Dipl.-Ing. Christoph Knauder

Investigations on the Mechanical Friction Losses of Different Engine Concepts

Doctoral Thesis

to achieve the university degree of
Doktor der technischen Wissenschaften
submitted to

Graz University of Technology

Supervisor and first examiner

Prof.h.c. Dipl.-Ing. Dr.techn. Theodor Sams
Institute of Internal Combustion Engines and Thermodynamics
Graz University of Technology, Austria

Second examiner

Assoc. Prof. Dr. Adolfo Senatore
Department of Industrial Engineering
University of Salerno, Italy

Graz, June 2021

Affidavit

I declare that I have authored this thesis independently, that I have not used other than the declared sources/resources, and that I have explicitly indicated all material which has been quoted either literally or by content from the sources used. The text document uploaded to TUGRAZonline is identical to the present doctoral thesis.

Date

Signature

Acknowledgments

This dissertation presents the key outcome of the long-term research project P27806-N30 funded by the Austrian Science Fund (FWF). The thesis was written at Virtual Vehicle Research GmbH in Graz and partially funded by the COMET K2—Competence Centers for Excellent Technologies Programme of the Federal Ministry for Climate Action (bmk), the Federal Ministry for Digital and Economic Affairs (bmdw), the Austrian Research Promotion Agency (FFG), and the Province of Styria and the Styrian Business Promotion Agency (SFG).

At the beginning, I would like to express my appreciation and gratitude to my PhD supervisor Prof.h.c. Theodor Sams from the Institute of Internal Combustion Engines and Thermodynamics at the University of Technology Graz for his persistent accompaniment, the many interesting conversations as well as continuing and inspiring remarks throughout my postgraduate studies. Special thanks also for the in-depth introduction to the field of scientific work after the diploma studies. Many thanks to Univ.-Prof. Helmut Eichlseder for the opportunity to carry out the supervision of the dissertation within the framework of the Institute of Internal Combustion Engines and Thermodynamics at the University of Technology Graz.

I would also like to thank Assoc. Prof. Adolfo Senatore for his comprehensive review. The detailed reflections and statements were essential to ensure that the work was written with appropriate scientific quality. The discussion and comments enabled an improvement of the quality of this thesis.

My gratitude to Priv.-Doz. Dr. Anton Fuchs and Dr. Jost Bernasch for the possibility and flexibility to realize the postgraduate study in coordination with my activities at the Virtual Vehicle Research GmbH.

Furthermore, I would like to thank my colleagues at the Virtual Vehicle Research GmbH, especially my current and previous team members of the tribology and efficiency team Stefan, Martin, Markus, Tomislav, Jakob and Walter for the support during the comprehensive testing activities and the innumerable and enduring discussions.

Very special thanks to my colleagues Dr. Hannes Allmaier and Dr. David Sander - their profound support greatly helped me to realize this thesis from including me to the funding application, introduction into the publication of peer-reviewed scientific publications, to final drafting of the manuscript. Their many years of experience and generated expert knowledge on journal bearing simulation was further an essential basis for the creation and implementation of simulation-based investigations on the main and big end bearings of the engines.

Additionally, I would like to express my deepest gratitude to my parents, for their always guiding and accompanying support throughout my life.

Last but not least and with deepest feelings I would like to thank my wife Bernadette and my children Johanna and Alexander, who have always accompanied and supported me in this dynamic, work intensive and demanding time for us as a young family.

Abstract

The ICE as part of future propulsion systems will play an essential role in purely ICE driven, hybrid and range extender systems beside the pure electrification of vehicle drives. Therefore, reducing the mechanical losses of internal combustion engines plays a central role in current and future engine development. Since the reduction of mechanical losses has a direct influence on fuel consumption, friction reduction on the engine level is a necessary measure for further steps to improve and meet current and future emission standards. To tackle these challenges in research, friction loss investigations on the sub-assembly level under heavy loaded operation conditions of different, currently available engine concepts are investigated in detail in this thesis. A further improvement of a friction loss analysis method combining testing and journal bearing simulation is conducted.

This thesis aims gaining a more detailed understanding of how base engine friction and lubrication conditions are affected by the engine concept, focusing on today's available conventional and high-power downsized engine concepts for passenger car applications. By engine concept conventional gasoline, downsized gasoline with high power density and modern diesel engines are meant.

A methodology using combined analysis results from engine tests and crankshaft journal bearing simulations is used to enable sub-assembly resolved comparisons also under load operation. For all engine concepts investigated, an identical and suitable SAE 5W30 lubricant is applied. This is an essential measure to prevent effects of different lubricant characteristics (even when using the same oil viscosity) like additive package composition on the results of the friction investigations and comparisons between the engine concepts.

Measurements of the friction losses on the base engine level are performed to enable both, determination of the base engine friction losses and the allocation of necessary input data for the journal bearing simulation model. From the tests conducted, results from the crankshaft main bearing friction losses are obtained as a basis for the verification of the crankshaft journal bearing simulation model. Measurements of the crankshaft journal bearing clearances and implementation in the contact model of the simulation result in an improvement of the calculated results. This enables the verification of the conducted calculations to measurement results from a conventional crank train system. Due to the subsequently updated contact model parameters a good applicability is shown. This is a vital finding for future work using the combined approach.

While the differences at the crankshaft journal bearing systems are insignificant, the main differences between the engine concepts investigated arise mainly from the piston group and valve train systems. A vital finding of the conducted work is assigned to the outcome that a holistic determination over the whole operation field of the engine is necessary because contrary results are obtained depending on the load state of the sub-assembly systems.

Reducing the lubricant viscosity is an important measure to decrease the friction losses in hydro-dynamic lubrication regime. By increasing the lubricant supply temperature significantly from 70 °C to 110 °C, analyses and comparisons are enabled focusing on sub-assembly resolved friction reduction potentials and risk assessment when FMEP changes arise. While at the base engine level friction potentials are investigated, an FMEP increase is determined at the valve train and piston group systems. Depending on the load state of engine operation friction loss reduction potentials up to 23%, 3% and 30% are determined for the piston group, valve train and crankshaft journal bearings, respectively.

On the other side at high loaded operation and low engine speeds disadvantages of up to 29% and 22% for the piston group and valve train system are resulting.

Finally, this thesis copes with the important aspect of the engine running-in (break-in) process providing detailed insights into the running-in behaviour and required run-in operation time at the sub-assembly level. The combined approach is applied to investigate this topic. The run-in period of 60 hours proved to be sufficient for the investigations carried out in this work. The influence of running-in is strongest at low engine speeds and high engine loads.

Kurzfassung

Der Verbrennungsmotor als Teil des zukünftigen Antriebssystems wird neben der reinen Elektrifizierung von Fahrzeugantrieben eine wesentliche Rolle bei rein verbrennungsmotorisch angetriebenen, hybriden und Range-Extender-Systemen spielen. Daher spielt die Reduzierung der mechanischen Verluste von Verbrennungsmotoren eine zentrale Rolle in der aktuellen und zukünftigen Motorenentwicklung. Da die Reduzierung der mechanischen Verluste einen direkten Einfluss auf den Kraftstoffverbrauch hat, ist die Reibungsreduzierung auf Motorebene eine notwendige Maßnahme für weitere Schritte zur Verbesserung und Erfüllung aktueller und zukünftiger Emissionsstandards. Um diese Herausforderungen in der Forschung anzugehen, werden in dieser Arbeit Reibungsverlustuntersuchungen auf Baugruppenebene unter hochbelasteten Betriebsbedingungen verschiedener, derzeit verfügbarer Motorkonzepte im Detail untersucht. Eine weitere Verbesserung einer Reibungsverlust-Analysemethode, die Versuch und Gleitlagersimulation kombiniert, wird durchgeführt.

Ziel dieser Arbeit ist es, ein detaillierteres Verständnis darüber zu erlangen, wie die Reibungs- und Schmierbedingungen des Basismotors durch das Motorkonzept beeinflusst werden, wobei der Schwerpunkt auf den heute verfügbaren konventionellen und hochleistungsfähigen Downsizing-Motorkonzepten für PKW-Anwendungen liegt. Mit Motorkonzept sind konventionelle Ottomotoren, Downsizing-Benzinmotoren mit hoher Leistungsdichte und moderne Dieselmotoren gemeint.

Um baugruppenaufgelöste Vergleiche auch im Last-Betrieb zu ermöglichen, wird eine Methodik verwendet, die kombinierte Analyseergebnisse aus Motortests und Kurbelwellen-Gleitlagersimulationen verwendet. Für alle untersuchten Motorkonzepte wird ein identischer und geeigneter SAE 5W30 Schmierstoff verwendet. Dies ist eine wesentliche Maßnahme, um Auswirkungen unterschiedlicher Schmierstoffeigenschaften (auch bei gleicher Ölviskosität) wie z.B. Additivpaketzusammensetzung auf die Ergebnisse der Reibungsuntersuchungen und Vergleiche zwischen den Motorkonzepten zu vermeiden.

Messungen der Reibungsverluste auf der Ebene des Basismotors werden durchgeführt, um sowohl die Bestimmung der Reibungsverluste des Basismotors als auch die Bereitstellung der notwendigen Eingangsdaten für das Gleitlagersimulationsmodell zu ermöglichen. Aus den durchgeführten Versuchen werden Ergebnisse der Kurbelwellen-Hauptlager-Reibungsverluste als Grundlage für die Verifizierung des Gleitlagersimulationsmodells gewonnen. Messungen der Lager-Spiele der Kurbelwellenlagerungen und deren Implementierung in das Kontaktmodell der Simulation führen zu einer Verbesserung der Berechnungsergebnisse. Dies ermöglicht die Verifizierung der durchgeführten Berechnungen mit Messergebnissen aus einem konventionellen Kurbeltrieb-System. Aufgrund der entsprechend aktualisierten Kontaktmodellparameter zeigt sich eine gute Anwendbarkeit. Dies ist eine wichtige Erkenntnis für zukünftige Arbeiten mit dem kombinierten Ansatz zur Reibungsverlustanalyse.

Während die Unterschiede an den Kurbelwellen-Gleitlagersystemen unbedeutend sind, ergeben sich die Hauptunterschiede zwischen den untersuchten Motorkonzepten vor allem bei den Kolbengruppen- und Ventiltriebsystemen. Eine wesentliche Erkenntnis der durchgeführten Arbeit ist dem Ergebnis zuzuordnen, dass eine ganzheitliche Ermittlung über das gesamte Betriebsfeld des Motors notwendig ist, da sich je nach Belastungszustand der Baugruppensysteme konträre Ergebnisse ergeben.

Die Reduzierung der Schmierstoffviskosität ist eine wichtige Maßnahme zur Verringerung der Reibungsverluste im hydrodynamischen Schmierungsregime. Durch die signifikante Erhöhung der Schmierstoffvorlauftemperatur von 70 °C auf 110 °C werden Analysen

und Vergleiche ermöglicht, die sich auf baugruppenaufgelöste Änderungen des FMEP konzentrieren. Während auf der Ebene des Basismotors Reibungsvorteile untersucht werden, wird an den Systemen Ventiltrieb und Kolbengruppe eine FMEP-Erhöhung ermittelt. Abhängig vom Lastzustand des Motorbetriebs werden für die Kolbengruppe, den Ventiltrieb und die Kurbelwellenzapfenlager Reibungsvorteile von jeweils bis zu 23%, 3% bzw. 30% ermittelt. Auf der anderen Seite ergeben sich bei steigender Belastung und niedrigen Motordrehzahlen Reibungserhöhungen von bis zu 29% und 22% für die Kolbengruppe und das Ventiltriebsystem.

Abschließend wird in dieser Arbeit der wichtige Aspekt des Motoreinlaufs (Einlaufvorgang) behandelt, indem detaillierte Einblicke in das Einlaufverhalten und die benötigte Einlaufzeit auf Baugruppenebene gegeben werden. Der kombinierte Ansatz wird angewandt, um dieses Thema zu untersuchen. Die Einlaufzeit von 60 Stunden hat sich für die in dieser Arbeit durchgeführten Untersuchungen als ausreichend erwiesen. Der Einfluss des Einlaufens ist bei niedrigen Motordrehzahlen und hohen Motorlasten am stärksten.

Abbreviations

ACEA	European automobile manufacturers association
API	American petroleum institute
BMEP	Brake mean effective pressure
CA	Crank angle
CO_2	Carbon dioxide
CAD	Computer-aided design
CDM	Crank degree marks
DAQ	Data acquisition
DOHC	Double overhead camshaft
DLC	Diamond like carbon
ECU	Engine control unit
EGR	Exhaust gas recirculation
EHD	Elasto-hydrodynamic
EU	European union
EUT	Engine under test
FE	Finite element
FCEV	Fuel cell electric vehicle
FEAD	Front end auxiliary drive
FMEP	Friction mean effective pressure
FRIDA	Friction dynamometer
FWF	Austrian science fund
GHG	Greenhouse gas
GMO	Glycerol mono-oleate
GUI	Graphical user interface
HTHS	High temperature high shear rate
ICE	Internal combustion engine
ILSAC	International lubricant standardisation and approval committee
IMEP	Indicated mean effective pressure
JASO	Japanese automotive standards organization
MBS	Multi body system
MoDTC	Molybdenum dithiocarbamate
NEDC	New european driving cycle
OEM	Original equipment manufacturer
SAE	Society of automotive engineers
RDE	Real driving emissions
TEHD	Thermo-elasto-hydrodynamic
TDC	Top dead center
TRG	Trigger signal
TST	Torque/Speed transducer
VI	Viscosity index
WLTP	World wide harmonized light vehicle test procedure
ZDDP	Zinc dialkyldithiosphosphate

Contents

Chapter 1

Introduction and scope of the thesis

The current situation in developing propulsion systems using ICE for the road transport sector is a challenging one. The global aim to reduce GHG-emissions to increase air quality and reduce air pollution yields to ever stricter emission limits. Based on globally driven agreements and subsequently increased customer awareness concerning the environmental impact of vehicles, major challenges for the automotive industry arise. Currently, the future of the ICE is generally being questioned for passenger cars [28].

To cope with related emissions by the ever-increasing number of vehicles used for individual and freight transport, fuel economy/vehicle emission standards have been developed in the past and take effect. Therefore, emissions from vehicles are a global climatic, political and economic issue that will gain momentum in the future due to the expected large increase in the number of vehicles on the road. An increase from 730 million (baseline year 2009) to 1.3 billion in the year 2030 is reported in [57] and a further market increase of about 2.4 billion vehicles until 2040 is reported in [103]. Today, all major countries worldwide have introduced vehicle emission standards/programs and fuel consumption targets for new engines and vehicles to reduce GHG emissions. This global trend ultimately manifests the importance of reducing vehicle emissions and fuel consumption, which was not pursued to this extent decades ago. Figure 1.1 shows the historical and current fleet CO_2 emissions performance from passenger cars.

The most ambitious fleet average target for passenger cars has historically been defined by the EU with a target of 95 gCO_2/km, followed by South Korea with a fleet average target of 97 gCO_2/km [104]. For exceeding the target limits, substantial fines have been defined. It should be noted that the EU fleet limit is not 95 gCO_2/km for all manufacturers, but depends on the average tare weight of the number of cars sold. The limit value curve for the CO_2 emissions related to the average vehicle mass is shown in figure 1.2.

A limit value of 95 gCO_2/km can be found in figure 1.2 at an average vehicle mass of 1.372 kg, which represents the average passenger car weight in the EU in 2015. To meet the 2020/21 targets and avoid substantial fines considerable progress in lowering the fleet CO_2 emissions is necessary in the next years [62]. Therefore, compliance mechanisms are included in the EU CO_2 standards. These mechanisms are mass-based $CO2_2$ targets, incentives for electric vehicles and innovative technologies, manufacturer pooling, derogations for small manufacturers and phase-in provisions [94]. In the near future, even stricter limits are defined and adopted. In the EU, a commission adoption concerning a proposal for a regulation of the new EURO 7 emission standard is currently discussed.

The official level of average CO_2 emissions is measured in the laboratory on chassis

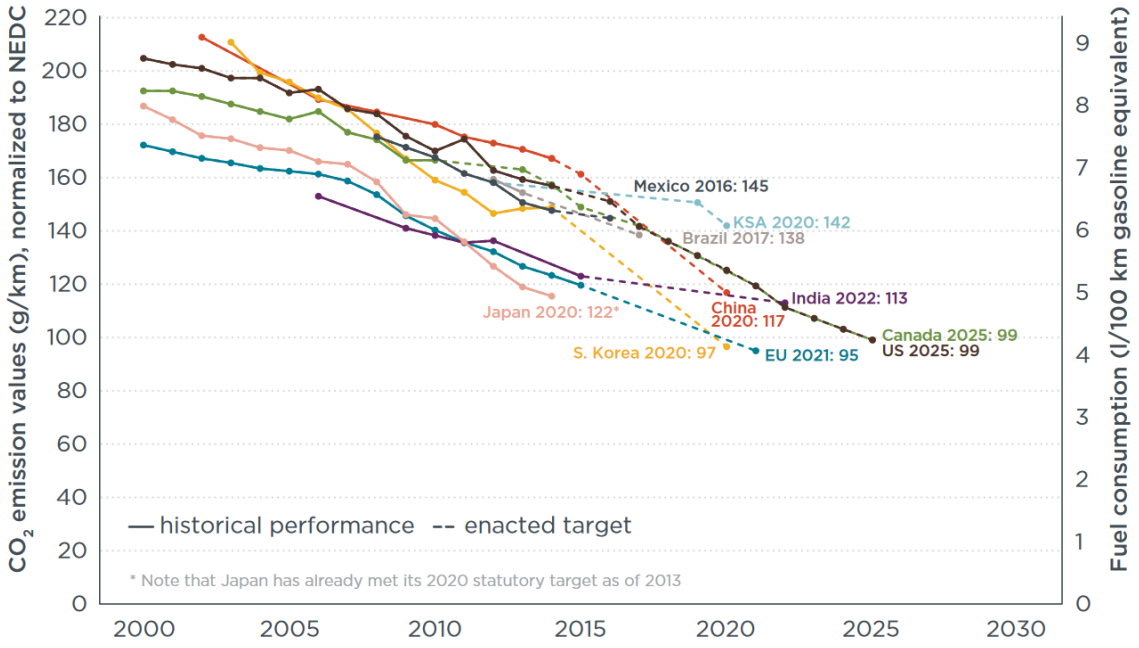

Figure 1.1: Historical fleet CO_2 emissions performance and current standards (gCO_2/km normalized to NEDC) for passenger cars [104]

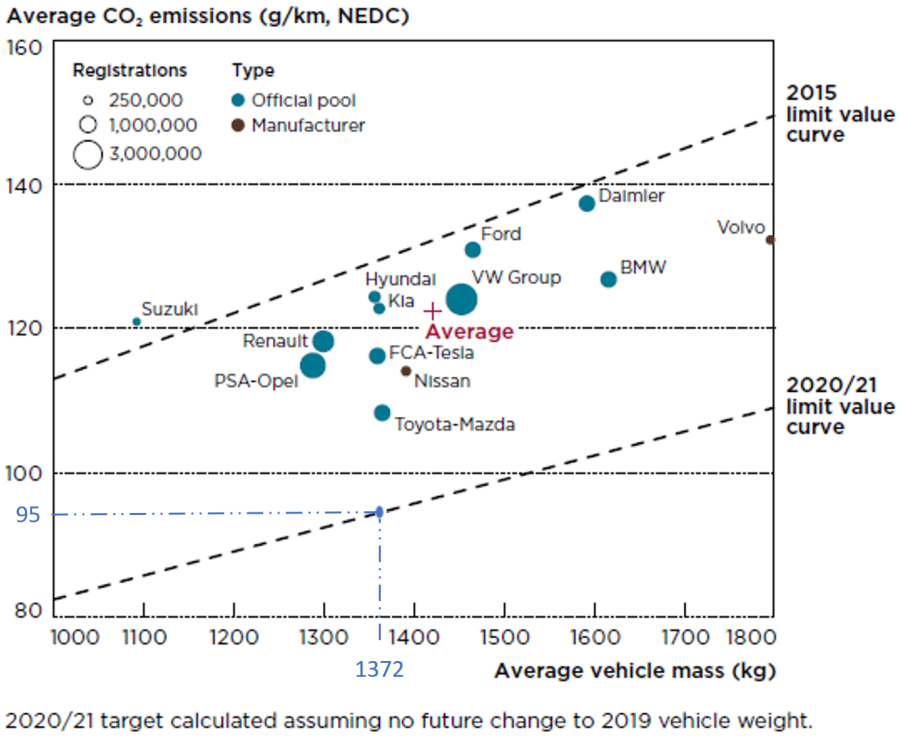

Figure 1.2: EU new passenger vehicles CO_2 emissions and weight in 2019 and corresponding 2020/21 targets (based on [62])

dynamometer using predefined and specified driving cycles. For the type-approval test, the NEDC (New European Driving Cycle) was used and has been replaced by the WLTP (World Wide Harmonized Light Vehicle Test Procedure) since September 2018 (phased-in since September 2017) [94]. These harmonized, predefined and specified tests with high time shares in the low/partial load range and therefore corresponding differences to real operation have led to targeted optimisation of operating conditions in the past. By introducing the WLTP test procedure the relevant engine operation points have shifted towards higher loaded conditions [6] but still only cover a partial area. In addition, the RDE (Real Driving Emissions) test procedure was phased-in in 2017 for on-road and other emissions testing and has been required since 2019 for all new vehicles in the EU. In this context, real-world tests are introduced resulting in higher emissions due to realistic vehicle operation compared to laboratory test. The regulation of how much higher the on-road test results are allowed to be is regulated with conformity factors. Beside real engine loads, the RDE test procedure also specifies cold temperature tests down to -7 °C [60], which differs strongly from previous test procedures. A clear trend can be derived that a holistic investigation at the conventional engine operation map (engine load, speed, temperature range) is necessary for a comprehensive investigation of fuel economy improvements. At the same time, the development and implementation of future friction improvements have to be realized within a reasonable cost frame. This strongly shows, that accurate development tools and methods are necessary to cope with future type-approval test procedure boundary conditions. This is also true for testing and improving the mechanical friction losses of the ICE.

The above-mentioned fuel economy/vehicle emission standards result in a so called „greening" of propulsion systems. The development of sustainable and greener vehicles is costly and promotes the need for investments to meet today's and future emission targets [106]. A current trend to reach the targeted emission levels is the electrification of the powertrain (e.g. using hybridisation (mild, full, plug-in) and the market launch of pure electrical driven vehicles (e.g. battery electric, fuel-cell electric). Research results and statistical analyses of market shares presented in figure 1.3 show that the global transition to electric vehicles is at an early stage and that the ICE will be the major part of the future vehicle propulsion systems for decades to come [20], [103].

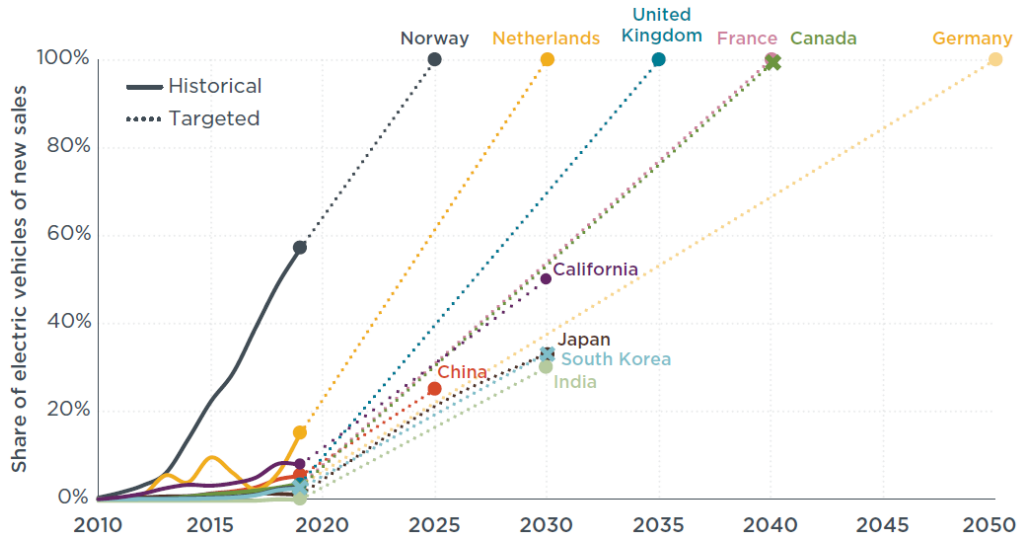

Figure 1.3: Historical and targeted electric shares of new passenger vehicles sales by markets and policy goals (based on [20] and [51])

It is reported in [103] that a market share of about 300 million purely electric driven vehicles is estimated by the year 2040, while the number of vehicles with an ICE in the propulsion system used (hybrid, range extender, purely ICE) will grow to 2.1 billion vehicles. Subsequently, beside the electrification also improvements of conventional technologies using the ICE as major propulsion component are and will be pursued by vehicle manufacturers. Within the further development of the ICE technology in terms of a sustainable, highly efficient and environmentally friendly system, the reduction of the mechanical friction losses is of major importance. Subsequently, the minimization of the ICE mechanical losses provides a significant contribution to high efficiency vehicles nowadays as well as in the foreseeable future. Even small contributions to a gain in fuel consumption are important. This becomes impressively obvious in a macroscopic view as examined in [35] and [103]. Additionally, reducing friction losses is one of the most economic ways to reduce fuel consumption [36], [49]. Finally, increasing the understanding in lubrication and friction represents important roles in energy conservation [102].

Because in the past basic research has been pushed and significant friction improvements have been made [89] future enhancements will be made up of small individual and more costly shares. These small shares are investigated and researched with special focus on the main components of the ICE, piston group, crankshaft journal bearings and valve train system. Work areas range from the design of the engine base geometries, the design of surface micro-geometries using advanced and new manufacturing technologies like honing and coating technologies and the combined application of advanced lubricants. An evaluation of these individual measures regarding frictional advantages and disadvantages at the main components is finally necessary at the engine level. Apart from the investigations on the component level, the interaction of the measures can only be considered holistically under realistic conditions in the engine system.

As the ICE gasoline and diesel combustion concepts work differently, it is currently interesting to gather a more detailed understanding of how the actual engine concept affects the base engine friction losses and lubrication conditions. Besides conventional concepts for gasoline and diesel engines for passenger car applications it is today a common way to use engine downsizing. Downsizing is nowadays also a common way to be applied at high power engines to minimize the number of lubricated contacts while maintaining the same power output. Subsequently, investigations of the base engine friction losses and lubrication conditions of high-power downsizing concepts is of additional interest. Furthermore, as the friction losses are generated at the base engine main components it is of interest to investigate the friction losses at the sub-assembly level during the study of the base engine. In this work, the focus is spent on the base engine main systems, the piston group, crankshaft main and big end bearing and valve train systems.

The assessment and assignment of engine friction losses in multi-cylinder engines is nowadays conventionally done by motored and fired friction tests. To reach conventional thermal boundary conditions as well as correct cylinder pressure phasing and gradient fired operation is ideal. At the same time it is challenging to keep necessary stability of engine operation and repeatability of tests which is required for comparisons. Motored engine tests offer reduced complexity of the test rig system due to the missing fuel system. At the same time different thermal boundary conditions as well as the absence of distinctive cylinder pressures acting on the pistons and bearings are affecting the results from these tests. Nevertheless, these tests are often used due to the limited effort needed to conduct comparisons of friction-improving measures on engine components [30]. Motored engine operation using an external charging system is able to create high peak

cylinder pressures and increased mechanical loads on the engine. In addition the method can be used to realise thermal conditions in the engine that are more similar to a fired operation, especially when using recirculation systems. Although the basic principle of motoring friction tests including external charging is known from the past [96], [97], it is currently used and developed further [15], [16] because of its advantageous measurement boundary conditions and the capability to simulate engine component mechanical loading comparable to fired operation. By the usage of recirculating systems between the engine inlet and outlet or the use of working gases other than air e.g. Argon [17] improves the thermal boundary conditions on the engine components during testing. A further description of commonly used measurement methods used to determine engine friction losses is presented in section 1.1.

A significant potential for friction loss determination under heavy loaded conditions is enabled when charged motoring tests are combined with predictive calculations of the journal bearing friction losses. The good reproducibility of the test method combined with the insights on the friction losses given by simulation enables new possibilities. Beside the sub-assembly resolved determination of the engine friction losses at conventional peak cylinder pressure ranges also related comparisons are enabled in great detail. Furthermore, this can be achieved without having to intervene significantly in the basic engine configuration.

This further development of new methods and tools for sub-assembly resolved friction loss investigations at highly loaded engine operation allows to holistically examine progress made at the component level (including ever smaller shares in future). Hybridisation of the domains' friction measurement technology and friction simulation is a key enabler in the development of future methodologies. Due to the considerable advancement in the field of friction simulation, predictive simulation models with time-efficient calculation durations have been developed and set up in conventional simulation environments available on the market e.g. [80]. Nevertheless, improvements and further research to enlarge public available data-sets for scientific work are necessary for the development of methodologies using simulation and measurements complementary to investigate ICE friction losses. The further improvement of simulation methods using specific measurement data from conventional ICE crank drives is also essential to further increase the accuracy of methods.

In the following subsection, current challenges and a state of the art is given for friction loss determination at the base engine level. It is not only given when determining the resulting friction losses at the crankshaft of the engine, but also when investigating the sub-assembly friction losses during base engine measurements. The further subsections contain and describe the aim, the research objectives and structure of the thesis. Finally the summary of research results is presented.

1.1 Current challenges and state of the art

Driven by ever stricter emission standards and related regulations, it is nowadays crucial to develop sustainable, highly efficient, and environmentally friendly vehicles. Besides a growing share of alternative drive systems (e.g. battery electric, fuel-cell electric), the ICE will be a predominant part of future propulsion systems e.g. in mild- and full-hybrid systems, using non-fossil based fuels like e-fuels or synthetic fuels for decades to come. Subsequently, the improvement of the mechanical friction losses is and will be of major interest.

To improve the overall mechanical efficiency of ICE and particularly at the base engine sub-assemblies, there are mainly three categories for reducing the friction losses and wear [102], [103]:

a): Mechanical design of the base engine sub-systems (power-cylinder unit, bearings and valve train) by defining configuration, properties and detailed micro-geometries of the major components.

b): Surface-, material- and machining-engineering e.g. advanced coating technologies like Nanocomposite or diamond-like carbon (DLC) coatings, honing processes and form honing.

c): Improved lubricant and additive package development to reduce hydrodynamic friction losses with the same engine service life and engine cleanliness e.g. by using ultra-low viscosity lubricants.

Care needs to be taken and specifically designed modifications are necessary from the categories mentioned above which can yield beneficial results and subsequently lowering the parasitic losses. [77]

For the identification and evaluation of measures from the above categories, the determination of the engine friction losses is an indispensable topic in engine development. New engine operation concepts e.g. downsizing, cylinder deactivation or advanced engine start-stop systems provide for a steady increase of the stress on engine components. The raise of stress (thermal and load) can lead to disadvantageous processes during operation leading to increased friction losses, high-temperature deposits and bearing material seizing. In [64], an adverse effect on the frictional performance of the compression ring and big-end bearing due to the introduction of cylinder deactivation is reported. This underlines the need for a holistic system view in order to determine the frictional losses when introducing new technologies and operating strategies. Especially high-power downsized engine concepts lead to highly loaded components which must be covered during engine design. Results of the highly loaded engine operation in combination with the trend to low-viscosity lubricants are enhanced areas of mixed lubrication at the contacting surfaces and potential increased risk of wear. In [23], the authors reported improvements of the boundary friction losses in the piston compression ring to cylinder liner conjunction when applying Nickel Nanocomposite coating technologies. This represents a good example of improvements in the frictional losses of engine components as a small single share, which, transferred to a fleet of vehicles, has a relevant global impact on fuel consumption and emissions reduction.

For the investigation of further friction reduction measures with the already good friction performance of today's modern ICE, methods and tools which can also dissolve and analyze small differences consistently over the operational range of the engines are necessary. For example, when analyzing the advantages of low viscosity engine oils, deviations in the friction torque of 0.1 Nm have to be resolved over the entire engine operation range [79]. When determining and assessing the friction losses of ICE, challenges arise for the methods used which are outlined briefly below:

Methods for friction determination at the base engine level:

- The precise measurement and analysis of engine friction under high load operation is not as easy as it may appear. In particular, the determination and assignment of the friction losses to the main components of the ICE under high peak cylinder pressures represents currently and in the future a considerable challenge. In [101], [100], a specifically designed friction measuring module is applied to

measure the friction loss shares via strip-measurements in fired operation. Other work specifically focuses on the sub-system piston group liner interaction using the „floating liner" friction test to investigate the resulting friction losses cyclically resolved [50], [47], [99] [59].

- For a long time, methods to measure the friction losses at the engine level in conventional fired and pure motored operation have been used [37], [67]. These methods are already standard procedures within the automotive industry to conduct investigations on the complete ICE system. For specific investigations at the piston group cylinder liner interaction single-cylinder test beds are used commonly [43]. Additionally, a methodology using charged motoring tests is used for measurements at the base engine level.
  - **Engine friction measurements under fired operation:** While an engine friction measurement in a fired operation is ideal because of the conventional thermal boundary condition as well as the correct cylinder pressure phasing and gradient, it is challenging to maintain the stability of the engine operation and the repeatability which is required for accurate measurements. Due to the combustion process, one is faced with strongly varying cylinder pressures from cycle to cycle. Furthermore, the inherently high indicated power produces highly alternating torques at the crankshaft. Therefore, a torque transducer with a larger measurement range is required for a fired operation compared to a motored operation. Furthermore, a fired engine operation also has an influence on the used pressure sensors of the cylinder pressure measurement system. Especially, the hysteresis effects during the conducted tests need to be accounted [100], and the usage of cooled pressure sensors is necessary.
  - **Engine friction measurements under pure motored operation:** The main drawback of pure motoring tests to identify the engine friction losses is the absence of load on the engine components from the non-predominant peak cylinder pressures of the combustion process. The application of pure motored engine tests results in a reduced complexity of the test rig due to the missing fuel system. Using a step-by-step disassembling process of engine components, the single component friction shares can be determined. However, different thermal boundary conditions as well as the absence of significant cylinder pressure levels acting on the pistons and bearings are affecting the friction results from these tests.
  - **Engine friction measurements using single-cylinder test engines under fired operation:** In the past, single-cylinder engines have been developed [66] and are currently improved for specific consideration of the friction losses of the piston rings, piston skirt and liner. This allows detailed insights into the cycle-resolved friction behaviour of single components, but cannot map the dynamic behaviour of the crank mechanism of multi-cylinder engines. Single-cylinder test beds using the floating-liner principle are commonly used for direct friction force measurements on the cylinder liner caused by the piston group under fired conditions. Here crank angle resolved friction loss investigations are possible. One main drawback is the missing possibility to use the conventional crank train of multi-cylinder engines. The methodology also has to deal with different boundary conditions like limited peak cylinder pressures, vibrations disturbing the force measurement signals, and stronger cylinder bore distortions due to the design of the test rig. However, in the last

years, improvements have been made regarding the sealing system between the floating liner and the cylinder head, and therefore, increased peak cylinder pressures can be reached. [50] Also, the difference in bore distortions has been minimized in the past using complex measurement and specific honing processes to reach comparable cylinder profiles as in conventional engines.

  - **Engine friction measurements under charged motoring engine operation:** In the recent past, a previously invented methodology using charged motoring tests [97], [96] is investigated and developed further [85], [55], [37], [15], [16]. This method for friction measurements is nowadays used also in industry applications (boost/motored friction test [37]). Limitations to thermal boundary conditions of piston and cylinder liner and different cylinder pressure phasing due to the motored operation of the engine without combustion have to be considered. Thermal boundary conditions of the piston group system can be improved when connecting the engine inlet and outlet (recirculating system) during the engine operation.

- The investigation of the engine friction losses should be carried out on the complete engine system. Replacing individual components (e.g. roller-bearings for camshaft support) without analyzing the effects on the main engine components (e.g. lubrication and cooling system, timing drive etc.) is not effective and does not allow the full potential of a friction reduction measure to be realized [11].

- Well-developed and established methods in the early development phase are used to perform tribological designs [27], [90], [24], [86]. However, the methods require results (experience-based, metrologically determined or derived from predecessor engines) in order to allow for a basic data set of the models. In the early stages of development, where no engine control unit including fuel system is available yet, methods are required which can carry out a metrological investigation.

- Today's engines operate with significantly increased maximum cylinder pressures compared to the past. For diesel engines, peak cylinder pressures of 200 bar and for turbocharged gasoline engines above 100 bar are state-of-the-art. This pressure increase results in more "diesel-like" loads in gasoline engines which affects the lubrication and behaviour of the engine components and interfaces [1]. When determining the friction losses of today's engine generations, the investigations have to be conducted under load conditions to gain insight in the frictional behaviour of the major engine components.

- Front loading of friction reduction studies in the early phase of engine development is a desired task during the engine development process. Therefore, the development and advancement of reliable and predictive simulation methods (journal bearings, piston/piston ring liner contact, valve train) are important topics besides enabling measurements on prototypes. Additionally, measurement methods with reduced complexity and costs (e.g. ECU and fuel system not needed) can be an advantageous addition in the early stage engine development phase.

Component design, surface engineering and coating technologies:

- Coating technologies and machining processes enable the production of contact surfaces with improved tribological behaviour (roughness, material properties (e.g. hardness), interaction with the lubricant (formation of tribofilms)). Low-friction coatings like diamond-like carbon (DLC) coatings are widely used in industry today, e.g. for valve train components or the piston group [63], [29]. At the same time, the

measures must be determined according to their friction minimizing properties, whereby the achievable friction advantages are quantitatively low. Methods for determining these small advantages must meet extraordinary boundary conditions in order to be able to represent a comparability of the measures on the engine level.

- The distortion of micro geometries due to the high stresses e.g deviations of the cylinder liner from the ideal cylindrical shape while operating under high temperatures and high loads are investigated numerically. In [8], the effect of a suitable conically shape of the liner in the engine cold state with nearly straight parallel walls in the hot state due to the impact of mechanical and thermal stresses is investigated by numerical calculations. The study revealed considerable potentials to reduce the friction losses by reducing ring pre-tension when combining the initially conical shape with a non-circular cross section to bring the liner even closer to the perfect cylindrical shape in the hot state. Therefore, when determining friction benefits resulting from these measures, tools and methods are necessary which can analyse the small fractions on the base engine levels.
- Measures on the component design level have to be metrologically recorded and determined. For example the reduction of bearing dimensions at individual engine bearings result in measurable friction reduction. In [13], a friction torque reduction of 0.3 Nm is reported for a conventional four-cylinder passenger car engine with five main bearings when reducing the main bearing dimensions from 52x18 mm to 47x18 mm (bearing diameter x width).
- Future electrified propulsion systems will reduce today's broad performance range of an engine family. Through modular systems in manufacturing this can be represented cost-efficiently for the industry. To give an example a wide power range can be offered e.g. for 2 litre 4-cylinder engines where the most powerful version can have twice the power of the lowest power version. This leads to disadvantageous friction performance, especially for the low power versions which are additionally often operated in part load conditions. Since the bearing dimensions and components must be designed for the engines' maximum power stage (incl. lubrication and cooling system), it is not possible to fully realize the possible friction-reducing potential for the lower power stages.

Component loads and lubrication

- The loading of engine components increased significantly in the past affecting the tribological boundary conditions engine components have to work within. In the EU, the average engine power for passenger cars has increased by 37% since 2001 [62]. At the same time, the average vehicle mass increased by 10% while the engine displacement decreased by 10%. Especially for the passenger car applications, the engine power for diesel engines increased significantly by 39% and for gasoline engines by 27% [61]. Charging, advances in combustion, material and production technologies make it nowadays possible to gain more power out of smaller engines. Additionally, engine operation modes like start-stop systems and engine coasting put additional stress on the engine sub-assembly systems.
- A proper layout and the knowledge of interaction between the surfaces and the lubricant determine the level of friction produced [74]. To reduce the hydrodynamic friction losses, low-viscosity lubricants are used and new lubricant classes and engine testing procedures are introduced [105], [68], [40], [69]. While it is beneficial in hydrodynamic lubrication regime to reduce the lubricant viscosity, it can be challenging for the contacting surfaces which already operate major in

mixed lubrication regimes like the valve train (e.g. cam lobe and follower contact). Subsequently, the reduction of lubricant viscosity reveals its benefits more likely in the power-cylinder components and the crankshaft bearings [102]. Therefore, the investigation of the component contact lubrication conditions is of great importance.

1.2 Aims of the thesis

This thesis aims at gaining a more detailed understanding of how base engine friction and lubrication conditions are affected by the engine concept. By engine concept conventional gasoline (turbocharged with conventional power density), downsized gasoline (turbocharged with high power density) and modern diesel engines (turbocharged with conventional power density) are meant.

Using a novel approach, combining friction measurements with predictive crankshaft journal bearing simulations, three different engine concepts for passenger car engines shall be investigated on the sub-assembly level. A data-set of the friction losses at the individual sub-assembly level of the three engines needs to be established as a basis for the further investigations. The capability of the EHD-simulation method to calculate the journal bearing friction losses of the crankshaft main and big-end bearings is verified with detailed measurement results at a conventional passenger car crank train system.

Following, it is the scope of this work to investigate not only how much friction is generated by the base engine sub-systems at highly loaded operation but also to gain an actual understanding of which type of friction is generated (friction generated in the hydrodynamic or mixed lubrication regime). While the so-called hydrodynamic losses do not harm the engine but increase the fuel consumption, the operation of contacting surfaces of engine components in the mixed lubrication regime can cause increased friction losses and detrimental wear to the engine. Based on the friction loss data-set of the three engines, friction loss reduction potentials and a risk assessment at the sub-assembly level need to be investigated.

Furthermore, by application of the novel approach the sub-assembly resolved investigation of engine running-in (break-in) is a further goal of this thesis.

In the course of this work, it should be noted at this point that the mechanical friction losses and the prevailing lubrication regime of the base engine sub-assemblies piston group, crankshaft journal bearings, valve train, timing drive, and shaft seals are being investigated intensively. The investigations in this work do not examine the pumping losses nor the friction losses of the auxiliary aggregates [34] which are disassembled or deactivated during the investigations.

1.3 Research objectives

This thesis targets towards increasing the knowledge of reducing the ICE friction losses applying sub-assembly resolved investigations under high load operation and realistic engine media supply temperatures. The novel approach used for highly detailed friction analysis is based on charged motored engine tests in combination with predictive EHD-simulations of the crankshaft journal bearings.

Therefore, this study investigates four different combined and building on each other application examples which are presented in the results chapter (see chapter 4). In the beginning of each application example, the specific topic is introduced and a review of the current and specific state of the art is presented.

Firstly, a combination of EHD-simulation and testing (semi-numerical approach so-called *virtual strip-down* approach) is used to investigate the friction losses and lubrication regimes for a modern 4-cylinder passenger car diesel engine. The measurements were performed on an engine test bed where motored tests with external charging of the intake air is realized to enable high loaded operation. In addition, external engine media supply units for the lubricant and coolant are used to establish realistic and stable engine media thermal boundary conditions for the tests. Furthermore, a recently developed journal bearing simulation methodology is used to calculate the hydrodynamic and asperity contact friction losses in a passenger car crank train system. The EHD-simulation methodology considers the elastic deformation of the involved components in contact and the complex rheological behaviour of the lubricant density and viscosity. In addition, conditions of mixed lubrication with undesired metal-metal contact are considered by the contact model. For a comprehensive parametrisation of the crankshaft journal bearing clearance, bearing clearance measurements have been conducted and the resulting values are integrated in the contact model of the simulation. For the verification of the EHD-simulation approach capability to calculate the crankshaft main and big-end journal bearing friction losses, specifically designed measurements are conducted. The extensive base engine measurement program includes a holistic strip-down measurement process. Measurements of the crankshaft solely without installed crankshaft seals (the crankshaft sealing has been replaced by a specifically designed sealing apparatus) are conducted to enable comparisons between calculations and measurement data. The generated crankshaft data-set is enabling a verification of the numerical analysis method to calculate the crankshaft journal bearing hydrodynamic and asperity contact friction losses (**PAPER I**).

Secondly, investigate different engine concepts to gather a deeper understanding of how actual engine concept designs affect the mechanical efficiency. In this context, the influence of conventional power density and highly increased power density (high-power downsizing concept) and combustion concept (diesel and gasoline) is investigated. In sum the rubbing friction losses of three 4-cylinder passenger car engines have been investigated using a combination of base engine measurements and predictive journal bearing simulations. By measuring the friction losses with a detailed and specifically designed measurement program, comparisons between the three engine concepts are enabled. For the crankshaft journal bearing system of all three engines, an EHD-simulation model is employed. Calculations of the journal bearing friction losses are performed at the identical operation points defined in the measurement program. The generated data-set is used to perform friction loss comparisons between the engines at the sub-assemblies piston group, crankshaft main and big-end bearings and valve train/timing drive system. By the comparison of the FMEP levels of the base engine sub-assemblies, the knowledge is increased where differences originate. Additionally, the impact of high-power downsized engine concepts on the mechanical friction losses is investigated in detail (**PAPER II**).

Thirdly, the usage of low viscosity lubricants enables the reduction of the hydrodynamic friction losses by decreasing the resistance due to lubricant shearing inside the lubrication film. At the same time, the likelihood for enlarged asperity contact friction is increasing, predominantly at high loads and low engine speeds. Comparing the friction shares at the sub-assembly level of the engine concepts at low and high lubricant temperatures, thus simulating a viscosity reduction, gives deeper insights into the systems level. A risk assessment evaluates potential FMEP increases and indicates the dominant lubrication regime under the different boundary conditions. By covering a wide range of operation points from low to full load operation, the comparison is conducted not only at identical

engine load conditions but also at identical thermal boundary conditions at low and high lubricant and coolant temperature levels. This enables the identification of potentials to reduce the friction losses by reduced lubricant viscosity and the investigation of negative influences resulting in friction drawbacks due to increasing metal-metal contact in the mixed lubrication regime (**PAPER III**).

Fourthly, as the process of engine running-in has a profound importance when performing engine friction measurements, the combined analysis approach is used to investigate this process of early engine operation. The friction loss determination, comparison and the investigation of the predominant lubrication regime is performed at the crankshaft main and big end bearings, valve train and piston group system. Subsequently, the engine running-in process is analysed using the novel approach not only for the base engine level but also the originate at the base engine sub-assembly level (**PAPER IV**).

1.4 Realization of the thesis

This study was part of a long-term research project P27806-N30 funded by the Austrian Science Fund (FWF). All investigations and work have been carried out at the VIRTUAL VEHICLE Research GmbH in Graz, Austria. The scientific supervision was realised by supervising the work at the Institute of Internal Combustion Engines and Thermodynamics at the University of Technology Graz. Numerous related discussions on fundamentals, the current state of the art as well as on the future development of engine friction contributed significantly to the design and realisation of the thesis. Involved partners in the broader project setting are the Mercedes-AMG GmbH, AVL List GmbH (AVL) and the Sloan Automotive Lab of the Massachusetts Institute of Technology. The supply of test equipment and simulation software tools as well as the detailed exchange and discussion of test results was conducted with the above-mentioned partners. This contributed significantly and best possibly when analysing the mechanical friction losses and lubrication conditions of the three engines and their sub-assemblies. The simulation model was set up in the commercially available AVL Excite software package. Besides the simulation environment, AVL also provided test bed measurement systems for the cylinder pressure measurements and crank angle determination as well as engine specific calibration work for the cylinder pressure sensors and amplifiers.

1.5 Structure of the thesis

The thesis is structured in four sections.

Section 1 focuses on the introduction of the area of work and the scope of the thesis. A holistic overview of the thesis is provided. After a general introduction into the field of interest, current challenges and state of the art as well as the research objectives are elaborated. Next, a description of the method used and the realization of the thesis with the general structure of the work is presented. The introductory section finishes with a summary of the research findings and an outlook on further research activities.

In Section 2, a general overview of the tribology of ICE with a specific focus on rubbing friction in the base engine system is given. The basic background of base engine system functions and terms used in this thesis is defined. Additionally, the mechanisms in lubricated contacts and the different lubrication conditions are presented. A general introduction of characteristics of rough surfaces and lubricant requirements and composition is given. Thereafter, the fundamentals of friction and wear in lubricated contacts and the interaction of engineering surfaces and the lubricant are described.

In Section 3, the methodology to investigate the frictional shares of the base engine sub-assemblies is described. The process of the combination of measurements and journal bearing simulation is outlined in detail by a description of both main components, the test-rig used to conduct engine measurements and the applied simulation method.

Section 4 presents the results of four content-related and building on each other application examples. It discusses the application of the methodology on reciprocating internal combustion engines. Furthermore, the investigation of friction losses and their comparison between the engines investigated in this thesis is described. The application examples are related to analyse the friction and lubrication as well as friction reduction potentials and arising risks at modern engine concepts. A validation of the journal bearing simulation methodology in a conventional engine crank train system is performed additionally in this study.

1.6 Summary of research results

The mechanical friction losses of three different 4-cylinder passenger car engine concepts are investigated on the base engine sub-assembly level using a combination of friction measurements and journal bearing simulation. The novelty of the work can be summarized as followed:

- Application of a developed friction investigation procedure (combination of base engine measurements and EHD journal bearing simulations) for different passenger car engine concepts to enable sub-assembly resolved friction loss investigations covering conventional engine loads (part and full load operation).
- Application and verification with measurement data of a parametrised journal bearing simulation model using actual simulation software functionalities (AVL Excite). The simulation method is used to calculate the crankshaft main- and big end bearing friction losses on a conventional passenger car crankshaft system.
- Investigations of the base engine and sub-assembly friction losses of three different passenger car engines working with the same or doubled specific power output.
- Sub-assembly resolved comparison of the friction losses of the different engine concepts.
- Assessment of reduction potentials and risks at the sub-assembly level of different engine concepts when increasing the lubricant supply temperature subsequently decreasing the lubricant viscosity.
- Sub-assembly resolved investigation of the impact of engine running-in effects at a passenger car gasoline engine.

A summary of the major research results is presented in the following:

- A developed analysis process merging results from base engine friction measurements and journal bearing simulations is holistically described in an application example [43]. Measurements are carried out at the base engine level where highly stable testing boundary conditions for peak cylinder pressure levels and thermal state of the engine media are realized. The motored engine tests with external charging of the air supplied to the engine intake bring up the power cylinder unit components' thermal state. The derived temperature levels are significantly increased compared to conventional motored tests due to the usage of a recirculation system between engine intake and exhaust manifold. The air supply temperature

can increase up to and maintain at supply temperature levels of 200 °C. In addition, increased gas forces acting on the crank system are realised due to the charging system. This puts the testing boundary conditions at more realistic levels of fired engine operation compared to pure motoring or charged motoring tests using an open exhaust system (without recirculation). By combining the recirculating external charging system with external supply units for lubricant and coolant, very stable testing boundary conditions even under high loads are realized. It is state of the art to keep the lubricant and coolant temperatures within a small range of $\Delta T = \pm 1$ °C. For the resulting peak cylinder pressure, variation ranges between $\Delta p = \pm 1$ bar are realised, even under high engine loads. This is an important feature of the test rig used for the measurements in this thesis, where peak cylinder cyclic deviations are insignificant compared to conventional fired operation. The stable testing conditions make it possible to resolve even small friction loss differences at the base engine level and its sub-assemblies' crankshaft journal bearings, valve train and piston group. This has been shown recently in specific applications e.g. presented in [79].

- The analysis of increased lubricant supply temperature and its influence on the subsequently reduced lubricant viscosity on the friction losses is in a first step conducted for the diesel engine concept in great detail. By stepwise increasing the engine media supply temperature from 70 °C to 110 °C during the executed test program, effects of the reduced lubricant viscosity on the friction losses are analysed. For the base engine, FMEP reductions up to 21% are determined. At the sub-assembly level, friction reduction is determined up to 45% at the crankshaft journal bearings. Simultaneously, an FMEP increase at the valve train and the piston group system for low engine speeds and high engine loads at the highest investigated lubricant supply temperature of 110 °C is assigned.

- In a sub study, a four-stage strip-measurement campaign is conducted at the diesel engine to experimentally analyse the friction losses of the valve train (including upper timing drive), the lower timing drive, crankshaft seals, and crankshaft main bearings. The valve train as well as the lower timing drive have shown a rather constant FMEP level at engine speeds higher than 2000 rpm. The FMEP level is 0,11 bar and 0,08 bar for the valve train (incl. upper timing drive) and lower timing drive respectively. At engine speeds below 2000 rpm, friction losses are increasing when elevating the lubricant supply temperature. The FMEP increase indicates mixed lubrication at this operation points. The most significant FMEP increase of 18% from 0,11 bar to 0,13 bar is found at the lowest investigated engine speed of 1000 rpm, which supports the conclusion of an increased amount of asperity contact.

- The crankshaft seal ring friction losses at the diesel engine range between an FMEP level of 0,02 bar and 0,04 bar. The highest friction losses result at the lowest lubricant supply temperature, while the lowest frictional losses appear at the highest lubricant supply temperature over the entire investigated engine speed range from 1000 rpm to 4000 rpm. This indicates predominant hydrodynamic lubrication. At engine speeds higher than 2000 rpm, a constant plateau for the friction losses is reached for each investigated engine media supply temperature of 70 °C, 90 °C and 110 °C. At engine speeds lower than 2000 rpm, the friction losses of the crankshaft seals are slightly decreasing. The effect of a stable plateau at specific levels of engine speed can be explained by the reduced amount of oil in the lubricated contact due to the recirculation effects of the sealing lip resulting in

lower friction losses due to lubricant shearing. Together with a further decrease of the radial force of the sealing lip due to a speed-dependent temperature increase, reduces the seal ring friction losses resulting in stable plateaus of friction losses.

- The journal bearing simulation model capable for calculations in hydrodynamic and mixed lubrication regime is set-up including an appropriate contact- and lubricant-model. In this context, the generated know-how from [82] and [84] is used. Important findings on the application, like using a constant friction coefficient, smoothing of contact surfaces and consideration of micro-hydrodynamic effects caused by the rough surfaces in the lubricated contacts by integration of correction factors (flow factors) are considered. Additionally, the running-in behaviour due to edge loading of the crankshaft bearings [83] is considered in the calculation process by preliminary calculations. The developed simulation model is applied in this thesis for friction loss calculations in a passenger car crankshaft system.

  Because the claim of predictive calculations of friction losses shall always exist (scientific studies, early development phase, calculation for existing prototypes and series engines), the surface roughness of shaft and bearing shell is not measured during the simulation model set-up in this work. Instead, the data and know-how to set up the contact model parameters to calculate both hydrodynamic and asperity contact friction losses from previous studies [5], [76] is used to investigate the capability of application at conventional crank trains. It is important to note that data from a surface measurement can be implemented at any time when required. The bearing clearance for the crankshaft journal bearings is set on a common value of 25 μm in a first step, which later on has been changed during a conducted validation process when comparing measurement and simulation results.

- The journal bearing simulation approach is validated and utilized in a conventional ICE crank train system in this work. The basis for the validation task are measurement results of the solely main bearing friction losses, which enabled a direct comparison between results from the EHD-simulation results to experimentally determined data. Calculations are conducted for the crankshaft main bearings friction losses, after the basic condition of the simulation model. The load and thermal boundary conditions for the calculations are set according to the conducted strip-test campaign results. Maximum deviations between the experimental and simulation results were found in the order of 20% (ΔFMEP=0.04 bar) at a lubricant supply temperature of 90 °C and an engine speed of 4000 rpm when using bearing clearances of 25 μm. After the measurement of the cold state bearing clearance of the main and big end bearings, an adjustment of the bearing clearance from 25 μm to 20 μm was made. This resulted in an improvement of the calculation results, which led to a maximum deviation of ΔFMEP=0,01 bar (7%) between measurement and simulation results at 90 °C. Over wide ranges of the engine speed band, the results' comparisons are below ΔFMEP=0,01 bar which proves the good suitability for using the simulation model in crank train applications and the usage in this study.

- The parametrised simulation model is applied and set-up to all three engines investigated in this thesis to calculate the journal bearing friction losses of the crankshaft main and big end bearings. It is interesting to note that for the individual engine concept investigated and hence resulting different maximum peak cylinder pressure, different trends for the load dependency of the journal bearing friction losses (sum of five main and four big end bearings) emerge. For the conventional gasoline engine where an operation with a maximum peak cylinder pressure of

70 bar has been realised, the dependency on engine load is about one third of the speed dependency (speed range 1000 to 5000 rpm). For the high-power downsized gasoline engine operated with a maximum peak cylinder pressure of up to 120 bar, the load dependency increases to half of the speed sensitivity of the journal bearing friction losses. The diesel engine operated with maximum peak cylinder pressure levels of 180 bar, the load dependency is about two third of the friction loss dependency on engine speed.

- Effect on friction losses from the combustion concept used:

  Globally, differences in engine friction were found between the three engines investigated, which was expected [44]. What was unexpected is that a large part of these differences can be attributed to the different valve trains used at the engines. If one neglects the different valve train systems and their different friction contributions, the remaining engine friction losses are rather similar. The valve actuation system has significant influence on the engine friction losses. Here the progress in the development of valve train systems away from flat-tapped based valve actuation systems used in gasoline engine 1 to roller finger follower systems with increased mechanical efficiency used in the other two engines is investigated. The modern roller finger follower systems investigated in this work show a temperature dependency with a negative effect on the friction losses when increasing the lubricant supply temperature. But at these systems, a much lower FMEP increase compared to the direct acting system used in gasoline engine 1 is analysed.

  For the diesel engine, the valve train friction losses are rather constant over engine speed with FMEP values ranging from 0,18 to 0,24 bar. A slight temperature dependency is noticeable with highest FMEP values resulting at the highest investigated temperature of 110 °C. Gasoline engine 1 uses a flat-based tappet valve actuation system with 5 valves per cylinder. This valve actuation system shows the highest FMEP level of all three engines and a significant temperature dependency of the friction losses. The overall FMEP level ranges from FMEP=0,32 bar to 0,51 bar. At the lowest engine speed and 110 °C engine media supply temperature, the FMEP value is 2.6 times higher compared to the other investigated engines. Noticeable mixed lubrication is investigated for this engine over the entire speed range but especially at engine speeds below 2000 rpm. At the lowest engine speed investigated, the FMEP level is about 35% higher at 110 °C compared to 70 °C.

  When analysing the piston group friction losses, the diesel engine showed rather similar friction losses to the gasoline concept of gasoline engine 1, which is a further remarkable result. At low engine speeds and low loads, differences are rather small with ΔFMEP=0,09 bar. At increased cylinder pressure levels of 70 bar, largest FMEP differences of ΔFMEP=0,12 bar are analysed. Especially the diesel engine was expected to show much higher friction losses due to the longer piston skirt and higher resulting side forces due to the very high peak cylinder pressures involved during the operation of this engine. It is reported [30] that for this engine, the piston group is particularly well friction-loss-optimized by increasing the piston clearance while lowering the piston pin offset. In addition, shorter ring heights in combination with lower tangential forces of the piston rings and friction reducing piston skirt coating are used to optimize the crank train.

- Effect on friction losses of high-power downsizing engine concepts:

  The influence of significantly increased power density on the base engine friction

losses is investigated in comparison to more conventional designs. The investigation of the high-power-density engine concept with doubled specific power (133 kW/L) of gasoline engine 2 compared to the other two engines revealed that investigations under load conditions are essential for a comprehensive analysis and interpretation of results.

At low loads up to maximum peak cylinder pressures of 50 bar, the piston group of the high-power downsizing concept has shown the best performance with advantages of up to ΔFMEP=0.15 bar. Under high load operation for engine speeds higher n = 1500 rpm and peak cylinder pressures above 70 bar, a maximum difference of ΔFMEP=0.5 bar in comparison to the diesel engine has been determined. This represents a good example of the potential and importance of tribological optimizations at the internal combustion engine and specifically at the piston group sub-assembly.

The comparison of the valve train system friction losses shows the lowest FMEP levels of the engines investigated for gasoline engine 2. The FMEP values vary between 0,15 bar and 0,38 bar. Nevertheless, the valve train friction losses of Gasoline engine 2 have shown a dependency on both lubricant supply temperature and engine speed. The FMEP level increased for higher lubricant supply temperatures investigated when the engine speed reaches levels below 1500 rpm and above 4500 rpm. At 6000 rpm, the FMEP increased at a higher extent than 30% between a lubricant supply temperature of 70 °C and 110 °C.

The crankshaft journal bearing losses are rather similar compared to the other engines with small advantages compared to gasoline engine 1 at higher engine speeds and insignificant disadvantages to the diesel engine at load operation (maximum difference ΔFMEP=0.05 bar).

- Friction reduction potential and risk assessment when reducing the lubricant viscosity:

  Comparisons and friction reduction potentials/arising risks due to the reduction of the lubricant viscosity are investigated. By varying the engine media supply temperature of the engine under test, the lubrication conditions in all contacts are simultaneously affected. A viscosity reduction is achieved by increasing the temperature, thus simulating the use of a low-viscosity engine oil. Consequently, the friction losses of the three engines are determined, analysed and compared for different media supply temperatures. If the determined FMEP value for the increased supply temperature does not change or even increase, this indicates the presence of significant amounts of asperity contact. Subsequently, an assessment which investigates the FMEP increase (risk) and decrease (reduction potential) using the previously presented combined friction analysis approach is performed. The assessment is conducted not only for the three base engines, but particularly for their sub-systems.

  The main and big end bearings at all three engines investigated show significant friction reduction potentials between 16% and 30%. For the piston group system of the diesel engine and gasoline engine 1, an FMEP reduction up to 16% is found. However, the reduction potential is identified at different engine operating conditions. While for gasoline engine 1 decreased FMEP values are found at low speed and low load operation, reduction potentials for the diesel engine are found at medium speed and low load operation. Both engines reveal mixed lubrication to

a minor extent for low engine speeds and high load operation when increasing the engine media supply temperature. Here the FMEP levels increase up to 7%.

Friction reduction potentials up to 23% are obtained for low load operation of gasoline engine 2. In contrast, the analysis' results at low engine speed and high load operation are significantly different. A significant FMEP increase is present at engine speeds below n=2000 rpm and maximum peak cylinder pressure levels above 50 bar. FMEP values increased by up to 29% were examined at these engine operating points.

Lowering the lubricant viscosity at the valve train system results in an FMEP increase between 9% and 11% for the diesel engine and between 9% and 18% for gasoline engine 1. At gasoline engine 2, a slight FMEP decrease of up to 3% is investigated at engine speeds between n=2000 rpm and n=4000 rpm. Contrary, at engine speeds below n=2000 rpm and above n=4000 rpm, the FMEP is increasing when the supply temperature is increased. While at the low engine speeds the increase is rather small (up to 9%), the increase at high engine speeds is significant (up to 22%). The results of the friction potential analysis at the base engine level of the engines represents a good example of the advantages using the combined approach for the sub-assembly resolved friction loss analysis. At the base engine level of e.g. gasoline engine 2, the increasing FMEP levels when lubricant viscosity is reduced are rated as rather small between 0% and -2% at low engine speeds and high loads. However, when analysing the friction reduction potential at the sub-assembly level, increased FMEP levels indicating mixed lubrication regimes are identified at the piston group and valve train system. Subsequently, a potential significant increase of friction loss of a single sub-system cannot be identified when the entire base engine is evaluated. For instance, friction reduction in the crankshaft journal bearings may cancel the increase of friction in the valve train or the piston group system, leading to possible misinterpretations.

- The impact of the engine run-in process:

  To assess the impact of the running-in process on the sub-assembly level of gasoline engine 1, a series of tests have been conducted. With the focus in this thesis on performing reproducible friction measurements enabling comparison of the results obtained, the newly developed method is used to determine the duration until stable levels of the friction torque in the initial operation phase of a new engine are reached. Derived from this investigation, a running-in program is to be defined that is used in the pre-phase of the friction measurements conducted at all three engines in this thesis. Specific focus is spent here on the running-in phase of the piston group and valve train system. Therefore, the main components of the valve train and piston group systems are replaced by new parts. The control of the running-in condition during the tests in this work is regularly checked. By repeated measurements after the individual test program has been run through and comparison with the value after the running-in phase, the completion of the running-in process is ensured. An additional aim of the investigations was to determine the duration of time until the end of the running-in process. It has been determined that the running-in process is finished after an operating time of about 60 hours. The FMEP of the base engine decreases by ΔFMEP=0,04 – 0,06 bar during the running-in phase. The influence is about as large as the temperature difference between 70 °C and 90 °C and its impact on the engine friction losses, where a 20 °C temperature change causes a friction reduction of about 0,08 bar. The largest change in FMEP due to running-in with a share of 70% occurs in the first 15

hours of operation. Within additional 15 hours of test-operation (between second and third test), a share of 20% and between the third and fourth test of about 10% is resulting. The direct acting valve train was affected strongest when analysing the sub-assembly systems with a change in FMEP of 0,06 bar. This represents a change of about 18% of the total valve train friction losses at the same operation point. The effect of running-in is strongest at the operation points where the sliding speed is lowest and asperity contact is strongest. The influence of running-in at the piston group system is between ΔFMEP= 0,02 - 0,04 bar. This is a remarkable result because the piston assembly is contributing considerably more to the friction losses than the valve train. In this engine design, two main explanations for the findings are the high number of five valves per cylinder and uncoated surfaces of cam and tappet. In contrast, the piston ring face and the piston skirt are coated and are subsequently more resistant to wear. The derived results regarding the required engine operation for comprehensive engine run-in showed that a holistic operating range (low and high engine load over the entire speed band) is necessary to obtain steady state operation over the full engine operation map. In addition, the operation of the engine at low and high engine media supply temperatures during the run-in phase is recommended. While the lubrication film is smallest at highest supply temperatures, specific oil additives may be activated at certain temperature levels to protect the surfaces in contact at elevated temperatures. Therefore, also lower temperature levels should be considered when conducting comprehensive engine run-in.

1.7 Outlook

The reduction of fuel consumption as well as greenhouse gas emissions are major drivers for a sustainable mobility in the future. Ever stricter fuel consumption and emission targets make it ever harder for car manufacturers to use conventional ICE propulsions systems including extensive exhaust after treatment systems because of rising costs. New technologies like alternative fuels (zero-carbon, produced from renewable energy) and the electrification of the passenger car power train are coming closer to the market introduction or are achieving ever larger market shares. Therefore, the carbon footprint in the transport sector is to be replaced by more environmentally friendly fuel alternatives or reduced by introducing other propulsion concepts such as electric mobility.

At present and in the near future, however, it is reported that the combustion engine will continue to be the major component in propulsion systems (pure or hybridised) for decades to come. Until substantial market shares of pure electric vehicles e.g. BEV, FCEV, the ICE will be an essential component to drive vehicles. Additionally, electrification can be seen as a positive addition to the ICE to improve the thermal efficiency as well as to improve the capability of operation in optimal working areas. Nevertheless, market studies assume further market growth in the coming years, also driven by high economic growth across the developing nations.

Regardless of the fuel used, improvements in the friction losses of internal combustion engines always bring significant benefits through a concomitant reduction in fuel consumption. With regard to the strict regulations of emission legislation, investments for improved friction losses of engine components instead of penalties for exceeding emission limits are becoming increasingly important.

Therefore, friction-minimizing measures are and will be an important part of the vehicle and engine development in the future. A focusing of the tribological requirements

on reduced operating conditions due to an expected decrease in the broad engine performance spectrum of current engine series is to be expected. Due to the increasing electrification of the power train, the operation field of the ICE is pushed to efficiency optimal operation points. Subsequently, the operation of the ICE in smaller or fixed thermal efficiency areas is expected by combining and coupling the ICE with electric motors.

This operation band limitation of an engine series and the associated reduction in the range of component loads to be controlled can be seen as advantageous with regard to the tribological development of components and their surfaces. Simplifications in that way will help to better design friction optimized engines as well as to significantly reduce costs. The cost savings are then available for investments in other technologies like coatings, production processes, materials or batteries and e-motors.

To identify and evaluate further improvements from individual measures when considering the ICE system as a whole, the investigation methods must be further developed both on the side of the experimental investigations and on the side of simulation. The combined method developed to investigate the frictional losses of ICE can make a contribution to this. On the one hand, friction-minimizing measures can be investigated on the overall engine system and on the other hand, it is possible to investigate the sub-assembly systems under high load conditions.

The investigation results for the piston group losses show the necessity for development and research on this topic in order to fully exploit the potential of this sub-assembly system. Current and future work on this topic [41], [56], [87], [65], [18], [92], [93], [25], [19] promises a further improvement of the understanding and a reduction of the friction losses.

In this context, the know-how of the developed journal bearing simulation methodology can be analysed for a transfer to develop simulation methods for the piston group. Results using the semi-numerical methodology can provide data for the verification of the simulation results. Further research on complementary opportunities of fired and externally charged motoring tests should be carried out to use full potential and synergies of the methods. A combination of the development tools in charged motoring operation in the engines' early development phase with the results from fired measurements in the later development phase could provide further insights and some more front-loading of tribological development work.

Furthermore, the enhancement of the friction measurement test bed capabilities with regard to extension of the thermal boundary conditions to very low temperatures (e.g. down to -20 °C) can be specified as a future work topic. Additionally, the investigation of further engines using enlarged thermal boundary conditions (e.g. very low temperatures) can expand the know-how and enlarge the data-set for the further development of simulation models. Finally, this results in an enrichment of the usable operation range of existing simulation models.

Chapter 2

Tribology in internal combustion engines (ICE)

The term „Tribology" defines the engineering and science of interacting surfaces in relative motion. It covers the interdisciplinary studies and application of the areas friction, lubrication and wear. Tribology as a subject became widely known through the work of Peter Jost [22], among others.

In this work, investigations are carried out on reciprocating ICE for passenger car applications, which work according to the four-stroke technique. The focus of the study is put on the friction losses (due to hydrodynamic and mixed lubrication) of the power conversion system (piston, conrod, crankshaft bearings) and valve train/timing drive system. ICE using other mechanisms than pistons are not in focus here.

Nevertheless, also the other systems involved in engine operation (e.g. turbocharger engine media pumps, EGR valve, FEAD components) are important to be investigated but have not been included in the investigations of this work.

In the following, the base engine systems and ICE lubricant fundamentals, requirements and composition are outlined. Furthermore, lubrication regimes as well as the basics of engineering surfaces, friction and wear including the engine running-in process are described.

2.1 Introduction and background

The development of the internal combustion engine at the end of the nineteenth century was the essential milestone of free and independent mobility of mankind. Since then, the ICE usage has ever-increasingly been leading to major technological developments in terms of available power, emissions and fuel consumption, but also reliability and failure minimization. The latter are mainly due to progress in the field of tribology.

There are several lubricated contacts in interaction in an ICE. The crankshaft bearings (main and big end bearings), the valve train/timing drive and the piston group are the main systems where about 90% of the engine friction losses occur [35]. These core systems together are commonly known as base engine system.

The friction loss shares from the lubricated working surfaces [102] of the crankshaft bearings (about 30%), the valve train/timing drive (about 15%) and piston group (about 55%) are in the focus of this thesis. Therefore, the main components and contacts are described hereafter.

2.1.1 Base engine systems

In this chapter, the main components and sub-assemblies of the ICE considered in this thesis are summarized. A detailed description can be found in relevant reference literature. [58], [34], [73], [52], [53], [54], [88], [98], [48], [31]

A reciprocating ICE consists roughly of 150-200 moving parts [1] transferring the gas forces from combustion acting at the piston into rotational movement at the crankshaft. The reliable mechanical function of the crank train system is dependent on these parts and their joints. An overview of the ICE main systems is shown in figure 2.1 for a four-cylinder engine designed for passenger car applications.

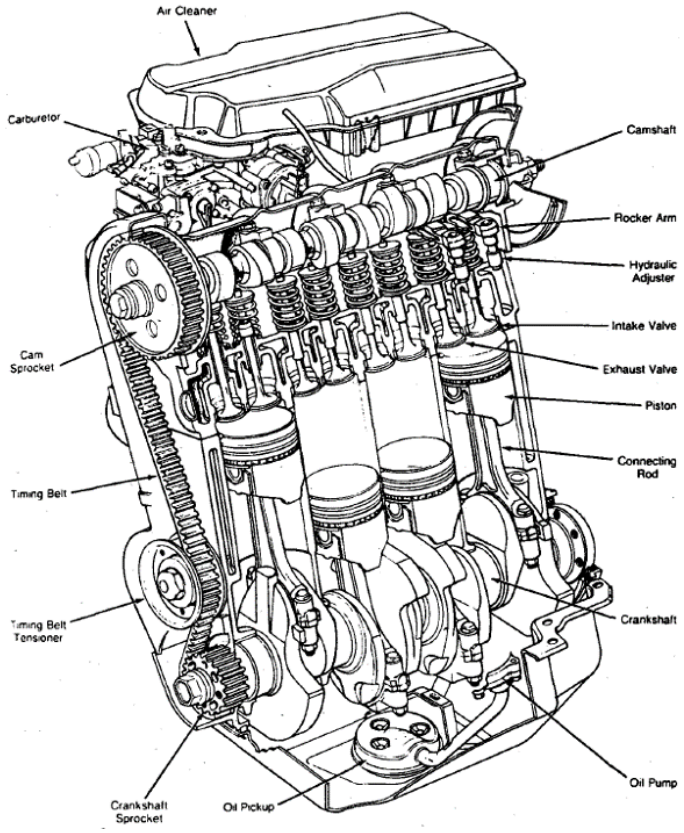

Figure 2.1: Overview of the ICE main systems [34]

The joints between the individual parts are mainly designed as journal bearings generally using engine oil as lubricant. In the lubricated contacts, fluid lubrication is predominant.

***Crankshaft journal bearings*:**

The crankshaft journal bearing system consists of the main and big end bearings. Next to special designs, the crankshaft in in-line concepts is conventionally supported in the crankcase at both ends and between each cranking. Subsequently, for the conventional design in an in-line four-cylinder passenger car engine, the crankshaft bearing system consists of five main and four big end bearings (see figure 2.2).

The crankshaft main bearings take up the forces (gas and oscillating/rotating mass forces) transmitted via the piston, piston pin, connecting rod and crankshaft. The forces are transferred via the bearing brackets to the engine crank case. Axial forces induced from different reasons (e.g when the clutch is operated, axial force components from

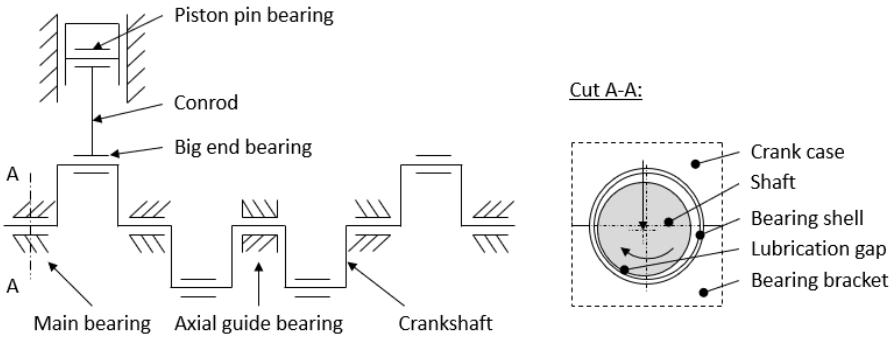

Figure 2.2: Overview crankshaft bearing system of an in-line four cylinder engine

manufacturing tolerances in the bearings or axial forces acting from helical gears at the crankshaft) also need to be supported from the crankshaft bearing system. Therefore, one crankshaft main bearing (e.g. main bearing number three in figure 2.2) is designed additionally as axial guide bearing and equipped with thrust washers for axial bearing support.

The crankshaft big end bearing directs the forces transmitted by the connecting rod to the crankshaft. At high engine speeds, mass forces are strongly increasing. At that operation points, the big end bearing is the highest loaded bearing in the combustion engine and subsequently the power-limiting component. The optimization of the conrod mass is particularly important for high-speed engines.

The bearing tribo-system consists of the bearing shaft (typically hardened), bearing shell (typically softer material than the shaft), bearing surrounding structure (bearing block and bracket) and the lubricant. All components may deform elastically during operation influencing the tribological processes in the lubricated contact.

The crankshaft friction contribution arises mainly from the main and big end journal bearings. In modern engines, the crankshaft bearings are working predominately in the hydrodynamic lubrication regime. At high loads, mixed lubrication regimes are added to this. Engine operation modes like start-stop systems or engine downsizing put additional stresses on the bearing systems.

***Valve train*:**

The valve train system consists of the camshafts (supported in the cylinder head), valves, valve guides, valve actuation system (cam directly acting, cam acting via leverage system) and sealing rings.

The design used today for passenger car engines is mostly the arrangement of two separate camshafts in the cylinder head (DOHC). Characteristic here are separate intake and exhaust camshafts (see figure 2.3) mainly due to reasons of speed rigidity and variable valve timing. [53]

The valve train friction losses are mainly influenced by the valve actuation system. The common actuation systems of today's passenger car engines can be separated into direct acting and not-direct acting constructions.

At the direct acting valve actuation systems, the cam is directly moving the valve conventionally using a bucket tappet. In-direct acting systems are using roller type cam follower systems and rocker arms to prevent the sliding contact between cam and tappet and replace it with more efficient rolling contact (figure 2.4).

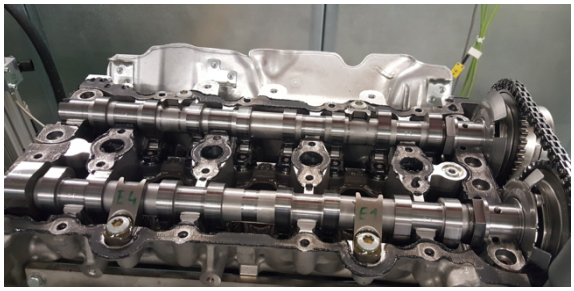

Figure 2.3: Double overhead camshaft (DOHC) system architecture for a in-line four-cylinder engine

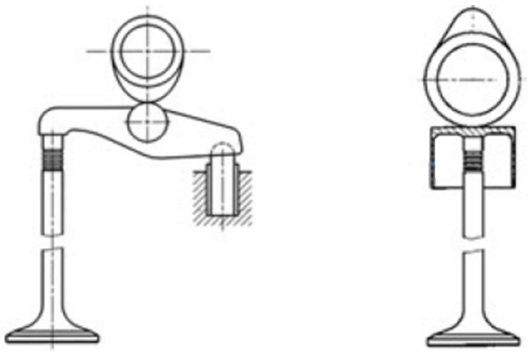

Figure 2.4: Valve actuation system: **left**: in-direct acting principle **right**: direct acting principle [53]

Especially at low engine speeds, where no hydrodynamic lubrication can evolve at the sliding contacts, the rolling contacts can show advantages regarding friction and wear. It is important to note that the camshaft speed is only half the speed (speed ratio 1:2) of the crankshaft at the widely used four stroke principle.

The main friction contribution at the valve train system comes from the cam and tappet interface, rocker arm/fulcrum interface and the camshaft journal bearings. Minor contribution results from the valve guides and valve seats. The valve train loads are mainly influenced by the valve spring forces and the inertia forces of the component masses. Subsequently, spring load and mass reduction are important goals when developing valve train systems.

***Timing drive*:**

The camshafts and the connected valve train system are driven by the crankshaft. The connecting element is the timing drive system. For passenger car applications, a common actuation is designed via chain or toothed belt systems. In the commercial vehicle sector, gear tooth systems are also common as drive systems. Figure 2.5 shows the timing drive system (chain drive and belt drive) of two engines under test in this thesis.

The timing drive system consists of the drive components (toothed belt/chain, cam and crankshaft sprockets), guiding rails, pulleys and the tensioning system. The main friction share for the chain drive occurs at both the chain and guiding rail plastic surface as well as the chain and tension rail plastic sliding contact interface. For the belt drive, the main friction sources come from the belt friction (tooth deformation work, belt inner friction), interface contact between pulleys and belt (tensioning system and idler pulley).

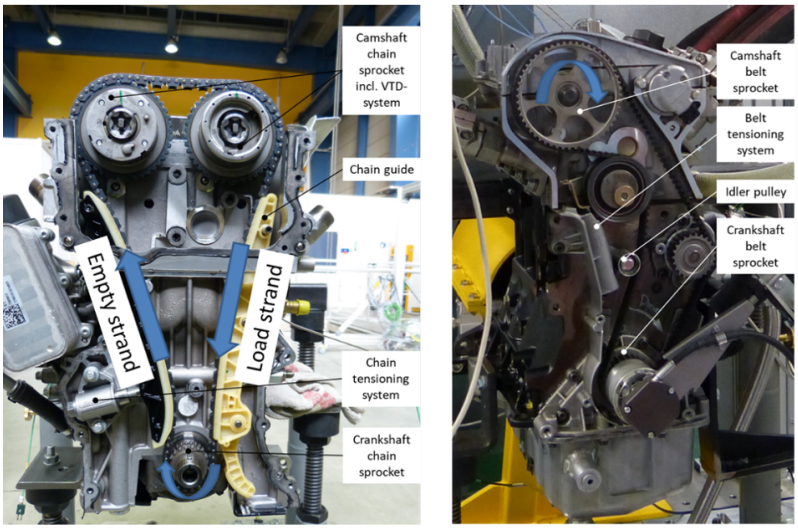

Figure 2.5: Mainstream timing drive systems for passenger car applications: **left**: Chain drive concept **right**: Toothed belt drive concept

***Piston group*:**

The piston group friction and wear originate mainly from the sliding of the reciprocating moving piston and piston rings in the cylinder liner. The main surfaces in contact with the liner are the piston skirt and land as well as the piston ring surface. In addition, the piston pin is supported in the pin bore bearing also contributing to the friction losses. It is understood that these contacts represent the areas in an ICE where the highest friction losses of all engine components occur [10]. Figure 2.6 shows an example of the piston group system used conventionally in passenger car applications.

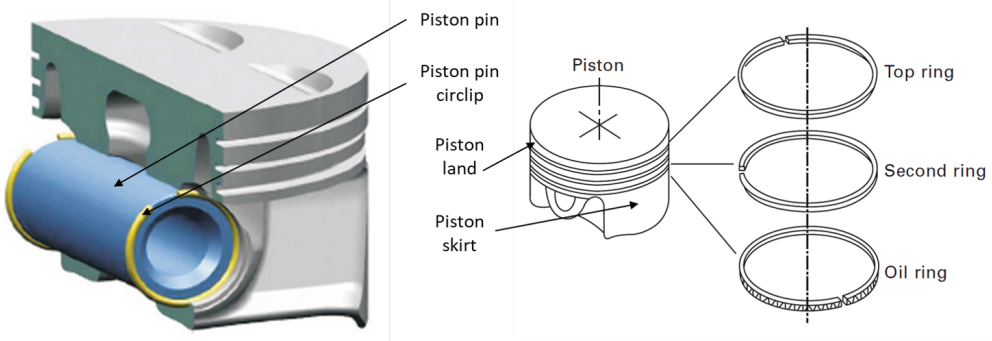

Figure 2.6: Main components of the piston group system (reprinted from: left [54], right [21])

The piston group for a modern passenger car consists of the piston, three piston rings (two compression rings and one oil ring), the piston pin and the piston pin circlips. While the piston skirt and the piston land carry the side load the piston rings seal the combustion chamber from the crankcase and control the lubricant film between the ring surface and the liner surface.

The top and second ring seal the combustion chamber to prevent blow by and keep the pressure in the combustion chamber to produce work at the piston. In addition, the piston rings have to maintain sufficient lubricant at the liner surface for proper lubricating the contacts thus minimizing friction and wear. Nevertheless, oil consumption needs to

be maintained at acceptable low levels at the same time. Furthermore, the piston rings are needed for the heat transfer to the coolant and liner surface to control the piston temperature. The piston ring and groove design complement each other e.g. to realize that the combustion gases can act also on the inner ring face to increase the radial load for increased sealing function.

During the installation of the piston rings, the rings are compressed and installed together with the piston conrod assembly into the cylinder. The in radial direction compressed rings result in a ring tension, which presses the ring's outer surface against the liner. This elastic tension and also the load and speed dependent gas pressure contributes to the ring friction. The compression rings are working in different lubrication regimes during one piston stroke. At the higher piston speed area after the top and bottom dead center, the ring face is designed to realize hydrodynamic lubrication. At the end of the stroke where the piston speed is low and even zero at the turning point, mixed and boundary friction is present. To control the oil film at the liner, the oil control ring has higher ring tension than the compression rings. Subsequently, the oil ring is working mainly in the mixed and boundary lubrication regime.

The piston skirt friction contribution comes mainly from hydrodynamic lubrication due to the fact that the large contact area between skirt and liner results in decreased loading in comparison to the piston ring contact area. To reduce the side thrust of the piston skirt, it is the aim to reduce the piston mass and use the opportunities of piston pin offset. Care needs to be taken to find an acceptable compromise between piston skirt friction loss reduction and noise emissions. Both effects are influenced contrarily using pin offsets.

2.1.2 Lubrication regimes

At the journal bearing joints, two surfaces are interacting which are in relative motion, e.g. crankshaft main bearing pin and main bearing shell or piston skirt/ring and liner. For this self-pressure generating lubricated contacts, four different forms of lubrication can be identified following [78]:

Hydrodynamic or full film lubrication: The two contacting surfaces are separated completely due to the sufficient high pressure in the lubricant. No metal-metal contact occurs. The friction force will come from shearing of the lubricant. As an example, in the crankshaft/bearing shell contact, the relative motion of the crankshaft pin creates the pressure in the lubricant.

Elasto-hydrodynamic lubrication: The surfaces are separated from each other. But the load is large enough in the hydrodynamic action to cause elastic deformation of the surfaces influencing the lubrication.

Mixed lubrication: In this lubrication regime, the fluid film pressure is not high enough, e.g. due to high load, low speed or reduced oil viscosity. Consequently, the fluid film is not separating the surfaces in complete manner anymore. Some of the surface asperities of the interacting surfaces begin to contact each other. But part of the bearing load is still supported by the fluid pressure.

Boundary lubrication: The interacting surfaces are not separated by the lubricant film and there is dominant asperity contact holding the load. The friction force is mainly caused by shearing surface films. Here the lubricant additive package (e.g. adsorbed molecules of friction modifiers) can have major influence on friction and wear.

In this work, investigations are carried out to increase the knowledge of when and where the different lubrication regimes dominate for the base engine sub-assembly systems. This knowledge can be used to reduce the friction losses aiming for fuel consumption improvements or determination of wear spots targeting engine lifetime increase.

The operation of a lubricated contact working in different lubrication regimes can be described by the Stribeck curve (see figure 2.7).

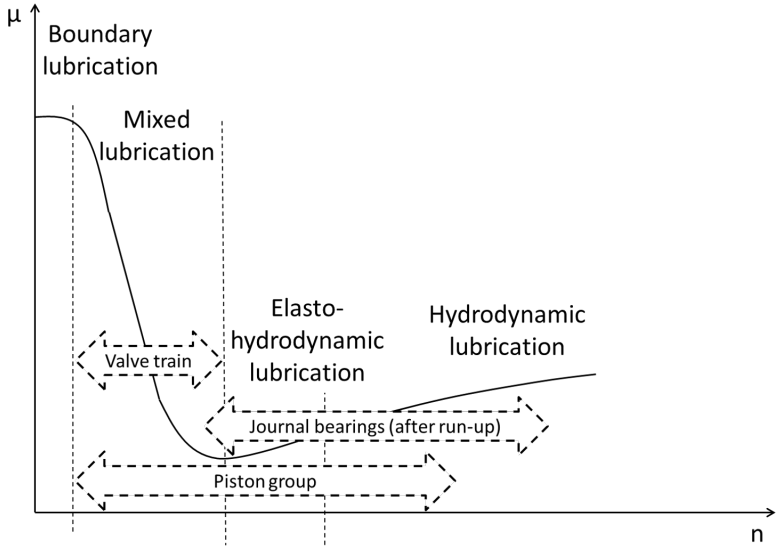

Figure 2.7: Description of the journal bearing lubrication regimes (Stribeck curve)

The highest friction coefficient (μ) occurs at the boundary lubrication regime. μ decreases strongly in the mixed lubrication regime when the shaft speed increases. Here one part of the surfaces is in direct contact the other is lubricated. Running the engine at the lowest friction coefficient, an operation near the bottom of the Stribeck curve is desired without affecting the engine's lifetime (no increased asperity contact). The shaft speed at the lowest value of μ is called detaching speed. At shaft speed higher than the detaching speed, full film lubrication starts and the surfaces are separated by the lubricant film. At higher shaft speeds, the resistance due to shearing the lubricant increases, resulting in increasing values of μ when the shaft speed is increasing.

2.1.3 Lubricant: Requirements and composition

In this work, the focus is on combustion engines for passenger car applications and therefore in this subsection, a brief overview of passenger car engine oils is given. Many engine development steps were and still are only possible today in combination with suitable further development of the lubricant. In the following, the main parameters of the lubricants are described. The information presented is based on the literature sources of [12], [2], [102], [39].

The role of a lubricant is a multifunctional one, especially in an ICE. The main requirements of engine oils are to reduce friction and wear, ensure proper heat transport away from the contact, carry away wear particles, prevent rust and corrosion, keep stability when getting in contact with water and combustion residues (e.g. acids, particulate, sludge) and have a good compatibility for different materials (e.g. metals and gasket

materials).

The areas of lubrication in an ICE cover all lubrication regimes (see figure 2.7) and specific challenges arise for the engine oil. For bearings, mostly elasto- and full hydrodynamic lubrication is expected, while for the valve train system boundary/mixed lubrication regime is anticipated. At the piston group system the situation is most complex. At the piston skirt, hydrodynamic lubrication is expected at the mid stroke region where high velocities are reached. At the lower speed regions and the dead centers on top and bottom of the stroke, mixed/boundary lubrication is present. For the piston rings, especially the oil control ring is expected to run in boundary/mixed lubrication regime due to the necessary ring pretension. For the top and second ring, the lubrication regime is expected to be equivalent to that of the piston skirt.

Additionally, the engine oil has a broad operation range and must cover operation in low and high ambient temperatures affecting the oil viscosity in great manner. Control of wear at engine systems and components where the engine start up can take considerable time is of great importance. Future aspects regarding thinner oils, longer service periods (oil drain intervals), higher loads and increased temperatures e.g. due to downsizing have to be handled to protect the component surfaces. The critical areas and issues related to friction and wear in an ICE are shown in figure 2.8.

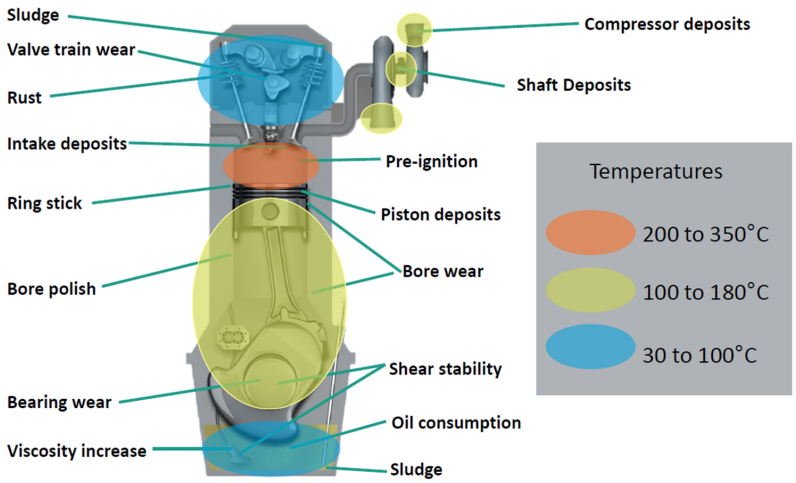

Figure 2.8: Critical areas and issues of friction and wear in ICE [39]

New engine operation strategies like advanced start/stop functions, cylinder deactivation (dynamic skip fire), engine downsizing and the usage of ultra-low viscosity lubricants put additional stress on the composition work. In order to meet the broad range of requirements, the lubricants are formulated using a base oil (mineral, synthetic or mixture base stock), viscosity modifiers and additive package. A typical share between base oil, viscosity modifier and additive package is shown in figure 2.9.

The base oil consists of the base stock components, which are molecule mixtures usable for lubricant production, primarily hydrocarbons. The mineral oil base stocks are refined from crude oil or by the use of processes like synthesis, conversion (hydrocracking) or separation (solvent extraction). Other base stock types are for example esters or polyalkylene glycol. Poly glycols have shown good friction performances in recent engine tests. [79] The base stock composition has a large effect on the lubrication properties like viscosity, oxidation, dispersancy and solvency, foaming and air entrainment, volatility

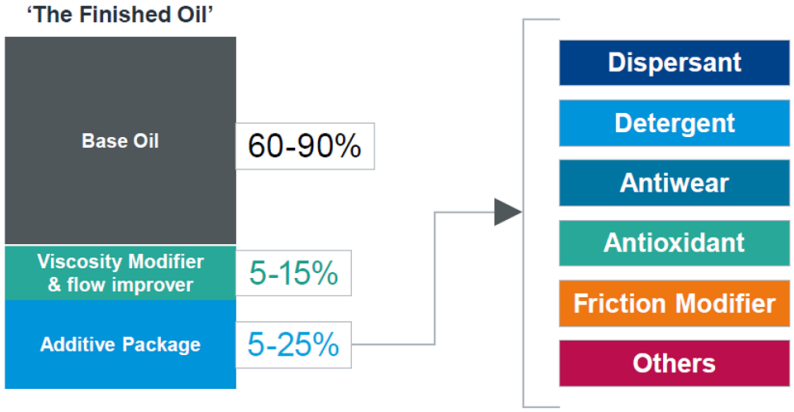

Figure 2.9: Composition and division of an engine oil [39]

(evaporation) and are of key importance.

The base oil composition is mainly responsible for the lubricant physical properties but cannot carry all lubricant requirements alone. As the base oil viscosity has a strong temperature dependence (viscosity is decreasing strongly when temperature is increasing) a standard was established to evaluate this behaviour called viscosity index (VI). To ensure a high viscosity index to reduce the influence of temperature on the viscosity, so called viscosity modifiers (viscosity index improvers) are added to the base oil. This enables efficiency benefits and better pumpability of the lubricant at low temperatures and prevents excessively thin oil films at higher temperatures. In simple terms, viscosity modifiers are polymer coils with high molecular masses solved in the base oil. Care needs to be taken when selecting the viscosity modifiers to maintain sufficient shear stability of the polymer molecules. When high shear stresses are applied, the polymer coils in the oil solution are stressed and aligned resulting in reversible and non-reversible (polymer coil break down) deformations. The alignment causes a shear thinning effect of the lubricant which can be temporary or permanent in case of non-reversible deformations. The non-Newtonian behaviour of modern low viscosity multi-grade engine oils can be attributed to the shear thinning behaviour of the composition of base oils and viscosity modifiers.

The base oil in combination with the viscosity index improvers are the starting base for low viscosity lubricants to maximize fuel economy. In addition, a proper additive package is necessary to improve the ability to protect the engine from wear, lubricant oxidation and destructive effects of deposits, sludge and corrosion. The following common additives are used in modern additive packages for engine lubricants:

Dispersant:

The function of dispersants is to mitigate the destructive effects of sludge, suspend soot and reduce the formation of deposits. Dispersants are metal based surfactants consisting of a small (low strength) polar head and a long non-polar tail.

Detergent:

Detergents are responsible to neutralize acid species and deposits. The structure of the ashless (metal free) surfactants is consisting of a strong polar head and a short non-polar tail.

Antiwear:

Antiwear agents like zinc dialkyldithiophosphates (ZDDP) or molybdenum dithiocarbamates (MoDTC) are added to reduce friction and metal-metal wear forming tribofilms. Using ZDDP, a polyphosphate film is formed at increased metal-metal contact due to prevailing high temperature and pressure. The phosphate film liquefies at the contact point at high temperature and is sacrificially lost to protect the metal surface. At hydrodynamic lubrication and no metal-to-metal contact, the phosphate layers would not be formed but would remain if they were formed beforehand.

Antioxidant:

Antioxidants are incorporated during oil composition to reduce and control oil oxidation and reduce the consequences like viscosity increase, formation of organic acids which attack engine surfaces, formation of deposits and sludge due to insolubles and additive depletion. They can be devided into primary and secondary antioxidants. ZDDP and MoDTC belong to the second category.

Friction Modifier:

The function of friction modifiers in engine oils is to reduce friction and wear in the mixed and boundary lubrication regimes. This is realized by providing a low shear surface forming a low friction coefficient layer. The surface-active additives can be categorized into organic and solid (chemical reactive) friction modifiers. The organic friction modifiers (e.g. glycerol mono-oleate (GMO)) are long chain hydrocarbon molecules with polar heads. They are not chemically transformed at the surface and anchor to the metal surface. The chemical reactive friction modifiers create an elastic tribofilm after a chemical transformation at the surface.

Others:

There are several other additives added to specific engine oil formulations having less impact on providing friction reduction and preventing wear, which is the focus of this study. Foam inhibitors, rust inhibitors, demulsifiers, seal compatibility agents, or extreme pressure additives are other examples for additional oil additives.

There are many organizations involved in the lubricant industry like oil companies, producers of additives, OEMs and test laboratories. Industry standards are established to define needs, parameters, licensing and administration of lubricant specifications. Therefore, national bodies, international associations and industry groupings represent their interest. Important organisations classifying the engine performance are ACEA (European Automobile Manufacturers Association), API (American Petroleum Institute), JASO (Japanese Automotive Standards Organization), ILSAC (International Lubricant Standardisation and Approval Committee) and the OEMs (e.g. Daimler, BMW, Volkswagen, General Motors, Ford etc.). While industry standards focus primarily on a minimum quality level for lubricants, OEM lubricant specifications put focus on OEM internal oil specifications for first and service fill applications (proper product performance) to satisfy OEM warranties. Aspects such as cleanliness of the engine (e.g. prevention of deposits, corrosion) and of the exhaust after treatment system (e.g. clogging of the particulate filters) play an important role. Additionally, OEM specifications continuously include the minimisation of fuel consumption, leading to ever lower viscosity oils reducing the hydrodynamic friction. These distinctive requirements and specifications subsequently affect the lubricant minimum quality level standards and make it necessary to introduce new higher performance base stocks e.g. replacement of API Group III with III+/IV/V base stocks [26]. Today, the SAEJ300 viscosity classification is used by all engine OEMs.

Currently the OEM recommended viscosity is lowered from 0W-16 to 0W-12 and 0W-8 to reach the fuel consumption and emission targets. Besides the low temperature and kinematic target values the high temperature high shear viscosity (HTHS-V) is an essential and characteristic parameter. The HTHS-V describes the measured viscosity of a heated and sheared engine oil at 150 °C and a shear rate of $10^6\ s^{-1}$.

The lubricant used in this work is a modern SAE 5W30 multi grade automotive lubricant. It is important to note that the lubricant is suitable for all engines investigated and is the only lubricant used during the investigations in this work to eliminate the effects of different engine oil formulations. The main rheological properties as well as the calculated dependencies of the viscosity on temperature, pressure and shear rate are presented in section 4.1.2.

2.1.4 Engineering surface and contact of rough surfaces

When describing surfaces which are in tribological contact, a simple description having length and breadth is not sufficient. The consideration of the surface thickness including the description of the significant depth of the surfaces is necessary. Therefore, the surface of a component can be the physical boundary of the component and the topography is the description (physical, chemical and functional). The top layer of an engineering surface can be significantly different from the underneath base material, having depths in the range of a few nanometers to micrometers.

During the manufacturing processes of engine components, characteristic marks are left behind referred to as surface topography or surface texture. This surface texture is measured using a special measurement instrument, the so called profilometer. The profilometer uses different measurement techniques to determine the surface topography characteristics like stylus measurements or laser reflection methods. The surface topography features, which are described by the profilometer measurement results, can be listed according to figure 2.10.

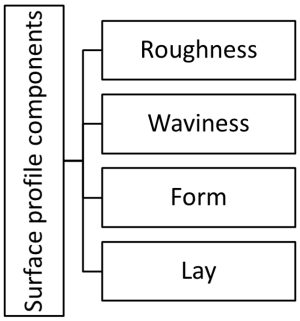

Figure 2.10: Components of a surface profile

The roughness plays an important role as component of the surface texture describing the closely spaced irregularities e.g. by cutting tool marks. The description of the surface roughness is done by digitisation of the surface profiles by measurement of the surface height at equal intervals and calculation of the mean surface height of the measurements to define a center line. Two values are then conventionally used which are describing the surface roughness depending on the distance from the central line Ra (roughness average) and Rq (root mean square deviation).

Waviness is referred to the texture component of the surface where the roughness is

superimposed (widely spaced irregularities e.g. tool vibration). The general shape of the components' surface, neglecting roughness and waviness variations is referred to as form (e.g. deviations by the ideal form due to inaccurate machine). The direction of the predominant surface finish pattern (determined usually by the machining method) is referred to as lay.

Contact of rough surfaces: When two surfaces get in contact, they first touch at the peaks of the highest asperities. The real contact area is the sum of the local asperity contacts and is very small in comparison to the overall component area in contact. Because the real area is small, the contact stresses are high and depend on the elastic and plastic properties of the contacts, the surface roughness and the asperity shapes. The elastic properties are conventionally described by the elastic modulus and Poison's ratio of the contacting materials. The plastic properties are normally described by the contacting material hardness (usually the magnitude of the indentation hardness is used).

At the contact area between two surfaces, the touching asperity peaks will be fully elastically, fully plastically and combined elastically/plastically deformed. A relation between the amount of elastic and plastic deformation under normal load is given by the *plasticity index* ψ [33]. Due to running-in of engine components, surfaces can change their initial characteristics because of occurring wear processes (e.g. smoothing and hardening of surfaces). Subsequently the plasticity index can change during the running-in phase and surface contacts can become almost entirely elastic resulting in very little wear.

2.1.5 Friction

The general term friction is a force of resistance to motion, both as a resistance against the initiation of a relative movement (static friction) or its maintaining (dynamic friction). The relation between the friction force F_f and normal force F_n is given by the coefficient of friction μ

$$\mu = \frac{F_f}{F_n} \tag{2.1}$$

Friction is subsequently a loss of energy, which is often low in today's ICE applications. Nevertheless, in the recent past and in the future economic needs to lower the ICE friction losses gain importance. Even if the fuel savings for a single vehicle seem relatively small, it is of immense magnitude for a global view. [35]

Dry contact friction will lead to malfunction of journal bearing systems, excessive wear and component damage. Therefore, lubricants are used to reduce friction. Different types of friction exist, characterised on the relative motion of the surfaces in contact.

Sliding friction is present during a sliding movement tangential to the contacting surfaces (e.g. journal bearings). One speaks of pure rolling friction when one body rolls on the other where the axis of rotation is parallel to the contact surface, and its direction of movement is perpendicular to the axis of rotation. In ball bearings or roller bearings, besides rolling also slip or micro-slip motion is occurring in the contact area. Here rolling friction and sliding friction exist in parallel.

As presented earlier in section 2.1.2, four different lubrication regimes are present during ICE operation. The friction losses in ICE lubricated contacts arise from the interaction between asperities of the surfaces in contact (boundary or asperity friction losses) and the "inner" friction generated by shearing of the lubricant (hydrodynamic friction losses). The transition between boundary lubrication and full hydrodynamic lubrication is the

mixed lubrication regime, where both, asperity and hydrodynamic friction losses are generated together.

Hydrodynamic friction

The friction in the hydrodynamic lubrication regime results from the shear stresses acting on the shaft. The viscosity of the lubricant is the parameter which describes the resistance of relative motion in the hydrodynamic lubrication regime. The general equation describing the resistance of the fluid (lubricant) is known as Newton's law of viscosity:

$$\tau = \eta \cdot \dot{\gamma}, \tag{2.2}$$

where the shear stress $\tau = \frac{F}{A}$, η is the dynamic viscosity of the lubricant in $\frac{(N \cdot s)}{m^2}$ and the velocity gradient $\dot{\gamma} = \frac{du}{dt}$. Equation 2.2 can be written in a different form to describe the force necessary to overcome the internal friction of the fluid (F). An exemplary description for a fluid film between two parallel plates results in

$$F = \eta \cdot A \cdot \frac{u}{h} \tag{2.3}$$

where A is the area of the plate, u is the velocity normal to the film height and h is the fluid film thickness.

Boundary friction

In the boundary friction regime, the lubricant base material has small impact on friction because the oil film height is smaller than the surface roughness. Here the friction force is dominated by the interactions between the asperities of the component surfaces or other elements involved such as hard contaminants and wear debris. In this lubrication regime, the designed lubricant additive package (friction modifier) generates tribo-films at the surfaces to prevent direct asperity contact where the loads are not too high. If the stresses are too high, direct asperity contact will occur.

The main friction mechanisms are adhesion, elastic and plastic deformations (slip mechanism) where plastic deformation and adhesion result in surface damage or wear. According to [91], elastic and plastic deformations dominate in boundary lubricated contacts and surface adhesion is prevented by tribo-films generated by the lubricant additive package. This mechanism results in moderate levels of friction coefficients. The wear mechanism is provided mainly by surface ploughing (grooving), micro-cutting and micro-fracture.

2.1.6 Wear and wear mechanisms

Wear is a consequence of tribological stresses, whereby progressive loss of material from the surface occurs. It results from direct contact of the individual asperities at the sliding interfaces. Archard formulated the well-known law of wear [9]

$$V = K \cdot I \cdot A_r = K \cdot I \cdot \frac{W}{H} \tag{2.4}$$

where the wear volume V is proportional to the real contact area A_r, a proportional wear coefficient (Archard coefficient) K and the sliding distance I. A_r can be written as the contact load divided by the Vickers hardness of the softer surface. Concerning wear between surfaces of solids from [91] there are major wear mechanisms known, which are summarized here for brevity:

Abrasive wear

Abrasive wear by particles (three-body abrasion) occurs usually due to embedding of a hard contaminant in one of the surfaces. The contaminant (particle, dirt or wear debris) is squeezed between the contacting surfaces which are in relative motion. If the particle is larger than the oil film thickness, it damages the surface. Damage to the surface is caused, for example, by cutting, ploughing and gouging. Mild abrasion by small particles can cause polishing of the surfaces.

In lubricated contacts, this can be prevented by lubricant filtration and by appropriate absorption and removal of wear particles from the interface by the lubricant. When a contaminant is not directly involved during abrasive wear and the metal asperities cut directly into the interacting surfaces, this is called two-body abrasion. When using low viscosity lubricants and subsequent reduction of the oil film thickness in today's ICE systems, special care needs to be taken to minimize surface roughness and using a proper lubricant additive package.

Adhesive wear

Adhesive wear occurs when the asperities of the contacting surfaces are bonded due to high loads, temperatures or pressures e.g. by spot-welding. Immediately after bonding the spot-welds are torn apart, shearing the material and transferring material from one surface to the other. As a result, the surface is damaged causing roughening and jagging. Conventional engine running-in is a form of mild adhesive wear. To prevent damage by adhesive wear in ICE systems, a proper layout of bearing loads (lower loading, no shock loading) in combination with the right choice of lubricant viscosity and additive package is necessary. Due to downsizing engines and subsequently higher loaded engine components, the lubricant additive package (e.g. extreme pressure and anti-wear additives) is an increasingly important component. The lubricant is then able to reduce or eliminate adhesion by providing low shear strength films between the surfaces.

Erosive wear

Erosive wear can be described as wear and subsequent material loss due to the interaction of the moving lubricant which often contains solid particles. It can be considered as a form of abrasive wear, where the impact of particles against the solid surface causes damage. Several wear mechanisms are involved in the term erosive wear, depending on the particle size, impact speed and angle of impingement. If not controlled, also the lubricant can cause as much damage as solid particles in the matter of erosive wear if the impact velocities are high enough (e.g. water jet cutting).

Fatigue wear

Cyclic mechanical stresses can cause components' fatigue wear. At non-conformal contacts like gears or roller bearings which operate in the EHD lubrication regime, the macroscopic fatigue wear is important. The microscopic fatigue wear is important at sliding asperity contacts. The form of initiated fatigue wear during sliding can be differentiated into surface and sub-surface fatigue mechanisms. In lubricated rolling contacts, the wear level is usually very low. Nevertheless, the bearing life is limited by fatigue. When the first wear fragments are produced (typically at impurity particles in the material structure), bearing lifetime ends. In sliding contacts, sub-surface deformations can lead to fatigue after the accumulation of many load cycles, even if asperity deformation is elastic. The mechanics of crack initiation, crack growth and fracture are determining the fatigue wear.

Corrosive wear

Corrosive wear is described by the loss of material caused by chemical/electrochemical reaction at the contact interface. Any form of mechanical wear (adhesive, abrasive, erosive, fatigue etc.) is related to corrosive wear in combination with a corrosive process. The corrosive process can be described as chemical reaction between the surface material and a corroding medium (chemical reagent, reactive lubricant, air) occurring due to mechanical and thermal stresses. In the ICE, degradation of engine oil is often the reason for corrosion when the additives (corrosion inhibitors) deplete. Then the additive package can no longer protect the metallic surfaces from corrosive fluids. The lubricant can become an increasingly acidic corrosive fluid when contaminated by moisture, unburned fuel and combustion gases or cooling fluid. Careful replacement of the engine oil helps to maintain the functionality of the additive package and avoid corrosive wear.

Running-in (break-in)

In the initial phase of the operation of a machinery or ICE an adjustment process takes place, when two surfaces in contact operate together for the first time. This running-in phase (also called break-in) is characterised by the altering of the original surface topography and the wear rate decreases until reaching a moderate long-term steady state value. The running-in process has been modelled as surface smoothing and is occurring by the removal of asperity peaks, which facilitates hydrodynamic lubrication [91]. It is reported from surface roughness measurements in [7] that the mean asperity heights at journal bearing shell edges (where the running-in occurs) is reduced from initially 0.4 μm to about 0.2 μm during the running-in phase. In addition, tribofilms are generated as surface layer in that early engine operation phase when the lubricant additive package is activated and reacting with the component surface for the first time. The formation of this layer is issued to a reduction of both friction and wear. In ICE, the valve train system and piston group system are mainly affected by running-in processes, which was investigated also in the work of this thesis [42]. The crankshaft journal bearings also underlay a running-in process which is of smaller magnitude [7] compared to the valve train and piston assembly in [42].

Chapter 3

Methodology of the investigation - Combining testing and simulation

For the investigation of the ICE friction losses, methodologies are necessary which can accurately break down the individual losses occurring at the lubricated contacts of the engine system. Today, measures to decrease the engine friction losses can be summarized in mechanical component design (macro and micro geometry), usage of low viscosity lubricants to minimize the hydrodynamic friction losses and the application of coating and surface finish techniques.

As the friction performance of ICE has made great progress in recent years methods are necessary which provide very stable boundary conditions and high measurement accuracy. These stable boundary conditions are vital to investigate even small differences in the friction loss shares resulting from friction loss and lubrication improvement measures. It is a challenging but with today's modern measurement technology feasible activity to recognize this part optimizations during component and system tests.

At the engine level, it is nowadays a common method to investigate the engine total friction losses using the indication method (IMEP-method). Here, the amount of work done by the engine per cycle is determined by the variation in combustion chamber volume, the cylinder pressure and the piston swept volume at a given time. At the same time, the BMEP is calculated by measurement of the resulting torque at the crankshaft for the same given time. The difference between the determined values of IMEP and BMEP results from the frictional losses of the engine systems and components, named FMEP.

Nevertheless, it is not usual to break down the individual friction shares of the engine sub-assemblies under load conditions. A friction breakdown under load conditions enables to assign the friction losses to the individual components under real dynamic conditions. Subsequently, a deeper understanding of the frictional performance is gained. With the exception of research test benches, the friction breakdown of the engine systems is normally done using the strip-down methodology. Here a step-by-step disassembly procedure is used to collect the individual friction shares of the components by subtraction of the results at the different stages. The main disadvantage of this approach is the missing component load both resulting from mechanical and thermal stresses.

Therefore, a methodology has been developed in the recent past where measurement results at the engine level are merged with predictive journal bearing simulation results

to enable sub-assembly resolved investigations. Figure 3.1 presents an overview of the methodology used to investigate the ICE friction losses.

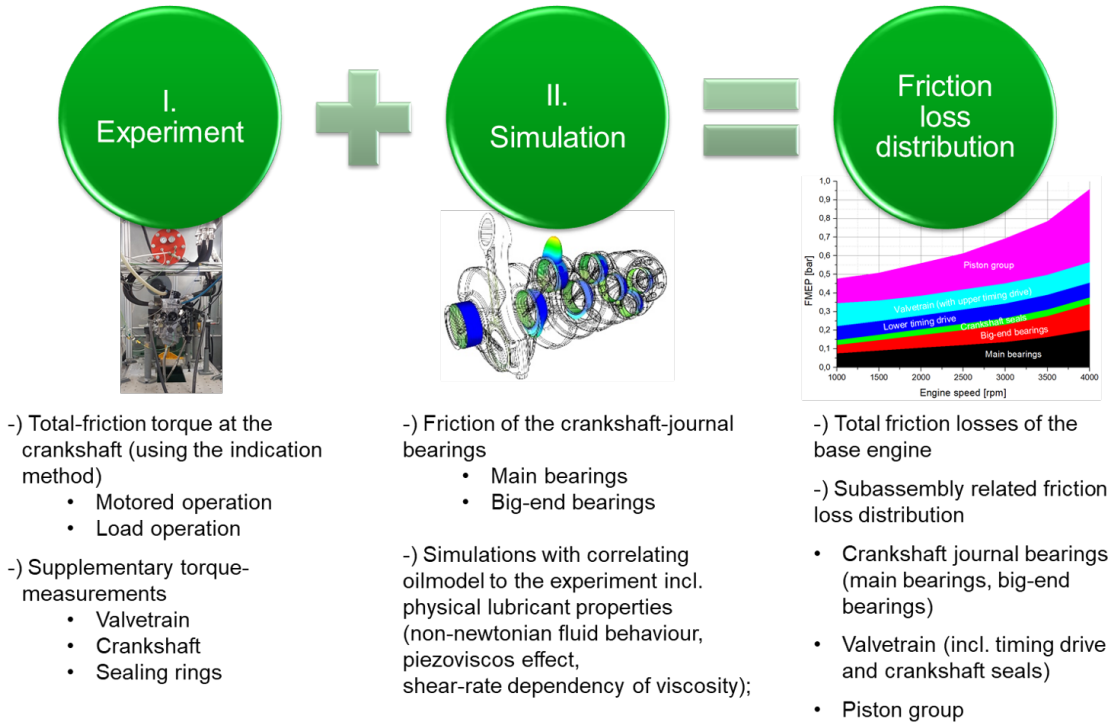

Figure 3.1: Overview of friction analysis methodology used to investigate the ICE friction losses

The base engine total friction losses are determined in the experimental part applying the indication method. In parallel, the journal bearing friction losses of the crankshaft's main and big end bearings are calculated using EHD-simulation techniques. For the simulation work, temperature and cylinder pressure measurement results are used besides a comprehensive description of the engine oil in the oil model to represent realistic boundary conditions.

A detailed process for investigating the ICE friction losses using the combined methodology has been developed for a uniform and comparable execution of the investigations, as is illustrated in figure 3.2.

In this thesis, three different engine concepts are investigated regarding their base engine friction power losses. It was the aim to gather a more detailed understanding of how the actual engine concept affects the friction losses. In this context, the term engine concept means that both the fuel used (diesel/gasoline) and the power density of the ICE (conventional/downsized concept) have profound influences. Table 3.1 lists the technical data of the engines under test.

The diesel engine and gasoline engine 1 represent conventional engine concepts with almost the same specific power output. Gasoline engine 2 is designed as a high-power downsized engine concept and has the doubled power density in comparison to the conventional concepts. Figure 3.3 shows the engines under test mounted and configured for the tests at the friction dynamometer test-rig.

In the following sections of this chapter, the single parts experiment and simulation of the applied methodology used for this study are described.

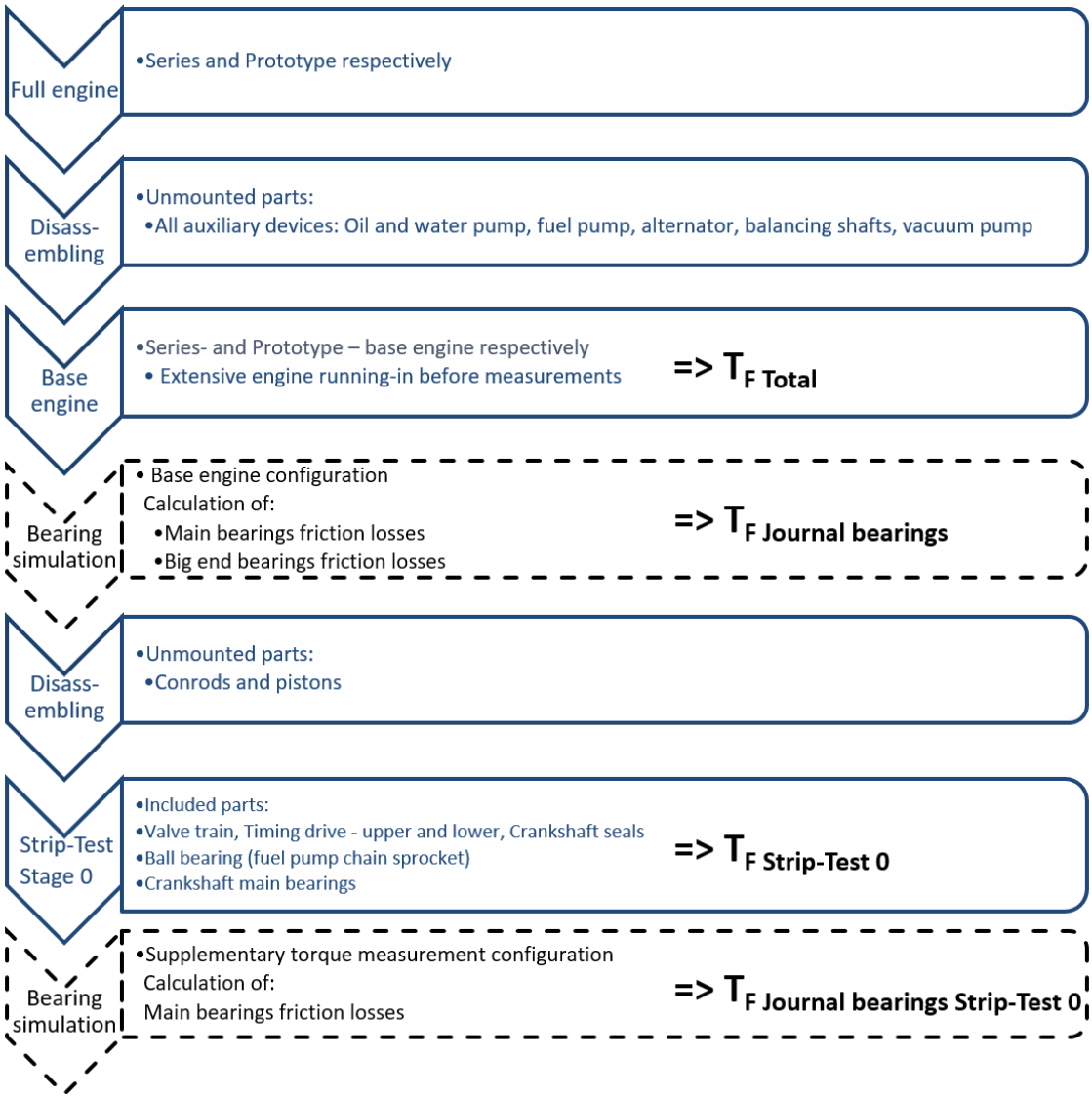

Figure 3.2: Process overview and process steps of the applied method (from the analysis of the diesel engine investigated in this work)

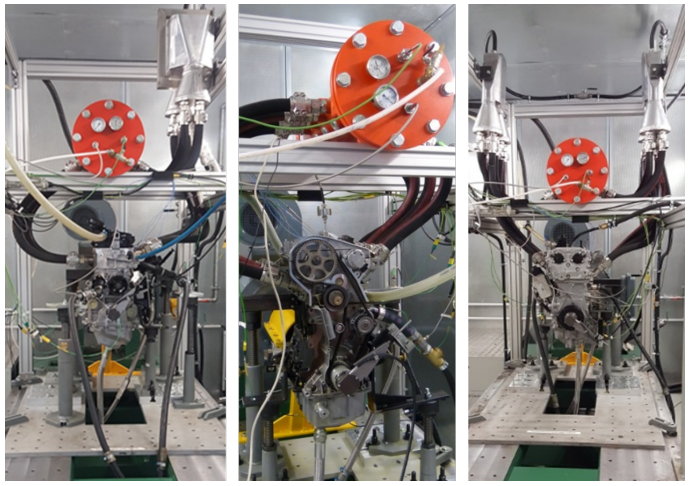

Figure 3.3: Overview of engines under test mounted at the friction dynamometer test-rig

Table 3.1: Technical data of the engines under test.

Parameter	Diesel Engine	Gasoline Engine 1	Gasoline Engine 2
Volume displacement	1995 cm^3	1781 cm^3	1991 cm^3
Compression ratio	16.5:1	9.5:1	8.6:1
Bore	84 mm	81 mm	83 mm
Stroke	90 mm	86.4 mm	92 mm
Nominal torque	380 Nm	235 Nm	422 Nm
Nominal Power	135 kW	130 kW	265 kW
Specific power	68 kW/L	73 kW/L	133 kW/L
Maximum Speed	4600 rpm	6600 rpm	6700 rpm
Cylinder distance	91 mm	88 mm	90 mm
Conrod length	138 mm	144 mm	138.7 mm
Main bearing diameter	55 mm	54 mm	55 mm
Main bearing width	25 mm	22 mm	19 mm
Main bearing clearance	20 µm	20 µm	20 µm
Big-End bearing diameter	50 mm	47.8 mm	48 mm
Big-End bearing width	24 mm	25 mm	19.4 mm
Valve-train	DOHC	DOHC	DOHC
Timing drive	chain	belt	chain
Valve-train type	roller-type cam follower	flat-base tappet	roller-type cam follower
Valves	4 per cylinder	5 per cylinder	4 per cylinder
Connecting rod ratio	0.326	0.3	0.332

3.1 Experiment: Engine friction test-rig

At the developed and established friction test-rig (referred to as "test-rig" hereafter), friction power loss measurements for common engine operating conditions up to 200 bar peak cylinder pressure (externally charged) and engine speeds up to 10.000 rpm are realized. During the test-rig measurements using the externally charged motoring technique, the IMEP-method is used to determine the engine friction losses. Here, the friction losses denoted as FMEP are determined by subtracting two similar sized quantities, the IMEP and the BMEP

$$FMEP = IMEP - BMEP \tag{3.1}$$

where the signs of IMEP and BMEP are negative for motored engine operation. The FMEP is a rather small quantity, therefore care needs to be taken when determining the IMEP and BMEP. Any significant error in the large quantities of IMEP and BMEP can easily lead to a measurement error of the same magnitude as the calculated FMEP.

The measured cylinder pressure data during the motored engine operation is used to calculate the pumping work distributed from the piston to the gas. This is expressed as indicated mean effective pressure (IMEP)

$$IMEP = \frac{\int p_{cyl} dV}{V_D}, \tag{3.2}$$

calculated by integrating the measured cylinder pressure ($pcyl$) over a working cycle divided by the volume displacement (V_D) of the engine. The measured total torque at the crankshaft to motor the engine (T) is related to the corresponding mean effective pressure:

$$BMEP = \frac{W}{V_D} = \frac{4\pi T}{V_D}, \tag{3.3}$$

where W refers to the work per cycle and V_D to the volume displacement of the engine under test. It is of key importance when using the IMEP-method to determine the quantities of IMEP and BMEP with great care to minimize measurement errors. Therefore, an AVL industry grade indication system is used to measure the cylinder pressure. The crank angle resolved referencing to the piston TDC is conducted with state-of-the-art measuring devices. In addition, the crankshaft torque is measured with a high accuracy torque transducer. A more detailed description is given in chapter 3.1.2 and the main components used are listed in table 3.3.

The following list summarizes the main goals of the test-rig measurements and figure 3.4 gives a schematic of the test-rig set-up.

- Enable early-stage friction measurements in the engine development process where systems for firing the engine are not yet available
- Enable measurements with reduced complexity and minimized costs
- Specific focus on the base engine configuration without auxiliaries
- Conduct friction measurements at more realistic component loads by operating the engine at conventional levels of engine speed and peak cylinder pressures
- Increase the temperature level for the piston assembly for partial temperature level compensation at the components due to the missing combustion
- Accurate determination of the IMEP and BMEP (for subsequent FMEP calculation) using high performance measurement equipment for cylinder pressure and torque measurements and piston TDC determination
- Reach very stable measurement boundary conditions for engine speed, cylinder pressure cyclic variations, engine media supply temperatures and pressures while operating the engine under high loads
- Enable accurate comparison of measurement results e.g. for evaluation of engine friction improvement measures
- Providing necessary data for the journal bearing simulation by means of cylinder pressure (bearing load) and main bearing temperatures (calculation of lubricant viscosity in the lubricated contacts)

The test-rig measurement hardware used to realize the specific goals of the test-rig measurements are described hereafter:

The test-rig is designed to conduct friction measurements for all kinds of ICE for passenger car applications and medium sized truck engines. The test-rig consists of a steel frame on which a dynamometer and the engine under test (EUT) can be flexibly mounted. During the tests, the EUT is operated in motored condition by the electric motor driven by a variable frequency drive. Directly at the dynamometer flange to drive shaft interface, the total friction torque is measured using a torque meter.

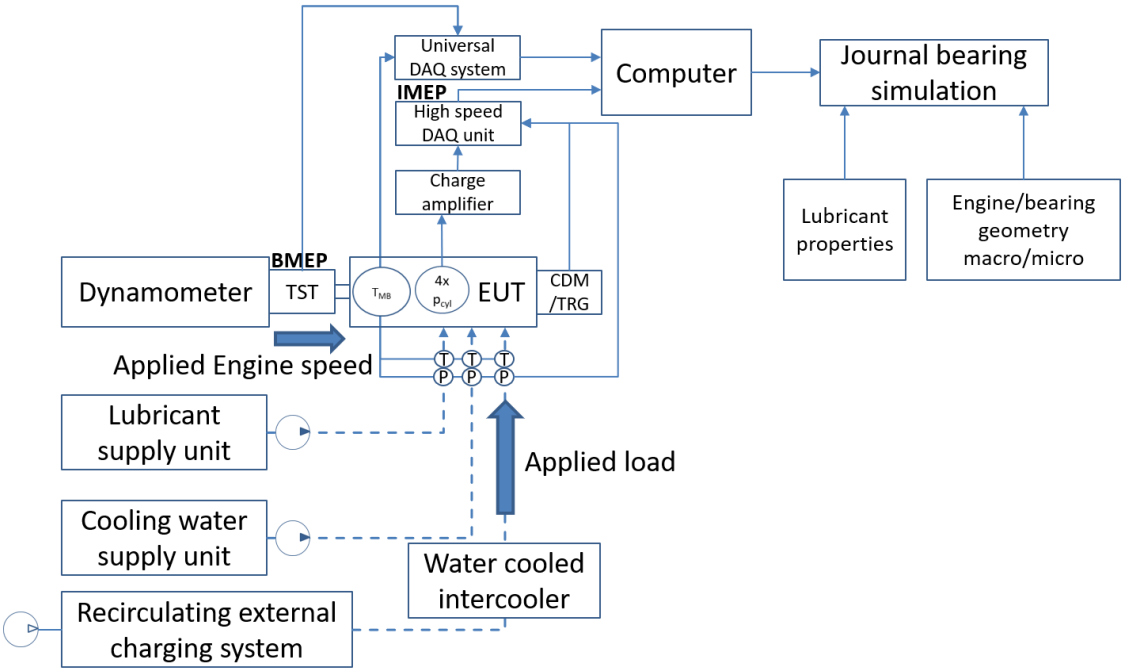

Figure 3.4: A schematic of the friction dynamometer test-rig

External engine media supply units enable test configurations without the auxiliary components oil and water pump, which are conventionally driven by the crankshaft. This enables to exclude the frictional torque shares of the pump systems. The heating and cooling function of the external supply units enables stable supply and thermal boundary conditions from low to high media temperatures and pressures. Load can be applied to the EUT via a recirculating external charging system supplying pressurized air to the engine inlet. The air is externally compressed, finely filtered and supplied to the EUT. The inlet pressure is controlled and variably adjusted using an externally controlled pressure control valve.

Connecting the engine outlet to the engine inlet enables to raise the inlet temperature significantly, especially at high engine speeds with correspondingly large air flow rates and short time for heat flux processes. To limit the maximum inlet temperature, a water-cooled intercooler system including a oil separation device in the air path is installed into the recirculation system. The limitation is necessary to prevent damage of the EUT and test-rig components due to possible self-ignition of the air and oil mist mixture. Inlet temperatures are limited to a maximum of 220 °C. Temperature sensors and pressure transducers are mounted at the EUT and peripheral test-rig systems for the regulation, control and monitoring of the tests. A comprehensive description is given in the following section 3.1.2 and table 3.3 lists the measurement equipment used at the test-rig.

3.1.1 Lubricant

In this work, one identical lubricant suitable for all engines put to test is used to neglect influences from different chemical composition e.g. additive package. Therefore, all investigations were carried out using a modern SAE 5W30 automotive lubricant. The physical properties are listed in table 3.2.

Table 3.2: Basic rheological properties of the lubricant

SAE class	5W30
Density at 15 °C	853 kg/m^3
Dynamic viscosity at 40 °C	59.88 mPas
Dynamic viscosity at 100 °C	9.98 mPas
HTHS[1] viscosity	3.57 mPas)

The physical properties are important input parameters to set up a realistic oil model that considers the non-Newtonian behaviour as well as piezoviscous effect. An overview of the journal bearing simulation is presented in section 3.2. The parameters used for the representation of the temperature and pressure dependency of the density and effects on the lubricant viscosity are provided in the results section in application example [43].

3.1.2 Measurement equipment

The main components of the measurement equipment used for the experimental investigations are listed in table 3.3.

Table 3.3: Test-rig main components

Group/Designation	Product/Type
Load unit and engine media conditioning	
High speed asynchronous dynamometer	KEB DQAT250-GZ01
Frequency converter incl. control and safety logic	KEB COMBIVERT F5
Lubricant supply unit	fabrication by PARR engineering
Cooling water supply unit	fabrication by PARR engineering
Water/air inter-cooler system	shaman equipment type 53
Measuring devices	
Piezoelectric cylinder pressure sensors	AVL ZI33 (gasoline), GU12P (diesel)
Piezo charge amplifier	AVL MicroIFEM
Crank angle encoder	AVL 365C
Capacitive TDC probe	AVL OT428
Combustion measurement system	AVL IndiModul Advanced GigaBit
IO systems and sensors	
Universal measuring amplifier	HBM QuantumX MX840A
Multi-I/O module	HBM QuantumX MX879
Temperature sensors	thermocouples type K, RTD PT100
Pressure sensors	BOSCH 0 261 230 112 (media resistant)
Mass flow meter	M+W mass-stream D6370
Digital torque transducer	HBM T12 nominal torque: 500 Nm

The crankshaft of the EUT is coupled to a 75 kW high speed asynchronous dynamometer. The dynamometer is driven by a variable frequency drive. It enables engine speeds up to 10.000 rpm, drive torques up to 250 Nm and is connected to the safety layer of

[1]HTHS: high temperature high shear rate viscosity (defined as the dynamic viscosity of the lubricant measured at 150 °C and at a shear rate of $10^6 s^{-1}$

the test-rig. External supply units for the engine cooling water and lubricant bring the media to the specified temperature and pressure level. The media supply units realise a temperature and pressure range from 50 °C to 130 °C/50 °C to 110 °C and 0 to 8 bar/0 to 4 bar for the lubricant and cooling water respectively. The temperature and pressure level is controlled to $\pm$0.1 °C and $\pm$0.05 bar.

By connecting the inlet and outlet manifolds of the engine by a recirculating external charging system, the air temperature at the inlet can be raised to temperature levels higher 200 °C during the tests. This allows a considerable increase of the temperatures at the components of the crank mechanism especially for piston crown and top ring.

To prevent damage at the EUT and test-rig due to possible self-ignition of the air/oil mist mixture, the temperature is limited to a maximum of 220 °C using a water to air inter-cooler system.

Load is applied to the EUT by the external charging system which supplies pressurized air to the engine intake. The intake pressure is externally controlled by a pressure control valve actuator. The limiting pressure for the inter-cooler system is 10 bar. Due to the intrinsic compression, peak cylinder pressures can be reached in a highly variable manner to correspond to peak levels of conventional fired operation. In practice, maximum peak cylinder pressures of more than 200 bar are realized.

The crankshaft torque and speed is measured by an HBM T12 digital torque/speed transducer (TST) with a measurement range of 500 Nm and an accuracy class of 0.03 (accuracy of $\pm$ 0.15 Nm). The total torque T is used to determine the BMEP in equation 3.3.

Several temperature sensors and pressure transducers are mounted at the EUT and peripheral test-rig systems for the regulation, control and monitoring of the tests. Temperature sensors at the lubricant circuit are placed at the main gallery, crankshaft main bearing shells and oil sump. Temperature sensors at the coolant circuit are placed at the inlet (near the thermostat) and outlet (near the water pump mounting position). Lubricant pressure is measured directly in the main supply bore of the oil gallery. Pressure transducers are mounted to measure the pressure in all cylinders of the engines.

The cylinder pressure indication system is realized using modern AVL industry standard systems. The system measures and processes the cylinder pressure sensor signals and references them to the TDC of the piston. The pressure sensors work according to the piezoelectric principle and are calibrated for the specific maximum peak cylinder pressures of the individual EUT. AVL ZI33 spark plug adapters and AVL GU12P glow plug adapters with integrated pressure sensors are used for the gasoline and diesel engine applications respectively investigated in this work.

A piezo amplifier system AVL MicroIFEM is used to process the piezo-electric signals from the pressure sensors to the high speed DAQ unit AVL Indimodul Advanced Gigabit. The high speed DAQ unit is connected to the test-rig computer to visualize, save and analyse the measured cylinder pressure data.

Precise TDC determination is conducted using a capacitive TDC probe system AVL OT428. The probe is installed at the position of the glow plug or diesel injector at cylinder one. TDC is determined with an accuracy of $\pm$0.01°CA while running the engine at a crankshaft speed of 2000 rpm for the engines investigated in this study. The TDC position is determined by using the angle of rotation between the TDC and a reference pulse from the crank angle encoder system mounted at the crankshaft.

A 3600 output pulse-per-revolution crank angle encoder AVL365C is used to reference the measured cylinder pressure to the TDC of the piston. By means of multiplication it is

possible to reference the cylinder pressure to the piston TDC by ±0.1°CA.

The recorded sensor signals at the EUT (with exception of the cylinder pressure measurements) and the test-rig environment are processed by a 24-bit universal measuring amplifier HBM QuantumX 840A and HBM QuantumX MX879 which are connected to the test-rig computer. The integrated DAQ software provides functionalities to visualize, save and analyse all relevant and safety critical sensor signals. The visualization is represented as a GUI for the test engineer conducting the measurements at the test-rig.

3.1.3 Testing procedure

The focus of this thesis is the investigation of the friction losses and shares of the base engine and its main assemblies, crankshaft journal bearings, valve train and piston group of three different engine concepts. Subsequently a procedure must be defined to ensure a consistent basis for the tests (figure 3.5). The testing boundary conditions vary between the different stages of the conducted tests. The engine speeds and loads are based on the corresponding operating map of the EUT, covering motored, low load and high load operation. Engine speeds up to 6000 rpm and peak cylinder pressures up to 200 bar are reached at specific test operation points.

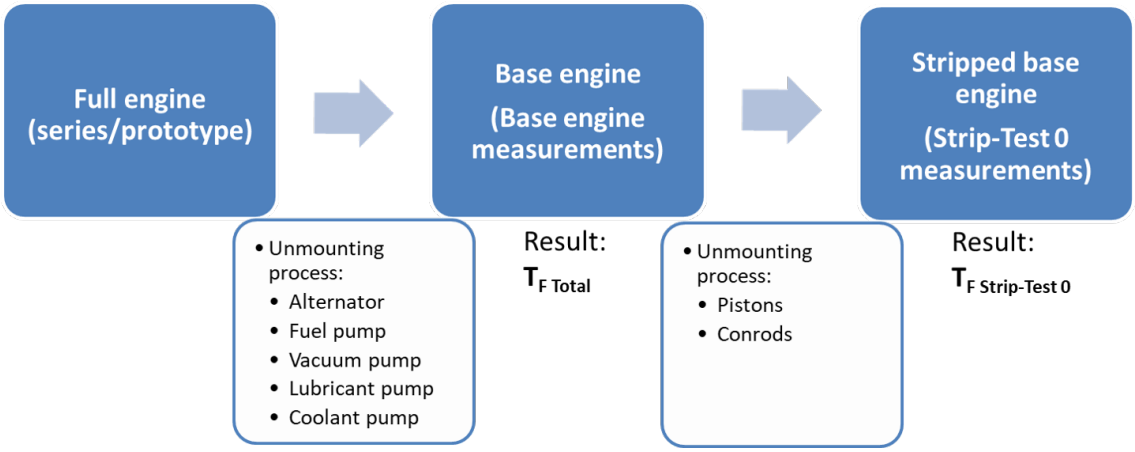

Figure 3.5: Defined test procedure

Starting point of the testing phase is an engine delivered from series production or at a prototype stage during engine development. The full engine is prepared for base engine measurements by unmounting all auxiliary systems and components which lead to additional friction shares. Also the lubricant and coolant pump systems are removed and the engine media circuits are prepared to be connected to external media supply units. The EUT is mounted on a base plate system attached to the dynamometer platform.

The preparation work includes the installation of pressure and temperature sensors at the lubricant and coolant circuits for the regulation of the external media supply units and the monitoring of the test boundary conditions. Engine inlet and outlet flanges are prepared and connected to the external charging system via hoses capable to withstand temperatures up to 220°C and pressures up to 10 bar. Temperature sensors, pressure sensors and a mass flow meter are installed to monitor the thermal boundary conditions of the charging system and check for leaks.

An essential step in the engine application is the installation of temperature sensors on the bearing brackets of the crankshaft main bearings. The temperature measurement

results are used for parameterization of the journal bearing simulation.

Torque measurements at the crankshaft are used to calculate the BMEP (equation 3.3) of the EUT. Crank angle resolved cylinder pressure measurements are used to perform the IMEP calculations (equation 3.2). Subsequently FMEP-maps of the base engine are resulting from the experiments at the base engine level (equation 3.1).

For the determination of the individual friction shares of the sub-assemblies at the base engine configuration, an additional strip measurement stage (strip-test 0) is conducted. After removing the pistons and conrods, master weights are placed at the big end bearings' position to compensate the missing rotational mass of the connecting rod. The result is the friction torque of the strip-test stage 0 configuration used to apply the friction analysis methodology in combination with the journal bearing simulation results.

A detailed description of the application work for the base engine and strip-test 0 stage tests is provided in the results section in application example [43].

3.2 Simulation: Journal bearing friction loss calculation

The virtual strip-down methodology for the sub-assembly resolved friction loss analysis requires the simulation of the crankshaft main and big end bearing friction losses. The simulation approach itself was developed and continuously improved in numerous long term research projects. It is published in several publications [75], [5], [76], [3], [4], [82], [83], [7], [84], [81] and was recently developed further with regard to today's operation of engine journal bearings under severe conditions (downsized engines, start-stop systems, cylinder de-activation, usage of ultra-low viscosity lubricants) in [81] and [80]. An overview of the developed journal bearing simulation is given here in a shortened form and is additionally presented in the results section in [43]. All details can be found in the original works cited above.

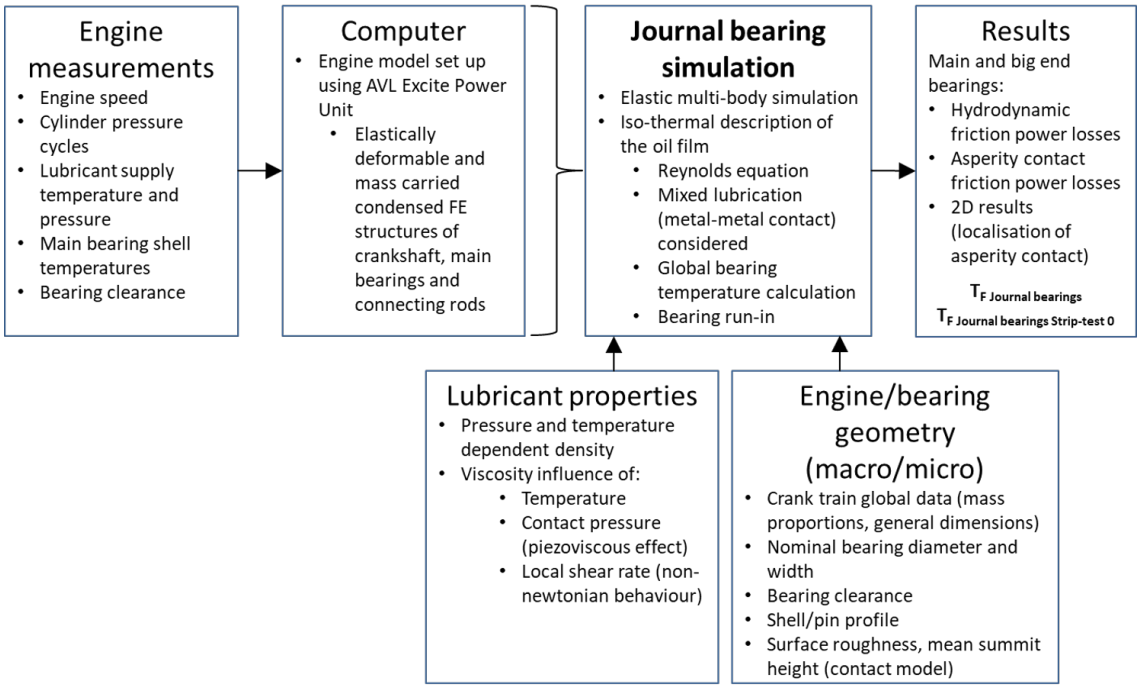

Figure 3.6: A schematic of the journal bearing simulation

Three main input streams to set up and parametrize the simulation model are used and are represented in a schematic in figure 3.6:

- Engine measurements
- Lubricant properties
- Engine/bearing macro and micro geometry

Engine measurements:

The input covers necessary measurement results of engine speed, crank angle resolved cylinder pressure cycles, lubricant supply temperature and pressure, main bearing shell temperatures and the bearing clearance. These parameters are used directly as boundary conditions for the EHD-calculations.

Lubricant properties:

The main lubricant properties density and viscosity (incl. HTHS-viscosity) of the automotive multi grade SAE 5W30 lubricant are mandatory simulation input parameters. The pressure and temperature dependency of the density is described by the approach of Dowson/Higginson. The dependency of the viscosity on temperature, piezo-viscous behaviour and the effect of shear rates are taken into account in the oil model using the equations according to Vogel, Barus and Cross, respectively.

Engine/bearing macro and micro geometry:

The general geometry data of the crank train components are derived by using provided CAD-data and drawings provided by the OEM and specific measurement of components. The determination of the bearing clearance is conducted using plastic gauge measuring strips with appropriate measuring scales. The surface roughness parameters for the contact model are dated from OEM informations and/or from empirical values from previous research projects.

3.2.1 Main equations used for the EHD-simulation to calculate the journal bearing friction losses in mixed lubrication

The determination of the journal bearing friction losses at highly loaded ICE passenger car bearings comprises the calculation of the hydrodynamic friction losses and losses due to metal-metal contact (asperity contact friction losses) in the mixed lubrication regime. A common form describing the friction losses is the representation as friction torque (T_F). By integration of the hydrodynamic shear stress τ_{hydr} and the asperity shear stress τ_{asp} over the bearing surface, the friction moment acting on the bearing surface in mixed lubrication is calculated:

$$T_\mathrm{F} = r \iint_A \left(\tau_{hydr} + \tau_{asp}\right) dxdy, \tag{3.4}$$

where r represents the nominal bearing shell radius and A is the bearing surface.

The fundamental equation to determine the hydrodynamic pressure in lubricated contacts is the Reynolds equation, developed by Osborne Reynolds in 1886 which is derived from the Navier Stokes equation using appropriate assumptions [80]. For the application in calculating the crankshaft journal bearing friction losses, several extensions are included to the Reynolds equation. These extensions include firstly the consideration of the non-Newtonian fluid behaviour of today's modern engine oils (change of the viscosity

with respect to the shear rate). Secondly the introduction of an averaged shear rate for reasons of simplification to calculate introduced coefficients to account for viscosity variations in film thickness direction. This results in an averaged form of the Reynolds equation. Thirdly, the averaged Reynolds equation is further extended for rough surfaces. This is of importance in micro-hydrodynamic effects where the minimum oil film thickness is lessened to such an extent that the contact surface asperities are affecting the hydrodynamic oil film as well as the oil flow. For the simulation work in this thesis, an indirect method considering rough surfaces in the lubricated contact is used, by adding correction factors (flow factors) according to the work of Patir and Cheng [70], [71] to the Reynolds equation.

$$\begin{aligned} &-\frac{\partial}{\partial x}\left(\phi_{\mathrm{x}}\frac{h^3}{12\eta}\frac{\partial p}{\partial x}\right)-\frac{\partial}{\partial y}\left(\phi_{\mathrm{y}}\frac{h^3}{12\eta}\frac{\partial p}{\partial y}\right)+ \\ &+\frac{\partial}{\partial x}\left(h\frac{u_1+u_2}{2}\right)+\frac{\partial}{\partial x}\left(\phi_{\mathrm{s}}\frac{u_1+u_2}{2}\sigma_s\right)+\frac{\partial h}{\partial t}=0. \end{aligned} \tag{3.5}$$

In equation 3.5, x and y denote the circumferential and the axial direction, respectively and h is the oil film thickness which is dependent on x and y. p represents the hydrodynamic pressure, while u_1 and u_2 are the sliding speeds of the facing contact surfaces. By the pressure flow factors ϕ_{x}, ϕ_{y} and the shear flow factor ϕ_{s} the influence of surface roughness is considered. The calculation of the flow factors by Patir and Cheng are conducted for numerically generated surfaces (including a Gaussian distribution of the asperity heights). Here, the surface asperities are concluded to be rigid and oriented along the circumferential or the axial direction. The asperity orientations at shaft and shell are parameters for the method besides the surface height. By using the definition of Peklenik [72], the asperity orientation is taken into account by Patir and Cheng:

$$\Gamma=\frac{\lambda_{0.5x}}{\lambda_{0.5y}}, \tag{3.6}$$

The autocorrelation length in circumferential and axial direction is represented by $\lambda_{0.5x}$ and $\lambda_{0.5y}$ respectively. The asperities are aligned with the circumferential direction if the value of Γ is greater than one.

The oil viscosity η dependency on temperature, pressure and shear rate is considered.

Besides the hydrodynamic contact pressure, also the asperity contact pressure is considered in the EHD-simulation of the crankshaft journal bearings. Here a contact model is employed to take metal-metal contact into account. To calculate the asperity contact pressure, the approach based on the contact of two nominally flat, random rough surfaces according to the work of Greenwood and Tripp is used. [32], [33]

The asperity contact pressure p_{asp} is defined according to equation 3.7,

$$p_{\mathrm{asp}}=KE^*F_{\frac{5}{2}}(H_s). \tag{3.7}$$

The elastic factor K is calculated according to

$$K=\frac{16\cdot\sqrt{2}\cdot\pi}{15}\cdot(\sigma_s\cdot\overline{\beta}_s\cdot\eta_s)^2\cdot\sqrt{\frac{\sigma_s}{\overline{\beta}_s}}, \tag{3.8}$$

where σ_s is the asperity summit roughness for journal ($\sigma_{s,J}$) and shell ($\sigma_{s,S}$) combined, calculated according to

$$\sigma_s = \sqrt{\sigma_{s,J}^2 + \sigma_{s,S}^2}. \tag{3.9}$$

Further factors are $\overline{\beta}_s$, the mean summit radius and η_s, the summit density.

E^* is the composite elastic modulus of the adjacent surfaces,

$$E^* = (\frac{1-\nu_1^2}{E_1} + \frac{1-\nu_2^2}{E_2})^{-1}, \tag{3.10}$$

where ν_i and E_i are the Poisson ratio and Young's modulus. $F_{\frac{5}{2}}(H_s)$ is the form function, which is an integral of the Gaussian distribution of asperity heights [80]. The approximated function according to [38] is used, who fitted the function using a power-law formula:

$$F_{\frac{5}{2}}(H_s) = \begin{cases} 4.4086 \cdot 10^{-5}(4-H_s)^{6.804}, & \text{if } H_s < 4 \\ 0, & \text{if } H_s \geq 4 \end{cases}, \tag{3.11}$$

In equation 3.11, H_s is a dimensionless clearance parameter, defined as

$$H_s = (h - \overline{\delta}_s)/\sigma_s), \tag{3.12}$$

where h is the nominal distance between the surfaces in contact and $\overline{\delta}_s$ being the combined mean summit height of the contacting surfaces with index '1' and '2':

$$\overline{\delta}_s = \overline{\delta}_{s,J} + \overline{\delta}_{s,S}. \tag{3.13}$$

Above a value of 4 for the dimensionless clearance parameter H_s the form factor $F_{\frac{5}{2}}(H_s)$ becomes zero. This describes the limit where no asperity contact occurs.

Calculation of the friction losses in hydrodynamic lubrication regime:

The hydrodynamic shear stress τ_{hydr} is calculated by

$$\tau_{hydr} = \eta \cdot \frac{u_1 - u_2}{h}(\phi_{\mathrm{f}} \pm \phi_{\mathrm{fs}}) \pm \phi_{\mathrm{fp}} \frac{h}{2} \cdot \frac{\partial p}{\partial x}, \tag{3.14}$$

where $+$ represents the shell surface and $-$ refers to the journal surface. ϕ_{f}, ϕ_{fs} and ϕ_{fp} represent the shear stress factors according to Patir and Cheng.

Calculation of the friction losses in mixed lubrication regime:

Asperity shear stress caused by shearing of the asperity peaks between the journal surface and the shell surface in the lubricated contact is calculated according to

$$\tau_{asp} = \mu_{\mathrm{Boundary}} \cdot p_a, \tag{3.15}$$

where μ_{Boundary} is the boundary friction coefficient and p_a represents the asperity contact pressure. In previous studies by Allmaier [5], investigations are carried out using

a constant value for the boundary friction coefficient with a value of μ_{Boundary}=0.02. The results of the study provided a solid basis for the usage of this value for lubricated contacts using modern engine oils in combination with proper additive package including friction modifier. Subsequently, μ_{Boundary} is assumed to be constant in the set-up of the simulation model used in this work using the value of 0.02.

3.2.2 Simulation environment and set-up

A multi body system (MBS) engine model is set up for each of the three engines investigated in this thesis using the software AVL Excite Power Unit [2]. Condensed finite element (FE) structures of the crankshaft, main bearings and connecting rods are used where all bodies are elastically deformable and mass carried. In a pre-processing step, the condensed bodies are created. For this work, pre-processing is conducted using Abaqus/standard [3]. For a detailed description of the pre-processing step, please refer to [80]. Joints connect the individual bodies.

In figure 3.7, the schematic representation of the in-line four-cylinder engine set-up used for calculations of the crankshaft journal bearing friction losses is shown.

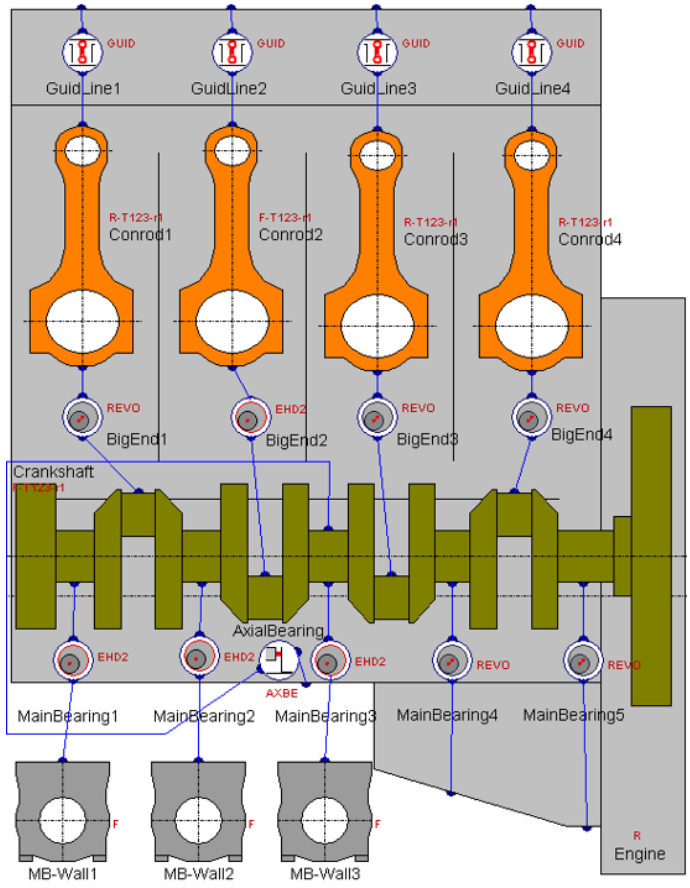

Figure 3.7: Schematic representation of the MBS to calculate the journal bearing friction losses

The principal set up of a simulation model is based on the general engine specification (bore, stroke, engine type, main bearing locations etc.), models of the engine components

[2] AVL List GmbH, Advanced Simulation Technology, Hans-List-Platz 1, 8020 Graz Austria, www.avl.com
[3] Dassault Systèmes, 10 rue Marcel Dassault, 78946 Vélizy-Villacoublay Cedex France, www.3ds.com

(engine block, crankshaft, conrods, main bearing body (wall)), connections (joints), lubricant model and load data (cylinder pressure profile).

Bearing temperature for iso-thermal simulation:

The journal bearing simulation basically consists of an elastic multi-body simulation with an isothermal description of the oil film (EHD simulation). Subsequently a general bearing temperature needs to be defined, representing an appropriate compromise for the entire journal bearing. A general temperature representing both the hot temperature in the highly loaded zone and cooler lubricant temperature in the non-loaded zone needs to be defined. In the recent past, a methodology to calculate an equivalent temperature has been developed [82], [4]. The developed equation is described in detail in the results section, in one application example [43]. The measured lubricant supply temperature and main bearing shell temperatures are used to calculate and describe the equivalent temperature.

Basic conditions of the surface contact model:

All surfaces in contact (journal and bearing shell) are considered as rough surfaces. For the calculation, the Greenwood and Tripp contact model type is chosen and parametrised. The simulation input parameters for the bearing shell and shaft is given in table 3.4.

Table 3.4: Surface roughness and simulation input parameters for the main bearing and big end bearing shell and the shaft

Parameter	Shell	Journal
Summit roughness (r.m.s) [μm]	0.2	0.2
Mean summit height [μm]	0.4	0.1
Young's modulus [N/mm^2]	63000	210000
Poisson's Ratio [-]	0.3	0.3
Elastic factor [-]	0.003	
Friction coefficient [-]	0.02	
Averaged Reynolds Equation - Type: According to Patir and Cheng	Shell	Journal
Surface roughness (r.m.s) [μm]	0.2	0.2
Roughness orientation [-]	2	4

It is generally known that lubricated contacts experience a running-in phase at the beginning of the engine operation, which is also considered in the journal bearing simulation. Therefore, initial wear calculations are performed with a duration of about 100 crankshaft revolutions (36000°CA) to consider the adaption of the bearing shells in the early phase of operation due to metal-metal contact. These initial simulations result in run-in shell profile geometries as a consistent starting point for the following friction loss calculations. In the results section, an application example [42] describes the importance to consider run-in phenomena when investigating ICE friction losses.

In this work, the developed simulation methodology is used in an engine crankshaft system, building on the developments and applications using a journal bearing test-rig in [80]. Furthermore, a first-time validation of the developed simulation methodology is conducted, directly comparing results from friction measurements of the crankshaft main bearings only and the calculations at a conventional engine crankshaft system. The verification work is presented in an application example [43] in section 4.

Chapter 4

Applications and development of the combined approach

In this chapter, the friction losses of three engine architectures are investigated. By using the developed combined analysis approach, the investigations are focusing not only on the base engine level but in particular on the sub-assembly systems' journal bearings, valve train and piston group. Using one identical lubricant for all tests conducted in combination with identical thermal boundary conditions for the engine media (oil and cooling water) through the use of external conditioning systems enables the realization of friction comparisons. The results are obtained at different engine media supply temperatures. Reducing the lubricant viscosity by increasing the supply temperature enables the discussion of the origin of the friction losses. An allocation is conducted from elasto-hydrodynamic lubrication regimes to severe mixed lubrication regimes. The use of an external charging system puts the influence of cylinder pressure fluctuations in friction determination into the background. The fluctuations can have a considerable influence on the comparability of the measurement results. Cylinder pressure variations in the order of Δp=1 bar between the cylinders also at high load operation can be achieved using the charging system. This is advantageous for comparative testing activities. The presentation of the friction analyses is based on a top-down approach. It ranges from the comparison of the base engines and sub-assembly systems to friction reduction potentials and risk assessment down to the sub-assembly level.

The first application example discusses the application and the developed process applying the combined approach to investigate the sub-assembly resolved base engine friction losses. The detailed description is exemplified by the diesel engine under investigation in this thesis. Since it is an important goal of the work to conduct the sub-assembly resolved investigations under load operation, focus is spent on the necessary step by step process to realize stable and reproducible test boundary conditions. The preparatory work for the experimental investigations as well as the set-up of the crankshaft journal bearing simulation model is discussed. Since the developed journal bearing simulation methodology is used for the first time in a conventional ICE crank drive, a verification of the simulation model with measured data is carried out. For this purpose, the engine is tested in a strip measurement campaign to measure the crankshaft losses alone (without crankshaft sealing rings). In order to demonstrate the application of the methodology as comprehensively as possible, the engine is operated in a speed range of 1000 - 4000 rpm and peak cylinder pressures up to 180 bar. To allow investigations regarding the predominate lubrication regime at the sub-assembly level, the lubricant viscosity is varied by increasing the lubricant supply temperature. Therefore, three different temperature

levels of 70 °C, 90 °C and 110 °C are realized during the measurements by the usage of external engine media supply units. Mixed lubrication is identified using the combination of measurements and journal bearing simulation. In addition, the test operation point map is adjusted accordingly to the other examined engines in this thesis to allow specific comparisons at identical speed and load.

The second application example uses the combined approach to investigate the sub-assembly resolved friction losses on two additional gasoline engines with the same and doubled specific power density of the diesel engine tested in application example one. Subsequently the friction losses are compared regarding the fuel used (comparison of diesel and gasoline engines) and with specific focus on the power density to investigate conventional and high-power downsizing engine concepts. A measurement program especially coordinated between the engines and correspondingly performed EHD simulations of the crankshaft journal bearings allows specific comparisons of the friction losses of the subsystems' crankshaft main/big end bearings, valve train and piston group. In addition to identical speeds between 1000 and 5000 rpm, comparisons are also made at identical peak cylinder pressures from motored engine operation to part and full load conditions. Peak cylinder pressures up to 130 bar are investigated, which represents modern highly loaded engine operation for series gasoline engine concepts. Different thermal boundary conditions at 70 °C, 90 °C and 110 °C allow further investigations of the resulting lubrication regime at the sub-assembly systems by reducing the lubricant viscosity. It is important to note again that the same suitable lubricant is used for the investigations at the three engines. This important boundary condition enables investigations neglecting influences from possible different additive packages influencing the friction losses for example in mixed lubrication regime by different anti wear and friction modifier supplements.

The third application example examines a sub-sequent investigation of the engine concepts focusing on friction reduction potentials and risk assessment at the engines' sub-assembly level. By analysing the results of the friction losses of the three engines at different lubricant temperature levels, the dominant lubrication regime is investigated. For pure hydrodynamic lubrication, a decreasing lubricant viscosity, e.g. when using ultra-low viscosity lubricants, results in decreasing friction losses by reduced work for the shearing of the lubricant in the lubricated contacts. Subsequently a reduction of the friction torque/friction power losses may result when increasing the lubricant temperature (simulating a viscosity reduction). At the same time, the oil film height is decreasing at the lubricated contacts, and mixed lubrication is possible when the oil film height is equal or lower than the surface roughness of the contacting surfaces. Especially at highly loaded lubricated contacts like the piston rings, big end bearings or contacts with low sliding speeds like at the valve train system, the risk for increased and harmful metal-metal contact increases. Because the engines are run-in in the preparation phase before the measurement campaign, an increase in friction torque/friction power loss is indicating increased asperity contact and sub-subsequently significant metal-metal contact.

The fourth application example uses the combined method of friction measurements and EHD crankshaft journal bearing simulation to investigate the running-in behaviour not only at the base engine configuration but at the sub-assembly systems' valve train and piston group. The investigations are carried out at gasoline engine 1 to gain insight into the effects on frictional behaviour and duration of the engine running-in phase. In a first step, the main components of the valve train and piston group are replaced by new parts. A series of tests are conducted for the full engine operation map at different thermal

boundary conditions ranging from 70 °C to 110 °C. As the run-in phase in the early stage of engine operation results in a smoothing of the asperities and surface roughness decreases, tests are performed until a steady state of the friction moment is resulting for the engine under test. The stable condition is checked after each completion of the test program.

In the first three application examples, the results of the friction analysis were published in a series of three peer-reviewed articles in the open access journal Lubricants of publisher MDPI AG. The papers are published in the special issue Automotive Tribology under supervision of the guest editor Prof. Dr. Adolfo Senatore, who is a renown expert in this field [43, 44, 45]. The fourth application example was published in the Proceedings of the Institution of Mechanical Engineers, Part J: Journal of Engineering Tribology [46]. The individual publications are included in each section. Summaries are provided as an introduction to each application example.

4.1 A combined approach for applying subassembly-resolved friction loss analysis on a modern passenger-car diesel engine

The comparison of ICE friction losses at different thermal and load conditions requires accurate analysis methods and processes. This enables to reliably identify even small friction benefits of today's engines with their already good friction performance. To achieve high precision for the full operational range, a recently in-house developed approach combining accurate measurements and state-of-the-art journal bearing simulations is applied. In this work, the developed approach is used to investigate the friction losses of a modern passenger-car diesel engine. By merging extensive experimental results with reliable journal bearing simulation, a detailed study is performed and allows a comparison of the piston group, crankshaft journal bearings and valve train friction losses at different operating conditions.

The resulting lubrication gap height in the lubricated contact has a significant influence on the prevailing friction regime (hydrodynamic lubrication, mixed lubrication, boundary lubrication) and thus on the friction losses. In the hydrodynamic range, the lubricant viscosity dominates the friction losses. With decreasing lubrication gap height and beginning contact of the roughness peaks of the contact surfaces it is more and more the metal-metal contact. In addition to the load from gas and inertial forces, a reduction of the lubricant viscosity e.g. by increasing the lubricant temperature or usage of low viscosity engine oils in particular leads to a decrease of the lubrication gap height.

To investigate and compare the sub-assembly friction losses at different load conditions, the engine is operated at a typical load range (varying cylinder pressure and engine speed). Peak cylinder pressures up to pcyl=180 bar and engine speeds from n=1000 rpm to n=4000 rpm are investigated. To study the influence of decreasing lubricant viscosity, the thermal boundary conditions are varied during the tests using engine media supply units. By conducting measurements at identical load conditions (cylinder pressure and engine speed) at three different supply temperature levels (70 °C, 90 °C and 110 °C), the influence of reduced lubricant viscosity is investigated. By using the developed methodology, friction comparisons and analyses of the prevailing friction regime are conducted. Thereby, critical mixed lubrication is identified in the sub-assembly systems.

Further measurements resulting in an additional friction breakdown of the valve train, timing drive, crankshaft seals and crankshaft journal bearings enable a deeper understanding of the friction behaviour and present lubrication regime on the sub-system level of the modern engine.

Friction torque measurements of the journal bearings solely at different thermal boundary conditions are performed. It is the basis for the verification of the journal bearing simulation approach utilization in a crankshaft system. Important input for the parametrisation of the contact model is generated. Direct comparison of the sole measurement to the journal bearing simulation results shows the suitability of the developed simulation methodology at a crankshaft system for the first time.

The details of the application of the developed combined approach and the results are described in [43] which are presented in section 4.1.2. The research findings of the publication are summarized here beforehand.

4.1.1 Summary of research findings

- Improvement of the measurement accuracy due to the realization of highly stable testing boundary conditions at the test bed and the definition of a detailed friction analysis procedure.
- Friction reduction of up to 21 % is determined at the base engine level when increasing the engine media supply temperature from 70 °C to 110 °C.
- The possible reduction potential obtained that especially for new engine modes of operation (start/stop systems, early engine stopping using hybridization), challenges arise for the thermal management system to keep the oil temperature at desired high levels to decrease the friction losses.
- While friction reduction is determined at the crankshaft main and big end bearings, mixed lubrication regimes are assigned simultaneously at the valve train and at the piston group at low engine speeds and high lubricant temperatures.
- Most significant friction loss increase is observed for the timing drive and valve train systems at the lowest engine speed investigated.
- Measurement results of the main bearings are direct input data for a comparison between EHD-simulation and experimental data.
- A validation of the developed journal-bearing simulation methodology in a conventional crank train system has shown good applicability. Adjustments at the contact model parametrisation for the bearing clearance are performed as a result of the conducted investigations.
- The maximum deviation in FMEP between measurements and journal bearing simulation at a lubricant supply temperature of 90 °C is ΔFMEP=0.01 bar (7%) at n=4000 rpm (highest investigated engine speed in the application example). At lower engine speeds, the difference is clearly below ΔFMEP=0.01 bar.

Annotation and additional reference

Besides an investigation of the crankshaft journal bearings, valve train and piston group systems in [43], also results were obtained for parts which are usually being considered as less relevant like the crankshaft rotary shaft seals. For this reason, these parts are normally not considered in discussions of the friction power losses of internal combustion engines. In a sub study, the friction losses of these machine elements are investigated. The results are presented and additionally discussed in another publication [46]. However, the results obtained within this sub study show that the quantity of these losses is surprisingly large. Contrary to common literature, the experimental results also show a discernible temperature dependency which appears to support the hypothesis that rotary shaft seals are predominantly hydrodynamically lubricated in this application example.

4.1.2 Paper I [82]

lubricants

MDPI

Article

Investigations of the Friction Losses of Different Engine Concepts. Part 1: A Combined Approach for Applying Subassembly-Resolved Friction Loss Analysis on a Modern Passenger-Car Diesel Engine

Christoph Knauder [1,*], Hannes Allmaier [1], David E. Sander [1] and Theodor Sams [2,3]

1 VIRTUAL VEHICLE Research Center, Inffeldgasse 21A, 8010 Graz, Austria; Hannes.Allmaier@v2c2.at (H.A.); David.Sander@v2c2.at (D.E.S.)
2 AVL List GmbH, Hans-List-Platz 1, 8020 Graz, Austria; Theodor.Sams@avl.com
3 Institute of Internal Combustion Engines and Thermodynamics—Graz University of Technology, Inffeldgasse 19, 8010 Graz, Austria
* Correspondence: christoph.knauder@v2c2.at

Received: 29 March 2019; Accepted: 17 April 2019; Published: 26 April 2019

Abstract: This work presents the application of a combined approach to investigate the friction losses in a modern four-cylinder passenger-car diesel engine. The approach connects the results from engine friction measurements using the indication method and the results from journal-bearing simulations. The utilization of the method enables a subassembly-resolved friction loss analysis that yields the losses of the piston group, crankshaft journal bearings, and valve train (including the timing drive and crankshaft seals). The engine and engine subassembly friction losses are investigated over the full speed and load range, covering more than 120 engine operation points at different engine media supply temperatures ranging from 70 to 110 °C. The subsequently decreasing lubricant viscosity due to higher engine media supply temperatures allow for the identification of friction reduction potentials as well as possible risks due to an onset of mixed lubrication. Furthermore, additional strip-tests have been conducted to determine the friction losses of the crankshaft radial lip seals, the timing drive, and the crankshaft journal bearings, thus enabling a verification of the calculated journal-bearing friction losses with measurement results. For the investigated diesel engine, a friction reduction potential of up to 21% could be determined when increasing the engine media supply temperature from 70 to 110 °C, at engine speeds higher than n = 1500 rpm and part load operating conditions. At low engine speeds and high load operations, the friction loss reduction potential is considerably decreased and below 8%, indicating mixed lubrication regimes at the piston group and valve train.

Keywords: engine friction; friction measurements; friction loss distribution; subassembly friction; journal-bearing simulation; valve train; journal bearings; piston group

1. Introduction

To improve fuel economy and, in particular, the overall mechanical efficiency, the determination of the friction losses of combustion engines is a crucial topic in modern engine development. Based on current challenges for manufacturers including stricter CO_2 emission limits from the legislative side, changing customer preferences (away from product towards function, e.g., car sharing and car rental) and a general focus on the environmental impact, it is nowadays crucial to develop highly efficient vehicles.

Especially for vehicles using internal combustion engines (ICE) which currently deal with bad public reputation due to the Diesel emission scandal, it is very important to present results on how to cut fuel consumption and to limit the exhaust gas emissions. The minimization of the mechanical losses provide a significant contribution to high efficiency vehicles nowadays as well as in the foreseeable future [1]. Measures to reduce the mechanical losses also often show advantages in terms of financial investments compared to hybridization and subsequently increases the overall efficiency of hybrid vehicles [2].

In internal combustion engines, the frictional losses of the base engine are generated by the subassemblies' piston group, crankshaft journal bearings, valve train, timing drive, and shaft seals. This means that friction reduction on these key assemblies continue to represent a significant goal for the development of low-friction base engines. Also, for the first calculations in the concept phase of engine development using empirical friction models [3–5], experimental data for the subassemblies, e.g., of the piston group, under realistic operation conditions is required. Furthermore, the need of advanced lubricant models including the non-Newtonian behaviour and of closer attention to the thermal conditions in the engine when developing engine friction models has been reported in the past [6]. Nowadays, the assessment and assignment of the engine friction losses to the subassemblies is generally done by fired and motored friction tests. Each mentioned measuring method has its area of application with its corresponding advantages and challenges which are briefly described below.

While an engine friction measurement in a fired operation is ideal because of the conventional thermal boundary condition as well as the correct cylinder pressure phasing and gradient, it is challenging to maintain the stability of the engine operation and the repeatability which is required for accurate measurements. Due to the combustion process, one is faced with strongly varying cylinder pressures from cycle to cycle. Furthermore, the inherently high indicated power produces highly alternating torques at the crankshaft. Therefore, a torque transducer with a much larger measurement range is required for a fired operation compared to a motored operation. In References [7,8] an overall methodology is presented which covers a systematic testing procedure from the calibration of the measurement chain to the exact measurement workflows to gain the highest possible repeatability of the conducted tests. Nevertheless, cyclic variations and necessary bigger torque transducer measurement ranges have to be accepted. The developed and used friction measuring module in Reference [8] needs to be specifically designed for the engines put to test. Furthermore, a fired engine operation also has an influence on the used pressure sensors of the cylinder pressure measurement system. Especially, the hysteresis effects during the conducted tests needs to be accounted [8], and the usage of cooled pressure sensors is necessary.

Single-cylinder test beds using the floating-liner principle, on the other hand, are commonly used for direct friction force measurements on the cylinder liner caused by the piston group under fired conditions. One main drawback is the missing possibility to use the conventional crank train of multicylinder engines. The methodology also has to deal with different boundary conditions like limited cylinder pressures, vibrations disturbing the force measurement signals, and stronger cylinder bore distortions due to the design of the test rig. However, in the last years, improvements have been made regarding the sealing system between the floating liner and the cylinder head, and therefore, higher cylinder pressures can be reached. Also, the difference in bore distortions has been minimized in the past using complex measurement and specific honing processes to reach comparable cylinder profiles as in conventional engines [9]. All improvements to enhance the function of the single-cylinder test bed result in high efforts on design and measurement requirements.

The application of conventionally motored (without external charging) engine tests results in a reduced complexity of the test rig due to the missing fuel system. However, very different thermal boundary conditions as well as the absence of a strong cylinder pressure acting on the pistons and bearings are affecting the friction results from these tests. External charging is able to create a mechanical load on the engine that is comparable to a fired operation as well as can be used to create thermal conditions in the

engine that is more similar to a fired operation than it is for conventional motored tests. Although the basic principle of motoring friction tests with external charging is known from the past [10,11], it came up again recently and is currently investigated [12]. Also, developments improving the thermal boundary conditions and reaching comparable load characteristics to a firing operation [13] have been achieved [14,15].

The major advantages of pressurized motoring tests are a significantly higher measurement accuracy due to a strongly reduced indicated mean effective pressure (IMEP; about factor 4 in comparison to a fired operation) and highly stable testing boundary conditions. The cycle-to-cycle cylinder pressure variations in a charged motoring operation are insignificant compared to the fired operation. Therefore, torque transducers with a much smaller measurement range and, consequently, a much higher measurement accuracy can be realized. The external charging is generally realized by supplying pressurized air or inert gases (e.g., nitrogen) to the engine intake. Due to the intrinsic compression of the engine, peak cylinder pressures can be reached which correspond to a conventional fired operation. By using a pressure control valve, the peak cylinder pressure representing the load of the engine can be controlled in a highly variable way which represents an engine operation in part and full load conditions. In contrast to a fired operation, the following limitations are assigned with a pressurized motoring: On the one hand, the position of the maximum cylinder pressure is always very close to the top dead center position of the engine. However, for diesel engines at full load, the resulting position of the pressure maximum occurs about +10 °CA (CA: Crank angle) after TDC (Top dead center) which results in a good agreement between the fired and charged motoring tests when a mechanical load is the dominating factor [15]. On the other hand, the thermal boundary conditions are different for the motoring test due to the missing thermal energy of the combustion processes. This limitation affects the results in particular at part load conditions when comparing the results from friction measurements in fired and pressurized motoring operation [16]. To reduce the lack of thermal energy in the engine during the pressurized motoring test, the charging system can be designed as a recirculation system. Therefore, the engine exhaust is connected to the engine intake. This enables a great increase in the intake temperature of the pressurized air, which subsequently strongly increases the temperature during the compression stroke. This affects the thermal operating conditions especially for the piston group.

For the investigation of further friction reduction measures with the already good friction performance of today's modern engines, methods and tools which can also dissolve and analyze small differences consistently over the operational range of the engines are necessary. To give an example, when analyzing the advantages of (ultra) low viscosity engine oils, deviations in the friction torque of 0.1 Nm have to be resolved over the entire engine operation range [17]. The same can be stated when analyzing small contributors to the friction losses like the crankshaft seals. The highest requirements regarding measurement accuracy and testing workflow have to be met to achieve highly accurate results [18].

Bringing together the advantages of both fields, simulation and testing, can result in new possibilities of analysing engine friction power losses. During the development process of a combined approach at the VIRTUAL VEHICLE Research Center, a friction analysis procedure has been defined which enables very good possibilities for comparisons of measures to reduce engine friction losses [14,15,19]. The developed friction analysis approach combines the results of a detailed elasto-hydrodynamic journal-bearing simulation and charged motoring tests with air recirculation. Due to the combination of simulations and measurements, it is possible to analyses the friction performance of the crankshaft journal bearings, valve train, and piston assembly over the entire engine operation range.

This work presents the application of the developed combined approach using the analysis procedure to investigate the friction losses of a modern passenger-car diesel engine in great detail. The primary aim of the study is to analyse the friction losses of the base engine and its subassembly crankshaft journal bearings, valve train, and piston assembly for different thermal boundary conditions. Therefore, the supply temperatures of oil and cooling water are varied between 70 and 110 °C. These additional investigations,

in particular, at highest temperatures, allow for the potential identification of critical mixed lubrication in subassemblies. The secondary aim is a further breakdown of the friction losses by additional measurements. The individual contribution of the valve train, timing drive, crankshaft seals, and crankshaft main bearings are identified. The measurement of the crankshaft main bearings friction losses enable a verification of the utilization of the journal-bearing simulation approach in a crankshaft system which represents the tertiary aim of this work. The simulation approach was developed on the basis of journal-bearing test-rigs. In this study, the sole measurement of the journal-bearing losses enables a direct comparison with the journal-bearing simulation approach for the first time.

2. Friction Losses Analysing Procedure: A Combined Approach Using Experiments and Predictive Journal-Bearing Simulation

The aim of the developed friction loss analysis procedure is the determination of the friction power losses of the base engine for motored and load operations and the breakdown of these losses to the individual components' crankshaft journal bearings, valve train (with timing drive and crankshaft seals), and piston group. For this purpose, an analysis approach combining motored engine test-bed measurements with external charging and a previously developed predictive and widely validated journal-bearing simulation method was developed. An overview of the developed approach is shown in Figure 1.

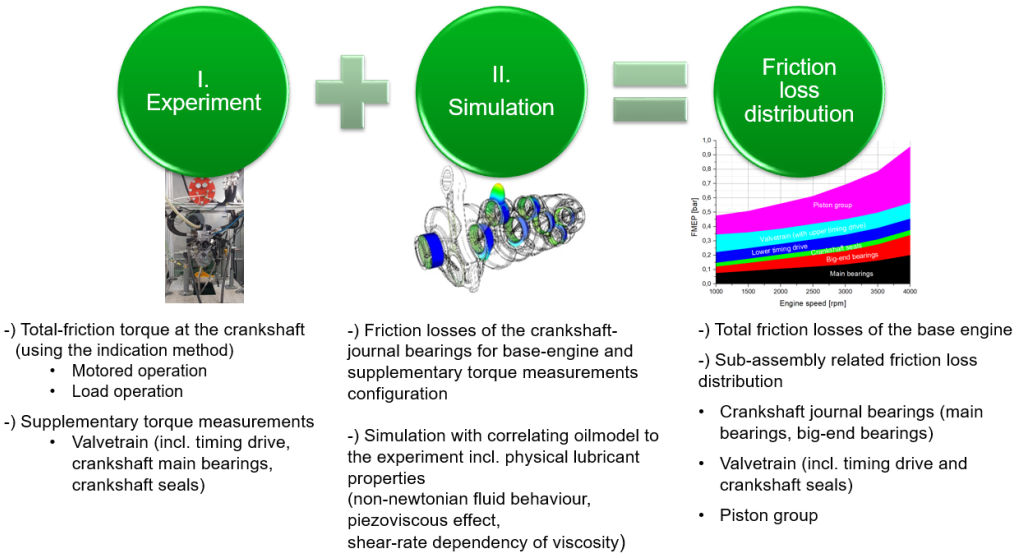

Figure 1. A general overview of the used combined approach to analyse the engine friction losses.

The combined approach connects the experimental results with the calculated journal-bearing friction losses from simulation models. This results, on the one hand, in the determination of the base engine total friction losses and, on the other hand, in a subassembly resolved friction loss distribution over the full engine operation range (speed and load).

The measurements are conducted using the indication method (IMEP (Indicated mean effective pressure) method). By using the IMEP-method, the friction losses denoted as FMEP (Friction mean effective pressure) are determined by the subtraction of two similar sized large quantities, the IMEP and the

BMEP (Brake mean effective pressure); see Equation (1). For a motored operation, the signs of IMEP and BMEP are negative in comparison to a fired operation. The FMEP is, in comparison, a rather small quantity.

$$FMEP = IMEP - BMEP \tag{1}$$

Therefore, great care needs to be taken in the determination of the IMEP and BMEP because any significant error in these large quantities can easily lead to a measurement error of the same magnitude as the calculated FMEP. The reduced IMEP (about factor 4 compared to the fired operation) when using charged motoring tests and insignificant cycle-to-cycle variations enable the usage of considerably smaller torque transducers and, therefore, an increased accuracy in BMEP determination. For an accurate IMEP determination, AVL List high-quality industry equipment for cylinder pressure measurements including a 720 ppr rotary encoder system is used. A corresponding calibration of the used measurement equipment is of great importance for reliable and accurate measurements.

Valve train friction: In addition to the total base engine friction (FMEP) tests, supplementary friction measurements are done with removed pistons and conrods to obtain the friction torque of the valve train with timing drive and crankshaft seals.

The simulation of the journal bearing friction losses: The simulation method is discussed in detail in a later section (Section 4). Here, only the basic applied scheme is outlined. The simulation is prepared in two steps: The first step uses the base-engine simulation model for the calculation of the main bearing and big-end bearing friction losses under the tested operating conditions. In the second step, a reduced engine model without pistons and conrods is used in combination with the supplementary torque measurements of the valve train friction. For detailed and accurate journal-bearing friction loss calculations, it is crucial to use lubricant models which correlate to the experiments and that describe closely the rheological properties of the used engine oil.

To determine the subassembly related friction loss distribution, the following workflow as shown in Figure 2 is used.

The full engine is reduced to the base-engine configuration by removing or deactivating all engine auxiliary devices. This enables to full focus on the base engine friction losses during the friction loss investigations. Before the friction tests are conducted, an extensive running-in procedure is performed to account for the processes affecting the results [20]. The first measurements are then carried out on the base engine to obtain the engine friction map ($T_{\text{F Total}}$) over the entire load and speed range of interest. The engine friction map is typically measured at different engine media supply temperatures to analyse the influence of different thermal boundary conditions on the friction losses of the engine. Parallel to the experimental part, the journal-bearing simulation model of the base engine is created. Besides the detailed geometrical and mass data of the whole crank train, the interaction between the simulation model and the experiments consists of the cylinder pressure curves and engine speeds for the bearing load and the main bearing temperature measurement data for the journal-bearing simulation methodology. The total friction losses (hydrodynamic and asperity friction losses) of the crankshaft main- and big-end bearings are calculated ($T_{\text{F Journal bearings}}$) for the same engine operation points as were used in the engine friction map measurements. After the engine friction map measurements are finished, the base-engine is stripped to engine strip-test stage 0 by removing the pistons and conrods. These so-called supplementary torque measurements ($T_{\text{F Strip-Test 0}}$) are then conducted at the same boundary conditions for the engine speed and engine media supply temperatures as were used for the engine friction map measurements. An additional journal-bearing simulation model in an engine strip-test stage 0 configuration is created to calculate and separate the main bearing friction losses for this strip stage ($T_{\text{F Journal bearing Strip-Test 0}}$). By subtracting the measured friction torque of the supplementary torque measurements ($T_{\text{F Strip-Test 0}}$) from the friction torque of the journal-bearing simulation correlating to the supplementary torque measurements ($T_{\text{F Journal bearing Strip-Test 0}}$), the valve train friction

torque ($T_{\text{F Valve train}}$) is determined; see Equation (2). Although for simplicity this friction torque is called the valve train friction torque in the following, it is important to note that the (comparatively smaller) friction losses of the timing drive and the crankshaft seal rings are included.

$$T_{\text{F Valve train}} = T_{\text{F Strip-Test 0}} - T_{\text{F Journal bearings Strip-Test 0}} \quad (2)$$

After the determination of the valve train friction losses (Equation (2)), the friction losses of the piston group can be determined. The resulting friction torque of the piston group ($T_{\text{F Piston group}}$) is calculated from the measured total friction torque of the base engine ($T_{\text{F Total}}$) by subtraction of the calculated friction torque of the valve train ($T_{\text{F Valve train}}$) and the calculated friction torque of the crankshaft journal bearings of the base engine configuration ($T_{\text{F Journal bearings}}$); see Equation (3).

$$T_{\text{F Piston group}} = T_{\text{F Total}} - T_{\text{F Valve train}} - T_{\text{F Journal bearings}} \quad (3)$$

With this combined approach, it becomes possible to determine the frictional losses of the subassembly piston group, valve train, and crankshaft journal bearings over the full range of engine operation conditions (entire engine speed and load range). This can be done for all kind of single- or multicylinder engines and prototypes, respectively, using conventional reciprocating crank trains. In addition, the cost benefits due to a reduced experimental effort arise, and a detailed insight in the tribological behaviour of the crankshaft main and big-end bearings becomes possible with the journal-bearing simulation results.

Figure 2. A detailed procedure to determine the subassembly-related friction losses using the combined approach.

Lubricants **2019**, *7*, 39

3. Experimental Investigation

The following subsections give detailed descriptions of the dynamometer, engine preparations, and the testing procedure for the experimental investigations.

3.1. The Dynamometer

The used motored engine test bench with external charging (FRIDA (FRIction DynAmometer)), was developed, designed, and built at the VIRTUAL VEHICLE Research Center. An overview of the experimental setup on the friction dynamometer is given in Figure 3.

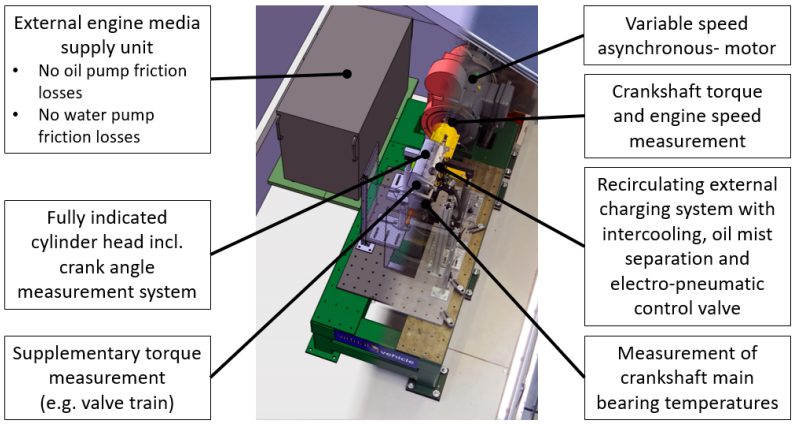

Figure 3. An overview of the experimental test setup for the analysis of the engine friction losses.

The fundamental aims of the experimental investigations on the motored engine test bench with external charging are to measure for the determination of the BMEP and the IMEP as well as to allocate the necessary data for the journal-bearing simulation model. For the determination of the BMEP, torque measurements at the crankshaft (brake torque) are conducted. The following equation relates the measured brake torque at the crankshaft (T) to the corresponding mean effective pressure ($BMEP$).

$$BMEP = \frac{W}{V_D} = \frac{4\pi T}{V_D}, \tag{4}$$

where W refers to the work per cycle and V_D referes to the volume displacement of the investigated 4-stroke engine. A highly accurate torque measurement system with an accuracy class of 0.03 (HBM T12) and integrated speed sensor is used to measure the brake torque and engine speed at the crankshaft. The IMEP determination of the pumping losses according to Equation (5) during the tests is done by integrating the measured cylinder pressure ($pcyl$) over a working cycle divided by the volume displacement of the engine.

$$IMEP = \frac{\int pdV}{V_D}, \tag{5}$$

For the IMEP determination, the cylinder pressures in all four cylinders are measured using piezoelectric pressure sensors (AVL GU12P) which are installed at the glow plug positions by using adapters. The measured piezoelectric charge is processed by a charge amplifier (AVL MicroIFEM). The complete cylinder pressure measurement chain (pressure sensors, cables, and charge amplifier) has been calibrated before the measurements. To allocate the measured cylinder pressure to the particular crank angle an 720 ppr angle encoder (AVL 365C) is used. One crucial point regarding the error sources

in the IMEP determination is the accurate determination of the piston TDC. Even small deviations of the correct TDC position results in large errors in the FMEP determination [21]. Consequently, the TDC determination has to be done with greatest possible precision and, therefore, a capacitive TDC sensor (AVL OT428) was used. The TDC determination using capacitive TDC sensors is one of the most precise techniques which can be used [21]. Ideally, the TDC determination should be done for every single operating point as the engine speed, load, and even the engine media supply temperature influence the exact position of the TDC. Practically, the TDC determination is done for an important engine operating point. For this engine, an engine speed of 2000 rpm and a lubricant supply temperature of 50 °C were selected. The mounted TDC sensor during the TDC determination is shown in Figure 4.

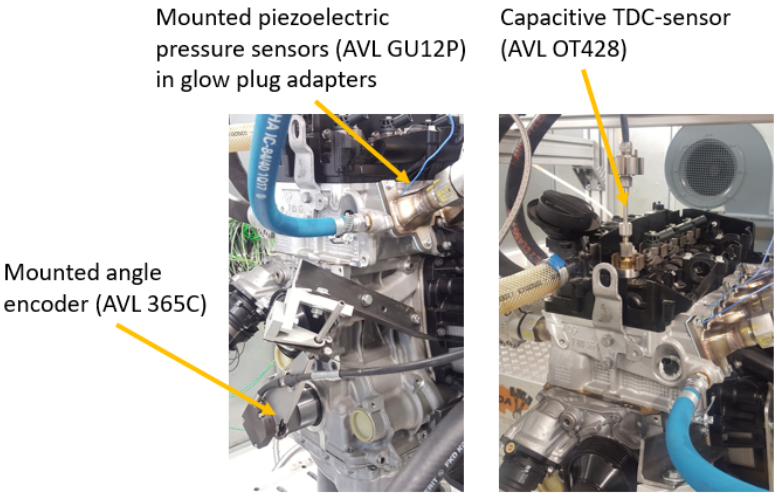

Figure 4. The mounted capacitive top dead center (TDC)-sensor and crank angle encoder during the TDC determination.

To obtain the required input data for the journal-bearing simulation and to ensure reproducible testing boundary conditions (thermal and load), an extensive engine preparation and sensor application are necessary which is described in the following subsection.

3.2. The Engine under Test and Necessary Engine Preparations

The experimental investigations were carried out for a modern in-line four-cylinder, four-stroke, turbo charged, passenger-car diesel engine with a nominal volume displacement of 2 L and a nominal power of 135 kW. The technical details of the engine are listed in Table 1.

The focus of the conducted friction loss investigation is on the base engine performance and its subassembly piston group, valve train, and crankshaft journal bearings. To analyse the friction losses of the base engine, all auxiliary devices like the oil and water pump, alternator, balancing shafts, vacuum pump, etc. have been removed from the engine or deactivated. Figure 5 shows the engine being installed for the measurements on the dynamometer.

Table 1. Technical data of the in-line four-cylinder turbocharged diesel engine under test.

Volume displacement	1995 cm^3
Compression ratio	16.5:1
Bore	84 mm
Stroke	90 mm
Nominal torque	380 Nm
Nominal Power	135 kW
Maximum Speed	4600 rpm
Cylinder distance	91 mm
Conrod length	138 mm
Main bearing diameter	55 mm
Main bearing width	25 mm
Main bearing mounting clearance	20 µm
Big-End bearing diameter	50 mm
Big-End bearing width	24 mm
Valve-train	DOHC
Timing drive	chain
Valve-train type	roller-type cam follower
Valves	4 per cylinder

It is important to note that all investigations were carried out using a modern SAE (Society of automotive engineers) 5W30 automotive lubricant with an HTHS (High-temperature high-shear-rate viscosity (defined as the dynamic viscosity of the lubricant measured at 150 °C and at a shear rate of 10^6 s^{-1})) viscosity of 3.57 mPas (The detailed oil data are listed in Table 2).

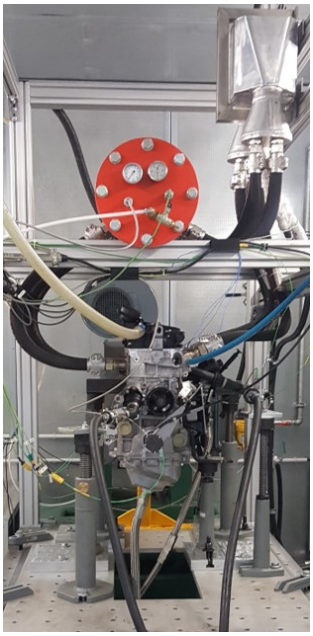

Figure 5. The engine on the dynamometer test rig.

The engine oil and coolant are provided by external supply units, and modifications are required on the oil module, oil pan, water pump, and oil- and coolant-circuits. Also, the coolant thermostat has been deactivated to ensure a full coolant flow. Figure 6 shows the deactivated water pump.

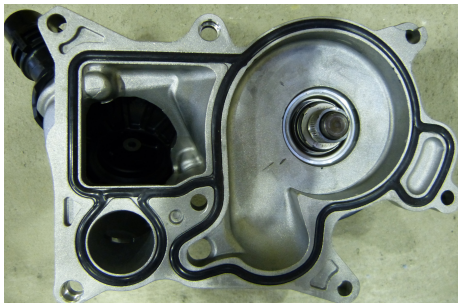

Figure 6. The deacitvated water pump.

The oil and coolant supply temperature and pressures are controlled within ± 0.1 °C and ± 0.05 bar, respectively. For the journal-bearing, simulation the main bearing temperatures for all tested operating points are required input parameters besides the measured cylinder pressures and bearing clearances. The bearing temperatures are measured in the high-load zone of the main bearings using type K thermocouples. As shown in Figure 7, three main bearing brackets are equipped with thermocouples.

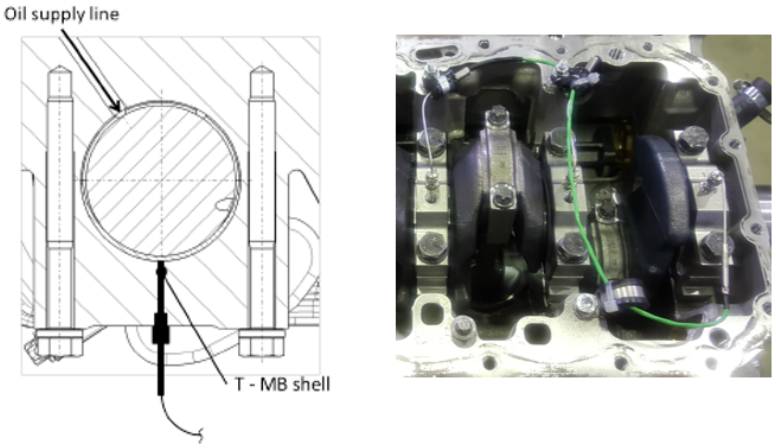

Figure 7. The measurement position of the main bearing temperatures: (**left**) A sectional view of the measuring point at the main bearing shell. (**right**) The mounted temperature sensors with cable guiding at the main bearing brackets 1, 2, and 3.

Bearing clearance measurements have been conducted at all five main bearings using measurement gauges. The conducted bearing clearance measurements result in bearing clearances of 20 µm. The high-pressure fuel pump is driven by the crankshaft utilizing a chain sprocket and the lower timing drive. As the friction losses of the fuel pump were not of interest, the connection of the chain sprocket to the pump shaft has been modified. Therefore, a ball bearing was mounted between the fuel pump drive shaft and chain sprocket to deactivate the high-pressure fuel pump drive (see Figure 8).

Lubricants **2019**, *7*, 39

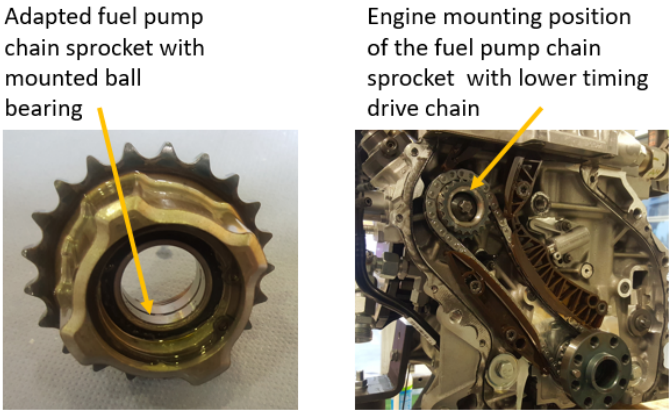

Figure 8. The deactivated fuel pump: (**left**) The adapted fuel pump chain sprocket. (**right**) The mounted fuel pump chain sprocket.

During the measurements, only a negligible contribution of the ball bearing comprised the friction torque of the engine [22].

3.2.1. Engine Preparations for Additional Torque Measurements

To separate the friction losses of the valve train from the overall base engine friction losses, supplementary measurements were conducted. For this task, the pistons and conrods were removed, and balancing weights were installed on the crank pins (see Figure 9). This was done to compensate the missing rotational mass forces of the conrods and to prevent excessive oil leakage from the otherwise open oil supply bores of the big-end bearings.

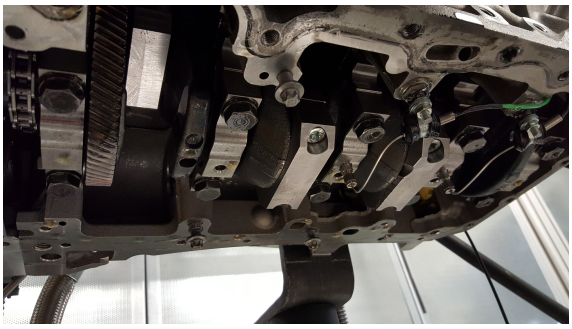

Figure 9. The mounted balancing weights at the crank pins.

The resulting valve train measurement setup includes the valve train, the timing drive (upper and lower), the ball bearing at the fuel pump chain sprocket, the crankshaft main bearings, and the crankshaft seals. As described in Section 2, the resulting valve train friction losses are calculated using Equation (2).

3.2.2. Engine Preparations for Crankshaft Seals Measurements

In the course of the measurement program, the friction torque of the crankshaft radial lip seals were analysed [18]. The measurements were performed with installed and with removed crankshaft seals. For a proper sealing of the engine crankcase during the tests, a simple sealing plug was installed on the FEAD (Front-end auxiliary drive) side of the engine. The sealing plug to seal the engine on the FEAD side is shown in Figure 10.

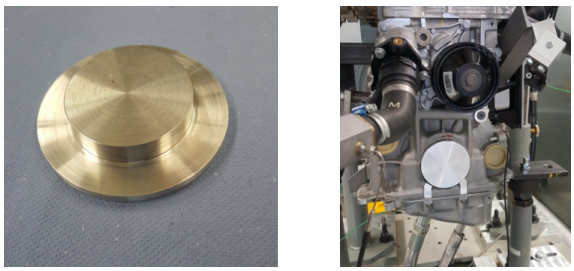

Figure 10. The sealing plug to prevent an oil leakage on the front-end auxiliary drive (FEAD) side of the engine.

A proper sealing of the engine on the flywheel side without a mounted crankshaft seal demands a special sealing apparatus to prevent an oil leakage. For this purpose, a custom sealing case was designed and realized and is shown in Figure 11.

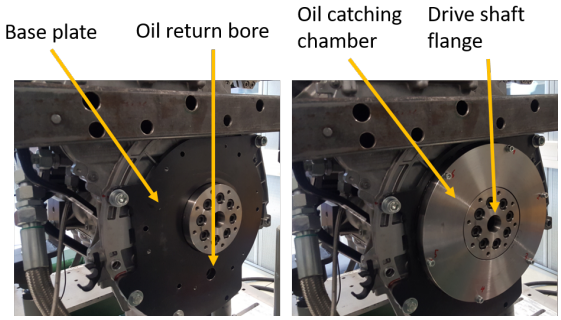

Figure 11. The realised crankshaft sealing system on the flywheel side.

For a complete description and detailed information about the realization of the sealing system, refer to Reference [18].

3.2.3. Engine Preparations for Crankshaft Measurements

The final strip-stage during the strip-test measurement campaign includes torque measurements of the crankshaft main bearings. Therefore, torque measurements were performed without a timing drive and crankshaft seals. This enables the possibility of comparing the main bearing simulation model with the experimental results of the base engine. For this task, the lower timing drive was deactivated by removing the lower drive chain and by deactivating the chain tension system. Figure 12 shows the engine on the flywheel side with an unmounted timing drive system.

Figure 12. The deacitvated timing drive system.

3.3. Testing Procedure

To investigate the friction losses of the base engine and its subassembly piston group, valve train, and crankshaft journal bearings, a wide range of tests were conducted. In the first step, engine friction map measurements to determine the FMEP of the base engine over the entire engine operation range were performed, and additional data for the journal-bearing simulation (cylinder pressure curves and journal-bearing temperatures) was collected. After the engine friction map measurements, a four-stage strip-test campaign was performed to determine the frictional losses of the subassemblies and to provide data for a comparison of the journal-bearing simulation results to the measurement results in a motoring operation of the crankshaft.

3.3.1. Measurement Program Base Engine

The base engine measurement program covers 120 different measurement points over a wide range of engine speeds and load points for three different engine media supply temperatures of 70 °C, 90 °C, and 110 °C. This results in detailed engine friction maps for different engine media supply temperatures. Figure 13 shows the performed measurement program both in the motored and load conditions.

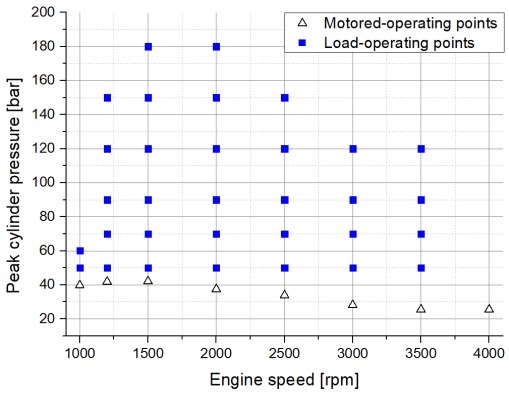

Figure 13. The realized measurement program (motored- and load-operating points).

Lubricants **2019**, *7*, 39

3.3.2. Additional Measurements: Strip-Test Procedure

To determine the frictional losses of the subassemblies, typically just one strip-test stage (strip-test stage 0) is necessary when applying the combined approach. Nevertheless, for this engine, additional measurements have been conducted to further separate the friction losses of the crankshaft seals, lower timing drive, and crankshaft journal bearings experimentally. Therefore, an extended strip-measurement campaign covering three additional strip-test stages has been conducted (see Figure 14). All strip-test stages have been investigated experimentally at engine media supply temperatures of 70 °C, 90 °C, and 110 °C to give detailed insight into the friction behaviour of the assemblies and components working under different thermal boundary conditions.

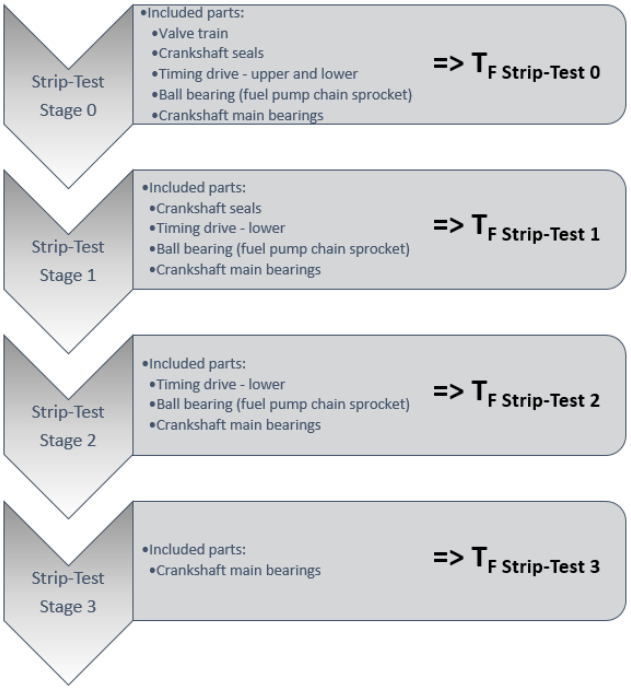

Figure 14. The measurement campaign for the additional torque measurements to determine the frictional losses of the subassemblies.

In the first strip-test stage (strip-test stage 0), the tests are performed after dismounting all pistons and conrods as well as all auxiliary devices (see Figure 2) resulting in friction torque $T_{\text{F Strip-Test 0}}$ which represents the basis for the determination of the valve train friction losses using the combined approach (see Equation (2)). In the next strip-test, stage 1 torque measurements are conducted without the valve train and the upper timing drive resulting in friction torque $T_{\text{F Strip-Test 1}}$. Equation (6) is used to calculate the resulting friction torque of the valve train and upper timing drive.

$$T_{\text{F Valve train and upper timing drive}} = T_{\text{F Strip-Test 0}} - T_{\text{F Strip-Test 1}} \quad (6)$$

After strip-test stage 1, the crankshaft radial lip seals have been dismounted and the friction torque $T_{\text{F Strip-Test 2}}$ was measured in strip test stage 2. The friction torque of the crankshaft seals are the results of using Equation (7) by a subtraction of the measured torques of strip-test stage 1 and strip-test stage 2.

$$T_{\text{F Crankshaft seals}} = T_{\text{F Strip-Test 1}} - T_{\text{F Strip-Test 2}} \tag{7}$$

Finally, in strip-test stage 3, the lower timing drive was unmounted and the friction torque $T_{\text{F Strip-Test 3}}$ of the crankshaft main bearings solely was measured. The friction losses of the lower timing drive are calculated using Equation (8).

$$T_{\text{F Lower timing drive}} = T_{\text{F Strip-Test 2}} - T_{\text{F Strip-Test 3}} \tag{8}$$

The particular results of the strip-measurements are plotted and discussed in the measurement results section.

3.4. Measurement Results

In this section, the results of the experimental investigations on the passenger-car diesel engine are presented. The measurement results are organised in the results of the base engine (engine friction maps) and the results of the conducted strip-measurement campaign. Due to the different engine media supply temperatures of 70 °C, 90 °C, and 110 °C, the influence of increased lubricant temperatures resulting in a lower lubricant viscosity is analysed.

3.4.1. Results Base Engine

The base engine friction map results are obtained at three different engine media supply temperatures covering 120 different measurement points. The resulting engine friction maps of the base engine are shown in Figure 15.

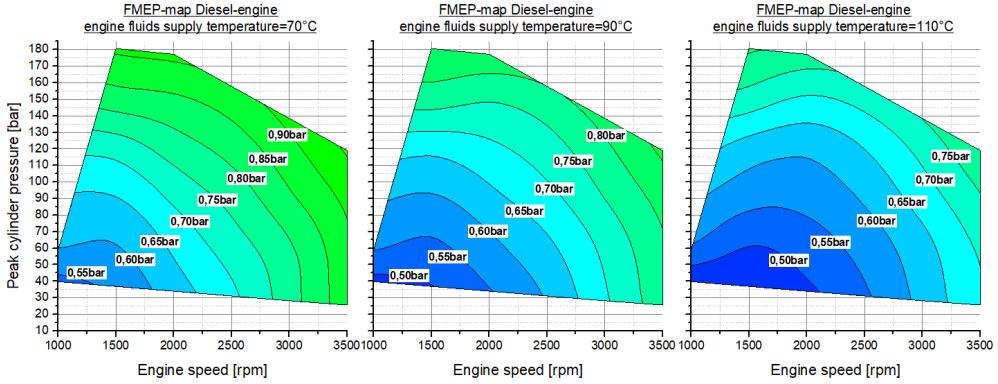

Figure 15. The resulting friction mean effective pressure (FMEP) maps for different engine media supply temperatures: (**left**) Supply temperature = 70 °C. (**middle**) Supply temperature = 90 °C. (**right**) Supply temperature = 110 °C.

The FMEP level of the modern diesel engine is generally low and comprises a good base engine performance regarding the mechanical efficiency. It is interesting to note that the highest FMEP-levels result at the lowest lubricant supply temperature of 70 °C and the lowest are at the highest lubricant supply temperature of 110 °C. The highest FMEP value of FMEP = 0.96 bar has been identified at an engine

speed of n = 3500 rpm and a peak cylinder pressure of 120 bar at an engine media supply temperature of 70 °C. The lowest FMEP results at the lowest engine speed of n = 1000 rpm with FMEP = 0.46 bar at the motored engine operation (pcyl = 40 bar) at an engine media supply temperature of 110 °C. With an increasing engine media supply temperature, the FMEP-level decreases over the entire engine speed and load range. By subtraction of the individual FMEP results between the different engine media supply temperatures, the friction reduction potential when increasing the engine media supply temperature can be calculated (see Figure 16).

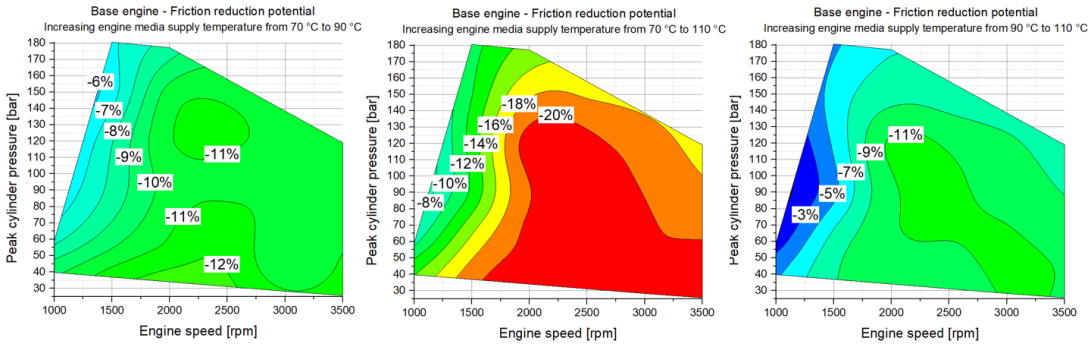

Figure 16. The friction reduction potential at the base engine when increasing the engine media supply temperature.

The increase in the engine media supply temperature shows advantages in the FMEP over the entire engine speed and load range. When increasing the engine media supply temperature from 70 °C to 90 °C, advantages up to 13% are investigated. At low engine speeds, the advantages of the FMEP are in the range of 6%. When increasing the engine media supply temperature from 70 °C to 110 °C, advantages of up to 21% in FMEP over a large area ranging from an engine speed of n = 1500 rpm up to n = 3500 rpm at part load conditions are observed. While the advantages at engine speeds higher than n = 1500 rpm are above 16%, they decrease at lower engine speeds. At an engine speed of n = 1000 rpm and load operation, the advantage in FMEP is 8%. It was further found that, when increasing the engine media supply temperature from 90 °C to 110 °C, the advantage at an engine speed of n = 1000 rpm is below 2% at load conditions.

The required journal-bearing temperatures for the journal-bearing simulations are measured in main bearings 1, 2, and 3 during all conducted measurements. Figure 17 shows the resulting temperatures at the main bearing shells in the high loaded zone (see Figure 7) determined during the engine friction map measurement campaign at an lubricant supply temperature of 90 °C.

As expected, the bearing temperatures show an influence on the engine speed and engine load whereupon the influence on the engine load is less distinctive. The highest bearing temperature was determined at an engine speed of n = 3500 rpm and high load conditions with 107 °C at main bearing 1. It is also interesting to note that the influence on the engine speed is less distinctive at main bearing 2. While at an engine speed of n = 3500 rpm, the main bearing temperature, at main bearing 1 and main bearing 3 are identical with 105.4 °C; the temperature at main bearing 2 is 100 °C. The results show that bearing temperature measurements at just one main bearing can lead to differences up to 5 °C in bearing temperature which are provided as input data to the journal-bearing, simulation affecting the calculated results of the journal-bearing friction losses.

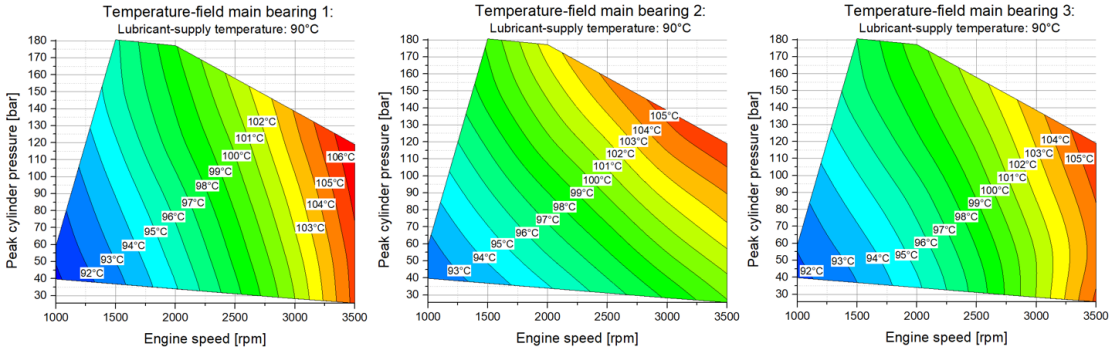

Figure 17. Measured main bearing temperatures: (**left**) Main bearing 1. (**middle**) Main bearing 2. (**right**) Main bearing 3.

3.4.2. Results Strip-Tests

The results of the strip-measurement campaign are presented under motored conditions ranging from an engine speed of n = 1000 rpm to n = 4000 rpm for three different engine media supply temperatures: 70 °C, 90 °C, and 110 °C. The results presented are the the calculated results of the individual strip-test stages from Equations (6)–(8) for the friction losses of the valve train (including the upper timing drive), crankshaft seals, and lower timing drive respectively. The individual measurement results of the strip-test stages are presented in Appendix A (Figures A1–A4).

Figure 18 shows the resulting friction torque of the valve train (including the upper timing drive) for three different engine media supply temperatures.

For engine speeds higher than n = 1500 rpm, the friction losses of the valve train and upper timing drive are almost constant over an engine speed ranging between 1.6 Nm and 1.75 Nm. At engine speeds lower than n = 1500 rpm, the friction torque shows a dependence on the engine media supply temperature. With an increasing engine media supply temperature, the friction torque also increases. Compared to 1.8 Nm at a supply temperature of 70 °C, the friction torque increases for a supply temperature of 90 °C and 110 °C to 2 Nm and 2.1 Nm, respectively. This indicates beginning mixed lubrication regimes at the investigated subassembly valve train (including the upper timing drive).

The outcome of the investigation of the crankshaft seals friction losses are presented in another publication and for further informations, refer to Reference [18]. For the sake of completeness, the resulting friction torque of the crankshaft seals are shown in Figure 19 for different engine media supply temperatures.

The determined friction losses of the lower timing drive are plotted in Figure 20 for 70 °C, 90 °C, and 110 °C engine media supply temperatures.

The friction torque of the lower timing drive is almost constant over the engine speed range from n = 1000 rpm to n = 4000 rpm ranging from 1.1 Nm to 1.3 Nm. A slight supply temperature dependence of the friction torque at engine speeds below n = 2000 rpm with differences in the friction torque of 0.14 Nm between supply temperatures of 70 °C and 110 °C was investigated. With an increasing engine media supply temperature, the friction torque increases from 1.1 Nm at n = 1000 rpm and a supply temperature of 70 °C to 1.24 Nm at a supply temperature of 110 °C. The friction torque results for a supply temperature of 90 °C are located between the results of 70 °C and 110 °C with 1.18 Nm. The friction torque of the lower timing drive also includes the friction loss of the ball bearing of the fuel pump chain sprocket. The grease-lubricated grooved ball bearing friction losses can be predicted from the manufacturers' information and literature. It is a minor friction contributor with a range of friction torque between 0.02 Nm to 0.04 Nm depending on the engine speed [22].

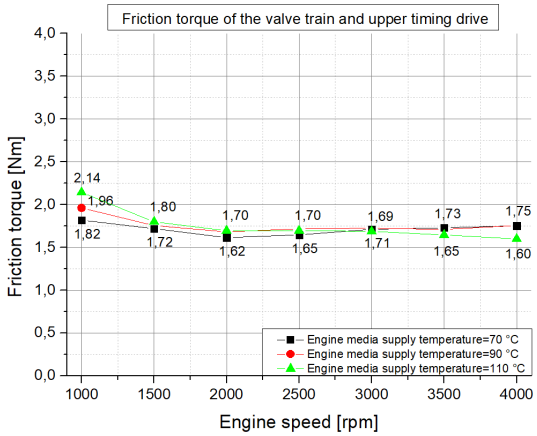

Figure 18. The resulting friction torque for different engine media supply temperatures: The valve train and upper timing drive using Equation (6).

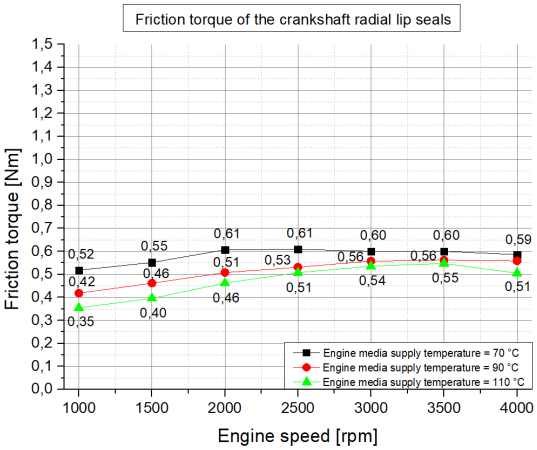

Figure 19. The resulting friction torque for different engine media supply temperatures: The crankshaft seals.

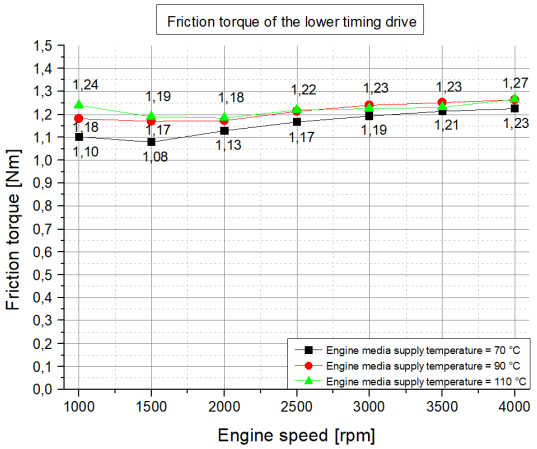

Figure 20. The resulting friction torque for different engine media supply temperatures: The lower timing drive.

Lubricants **2019**, *7*, 39

The last step of the strip-test campaign enables the investigation of the friction losses of the crankshaft main bearings in a strip-test configuration. Due to the used sealing system for measurements without mounted crankshaft seals, the friction torque of the main bearings solely can be obtained. Figure 21 shows the friction torque of the crankshaft main bearings over the engine speed for different engine media supply temperatures.

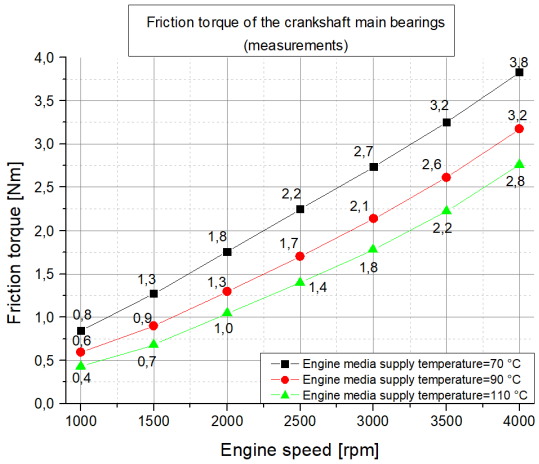

Figure 21. The resulting friction torque for different engine media supply temperatures: The crankshaft main bearings.

As expected, a strong influence of the engine speed was derived from the friction torque results plotted in Figure 21. Furthermore, a decrease in the friction torque with an increasing engine media supply temperature was investigated. The lowest friction torque occurs at the highest supply temperature of 110 °C ranging from 0.4 Nm at an engine speed of n = 1000 rpm to 2.8 Nm at an engine speed of 4000 rpm. The highest friction torque occurs at the lowest lubricant supply temperature of 70 °C ranging from 0.8 Nm at 1000 rpm to 3.8 Nm at 4000 rpm. The obtained friction torque measurements of the crankshaft main bearings can also be used for a verification of the calculated journal-bearing friction losses from the used simulation methodology. The results of the verification are presented in Section 4.1.

4. Journal-Bearing Friction Loss Simulation

The simulation approach for determining the friction losses of the crankshaft journal bearings consists basically of a elastic multi-body simulation with an isothermal description of the oil film using the Reynolds equation in combination with the approach of Greenwood and Tripp to describe the metal-to-metal contact. The simulation methodology was realised in numerous long-term research projects. It is capable of calculating the friction losses in journal bearings accurately as could be shown in a direct comparison to the experimental data [23,24]. In previous works, a wide range of aspects have been investigated and discussed like the extension of the simulation model to TEHD (Thermo elasto hydro dynamic) [25] simulations under severe mixed lubrication [26] or journal bearing simulations with new engine operation technologies like start/stop systems [27]. Also, the investigation of friction reduction potentials using low viscosity lubricants as well as the resulting possible risks due to increased mixed lubrication regimes have been conducted in the past using the developed simulation methodology [28,29]. In the following, a short summary is reproduced here for brevity, and for a rather complete overview, we refer to References [30–32]. To calculate the journal-bearing friction losses of the engine using the developed simulation approach, a engine model based on the MBS (Multi-body system) AVL Excite Power Unit (AVL EXCITE Power

Unit Version 2017.1, AVL List GmbH, Advanced Simulation Technology, Hans-List-Platz 1, 8020 Graz, Austria, www.avl.com.) was set up for the engine. The engine model consists of condensed FE (Finite element) structures of the crankshaft, main bearings, and connecting rods, with all bodies being elastically deformable and mass carried [33,34]. The following Figure 22 shows the schematic structure of the engine model for the journal-bearing simulations.

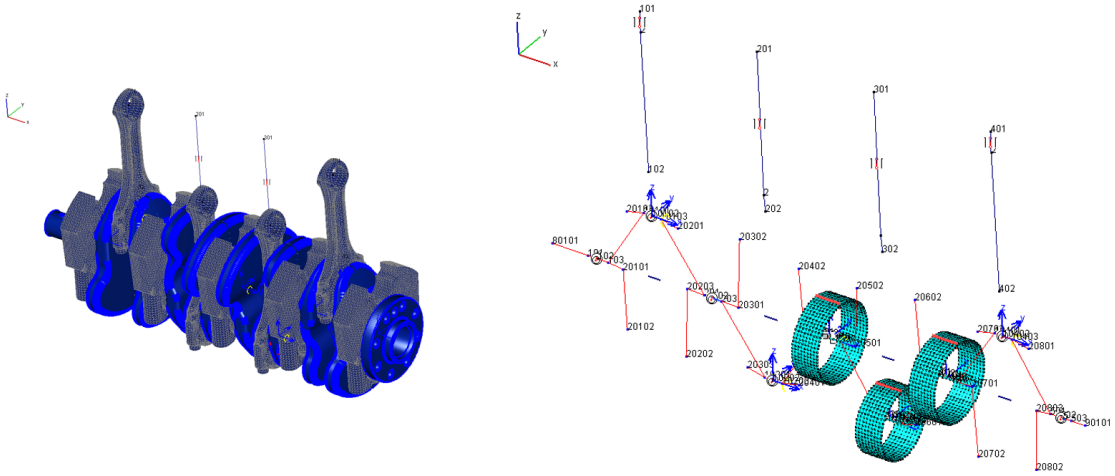

Figure 22. The engine model for the journal-bearing simulation: (**left**) The Finite Element model. (**right**) The condensed model.

Besides the geometrical dimensions (macro- and micro-geometry), the required input data for the journal-bearing simulation model are the main and big-end bearing temperature, the lubricant supply temperature and pressure, the cylinder pressure profile over the crank angle, and the engine speed which are provided from the experimental investigations on the motored test rig. The basic physical properties of the SAE 5W30 lubricant used in this work are listed in Table 2.

Table 2. The basic rheological properties of the lubricant.

SAE class	5W30
Density at 15 °C	853 kg/m^3
Dynamic viscosity at 40 °C	59.88 mPas
Dynamic viscosity at 100 °C	9.98 mPas
HTHS viscosity	3.57 mPas

HTHS: high-temperature high-shear-rate viscosity (defined as the dynamic viscosity of the lubricant measured at 150 °C and at a shear rate of 10^6 s^{-1}).

To describe the physical properties of the lubricant in the simulation model, an extensive rheological model is employed [35]. For the description of the pressure- and temperature-dependent density, the widely used Dowson/Higginson equation is used (see Equation (9)), applying the parameters listed in Table 3.

$$\rho(p,T) = \rho_0 \cdot \left(1 + \frac{f_1 \cdot p}{1 + f_2 \cdot p}\right) \cdot (1 - f_3 \cdot (T - T_0)) \quad (9)$$

Finally, Figure 23 shows the calculated density vs. temperature relation of the lubricant for different contact pressures.

Table 3. The rheological parameters for Equation (9) of the SAE 5W30 lubricant.

ρ_0	853	kg/m^3
T_0	15	°C
f_1	0.001	1/MPa
f_2	0.003	1/MPa
f_3	8.5×10^{-4}	1/°C

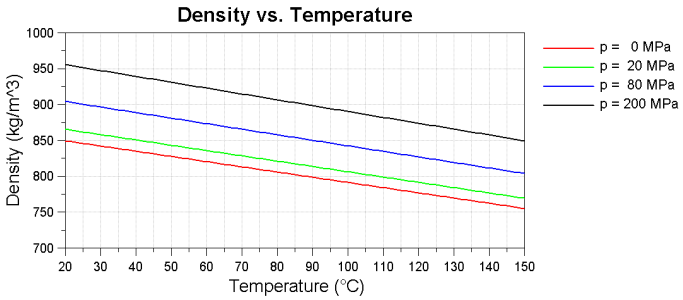

Figure 23. The calculated lubricant density.

Besides the description of the density–pressure relation using Equation 9, the description of the physical properties describing the influence on lubricant viscosity, the temperature dependence, the pressure dependence (piezoviscos effect), and the non-Newtonian behavior (the dependence of the viscosity on the local shear rate) of the modern multigrade lubricant is comprehensively taken into account in the calculation [24,36]. Using the Vogel equation [37] for the dependence on the temperature (T), the Barus equation [38] for the piezoviscous behaviour (p), and the Cross equation [39] to describe the influence of the shear-rate ($\dot{\gamma}$), the influences on the viscosity (η) can be described using Equation (10).

$$\eta(T, p, \dot{\gamma}) = A \cdot e^{\frac{B}{T+C}} \cdot e^{\alpha \cdot p} \cdot \left(r + \frac{1-r}{1+(K \cdot \dot{\gamma})^m} \right) \tag{10}$$

The applied parameters are listed in Table 4 and are calculated using results from previously published work [24] and from lubricant characteristics obtained from a conducted laboratory oil analysis.

Table 4. The rheological parameters for Equation (10) of the SAE 5W30 lubricant.

A	0.064	mPas
B	1124.7	°C
C	125.48	°C
m	0.79	-
α	0.0009	1/bar
r	0.75	-
K	3.5×10^{-7}	s

The computed viscosity behaviour including the influences of the lubricant temperature, contact pressure, and shear-rates are plotted in Figure 24.

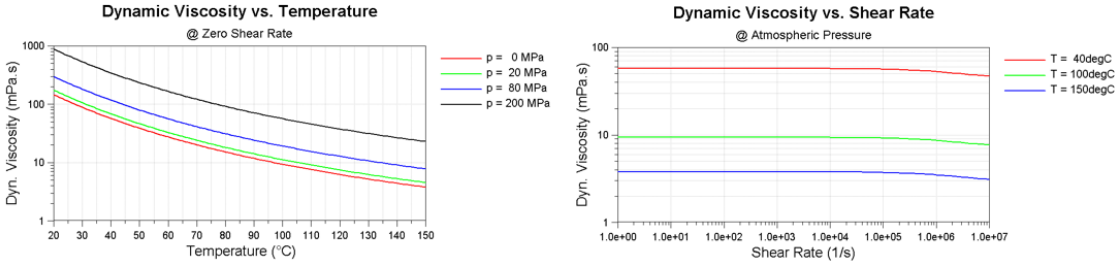

Figure 24. Lubricant viscosity dependences: (**left**) The viscosity–temperature curve for different contact pressures. (**right**) The viscosity–shear rate curves for different temperatures.

As the simulation model is carried out as an EHD (Elasto hydro dynamic)-calculation, a global bearing temperature has to be defined, which represents a suitable compromise for the entire journal bearing (hot oil temperature in the high loaded zone and cooler oil temperature in the non-loaded zone). In recent projects, a methodology to calculate an equivalent temperature was developed [24,25]. Therefore, thermal processes and heat flows have been investigated [25] using measurements and simulations. To describe the equivalent temperature of the journal bearing, measured temperatures (oil supply temperature and main bearing shell temperature) are used.

$$T_{\text{Equiv}} = T_{\text{MB Shell}} - \left(\frac{T_{\text{MB Shell}} - T_{\text{MB Supply}}}{4} \right) \tag{11}$$

where $T_{\text{MB Supply}}$ is the lubricant supply temperature and $T_{\text{MB Shell}}$ is the temperature in the high load zone of the main bearing. Using Equation (11) results in the equivalent temperature of the journal bearing. $T_{\text{MB Supply}}$ and $T_{\text{MB Shell}}$ are provided from the experimental investigations on the motored test rig. By applying temperature sensors at the individual main bearings during the experiments (see Figure 7), the equivalent main bearing temperatures of the individual main bearings can be calculated and provided to the journal-bearing simulation model. Due to the higher loads acting on the big-end bearings, they have to work at increased temperatures compared to the main bearings. Published experimental data show an increase in the big-end temperature at the bearing shell of about 3–5 °C compared to the main bearings [40]. Nowadays, modern diesel engines work under much higher bearing loads, and therefore, a further increase of the big-end bearing temperatures is expected. Recent results from measurements at journal-bearing test rigs confirm these expectations [23,24]. For that reason, the temperatures of the big-end bearings are approximated to be about 7 °C higher than the calculated equivalent temperatures of the main bearings. Figure 25 shows the resulting equivalent bearing temperature for main bearing 2 and the big-end bearing 2. For the sake of completeness, the calculated equivalent bearing temperatures for main bearing 1 and main bearing 3 are presented in Appendix A in Figure A5.

While the adjustment of a few single degree Celsius only has a marginal influence on the results, the usage of the measured main bearing shell temperatures is significant because the deviation between the oil supply temperature and bearing shell temperature can easily be above 20 °C, resulting in major reductions of the lubricant viscosity (see Figure 24). As can be seen from the shown temperatures, there is a strong dependence on the engine speed and load present that counteracts the increase in the friction power losses of the journal bearings at high engine speeds and loads.

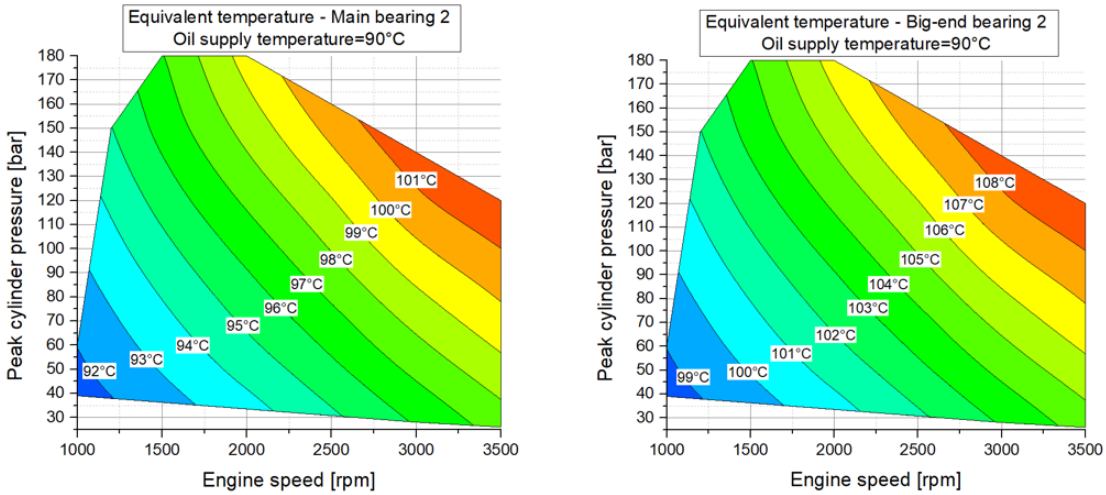

Figure 25. The equivalent temperatures for the isothermal journal-bearing simulation for main bearing 2 and big-end bearing 2 calculated using Equation (11).

4.1. Simulation Results

The calculation of the journal-bearing friction losses using the developed simulation methodology was carried out for the equal engine operation points of the measurement campaign (see Figure 13) for three different engine media supply temperatures: 70 °C, 90 °C, and 110 °C. Consequently, 120 different engine operation points have been calculated to obtain the crankshaft journal-bearing friction losses. The resulting FMEP of the main- and big-end bearings for an engine media supply temperature of 90 °C is shown in Figure 26.

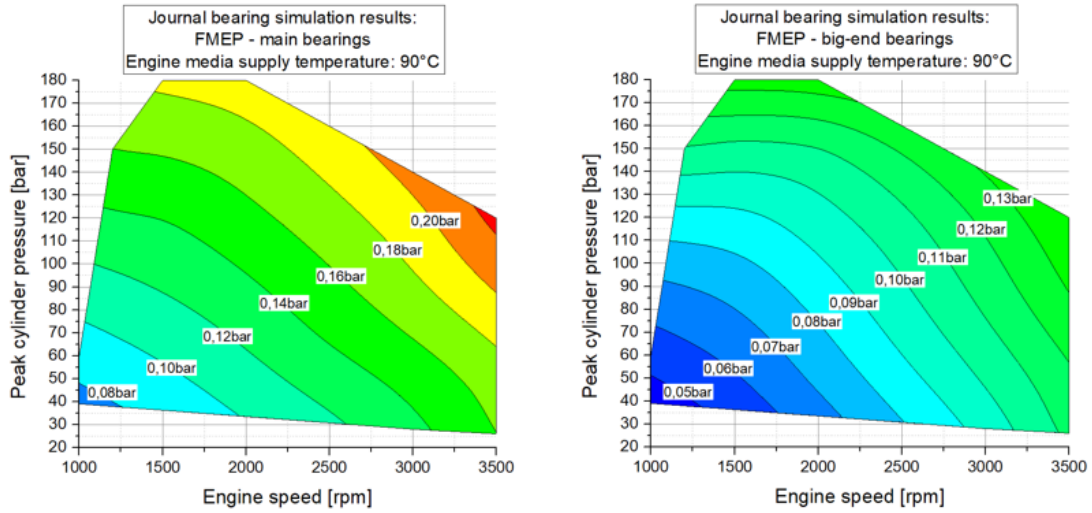

Figure 26. The resulting FMEP using the journal-bearing simulation method: (**left**) Main bearings. (**right**) Big-end bearings.

The results in Figure 26 show the determined FMEP of the five main bearings ranging from 0.07 bar at an engine speed of n = 1000 rpm in a motored operation to 0.23 bar at an engine speed of n = 3500 rpm

at an peak cylinder pressure of 120 bar. The friction losses of the four big-end bearings range from 0.04 bar at an engine speed of n = 1000 rpm in a motored operation to 0.14 bar at an engine speed of n = 3500 rpm at a peak cylinder pressure of 120 bar. The resulting FMEP of the main and big-end bearings at a lubricant supply temperature of 70 °C and 110 °C can be found in Appendix A for the sake of completeness and are plotted in Figures A6 and A7. In addition, it is interesting to investigate the friction reduction potential when increasing the engine media supply temperature. Due to the calculation at different lubricant supply temperature levels, 70 °C, 90 °C, and 110 °C, this was realized and the results are shown in Figure 27.

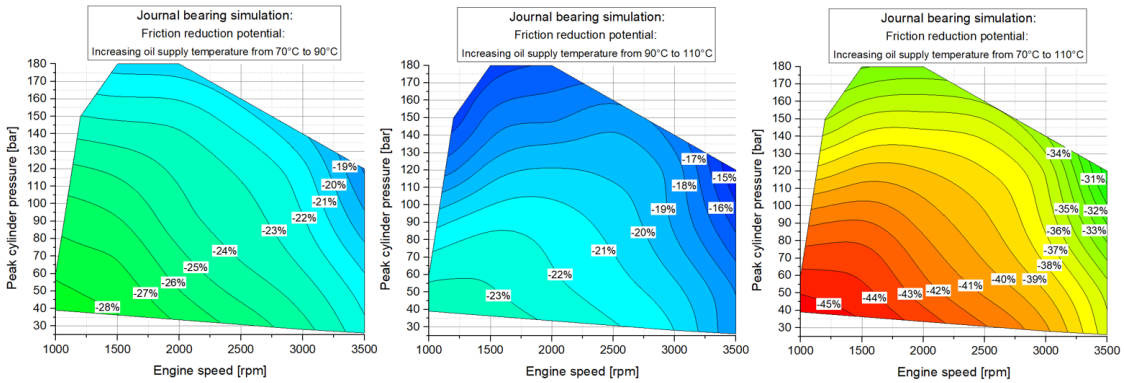

Figure 27. The friction reduction potential when increasing the oil supply temperature.

The most significant friction reduction potential for the crankshaft journal bearings has been observed when the supply temperature is increased from 70 °C to 110 °C at engine speeds below n = 2000 rpm and at peak cylinder pressures smaller 80 bar. Here, the maximum friction reduction with more than 45% could be determined. It was further found that, at the crankshaft journal bearings, no mentionable mixed lubrication regime occurred over the entire investigated engine speed and load range.

Simulation Results: Supplementary Torque Measurement Configuration (Strip-Test Stage 0)

To obtain the valve train friction losses using Equation (2) of the developed combined friction break down approach, the journal-bearing friction losses at the engine configuration for strip-test stage 0 (without pistons and conrods but with the mass of the master weights at the crank pins) have been calculated. The resulting FMEP of the journal-bearing simulations in a strip-test stage 0 configuration is shown in Figure 28 over the engine speed for different lubricant supply temperatures.

When comparing the calculated journal bearing friction losses to the results from the conventional base engine model, the strip-test stage 0 configuration shows a decreased FMEP level. This can be stated to the missing load transmitted by the pistons and conrods, which are not installed during the strip-test stage 0 investigations. Also, a clear temperature dependency is found in Figure 28, where the highest friction losses occur at the lowest lubricant supply temperature and the lowest friction levels are investigated at the highest supply temperature. A possible explanation for this result is the decreasing viscosity of the lubricant with an increasing temperature (see Figure 24), which yields a strong decrease of the hydrodynamic friction losses. In addition, high shear rates at high engine speeds are further responsible for a decreasing behaviour of the lubricant viscosity, which results in a continuing reduction of the journal-bearing friction losses as long as no severe mixed lubrication is present.

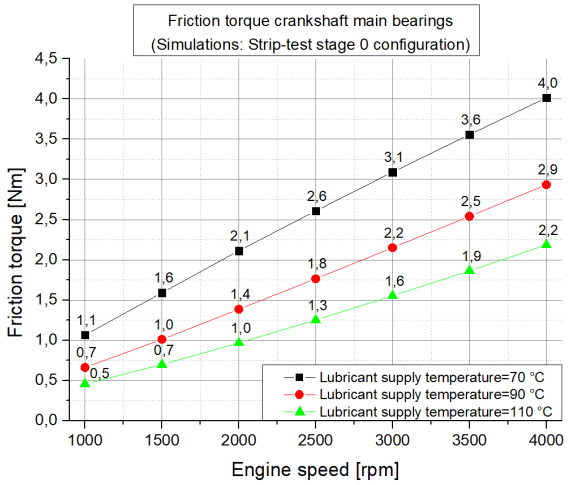

Figure 28. The resulting friction torque using the journal-bearing simulation method: The strip-test stage 0 configuration.

Another investigation using the calculated friction losses of the journal-bearing simulation can be conducted when performing comparisons to the conducted measurements. Therefore, the results of the calculations with the journal-bearing simulation model in the strip test stage 0 configuration (see Figure 28) have been compared to the measurement results in the engine strip-test stage 3 configuration (see Figure 21). Figure 29 shows the comparison carried out for a lubricant supply temperature of 90 °C.

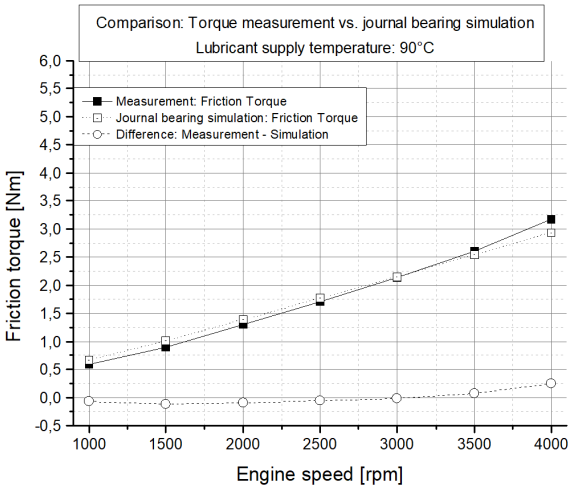

Figure 29. A comparison between the measurement and journal-bearing simulation for a lubricant supply temperature of 90 °C.

The comparison of the journal bearing simulation with the measurement data shows a good compliance over the investigated engine operation points. The deviation in friction torque between the measurement and simulation at an lubricant supply temperature of 90 °C is within 0.1 Nm up to an engine speed of n = 3500 rpm and 0.24 Nm at n = 4000 rpm. It is important to mention that no specific matching between the developed simulation methodology and the measurement results has

Lubricants **2019**, *7*, 39

been conducted. For brevity, the comparison for a lubricant supply temperature of 70 °C and 110 °C are presented in Appendix A in Figure A8.

Summarizing, it is concluded that the conducted comparisons between the measurements in strip-test stage 3 and the journal-bearing simulation represent the worst case scenarios for the developed journal-bearing simulation methodology. The reason for that is that the validation process during the development of the journal-bearing simulation model has been performed with the experimental data from journal-bearing test-rig measurements where the bearing load is a dominant factor for the resulting journal-bearing friction losses. For that reason, it can be expected that the calculation results of the journal-bearing friction losses are significantly improved for load conditions using the simulation model of the base engine including the conventional crank train.

5. Applying the Combined Approach: A Subassembly-Resolved Friction Loss Distribution

In the following section, the results of the friction loss investigations conducted in the passenger-car diesel engine (for specifications, see Table 1) using the combined approach are presented and discussed. In the first part, the results of the valve train friction losses (including the timing drive and crankshaft seals) using the combined friction analysis approach will be presented. In the second part, the subassembly-resolved friction analysis of the base engine, namely crankshaft journal bearings, valve train, and piston group, are described for different engine operation conditions.

5.1. Resulting Valve Train Friction Losses Using the Combined Friction Analysis Approach

One of the main advantages when using the developed combined approach to analyse the friction losses is the possibility to determine the valve train friction losses with a reduced experimental afford during the conducted friction tests at the motored engine test rig. Therefore, the extended valve train friction losses are obtained using the measurement results of engine strip-stage 0 (see Figure 2) in combination with the calculated friction losses of the journal-bearings simulation methodology by applying Equation (2). It is important to note that the friction losses of the timing drive and the crankshaft seals are included in the valve train results when using the combined approach which are shown in Figure 30. This needs to be taken into account and attention has to be spent to not compare the results of the combined approach to the results from the experimental strip-test campaign presented in Figure 18.

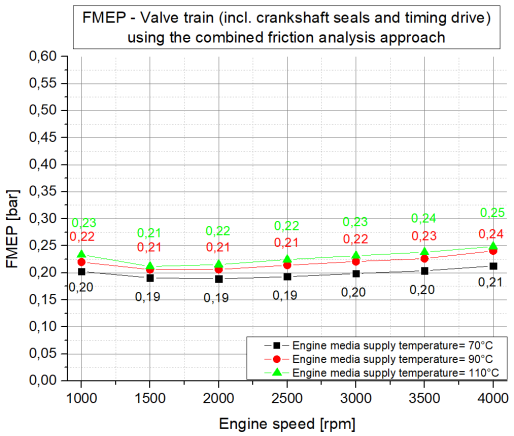

Figure 30. The resulting FMEP: The valve train (including the crankshaft seals and timing drive) for different engine media supply temperatures.

Lubricants **2019**, *7*, 39

The resulting FMEP of the valve train (including the timing drive and crankshaft seals) shows a slight temperature dependence in the range of ΔFMEP = 0.03 bar at n = 1000 rpm and ΔFMEP = 0.04 bar at n = 4000 rpm between a lubricant supply temperature of 70 °C and 110 °C. The overall FMEP level is nearly constant over an engine speed ranging between ΔFMEP = 0.02 bar between n = 1000 rpm and n = 4000 rpm at the individual lubricant supply temperatures of 70 °C, 90 °C, and 110 °C. The determined valve train friction losses with timing drive and crankshaft seals included are used to calculate and allocate the subassembly friction losses according to Equation (3).

5.2. Subassembly-Resolved Friction Loss Distribution for the Base Engine

After the determination of the base engine friction map, the valve train friction losses using the combined approach, and the calculation of the journal-bearing friction losses, it is possible to perform the subassembly-resolved friction loss analysis of the base engine. Therefore, the basic equation of the combined approach according to Equation (3) is used to calculate the friction losses of the piston group. Figure 31 shows the results of the subassembly-resolved friction losses of the base engine for a motoring operation and different engine media supply temperatures.

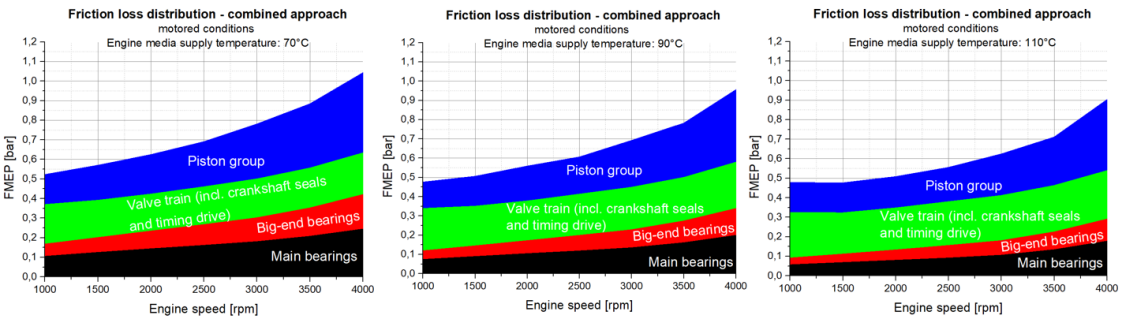

Figure 31. The friction loss distribution using the combined approach for different engine media supply temperatures—motored conditions.

Figure 31 shows a typical friction loss distribution for an engine speed of n = 4000 rpm, where the piston group has the highest FMEP share of about 40% followed by the crankshaft journal bearings with 35% and the valve train with about 25%. In contrast, at the lowest engine speed, the FMEP share is inverted compared to the results at n = 4000 rpm. At an engine speed of n = 1000 rpm and an engine media supply temperature of 110 °C, the valve train friction losses (including timing drive and crankshaft seals) are dominating with an FMEP share of up to 49% followed by the piston group with 32% and the crankshaft journal bearings with 19%. It is further interesting to note that the friction losses of the piston group and crankshaft journal bearings show a strong increase over the engine speed, whereas the friction losses of the valve train are rather constant for engine speeds higher n = 1500 rpm. For engine speeds smaller than n = 1500 rpm, a slight increase in the FMEP level of the valve train could be observed. It was found that the friction losses of the piston group and the crankshaft journal bearings decrease with an increasing engine media supply temperature, but the valve train friction losses showed a slight increase. A possible explanation for this result is that the friction losses of the crankshaft journal bearings and the piston group are dominated by hydrodynamic friction losses while in the subassembly valve train (including timing drive and crankshaft seals), mixed lubrication regimes occur leading to higher friction losses at increased lubricant supply temperatures and low rotational speeds.

The main advantage of applying the combined approach is that the friction loss distribution can be conducted also at a loaded engine operation. An analysis under the load operation has been done for all

investigated engine speeds according to the base engine measurement program (see Figure 13), and Figure 32 presents the results at an engine speed of n = 1200 rpm for different engine media supply temperatures.

The crankshaft journal bearings and the piston group revealed an increase of the friction losses with an increasing load and a decrease of the friction losses when increasing the lubricant supply temperature. This indicates that the journal bearings and the piston group are operating mainly in a hydrodynamic lubrication regime without excessive mixed lubrication. As already described in the discussion on the motored friction loss distribution results, the valve train friction loss shares slightly increase with an increasing engine media supply temperature. The FMEP share for high load conditions at an engine media supply temperature of 70 °C is dominated by the crankshaft journal-bearings friction losses of 42% followed by the piston group with 34% and the valve train with 24%. At an engine media supply temperature of 110 °C and high load conditions, the FMEP share of the piston group is 39% followed by the crankshaft journal bearings with 31% and the valve train with 30%.

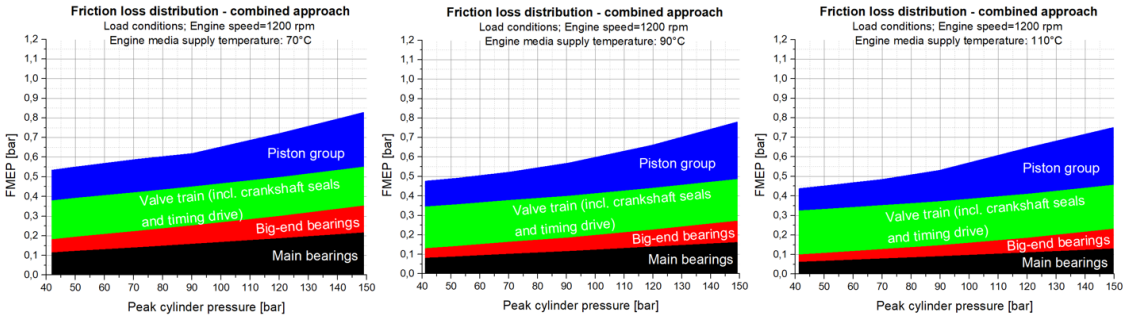

Figure 32. The friction loss distribution using the combined approach for different engine media supply temperatures—engine speed n = 1200 rpm, load conditions.

Figure 33 presents FMEP results over the engine load at an engine speed of n = 3500 rpm for different engine media supply temperatures of 70 °C, 90 °C, and 110 °C.

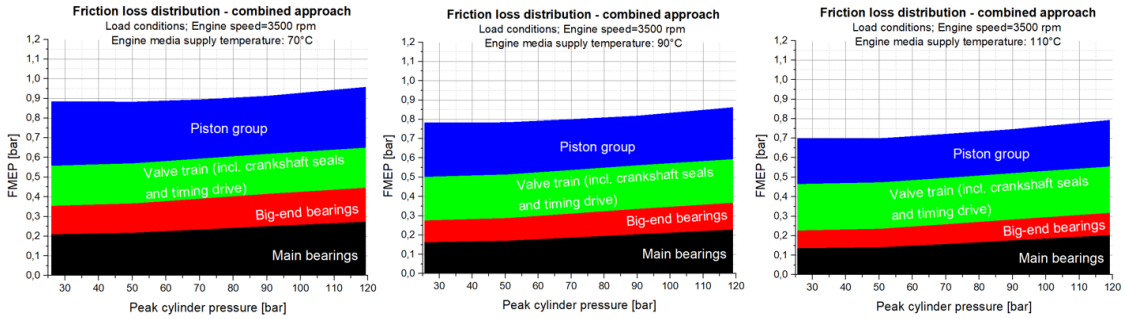

Figure 33. The friction loss distribution using the combined approach for different engine media supply temperatures—engine speed n = 3500 rpm, load conditions.

As expected, the friction level for the increased engine speed of n = 3500 rpm increased to FMEP = 0.9 bar at an engine media supply temperature of 70 °C. Also, in terms of the influence of acting gas forces, the friction losses of the piston group slightly decreased when the gas pressure partly compensated the acting mass forces of the piston group in low load conditions up to peak cylinder pressures of 50 bar. It was found that the friction losses of the crankshaft journal bearings as well as the piston group showed only small influences on the engine load at this engine speed level. The FMEP share at high load conditions at

an engine media supply temperature of 70 °C was dominated by the crankshaft journal-bearings friction losses of 46% followed by the piston group with 32% and the valve train with 22%. At an engine media supply temperature of 110 °C and high load conditions, the FMEP share of the crankshaft journal bearings was 40% followed by the piston group with 30% and the valve train with 30%. Summarizing, it can be said that the piston group of this engine was very efficient in terms of friction losses. Also, at very high engine loads in combination with high engine media supply temperatures, no increased FMEP could be investigated. It can also be found in the literature [41] that the piston group of this engine was friction-loss-optimized by increasing the piston clearance while lowering the piston pin offset. In addition, shorter ring heights in combination with lower tangential forces of the piston rings and friction reducing piston skirt coating was used to optimize the crank train. In another publication [16] where investigations on the friction loss potentials of the piston group were performed and analysed, it was also shown that the piston installation clearance had a marginal influence on the friction losses of the piston group among other design parameters.

6. Conclusions

A combined approach using measurements and a simulation to determine the friction power losses of a modern passenger-car diesel engine was used to analyse the tribological behaviour of the base engine and its subassembly crankshaft journal bearings, valve train, and piston group over the entire engine speed and load operation conditions. The approach brought together the experimental data resulting from engine friction measurements and predictive journal bearing friction loss simulations. The experimental tests were conducted using a motored engine test bed with external charging and an air recirculation system to improve the thermal boundary conditions of the piston group. The measurements were performed for different engine media supply temperatures varying between 70 °C and 110 °C to determine the tribological engine performance under changing thermal boundary conditions. In addition, a four stage strip-measurement campaign was conducted for this engine to experimentally analyse the friction losses of the valve train (including upper timing drive), lower timing drive, crankshaft seals, and crankshaft main bearings.

For the simulation part, a simulation model of the engine was created using detailed geometry, surface, and lubricant data using the approach developed by the authors that is well-documented and has a proven accuracy.

The experimental tests show that, for the entire base engine, a friction reduction potential above 20% could be realized by increasing the engine media supply temperatures from 70 °C to 110 °C. This showed that, especially for new engine modes of operation like start/stop systems and more advanced strategies like early engine stopping (e.g., at vehicle speeds below 30 km/h) using hybridization, challenges arise for the thermal management systems to keep oil temperatures at desired high levels to decrease the friction losses of the combustion engine and to maintain an optimal fuel economy. The usage of low viscosity lubricants could further improve the friction losses of the engine, especially when operating the engine at low lubricant temperatures. However, at the same time, care had to be taken regarding increased mixed lubrication in particular for low engine speeds and high lubricant supply temperatures.

The assignment of friction reduction potentials to the base engine subassemblies was possible in great detail due to the usage of the combined numerical/testing approach and the conducted extensive strip-test campaign. The main subassemblies that showed decreasing friction losses with an increasing the engine media supply temperature were the crankshaft journal bearings and the piston group. The valve train as well as the lower timing drive and crankshaft seal rings showed a rather constant level of the friction losses at engine speeds higher than 2000 rpm. While the friction torque of the crankshaft seals was slightly decreasing for engine speeds lower than 2000 rpm when increasing the lubricant supply temperatures,

the lower timing drive and the valve train showed a different behaviour. The friction torques of the lower timing drive and the valve train were increasing with an increasing lubricant supply temperature at engine speeds lower than 2000 rpm. The most significant increase could be observed at the lowest investigated engine speed of 1000 rpm. For these subassemblies, care needed to be taken regarding mixed lubrication regimes when further increasing the lubricant supply temperature and, in addition, decreasing the engine speed, resulting in low rotational shaft speeds (especially for the performance of the valve train which was working at half the speed of the crankshaft due to the required gear reduction for the timing of the engine control). Also, when considering the usage of low viscosity lubricants, the impact on the friction losses of the valve train and timing drive needed to be carefully investigated. Finally, it can be said that the piston group of the investigated diesel engine showed a very good tribological performance even under very high loads and high lubricant supply temperatures. A possible explanation for this result is that the piston group had been particularly well friction-loss-optimized by increasing the piston clearance while lowering the piston pin offset. In addition, shorter ring heights in combination with lower tangential forces of the piston rings and friction reducing the piston skirt coating had been used to optimize the crank train.

As expected for an engine that is commercially sold in the thousands, some results from the simulation were that the friction losses of the main bearings and big-end bearings were dominated by the hydrodynamic friction losses and that no severe mixed lubrication occurred for the journal bearings over the investigated engine operation range. In agreement with this result is that friction reduction potentials above 45% had been determined for the main and big-end journal bearings when increasing the lubricant supply temperatures from 70 °C to 110 °C.

The measurement of the crankshaft main bearings friction losses solely during the additionally conducted strip-test campaign enabled the verification of the utilization of the journal-bearing simulation approach in a crankshaft system for the first time. The verification between the measurement and simulation showed a good agreement of the results with a maximum deviation in the friction torque of 0.24 Nm at an engine speed of 4000 rpm and an engine media supply temperature of 90 °C. At lower engine speeds, the results were within 0.1 Nm, which confirms the good applicability of the previously developed journal-bearing simulation method.

Summarizing, the combined approach used in this work can be applied to analyse in detail the friction losses of reciprocating engines and its subassemblies crankshaft journal bearings, valve train, and piston group. This analysis can be conducted over the entire engine speed and load range for different thermal boundary conditions with a high accuracy and enables the analysis of the influence of friction reduction measures like low viscosity oils, design parameter variants of the crank train components, or comparisons between different engine concepts.

Author Contributions: C.K., H.A. and D.E.S. conceived and designed the experiments; C.K., H.A. and D.E.S. performed the experiments; C.K. and D.E.S. build up the simulation models; C.K. performed the calculations; All authors analysed and discussed the data; C.K. wrote the paper; D.E.S. and H.A. reviewed and edited the paper.

Acknowledgments: The publication was written at VIRTUAL VEHICLE Research Center in Graz and was partially funded by the COMET K2—Competence Centers for Excellent Technologies Programme of the Federal Ministry for Transport, Innovation, and Technology (bmvit); the Federal Ministry for Digital, Business, and Enterprise (bmdw); the Austrian Research Promotion Agency (FFG); the Province of Styria; and the Styrian Business Promotion Agency (SFG). Furthermore, we acknowledge the partial financial support of the Austrian Science Fund (FWF): P27806-N30.

Conflicts of Interest: The authors declare no conflict of interest.

Lubricants **2019**, *7*, 39

Appendix A

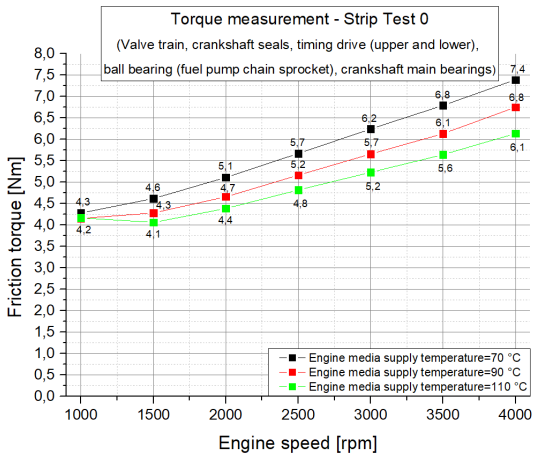

Figure A1. The resulting torque for different engine media supply temperatures: Strip-test stage 0.

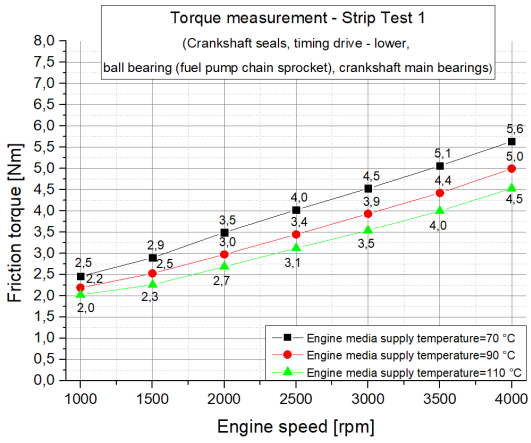

Figure A2. The resulting torque for different engine media supply temperatures: Strip-test stage 1.

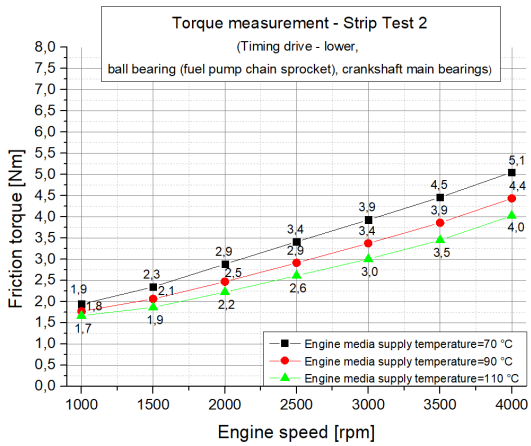

Figure A3. The resulting torque for different engine media supply temperatures: Strip-test stage 2.

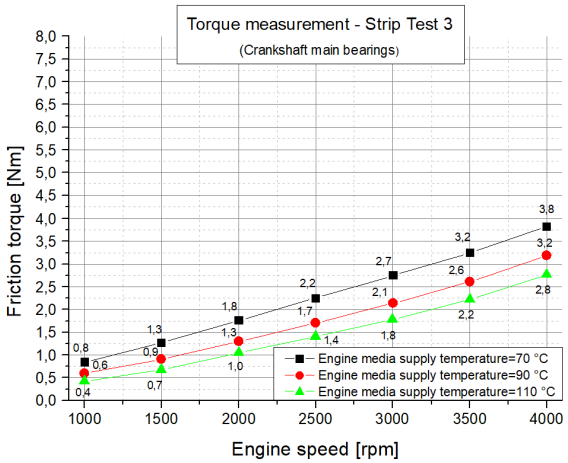

Figure A4. The resulting torque for different engine media supply temperatures: Strip-test stage 3.

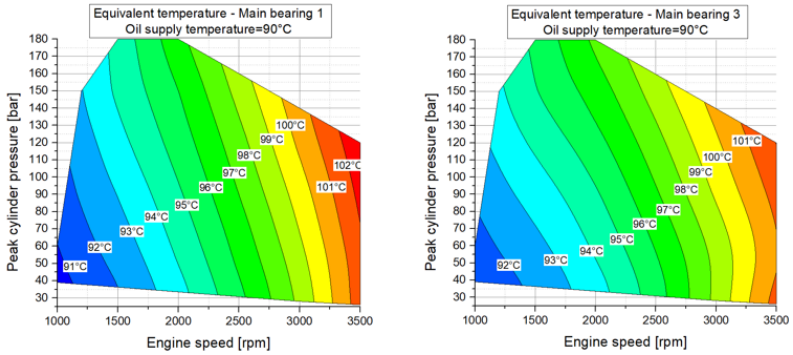

Figure A5. The equivalent temperature for the isothermal journal-bearing simulation for main bearing 1 and 3 calculated using Equation (11).

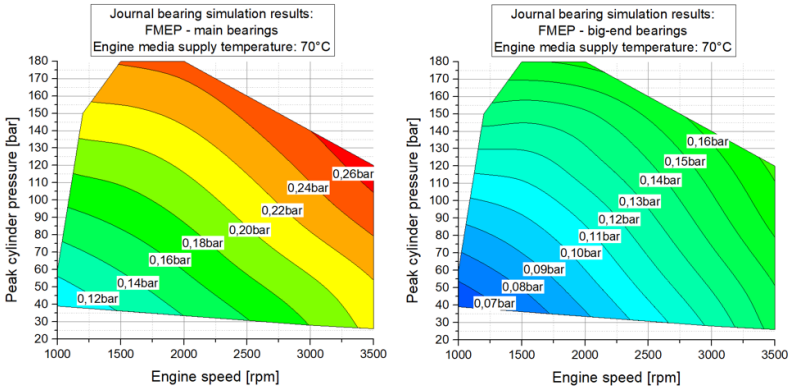

Figure A6. The resulting FMEP using the journal-bearing simulation method for main bearings and big-end bearings: lubricant supply temperature 70 °C.

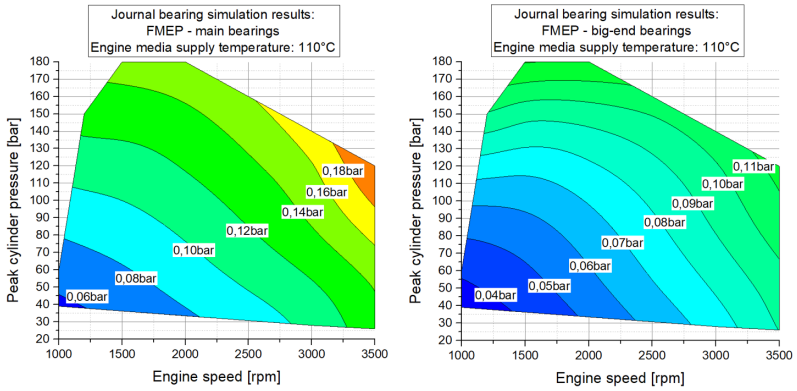

Figure A7. The resulting FMEP using the journal-bearing simulation method for main bearings and big-end bearings: lubricant supply temperature 110 °C.

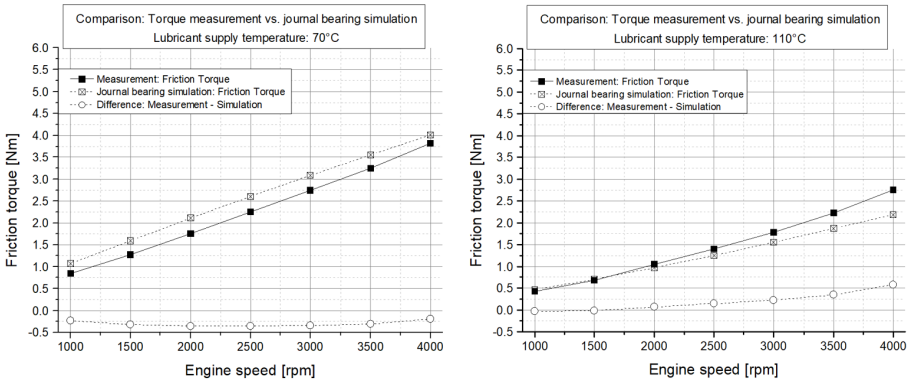

Figure A8. A comparison between the measurement and journal-bearing simulation for a lubricant supply temperature of 70 °C and 110 °C.

References

1. Holmberg, K.; Andersson, P.; Erdemir, A. Global energy consumption due to friction in passenger cars. *Tribol. Int.* **2012**, *47*, 221–234. [CrossRef]
2. Schwaderlapp, M.; Dohmen, J.; Janssen, P.; Schürmann, G. Friction Reduction–The contribution of engine mechanics to fuel consumption reduction of powertrains. In Proceedings of the 22nd Aachen Colloquium Automobile and Engine Technology, Aachen, Germany, 7–9 October 2013; pp. 1273–1292.
3. Chmela, F.; Pirker, G.; Wimmer, A. Grundlagen der Motorprozessrechnung. In *Grundlagen Verbrennungsmotoren—Funktionsweise, Simulation, Messtechnik*; Merker, G.P., Teichmann, R., Eds.; Springer Fachmedien: Wiesbaden, Germany, 2014; pp. 633–707.
4. Fischer, G.D. Expertenmodell zur Berechnung der Reibungsverluste von Ottomotoren. Ph.D. Thesis, Technische Universität Darmstadt, Darmstadt, Germany, 2000.
5. Schwarzmeier, M. Der Einfluss des Arbeitsprozeßverlaufs auf den Reibmitteldruck von Dieselmotoren. Ph.D. Thesis, Technische Universität München, München, Germany, 1992.
6. Dowson, D.; Taylor, C.M.; Yang, L. Friction Modelling for Internal Combustion Engines. In *The Third Body Concept Interpretation of Tribological Phenomena*; Dowson, D., Taylor, C.M., Childs, T.H.C., Dalmaz, G., Berthier, Y., Flamand, L., Georges, J.-M., Lubrecht, A.A., Eds.; Elsevier Science B.V.: Amsterdam, The Netherlands, 1996; pp. 301–318.

7. Wichtl, R.; Schneider, R.; Grabner, P.; Eichlseder, H. Experimental and Simulative Friction Analysis of a Fired Passenger Car Diesel Engine with Focus on the Cranktrain. *SAE Int. J. Engines* **2016**, *9*, 2227–2241. [CrossRef]
8. Wichtl, R.; Eichlseder, H.; Mallinger, W.; Peterek, R. Friction Investigations on the Diesel Engine in Combustion Mode A New Measuring Method. *MTZ Worldw.* **2017**, *78*, 26–31. [CrossRef]
9. Lösch, S.; Priestner, C.; Thonhauser, B.; Zieher, F.; Hick, H. Advances in Determination of Piston Group Friction Losses at High Speeds and Loads using the AVL FRISC Single-Cylinder Engine. In Proceedings of the Reibungsminimierung im Antriebsstrang, Esslingen am Neckar, Germany, 1–2 December 2015; pp. 184–202.
10. Ullmann, K. Die Reibungs- und Pumpverluste des schnellaufenden Otto- und Dieselmotors. *ATZ-Automobiltechnische Zeitschrift* **1939**, *42*, 397–406.
11. Ullmann, K. Die mechanischen Verluste des schnelllaufenden Dieselmotors und ihre Ermittlung im Schleppversuch. *Deutsche Kraftfahrtforschung* **1939**, *34*.
12. Caruana, C.; Farrugia, M.; Sammut, G. *The Determination of Motored Engine Friction by Use of Pressurized 'Shunt' Pipe between Exhaust and Intake Manifolds*; SAE Technical Paper 2018-01-0121; SAE International: Warrendale, PA, USA, 2018.
13. Mauke, D.; Dolt, R.; Stadler, J.; Huttinger, K.; Bargende, M. *Methods of Measuring Friction under Motored Conditions with External Charging*; Kistler Group: Winterthur, Switzerland, 2016.
14. Allmaier, H.; Knauder, C.; Sander, D.E.; Reich, F. Combination of Measurement and Simulation to Analyse Engine Friction. *MTZ Worldw.* **2016**, *77*, 66–71. [CrossRef]
15. Allmaier, H.; Knauder, C.; Salhofer, S.; Reich, F.M.; Schalk, E.; Wagner, A. An experimental study of the load and heat influence from combustion on engine friction. *Int. J. Engine Res.* **2016**, *17*, 347–353. [CrossRef]
16. Deuss, T.; Ehnis, H.; Freier, R.; Künzel, R. Friction power measurements of a fired diesel engine piston group potentials. *MTZ Worldw.* **2010**, *71*, 20–24. [CrossRef]
17. Sander, D.E.; Knauder, C.; Allmaier, H.; Damjanovic-Le Baleur, S.; Mallet, P. Friction Reduction Tested for a Downsized Diesel Engine with Low-Viscosity Lubricants Including a Novel Polyalkylene Glycol. *Lubricants* **2017**, *5*, 9. [CrossRef]
18. Knauder, C.; Allmaier, H.; Sander, D.E.; Sams, T. Measurement of the Crankshaft Seals Friction Losses in a Modern Passenger Car Diesel Engine. *Proc. Inst. Mech. Eng. J.* **2019**, under review.
19. Sander, D.E.; Allmaier, H.; Priebsch, H.H.; Reich, F.M. Determination of friction losses in combustion engines—Combination of measurement and validated EHD journal bearing simulation. In Proceedings of the VDI-Berichte 2202, Schweinfurt, Germany, 23–24 April 2013; pp. 165–175.
20. Knauder, C.; Allmaier, H.; Salhofer, S.; Sams, T. The impact of running-in on the friction of an automotive gasoline engine and in particular on its piston assembly and valve train. *Proc. Inst. Mech. Eng. J.* **2017**, *232*, 749–756. [CrossRef]
21. Teichmann, R.; Wimmer, A.; Winklhofer, E. Verbrennungsdiagnostik. In *Grundlagen Verbrennungsmotoren—Funktionsweise, Simulation, Messtechnik*; Merker, G.P., Teichmann, R., Eds.; Springer Fachmedien: Wiesbaden, Germany, 2014; pp. 549–629.
22. Meyer, C. Reibung in hoch belasteten EHD-Wälzkontakten. Ph.D. Thesis, Gottfried Wilhelm Leibniz Universität Hannover, Hannover, Germany, 2010.
23. Allmaier, H.; Priestner, C.; Six, C.; Priebsch, H.H.; Forstner, C.; Novotny-Farkas, F. Predicting friction reliably and accurately in journal bearings—A systematic validation of simulation results with experimental measurements. *Tribol. Int.* **2011**, *44*, 1151–1160. [CrossRef]
24. Sander, D.E.; Allmaier, H.; Priebsch, H.H.; Reich, F.M.; Witt, M.; Füllenbach, T.; Skiadas, A.; Brouwer, L.; Schwarze, H. Impact of high pressure and shear thinning on journal bearing friction. *Tribol. Int.* **2015**, *81*, 29–37. [CrossRef]
25. Allmaier, H.; Priestner, C.; Reich, F.M.; Priebsch, H.H.; Novotny-Farkas, F. Predicting friction reliably and accurately in journal bearings—Extending the simulation model to TEHD. *Tribol. Int.* **2013**, *58*, 20–28. [CrossRef]
26. Sander, D.E.; Allmaier, H.; Priebsch, H.H.; Witt, M.; Skiadas, A. Simulation of journal bearing friction in severe mixed lubrication—Validation and effect of surface smoothing due to running-in. *Tribol. Int.* **2016**, *96*, 173–183. [CrossRef]

27. Sander, D.E.; Allmaier, H.; Witt, M.; Skiadas, A. Journal Bearing Friction and Wear in Start/Stop Operation. *MTZ Worldw.* **2017**, *78*, 46–51. [CrossRef]
28. Knauder, C.; Allmaier, H.; Sander, D.E.; Salhofer, S.; Reich, F.M.; Sams, T. Analysis of the journal bearing friction losses in a heavy-duty diesel engine. *Lubricants* **2015**, *3*, 142–154. [CrossRef]
29. Sander, D.E.; Allmaier, H.; Knauder, C.; Strömstedt, F. Potentials and Risks of Reducing Friction with Future Ultra-low-viscosity Engine Oils. *MTZ Worldw.* **2018**, *79*, 20–27. [CrossRef]
30. Allmaier, H.; Priestner, C.; Sander, D.E.; Reich, F.M. Friction in automotive engines. In *Tribology in Engineering*; Pihtili, H., Ed.; Intech: Rijeka, Croatia, 2013; pp. 149–184.
31. Sander, D.E.; Allmaier, H.; Priebsch, H.H. Friction and Wear in Automotive Journal Bearings Operating in Today's Severe Conditions. In *Advances in Tribology*; Darji, P.H., Ed.; Intech: Rijeka, Croatia, 2016; pp. 143–172.
32. Sander, D.E. A Validated Elasto-Hydrodynamic Simulation for Journal Bearings Operating Under Severe Conditions. Ph.D. Thesis, Technische Universität Graz, Graz, Austria, 2016.
33. Offner, G. Modelling of condensed flexible bodies considering non-linear inertia effects resulting from gross motions. *Proc. Inst. Mech. Eng. Part K J. Multi-Body Dyn.* **2011**, *225*, 204–219. [CrossRef]
34. Offner, G. Friction power loss simulation of internal combustion engines considering mixed lubricated radial slider, axial slider and piston to liner contacts. *Tribol. Trans.* **2013**, *56*, 503–515. [CrossRef]
35. Allmaier, H.; Priestner, C.; Reich, F.M.; Priebsch, H.H.; Forstner, C.; Novotny-Farkas, F. Predicting friction reliably and accurately in journal bearings—The importance of extensive oil-models. *Tribol. Int.* **2012**, *48*, 93–101. [CrossRef]
36. Coy, R.C. Practical applications of lubrication models in engines. *Tribol. Int.* **1998**, *31*, 563–571. [CrossRef]
37. Vogel, H. The law of the relation between the viscosity of liquids and the temperature. *Phys. Z.* **1921**, *22*, 645–646.
38. Barus, C. Isothermals, isopiestics and isometrics relative to viscosity. *Am. J. Sci.* **1893**, *45*, 87–96. [CrossRef]
39. Cross, M.M. Rheology of non-Newtonian fluids: A new flow equation for pseudoplastic systems. *J. Colloid Sci.* **1965**, *20*, 417–437. [CrossRef]
40. Furuhama, S.; Oya, Y.; Hikari, S. Temperature measurements of the connecting rod, piston pin and crankpin bearing of an automobile gasoline engine. *Bull. JSME* **1966**, *9*, 181–189. [CrossRef]
41. Gießauf, G. Bewertung Unterschiedlicher Reibungsrelevanter Maßnahmen beim PKW-Dieselmotor. Master's Thesis, Technische Universität Graz, Graz, Austra, 2013.

4.2 Sub-assembly resolved friction loss comparison of three engines

The minimization of the ICE mechanical losses provides a significant contribution to save fuel and reduce emissions nowadays as well as in the foreseeable future. In the recent past, so-called downsizing has been used to increase engine efficiency. By moving the operating state to higher mean pressures by reducing the displacement, the engine operation is shifted to advantageous high-efficiency areas in the engine map.

Downsizing is also applied to sports engines. This enables very high power outputs to be realised with 4-cylinder engines, which until a few years ago could only be achieved by engines with more cylinders. The high available power with simultaneously reduced displacement results in very high specific power of the engines. This results in additional challenges for the power unit with regard to the controllability of increased loads from high gas forces. This affects the layout and design of the engine sub-assemblies. In comparison to conventional gasoline engines, robust components are required to withstand increased load.

Conventional gasoline engines achieve their power and torque at higher speeds and low loads. In contrast, diesel engines are exposed to very high gas forces due to the self-ignition concept with indispensable high compression ratios. The mechanical friction losses for conventional gasoline and diesel engines are well investigated and analysed in literature. But a lack of literature can be found regarding direct comparisons between the different engine conceptual designs at the same specific power output. However, the mechanical losses of downsized engines have not yet been studied much. Especially direct comparisons to conventional diesel and gasoline engine concepts are not covered in the literature.

Therefore in this work, the sub-assembly resolved friction losses for three different in-line four-cylinder, four-stroke, turbo charged engines for passenger car applications are investigated. Two gasoline engines (a conventional and a downsized gasoline engine with twice the specific power output) and a diesel engine (very similar specific power output than the conventional gasoline engine) have been analysed.

In [43] it was shown that the method is very well suited for comparisons under different boundary conditions regarding load, speed and media temperature. The developed combined friction analysis method is therefore used to conduct investigations on all three engines.

Because the lubricant can have a considerable influence on the results of the friction losses (even with the same viscosity class), an identical SAE 5W30 lubricant suitable for all engines was used for all tests. The lubricant was also used in the previous investigation in [43].

Any deviation in the execution of the tests, e.g. due to differences in the configuration of the engines on the test bench (auxiliary units not uniformly mounted between the engines or partially assembled) or different thermal boundary conditions during the test, has a considerable influence on the results of the friction comparisons. For this reason, a number of strict boundary conditions were defined for the comparisons between the different engine concepts and were adhered to in all tests.

- Disassembly of all three engines from the complete engine to the base engine configuration without all auxiliaries.

- Supply of the engines with the engine media engine oil and cooling water by external supply systems.
- By using the external supply units, temperature levels and supply pressures of the engine media are ensured with an accuracy of $\pm$ 0.1 °C and $\pm$ 0.05 bar.
- Extensively run-in of the engines using a defined procedure covering low and high engine speeds and loads, at low and high engine media supply temperatures.
- Especially designed measurement programs at identical engine speeds, loads and engine media supply temperatures/pressures to obtain comparable friction loss data maps of the three base engines and their sub-assemblies.
- Because the cycle-to-cycle cylinder pressure variation is very small when using the external charging system of the friction analysis methodology, the effect of engine load variation between the engines is very small with peak cylinder pressure variations in the order of $\pm$ 1 bar.

The details of the sub-assembly resolved investigations conducted at all three engines and the comparison of the engine concepts are described in [44] which are presented in section 4.2.2. The research findings of the publication are summarized here beforehand.

4.2.1 Summary of research findings

- The friction losses of the piston group system, crankshaft journal bearings (five main bearings and four big end bearings) and valve train of three engine concepts for passenger car applications with the same or doubled specific power output have been investigated using one SAE 5W30 lubricant (suitable for all three engines) at identical boundary conditions for engine speed, engine load and thermal ancillary conditions.
- By carrying out the investigations at 70 °C, 90 °C and 110 °C, a comprehensive consideration of the friction losses at reduced lubricant viscosity is performed. As a rule of thumb, the viscosity of the lubricant is halved with a temperature increase of 20 °C.
- For a comprehensive analysis of the entire base engine friction losses, the investigations of the friction losses have to be conducted under load conditions. Measurements without load cannot represent the overall results of engine friction tests or give contradictory results.
- All three engines showed a friction reduction potential at the base engine level over the whole operation range when increasing the lubricant supply temperature. Only with gasoline engine 1 at the lowest investigated engine speed of n=1000 rpm, identical FMEP levels were found at 70 °C and 110 °C. These results show increasing friction at low lubricant viscosity and subsequent beginning of mixed lubrication.
- The crankshaft journal bearings (main and big end bearings) showed only small differences (main bearings up to ΔFMEP=0.05 bar, big end bearings up to ΔFMEP=0.03 bar) when comparing the base engines. This is explained by the comparable bearing geometry and measured bearing temperatures during the tests.
- The main differences between the engine concepts arise mainly from the piston group and valve train systems.

- At low engine speeds and low load operation, the piston group friction losses of gasoline engine 2 are lowest for all three engines. In contrast, at high load operation gasoline engine 2 shows increased FMEP levels with considerable differences in the FMEP of the piston group of up to ΔFMEP=0.5 bar.
- The high-power downsizing gasoline engine concept showed the best friction performance in motored and low load operation mainly driven by a good performance of the valve train and piston group system.
- The diesel engine showed the best friction loss performance at highly loaded engine operation due to the good performance of the piston group system.
- As is generally known, the design of the valve train is decisive for the friction losses. Nevertheless, in this thesis it was possible to quantify the valve train losses in a direct comparison of the concepts' flat tappet based valve actuation systems used in gasoline engine 1 and roller finger follower systems used in the gasoline engine 2 and the diesel engine.
- At low engine speeds and subsequent low sliding speeds at the lubricated contacts of the valve actuation system, disadvantages of up to ΔFMEP=0.28 bar arise between the different valve actuation systems.
- When disregarding the disadvantageous valve train friction losses at gasoline engine 1, the other sub-assemblies namely piston group and crankshaft journal bearings of the conventional engine concepts are showing a good performance and partly better results in comparison to the high-power downsizing concept.

4.2.2 Paper II [44]

lubricants

MDPI

Article

Investigations of the Friction Losses of Different Engine Concepts. Part 2: Sub-Assembly Resolved Friction Loss Comparison of Three Engines

Christoph Knauder [1,*], Hannes Allmaier [1], David E. Sander [1] and Theodor Sams [2,3]

1 VIRTUAL VEHICLE Research Center, Inffeldgasse 21A, 8010 Graz, Austria; hannes.allmaier@v2c2.at; david.sander@v2c2.at
2 AVL List GmbH, Hans-List-Platz 1, 8020 Graz, Austria; Theodor.Sams@avl.com
3 Institute of Internal Combustion Engines and Thermodynamics—Graz University of Technology, Inffeldgasse 19, 8010 Graz, Austria
* Correspondence: christoph.knauder@v2c2.at

Received: 29 October 2019; Accepted: 20 November 2019; Published: 25 November 2019

Abstract: In this work, friction loss investigations and comparisons of three different four-cylinder engines for passenger car applications are presented, using a recently developed combined approach. By merging extensive experimental with reliable and predictive journal bearing simulation results, a sub-assembly-resolved friction loss analysis of the piston group, crankshaft journal bearings and valve train is conducted for all three engines. The engines have been chosen individually based on their specific power output and crank train geometry. The measurement program covers a wide range of corresponding engine operation points (identical speed, load and thermal boundary conditions). In addition, the investigations are carried out for different engine media supply temperatures ranging from 70 °C to 110 °C for a comprehensive consideration of the friction losses at reduced lubricant viscosity. For reasons of comparability, all investigations conducted in this work have been carried out using the same modern SAE 5W30 lubricant. This is done to exclude influences from different lubricant properties which may have significant effects on the tribological behaviour of the engines' sub-assemblies. While the diesel engine showed a friction reduction potential over the entire engine operation range when increasing the engine media supply temperatures, the gasoline engines showed a different behaviour. For the gasoline engines, disadvantages arise especially at low engine speeds. By using the developed combined approach, it was possible to assign mixed lubrication regimes at the valve train systems and at the piston groups.

Keywords: engine friction; friction comparison; friction measurements; friction loss distribution; sub-assembly friction; journal bearing simulation; valve train; journal bearings; main bearings; big end bearings; piston group

1. Introduction

In internal combustion engines (ICE), the friction losses of the base engine are divided into the sub-assemblies piston group, crankshaft journal bearings, valve train, timing drive and shaft seals. Looking at a passenger car powerd by an ICE, approximately 30% of fuel consumption is used to overcome friction losses [1]. Subsequently, the reduction of the friction losses on these sub-assembly systems is currently and in future a significant aim during the base-engine development process [2–5].

From literature detailed friction loss investigations on single cylinder engines are available [6–8]. Also a number of reasearchers have investigated the friction losses of passenger car engines both for gasoline [9–11] and diesel engines [12–15]. Furthermore, individual comparisons between modern

Lubricants **2019**, *7*, 105

diesel and gasoline engine friction losses focusing on lubricant sensitivities [16], a comparison of two gasoline engines for passenger car applications [17] and a comparison of two diesel engines for passenger car applications [18] are available in literature. Also detailed investigations dealing with ICE design aspects on friction losses are available [19]. But a lack of literature is found which is focusing on ICE friction loss investigations and comparisons with identical engine displacement and power density. In addition comparisons on the engines sub-assembly level for different engine media supply temperatures over a wide range of the engine operation map (engine speed, engine load) are not known to the author.

In this study, three different engines are investigated in detail. Two gasoline engines (a conventional and a downsized gasoline engine with twice the specific power output) and a diesel engine (very similar specific power output than the conventional gasoline engine) have been analysed. While conventional gasoline engines achieve higher speeds with relatively low loads, downsizing engines are working in addition under high peak cylinder pressures (see Figure 1).

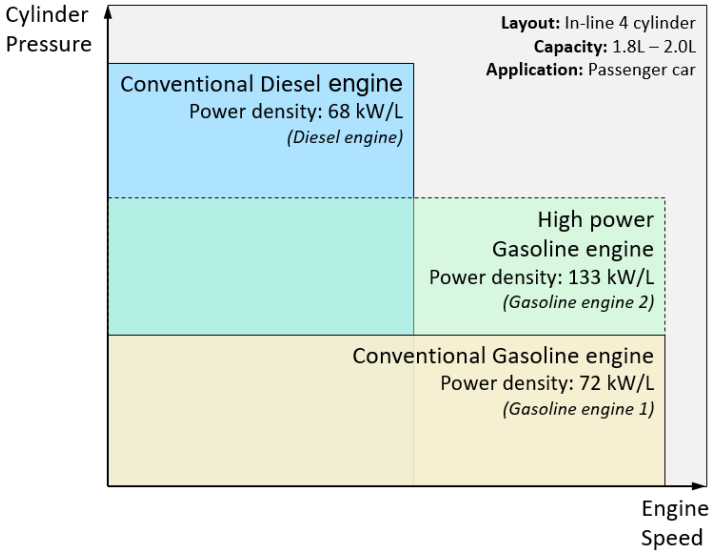

Figure 1. Simplified overview of the engine concepts operation field.

Diesel engines are conceptually exposed to very high loads due to the high gas forces resulting from the self-ignition combustion design with indispensable high compression ratios. The aim of engine "downsizing" is to increase the engine efficiency by moving the engine operation to advantageous high-efficiency areas in the engine map. The operation range is shifted to higher mean pressures subsequently by reducing the volume displacement. Torque buffers have to be included which are essential for acceleration phases [20]. For high performance downsizing engine concepts (realized at gasoline engine 2) the ICE power output and torque is put to the same or increased level than at bigger engines using a higher number of cylinders. Consequently, additional needs regarding the controllability of increased loads due to high gas forces arise for the power unit. This affects the layout and design (construction and materials) of the engine sub-assemblies. In comparison to conventional gasoline engines robust components are required for downsizing and diesel engine concepts to withstand these increased stresses. The different layouts are exemplary shown in Figure 2 for the conrod/piston group assembly of the engines investigated in this work.

Lubricants **2019**, *7*, 105

Figure 2. Mass comparison of conrod incl. pistons of the investigated engine concepts in this work: (**left**) Diesel engine: m = 1584 g, (**middle**) Gasoline engine 1: m = 1000 g, (**right**) Gasoline engine 2: m = 914 g.

In addition to the increased loads resulting from the high gas forces, the diesel engine must withstand higher mass forces of the moving crank drive components due to the larger component masses. For the downsizing concept, not only increased peak cylinder pressures but also increased engine speeds are realized. These design parameters require low component masses to reduce the acting mass forces, but at the same time connecting rods and pistons must also be able to withstand the resulting higher loads (see Figure 2).

Regarding the different engine layouts, specific interests and aims to investigate the mechanical efficiency of the three different engine concepts arise:

- Determination of the friction losses on the base engine key sub-assemblies: Piston group, crankshaft journal bearings (main- and big end bearings) and valve train.
- Sub-assembly-resolved comparison of the friction losses between the different engine concepts
- Overview and discussion of the base engine friction losses

To conduct the friction loss analysis for all engines presented in this work, a combined approach using the advantages of both, experimental investigations and simulation capabilities, is applied. The combined methodology has been presented and described in detail in part 1 of this publication series "Investigations of the Friction Losses of Different Engine Concepts. Part 1: A Combined Approach for Applying Sub-assembly-Resolved Friction Loss Analysis on a Modern Passenger-Car Diesel Engine" [21]. At this point it is noted, that for the understanding of the results presented in this work the content presented in [21] is recommended.

2. The Engines Under Test

The friction investigations were carried out on three different in-line four-cylinder, four-stroke, turbo-charged, passenger car engines. The engines have been specifically chosen to enable comparisons not only between the different engine concepts but also with focus on their specific power output. The diesel engine and gasoline engine 1 are representing two engines with almost identical specific power output. In contrast, gasoline engine 2 represents a downsizing concept with doubled power density in comparison to the conventional engines. The technical details of the engines are listed in Table 1.

Table 1. Technical data of the engines under test.

Parameter	Diesel Engine	Gasoline Engine 1	Gasoline Engine 2
Volume displacement	1995 cm^3	1781 cm^3	1991 cm^3
Compression ratio	16.5:1	9.5:1	8.6:1
Bore	84 mm	81 mm	83 mm
Stroke	90 mm	86.4 mm	92 mm
Nominal torque	380 Nm	235 Nm	422 Nm
Nominal Power	135 kW	130 kW	265 kW
Specific power	68 kW/L	73 kW/L	133 kW/L
Maximum Speed	4600 rpm	6600 rpm	6700 rpm
Cylinder distance	91 mm	88 mm	90 mm
Conrod length	138 mm	144 mm	138.7 mm
Main bearing diameter	55 mm	54 mm	55 mm
Main bearing width	25 mm	22 mm	19 mm
Main bearing clearance (cold)	20 µm	20 µm	20 µm
Big-End bearing diameter	50 mm	47.8 mm	48 mm
Big-End bearing width	24 mm	25 mm	19.4 mm
Valve-train	DOHC	DOHC	DOHC
Timing drive	chain	belt	chain
Valve-train type	roller-type cam follower	flat-base tappet	roller-type cam follower
Valves	4 per cylinder	5 per cylinder	4 per cylinder
Connecting rod ratio	0.326	0.3	0.332

It is important to note that all investigations conducted in this work are carried out using the same modern SAE 5W30 lubricant. This represents a fundamental boundary condition to exclude arising influences from different lubricant properties which may have significant effects on the engines sub-assemblies. As an example using different base oils and/or different additive packages may affect the beginning of mixed lubrication or change lubricant viscosity when high pressure and shear rates occure in the lubricated contacts [22]. Therefore, one lubricant has been selected for the research tasks, which is suitable for all three engine concepts. The basic physical properties of the SAE 5W30 lubricant used in this work are listed in Table 2.

Table 2. Basic rheological properties of the lubricant used for all investigations.

SAE class	5W30
Performance level	ACEA C3, ACEA A3/B4
Density at 15 °C	853 kg/m^3
Dynamic viscosity at 40 °C	59.88 mPas
Dynamic viscosity at 100 °C	9.98 mPas
HTHS viscosity	3.57 mPas
Viscosity index	153

HTHS: high temperature high shear rate viscosity (defined as the dynamic viscosity of the lubricant measured at 150 °C and at a shear rate of 10^6 s^{-1}.

Furthermore it is a mandatory boundary condition for the friction loss investigations, that the engines are proper run-in before the friction measurements are conducted. Therefore the engines are extensively run-in using a defined procedure to account for occurring run-in processes affecting the results [23–26].

Measurement Program

The measurement programs, which have been conducted at different engine media supply temperatures ranging from 70 °C to 110 °C are designed and coordinated regarding the comparability of engine speed, peak cylinder pressures and engine media supply temperatures/pressures. The coordination effort results in detailed and comparable friction maps for the investigated engines. Figure 3 shows the executed engine operation points both in motored and load conditions.

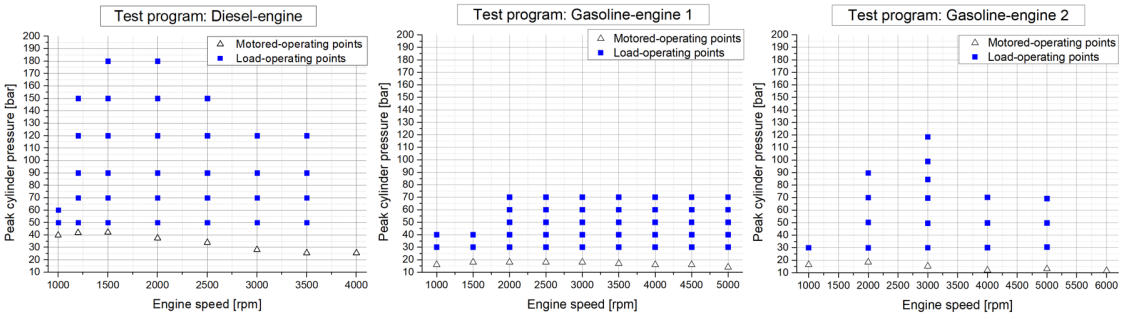

Figure 3. Realized measurement program for the three different engines (motored- and load-operating points): (**left**) Diesel engine (**middle**) Gasoline engine 1 (**right**) Gasoline engine 2.

The base engine measurement programs are covering pure motoring tests and load tests ranging from part load up to full load conditions. It covers 120, 144 and 46 different measurement points for the diesel engine, gasoline engine 1 and gasoline engine 2, respectively. The minimum engine speed was defined with n = 1000 rpm. The maximum engine speed was limited with n = 4000 rpm, n = 5000 rpm and n = 6000 rpm for the diesel engine, gasoline engine 1 and gasoline engine 2 respectively. Load tests have been conducted at comparable engine speeds between the aggregates working at peak cylinder pressures up to p_{cyl} = 180 bar, p_{cyl} = 70 bar and p_{cyl} = 120 bar for the diesel engine, gasoline engine 1 and gasoline engine 2. It is important to note that equal cylinder pressure levels have been chosen between the different engines to allow friction loss comparisons at identical boundary conditions. It is mandatory to minimize influences of different thermal boundary conditions affecting e.g., lubricant viscosity and density, installation clearances of journal bearings and pistons when conducting friction comparisons.

3. Sub-Assembly Resolved Friction Losses of the Three Engine Concepts

The applied analysis approach [21] connects results from engine friction measurements and from predictive journal bearing simulations. When applying the combined approach, following basic set of formulas is used to determine the individual proportions of the sub-assemblies:

The friction loss of the base engine, denoted as FMEP (friction mean effective pressure) is calculated by the subtraction of the IMEP (indicated mean effective pressure) and the BMEP (brake mean effective pressure) according to Equation (1) when using the IMEP-method.

$$FMEP = IMEP - BMEP \tag{1}$$

Equation (2) relates the measured brake torque at the crankshaft (T) to the corresponding mean effective pressure (BMEP)

$$BMEP = \frac{W}{V_D} = \frac{4\pi T}{V_D} \tag{2}$$

where W refers to the work per cycle and V_D to the volume displacement of the investigated four-stroke engine. The IMEP calculation is done according to Equation (3) by integrating the measured cylinder pressure ($pcyl$) over a working cycle divided by the volume displacement of the engine.

$$IMEP = \frac{\int pdV}{V_D} \tag{3}$$

To receive the FMEP for the sub-assemblies valve train, journal bearings and piston group during the application of the developed friction analysis approach, the individual FMEP shares are calculated as follows:

$$FMEP_{\text{Valve train}} = \frac{W}{V_D} = \frac{4\pi T_{\text{F Valve train}}}{V_D} \tag{4}$$

$$FMEP_{\text{Main bearings}} = \frac{W}{V_D} = \frac{4\pi T_{\text{F Main Bearings}}}{V_D} \tag{5}$$

$$FMEP_{\text{Big end bearings}} = \frac{W}{V_D} = \frac{4\pi T_{\text{F Big end bearings}}}{V_D} \tag{6}$$

$$FMEP_{\text{Piston group}} = \frac{W}{V_D} = \frac{4\pi T_{\text{F Piston group}}}{V_D} \tag{7}$$

In the following subsections the resulting FMEP results of the individual sub-assemblies are presented for all three engines for different engine media supply temperatures ranging from 70 °C to 110 °C.

3.1. Piston Group Friction Losses

The friction losses of the piston group for the three engines investigated are plotted in Figure 4 for three different engine media supply temperatures. It is important to note that the sub-assembly piston group includes the friction losses of the pistons, piston rings (top-, second- and oil-rings), piston pins and conrod small end bearings.

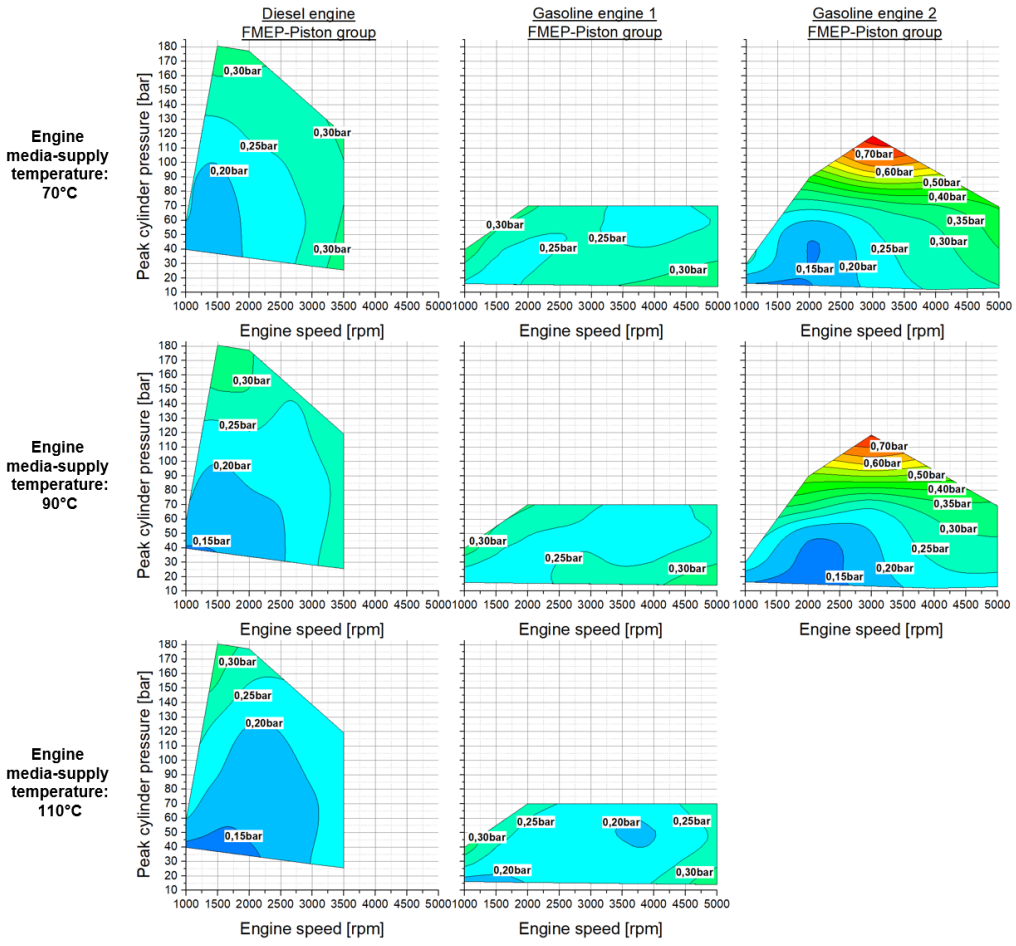

Figure 4. Resulting FMEP-maps for the piston group (**left**) Diesel engine (**middle**) Gasoline engine 1 (**right**) Gasoline engine 2.

Diesel engine:

A clear temperature trend is observed when analysing the piston group friction losses, even though the highest peak cylinder pressures are reached for this engine with p_{cyl} = 180 bar. At the lowest engine media supply temperature the maximum FMEP levels are resulting with FMEP = 0.33 at an engine speed of n = 3500 rpm. When the temperature is increased, the FMEP levels are decreasing with the exception of high load operation at n = 1500 rpm. At this operation point the FMEP levels of the piston group are slightly increasing indicating mixed lubrication. The lowest FMEP level for the piston group of the diesel engine are resulting at the highest engine media supply temperature of 110 °C and motored operation at n = 1000 rpm with FMEP = 0.13 bar.

Gasoline engine 1:

For gasoline engine 1 the FMEP results show a different behaviour in comparison to the diesel engine. At the lowest engine media supply temperature the maximum FMEP levels with FMEP = 0.35 bar are determined at two different operation points in the engine map. On one hand the maximum level results at the maximum engine speed n = 5000 rpm at motored operation. On the other hand the same FMEP level is found at the lowest engine speed of n = 1000 rpm at an peak cylinder pressure of p_{cyl} = 40 bar. This result indicate that the piston group is running in the whole field of lubrication regimes ranging from boundary/mixed lubrication at the TDC/BDC and pure hydrodynamic lubrication during the up and down stroke of the piston. While at n = 1000 rpm a possible explanation of the high FMEP level can be increased mixed lubrication at low engine speeds and high loads. In contrast, the friction losses at an engine speed of n = 5000 rpm can be explained by increased hydrodynamic friction losses due to lubricant shearing at positions of high piston speeds during the piston stroke. Furthermore, a temperature trend is found for the piston group of gasoline engine 1. When increasing the engine media supply temperature, the FMEP levels are decreasing but remain almost constant for n = 1000 rpm and p_{cyl} = 40 bar supporting the explanation of the high FMEP levels caused by mixed lubrication regimes. The lowest FMEP level is found at the lowest engine speed of n = 1000 rpm and motored operation with FMEP = 0.17 bar at an engine media supply temperature of 110°C.

Gasoline engine 2:

For gasoline engine 2 very interesting results are received when applying the analysis procedure of the combined approach. For motored and low load engine operation, the FMEP levels of the piston group are indicating a good friction performance. The lowest FMEP level is resulting at an engine speed of n = 2000 rpm and motored operation with FMEP = 0.13 bar at an engine media supply temperature of 90 °C. It is interesting to note that for motored operation gasoline engine 2 shows the lowest FMEP levels of all three engines at 90 °C (Diesel engine: FMEP = 0.14 bar; Gasoline engine 1: FMEP = 0.2 bar). With increasing peak cylinder pressures the FMEP levels are also strongly becoming larger. The highest FMEP level is resulting at a peak cylinder pressure of p_{cyl} = 120 bar at an engine speed of n = 3000 rpm and an engine media supply temperature of 70 °C with FMEP = 0.77 bar. Nevertheless, a clear temperature trend is observed from the results. When increasing the engine media supply temperature the FMEP levels of the piston group are decreasing over a wide range of the engine operation map for low load operation. For high load operation at an engine speed of n = 2000 rpm the FMEP levels are increasing when the lubricant viscosity is decreasing. This results are indicating beginning mixed lubrication regimes for the piston group of gasoline engine 2.

The piston group FMEP results are clearly showing, that friction investigations under load conditions are essential for a holistic analysis of the sub-system. It is interesting to note that the FMEP level of the piston group at motored engine operation is lowest for gasoline engine 2. The FMEP difference to the other engines under motoring engine operation reaches values of up to ΔFMEP = 0.12 bar. But the situation under load operation is different. Here, gasoline engine 2 revealed increased FMEP levels for engine speeds higher n = 1500 rpm and peak cylinder pressures above p_{cyl} = 70 bar either when comparing the results with the conventional gasoline and diesel concept. The diesel

engine piston group shows a very good performance in terms of generated friction losses under high load operation.

The piston group friction losses are calculated by subsequent subtraction of individual friction losses from the results of the base engine friction measurements due to the applied procedure [21]. It is therefore expected that the FMEP results of the piston group are showing the largest uncertainties of the sub-assembly system results.

3.2. Crankshaft Journal Bearing Friction Losses

The friction losses of the crankshaft main and big end bearings are calculated for the equal engine operation points of the base engine measurement campaigns presented in Figure 3. Consequently, 310 different operation points have been calculated to obtain the crankshaft journal bearing friction losses of the diesel, gasoline engine 1 and gasoline engine 2. For the calculations measured journal bearing temperature data as well as the measured cylinder pressures at all cylinders are important input data for the simulations beside detailed geometry data (macro- and micro-geometry). The results are separated into results of the five crankshaft main bearings and four big end bearings. The subsequent FMEP-maps are plotted in Figures 5 and 6.

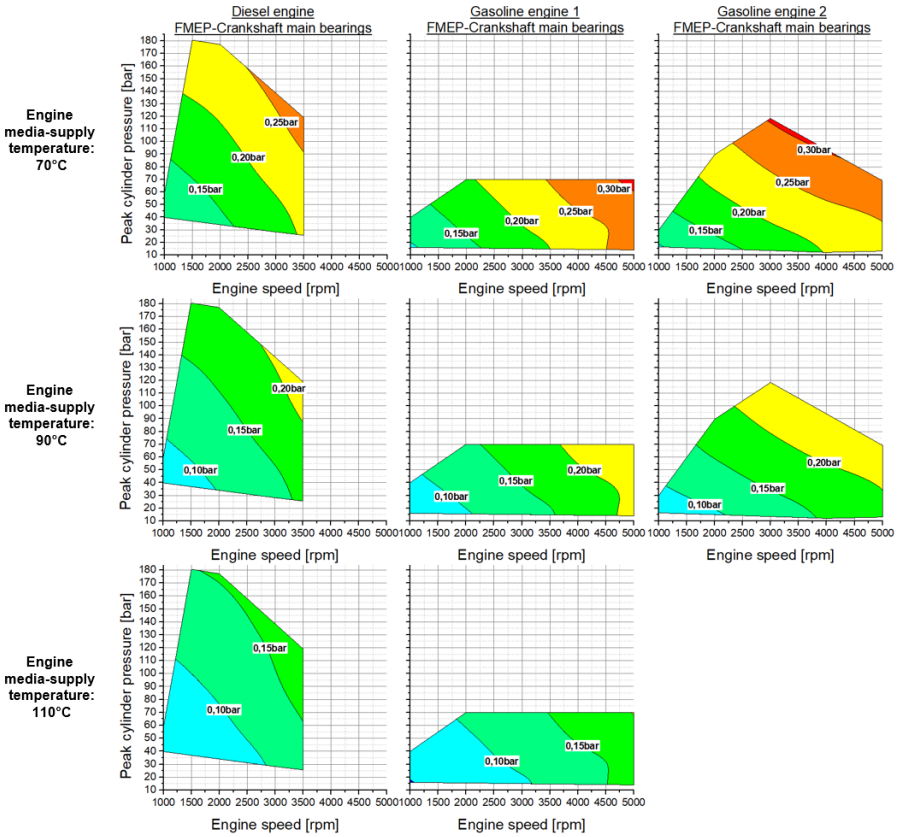

Figure 5. Resulting FMEP-maps for the crankshaft main bearings using the journal bearing simulation method (**left**) Diesel engine (**middle**) Gasoline engine 1 (**right**) Gasoline engine 2.

The results in Figure 5 show the determined FMEP of the five main bearings for all three investigated engines at different engine media supply temperatures. In general, the results show a FMEP increase when increasing engine speed and load.

Diesel engine:

For the diesel engine the FMEP-values of the main bearings are showing an increase over engine speed and engine load. In addition a clear temperature dependency and trend is found. The highest

FMEP level with FMEP = 0.27 bar was found at the lowest engine media supply temperature of 70 °C at the highest investigated engine speed of n = 3500 rpm and a peak cylinder pressure of p_{cyl} = 120 bar. The lowest FMEP level on the other hand with FMEP = 0.06 bar was found at an engine speed of n = 1000 rpm in motored operation at 110 °C. The FMEP levels are decreasing significantly over the whole engine operation map when increasing the engine media supply temperature.

Gasoline engine 1:

The main bearing friction losses of gasoline engine 1 showed an increase over engine speed and engine load as well as a clear trend when increasing the engine media supply temperature. The highest FMEP level with FMEP = 0.31 bar was found at the lowest engine media supply temperature of 70 °C at an engine speed of n = 5000 rpm and a cylinder pressure of p_{cyl} = 70 bar. The lowest FMEP level on the other hand with FMEP = 0.05 bar was found at an engine speed of n = 1000 rpm in motored operation at 110 °C. It was found that the FMEP levels are decreasing significantly over the whole engine operation map when increasing the engine media supply temperature.

Gasoline engine 2:

For gasoline engine 2 the FMEP-values of the main bearings are showing a clear dependency on engine load, engine speed and engine media supply temperature. The highest FMEP level with FMEP = 0.31 bar was found at the lowest engine media supply temperature of 70 °C at the highest investigated peak cylinder pressure of p_{cyl} = 120 bar at an engine speed of n = 3000 rpm. The lowest FMEP level with FMEP = 0.07 bar was found at an engine speed of n = 1000 rpm in motored operation at 90 °C. The FMEP levels are decreasing significantly over the whole engine operation map when increasing the engine media supply temperature.

In Figure 6 the summed big end bearing FMEP (four big end bearings) are presented at different engine media supply temperatures.

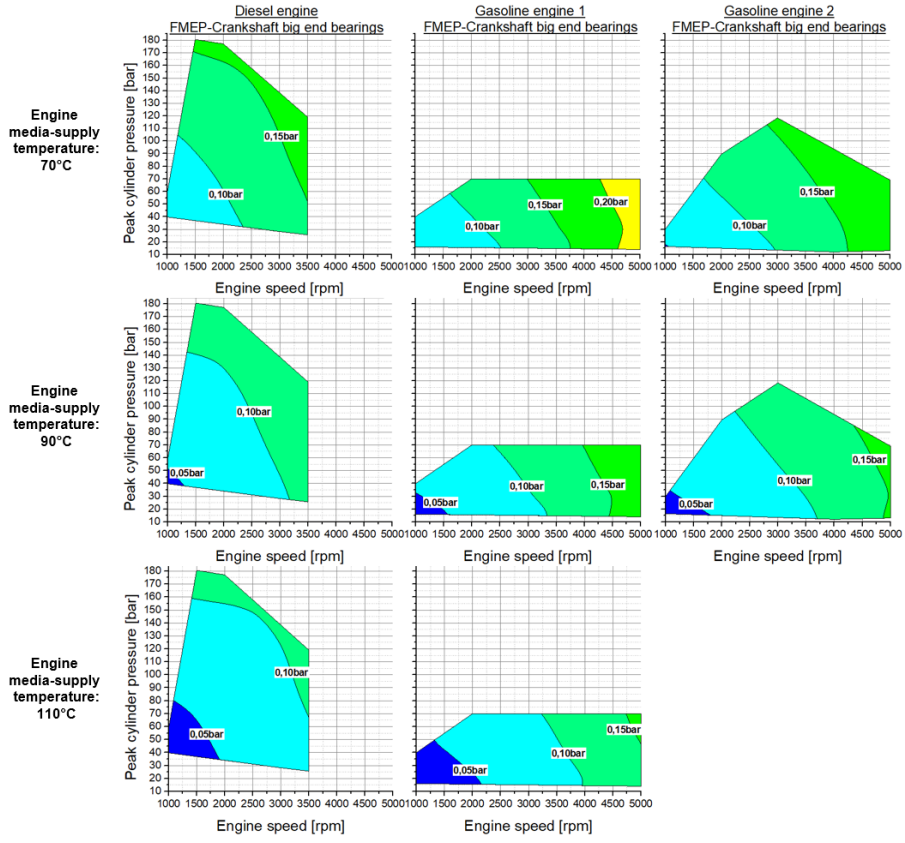

Figure 6. Resulting FMEP-maps for the big end bearings using the journal bearing simulation method (**left**) Diesel engine (**middle**) Gasoline engine 1 (**right**) Gasoline engine 2.

As expected, the FMEP results show a increase when increasing engine speed and load. Also a clear temperature trend was found when analysing the results at different engine media supply temperatures.

Diesel engine:

For the diesel engine the FMEP values of the four big end bearings are showing an increase over engine speed and engine load. In addition a clear temperature dependency and trend is found. The highest FMEP level with FMEP = 0.17 bar was found at the lowest engine media supply temperature of 70 °C at the highest investigated engine speed of n = 3500 rpm and a peak cylinder pressure of p_{cyl} = 120 bar. The lowest FMEP level on the other hand with FMEP = 0.03 bar was found at an engine speed of n = 1000 rpm in motored operation at 110 °C. The FMEP levels are decreasing significantly over the whole engine operation map when increasing the engine media supply temperature.

Gasoline engine 1:

The big end bearing friction losses of gasoline engine 1 showed an increase over engine speed and engine load as well as a clear trend when increasing the engine media supply temperature resulting in reduced lubricant viscosity. The highest FMEP level with FMEP = 0.23 bar was found at the lowest engine media supply temperature of 70 °C at an engine speed of n = 5000 rpm and a cylinder pressure of p_{cyl} = 70 bar. The lowest FMEP level on the other hand with FMEP = 0.03 bar was found at an engine speed of n = 1000 rpm in motored operation at 110 °C. It was found that the FMEP levels are decreasing significantly over the whole engine operation map when increasing the engine media supply temperature.

Gasoline engine 2:

For gasoline engine 2 the FMEP-values of the main bearings are showing a clear dependency on engine load, engine speed and engine media supply temperature. The highest FMEP level with FMEP = 0.20 bar was found at the lowest engine media supply temperature of 70 °C at a peak cylinder pressure of p_{cyl} = 70 bar at an engine speed of n = 5000 rpm. The lowest FMEP level with FMEP = 0.04 bar was found at an engine speed of n = 1000 rpm in motored operation at 90 °C. The FMEP levels are decreasing significantly over the whole engine operation map when increasing the engine media supply temperature.

Summarizing the results of the crankshaft journal bearing friction losses, it was found that the friction losses are significantly decreasing when increasing the lubricant supply temperature. While the main bearing friction losses are influenced in a greater matter by the engine peak cylinder pressure, the big end bearings showed a increased dependency on engine speed, compared to the main bearings. In addition it can be stated, that the simulation results of the journal bearing friction losses are confirming predominantly hydrodynamic lubrication regimes at all three engines.

3.3. Valve Train Friction Losses

The valve train friction losses of the individual engines are investigated for the identical engine speeds for three different engine media supply temperatures ranging from 70 °C to 110 °C. It is important to note that the investigations of the valve train friction losses are carried out in motored operation and are assumed to be not sensitive to engine load. In previous research projects extensive investigations have been conducted using torque measurement systems applied at camshafts to measure the valve train drag torque under load operation at different thermal and load boundary conditions. Based on the results of this study which revealed insignificant influence of the engine load on the valve train friction losses, the friction losses in this work are soley obtained in motored operation. From literature it can be further found, that the same assumptions are used [27] and that regarding the friction losses highly loaded engine concepts are mostly affecting the crank train system. The valve train loads are insignificantly affected by the high loaded engine operation, apart from thermal loads [20].

The resulting FMEP values for the individual engines are plotted in Figure 7. It is important to note that the resulting FMEP of the individual valve train systems are including the timing drive and crankshaft seals friction losses.

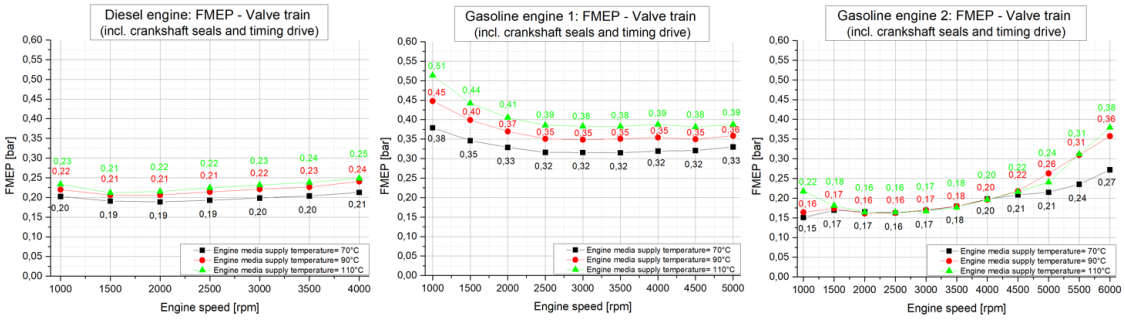

Figure 7. Resulting FMEP-levels for the valve train (including timing drive and crankshaft seals friction losses) (**left**) Diesel engine (**middle**) Gasoline engine 1 (**right**) Gasoline engine 2.

Diesel engine: The results of the diesel engine valve train are almost constant over engine speed. Nevertheless, an interesting trend is observed. The highest FMEP level of FMEP = 0.25 bar is resulting at an engine speed of n = 4000 rpm at an engine media supply temperature of 110 °C. On the other hand, the lowest FMEP level with FMEP = 0.19 bar is resulting at an engine speed of n = 2000 rpm at an engine media supply temperature of 70 °C. The results show a slight temperature dependence with increased FMEP levels when increasing the engine media supply temperature indicating beginning mixed lubrication in the sub-assembly system.

Gasoline engine 1: At gasoline engine 1 the results of the valve train friction losses are significantly different in comparison to the other two engines. The reason for the different behaviour is the different valve train design type of gasoline engine 1 which is realised as flat-base tappet valve actuation system. In addition, the valve train assembly is equipped with 5 valves per cylinder in comparison to 4 valves per cylinder at the other two engines. The valve train friction losses at gasoline engine 1 show a significant temperature dependence in the range of ΔFMEP = 0.13 bar at n = 1000 rpm and ΔFMEP = 0.06 bar at n = 5000 rpm between a lubricant supply temperature of 70 °C and 110 °C. Especially at engine speeds below n= 2500 rpm the FMEP levels are increased for all engine media supply temperatures investigated.

The highest FMEP level is found at the lowest engine speed and the highest engine media supply temperature of 110 °C with FMEP = 0.51 bar. This behaviour can be explained by the appearance of increased mixed lubrication in the lubricated contact between the camshaft and the flat tappet. The mixed lubrication regimes are further increased at high engine media supply temperatures due to further reduced lubricant viscosity at the lubricated contacts. In comparison to today's modern roller-type cam follower actuation sytems, the FMEP of the flat-base tappet system is increased by more than factor 2.3 at 1000 rpm and high engine media supply temperatures. The lowest FMEP level with FMEP = 0.32 bar results at an engine media supply temperature of 70 °C at engine speeds higher n = 2500 rpm as stable plateau. It is interesting to note that the valve train system of gasoline engine 1 shows this FMEP plateau behaviour also at the higher engine media supply temperatures at engine speeds higher n = 2500 rpm with FMEP = 0.35 bar at 90 °C and FMEP = 0.38 bar at 110 °C.

Gasoline engine 2: The resulting valve train FMEP levels of gasoline engine 2 show similar behaviour in comparison to the diesel engine up to an engine speed of n = 5000 rpm. Though the FMEP level is slightly decreased compared to the diesel engine with FMEP = 0.15 bar, FMEP = 0.16 bar and FMEP = 0.22 bar at n = 1000 rpm and engine media supply temperatures of 70 °C, 90 °C and 110 °C respectively. It is interesting to note that for n = 1000 rpm the FMEP level of the valve train is increasing with increasing engine media supply temperature indicating mixed lubrication. For engine speeds above 1500 rpm and below 4500 rpm the FMEP level of the valve train is almost identical for the different engine media supply temperatures. Above n = 4500 rpm the FMEP is increasing for the

Lubricants **2019**, *7*, 105

higher engine media supply temperatures with values up to FMEP = 0.38 bar at an engine speed of n = 6000 rpm and an engine media supply temperature of 110 °C.

4. Sub-Assembly Friction Loss Comparison between the Three Engine Concepts

The friction loss comparisons have been conducted under motored and load operation for all comparable engine speeds, according to the presented base engine measurement programs in Figure 3. In the following the conducted comparisons between the individual engines on the sub-assembly level are presented and analysed.

4.1. Friction Loss Comparison Gasoline Engines

The comparison of the gasoline engines enables the comparison of a conventional engine concept and high-power downsizing engine concept. The results are presented in Figure 8 for an engine media supply temperature of 90 °C. The considered engine speeds are ranging from n = 1000 rpm up to n = 5000 rpm. The maximum peak cylinder pressure is limited by gasoline engine 1 with p_{cyl} = 70 bar which is applied for engine speeds of 2000 rpm and higher. For engine speeds below n = 2000 rpm the peak cylinder pressure is limited to p_{cyl} = 30 bar.

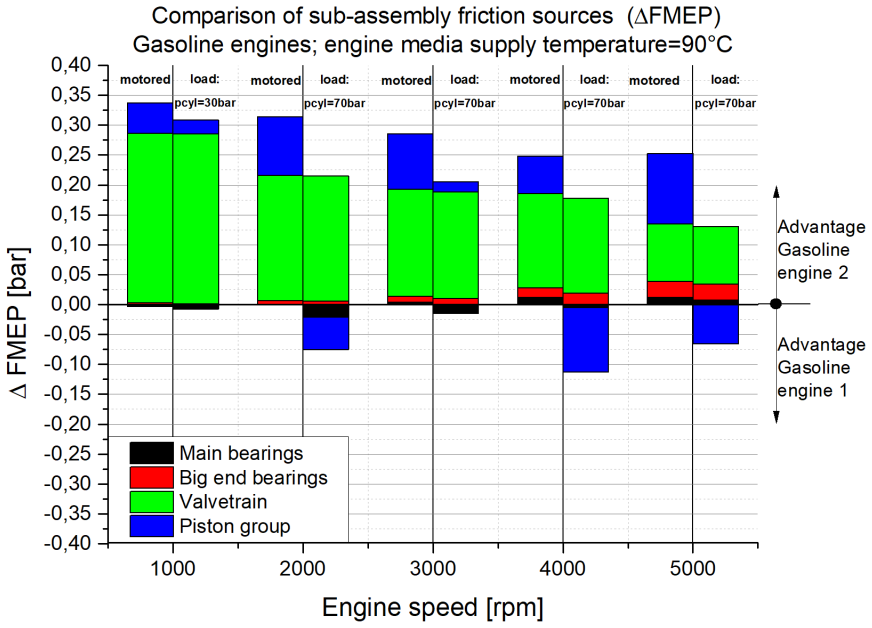

Figure 8. Gasoline engines: Friction loss comparison—engine media supply temperature = 90 °C.

In Figure 8 the engine operation points are applied for the individual engine speeds. At each engine speed, two different load points are indicated. The motored operation condition is shown on the left side, the load operation condition on the right side.

When analysing the gasoline engines, a major difference in the valve train friction losses is noticeable. Especially at low engine speeds, the FMEP difference is highest with ΔFMEP = 0.28 bar. When the engine speed is increasing, the FMEP difference decreases to ΔFMEP = 0.10 bar at an engine speed of n = 5000 rpm. The reason for the big difference is arising from the different valve train design. For gasoline engine 1 the valve actuation is designed as flat-based tappet, which especially at low engine speeds results in significant disadvantages compared to the roller type cam follower system used in gasoline engine 2. The friction comparison for the crankshaft journal bearings shows small differences for the investigated engine operation points. The main bearing friction losses are ranging below ΔFMEP = 0.02 bar. The biggest difference in the FMEP levels for the big end bearings is ΔFMEP = 0.03 bar at an engine speed of n = 5000 rpm. The friction loss comparison of the piston group

Lubricants **2019**, *7*, 105

clearly shows that detailed friction investigations under load conditions are essential for a holistic analysis of the friction behaviour of the engines. While the piston group of gasoline engine 2 shows advantages of up to ΔFMEP = 0.12 bar under motoring engine operation, the situation under load conditions (p_{cyl} = 70 bar) is different. Under load operation up to a engine speed of n = 3000 rpm the FMEP differences for the piston groups are low with ΔFMEPmax = 0.05 bar at n = 2000 rpm. For engine speeds of n = 4000 rpm and 5000 rpm and peak cylinder pressures of 70 bar the piston group of gasoline engine 1 shows advantages of ΔFMEP = 0.11 bar and ΔFMEP = 0.07 bar, respectively.

4.2. Friction Loss Comparison Gasoline Engine 1 and Diesel Engine

The comparison between gasoline engine 1 and the diesel engine which are designed as conventional concepts, enables on one hand the friction loss comparison between a gasoline and a diesel concept. On the second hand, the comparison between engine concepts with the same specific power output is realized. Figure 9 shows the sub-assembly-resolved friction loss comparison between the two engines at different engine operation points. The investigated engine speeds are ranging from n = 1000 rpm to n = 3500 rpm. The maximum peak cylinder pressure is limited by gasoline engine 1 with p_{cyl} = 70 bar which is applied from engine speeds n = 2000 rpm onwards. At the lower engine speeds, the peak cylinder pressure was limited to p_{cyl} = 40 bar. It is interesting to note that for gasoline engine 1, a peak cylinder pressure of p_{cyl} = 40 bar already represents a high part load operation point. In contrast, p_{cyl} = 40 bar represents the resulting peak cylinder pressure at the motored operating point at an engine speed of n = 1500 rpm for the diesel engine.

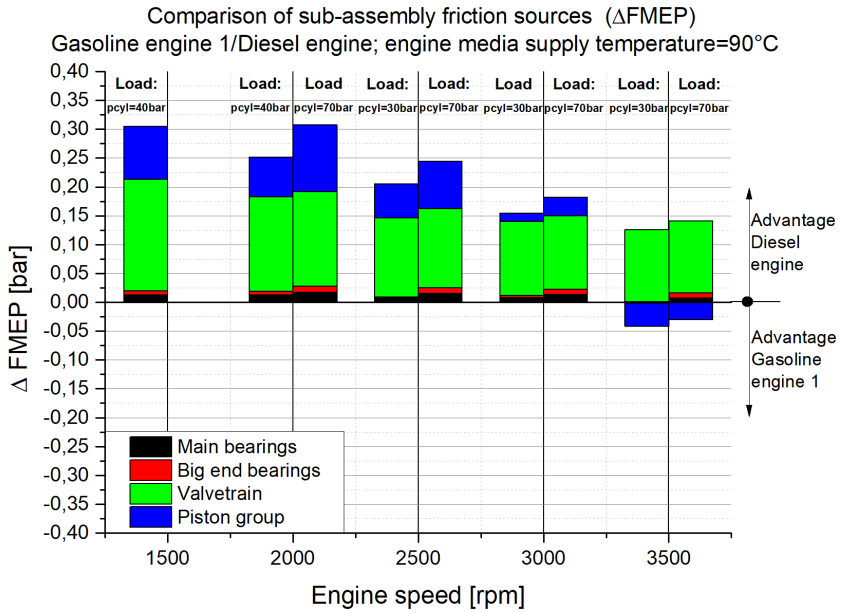

Figure 9. Gasoline engine 1/Diesel engine: Friction loss comparison—engine media supply temperature = 90 °C.

When comparing the two engines, the largest friction loss difference arises at the valve train assembly. The diesel engine, equipped with a roller type cam follower system, shows significant advantages in comparison to the flat-tappet based valve actuation system of gasoline engine 1. The determined FMEP difference at an engine speed of n = 1500 rpm is ΔFMEP = 0.19 bar but decreases when increasing engine speed. At n = 3500 rpm the FMEP difference results in ΔFMEP = 0.12 bar. For the crankshaft main and big end journal bearings small differences are observed over the entire investigated engine speed and load range. The largest FMEP difference is assigned to the main bearings with ΔFMEP = 0.02 bar. The piston group of the diesel engine shows advantages compared to gasoline engine 1 for engine speeds up to n = 3000 rpm. While the FMEP difference at low load

is ΔFMEP = 0.09 bar, the FMEP advantage for the diesel engine is slightly increased under high load operation (p_{cyl} = 70 bar) with ΔFMEP = 0.12 bar. When analysing the friction losses of the piston group at an engine speed of n = 3500 rpm, gasoline engine 1 shows slight advantages (ΔFMEP = 0.04 bar) compared to the diesel engine.

4.3. Friction Loss Comparison Gasoline Engine 2 and Diesel Engine

The friction loss comparison between gasoline engine 2 and the diesel engine enables primary the general comparison between a gasoline and a diesel concept. But especially it is possible to conduct comparisons between a gasoline engine with doubled specific power output compared to the diesel engine. Both engines are operated with significantly increased peak cylinder pressures (gasoline engine 2: p_{cylmax} = 120 bar; diesel engine: p_{cylmax} = 180 bar) compared to gasoline engine 1 (p_{cylmax} = 70 bar). The following Figure 10 shows the sub-assembly-resolved friction loss comparison at different engine operation points.

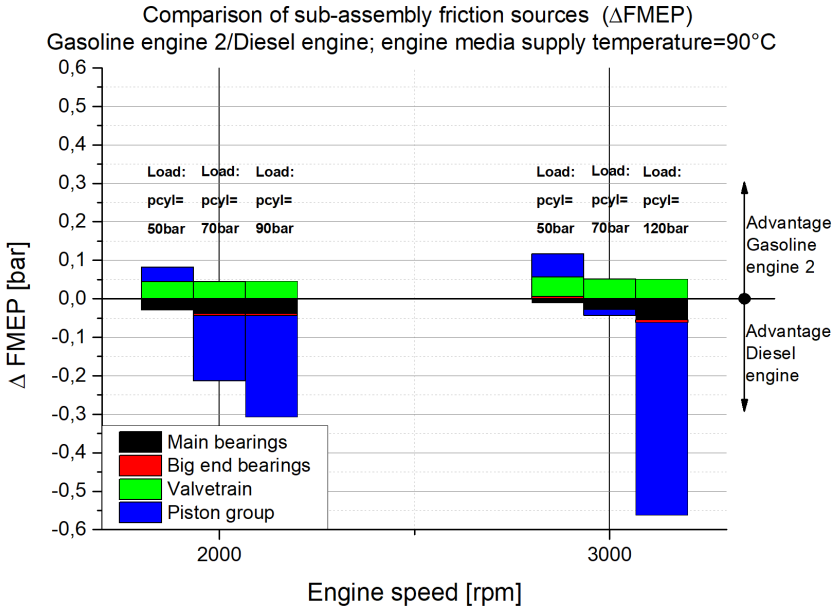

Figure 10. Gasoline engine 2/Diesel engine: Friction loss comparison—engine media supply temperature = 90 °C.

The friction comparison has been performed at engine speeds of n = 2000 rpm and n = 3000 rpm. The peak cylinder pressure was limited by gasoline engine 2 with p_{cyl} = 120 bar. At an engine speed of n = 2000 rpm the peak cylinder pressure was limited to p_{cyl} = 90 bar. The comparison of the valve train friction losses shows small differences between the two engines because of the similar design of the valve train actuation system which is configured as roller-type cam follower system at both engines. Anyway, gasoline engine 2 shows minor advantages with ΔFMEP = 0.05 bar for the engine speeds shown in Figure 10. The crankshaft main bearings of the diesel engine shows slight advantages with a maximum difference of ΔFMEP = 0.05 bar over the engine operation points investigated. For the crankshaft big end bearings the FMEP differences are very small with ΔFMEP < 0.01 bar.

The major variation in the friction loss comparison results at the piston group sub-assembly system. At low load conditions (p_{cyl} = 50 bar), gasoline engine 2 shows advantages with ΔFMEP = 0.04 bar at an engine speed of n = 2000 rpm and ΔFMEP = 0.06 bar at n = 3000 rpm. With increasing engine load and subsequently increasing gas-force effects, the piston group of gasoline engine 2, shows significant disadvantages compared to the diesel engine. At an engine speed of n = 2000 rpm the friction loss comparison of the piston group at a peak cylinder pressure of p_{cyl} = 70 bar shows a FMEP advantage for the diesel engine of ΔFMEP = 0.17 bar, at p_{cyl} = 90 bar of ΔFMEP = 0.26 bar. It is interesting to

note that at an engine speed of n = 3000 rpm and a peak cylinder pressure of p_{cyl} = 70 bar, the piston group friction losses are almost identical. Nevertheless, if the peak cylinder pressure is increased to p_{cyl} = 120 bar, significant disadvantages of the piston group of gasoline engine 2 have been analysed. At this high load engine operation point the piston group of the diesel engine shows advantages of ΔFMEP = 0.5 bar. The results are proving a better suitability of the diesel engine for engine operation under the effect of high gas force action.

4.4. Summary

Summarizing the presented investigations, it can be said that the main FMEP differences between the three investigated engine concepts arise mainly from the piston group and valve train systems. While the diesel engine piston group shows a very good performance in terms of generated friction losses under high load operation the gasoline engine 2 shows increased FMEP levels. It can be found in the literature [13], that the piston group of the diesel engine has been extensively friction loss optimized by increasing the piston clearance while lowering the piston pin offset. In addition shorter ring heights in combination with lower tangential forces of the piston rings and a friction reducing piston skirt coating is used to optimize the system. At low speed and low load operation the piston group friction losses of gasoline engine 2 is advantageous. Concerning the valve train friction losses, gasoline engine 2 shows the best performance. The main difference in the valve train friction losses between gasoline engine 1 and the other two engines arise from the different valve actuation design in addition with the increased number of five valves per cylinder.

5. Overview Base Engine Friction Losses and Discussion

It is further very interesting to observe the base engine total friction losses of the individual engine concepts. The base engine friction results are obtained at engine media supply temperatures ranging from 70 ^{c}*irc*C to 110 °C covering all engine operation points presented in Figure 3. The FMEP-maps for the three engine concepts are presented in Figure 11 and show large differences in the FMEP-levels of the base engines. Generally, the FMEP-levels of the engines decrease with increasing engine media supply temperature. The highest FMEP-levels subsequently result at the lowest investigated engine media supply temperature of 70 °C with a maximum FMEP-level of FMEP=0.96 bar for the diesel-engine, FMEP = 1.18 bar for the gasoline engine 1 and FMEP = 1.40 bar for the gasoline engine 2. It is interesting to note that the highest FMEP-levels result at different engine operation conditions. While for the diesel engine and gasoline engine 2 the highest FMEP-level results at high load conditions, gasoline engine 1 shows a different behaviour. For gasoline engine 1 the highest FMEP results at motored conditions at the highest investigated engine speed of n = 5000 rpm.

The holistic consideration of the friction losses solely by measurements at the base engine level, implies possible distortion in the interpretation of the results by the lack of details. This can be clearly explained, by analysing the FMEP-maps results of the three base engines investigated in this work.

Conventionally, the usage of a combined approach in the automotive industry development processes to analyze and determine the friction losses of the base engine sub-assemblies and their tribological performance is not known to the author. Despite far-reaching developments of simulation methods, appropriate rig and engine test programs are used (based mainly on empirical knowledge and extensive experience) to ensure the prescribed limits in terms of wear and fatigue [28]. This is done because simulation models for predictive wear calculations without a number of iterations are not available at the moment in practice which can guaranty sufficient accuracy compared to measurements. For inital engine design and layout stages, helpful design tools have been developed for friction modelling based on analytical and empirical component models to support the engineers e.g., in [9,10,29,30].

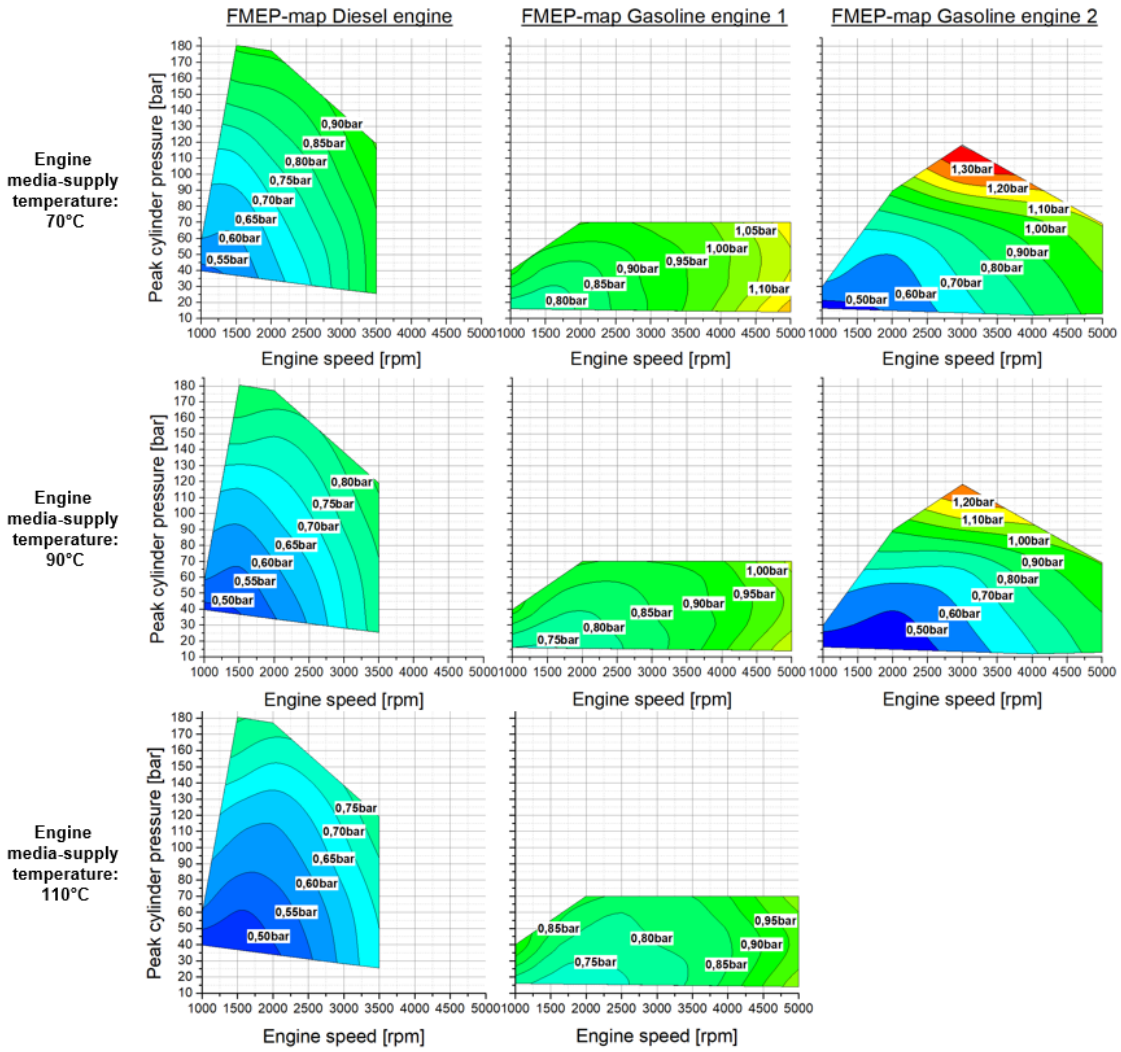

Figure 11. Resulting FMEP-maps for different engine media supply temperatures: (**left**) Diesel engine (**middle**) Gasoline engine 1 (**right**) Gasoline engine 2.

Without detailed informations regarding the increased friction losses of the valve train at gasoline engine 1 due to its different design one may come to the result, that the whole base engine shows disadvantageous friction performance. But when disregarding the valve train friction losses, the other sub-assemblies namely piston group and crankshaft journal bearings are showing a good performance and partly better results in comparison to the other engine concepts.

With the knowledge of the sub-assembly-resolved friction loss investigations presented in this work, one is able to assign the arising potentials and risks to the individual sub-assembly systems. This enables prioritized and more specific development activities when using the capabilities of both, accurate friction measurements and predictive simulation methodologies.

6. Conclusions

The friction losses of three different in-line four-cylinder, four-stroke, turbo charged engine concepts for passenger car applications have been investigated. The engines put to test have been specifically chosen, to enable comparisons not only between the different engine concepts of diesel and gasoline engines but also with focus on their specific power output focusing on modern high-power downsizing engine concepts available in series production. For that purposes one diesel engine and one gasoline engine has been selected with almost similar power density, to conduct investigations

regarding the base engine friction performance for diesel and gasoline engines. In addition a gasoline engine with doubled power density compared to the conventional engine concepts has been chosen for investigations on a gasoline concept working under high loaded engine operation. All investigations conducted in this work have been carried out using the same modern SAE 5W30 lubricant to exclude arising influences from different lubricant properties which may have significant effects on the engines sub-assemblies.

The friction losses have been determined using a recently developed combined analysis approach. By applying the combined approach it was possible to analyse and conduct comparisons on the base engine sub-assemblies crankshaft journal bearings (main and big end bearings), valve train (incl. timing drive and crankshaft seals) and piston group. The friction loss analysis and comparisons have been conducted not only for different engine operation points ranging from motored to high load operation but also at different thermal boundary conditions. This has been realized by supplying the engine media (cooling water and lubricant) from precisely controllable external supply units. The applied supply temperature levels have been ranging from 70 °C up to 110 °C.

The base engine measurement programs covered 120, 144 and 46 different measurement points for the diesel engine, gasoline engine 1 and gasoline engine 2 (high-power engine), respectively. For the calculation of the crankshaft journal bearing friction losses, simulation models of the three engine crank trains have been set up. The calculations have been carried out directly connected to the measurement programs of the base engines. By combination of measurement and journal bearing calculation results, the valve train friction losses for the individual engines have been obtained. Furthermore, the piston group friction losses have been calculated by subtraction of the valve train friction losses and crankshaft journal bearing friction losses from the base engine measurement results.

It was found that investigations under load conditions are necessary for a comprehensive analysis of the entire base engine friction losses. The high-power downsizing gasoline engine concept showed the best friction performance in motored and low load operation mainly driven by a good performance of the valve train and piston group system. In contrast, the diesel engine showed the best friction loss performance at highly loaded engine operation due to its friction optimized piston group system. The most significant result during the comparison of the piston group friction losses was investigated at high load operation. Here gasoline engine 2 revealed increased FMEP levels for engine speeds higher n = 1500 rpm and peak cylinder pressures above p_{cyl} = 70 bar and FMEP differences of up to ΔFMEP = 0.5 bar in comparison to the diesel engine could be determined. The crankshaft journal bearings showed only small differences when comparing the base engines. This can be explained by the comparable geometry of the bearings. One of the most significant result of the conducted work can be assigned to the design of the valve train system. In particular the valve actuation system, has significant influence on the engine friction performance. Here the progress in the development of valve train systems away from flat-tapped based valve actuation systems which is used in gasoline engine 1 to roller finger follower systems with increased mechanical efficiency used in the other two engines has been investigated. When disregarding the disadvantageous valve train friction losses at gasoline engine 1, the other sub-assemblies namely piston group and crankshaft journal bearings are showing a good performance and partly better results in comparison to the other engine concepts.

Future work could address the analysis of friction reduction potentials and possible risks due to mixed lubrication on the base engine sub-assembly level. Furthermore future work could address the development of detailed simulation models for the piston group and valve train system. This could enable advanced investigations of the tribological performance down to the component level of the base engines.

Author Contributions: C.K., H.A. and D.E.S. conceived and designed the experiments; C.K., H.A. and D.E.S. performed the experiments; C.K. and D.E.S. build up the simulation models; C.K. performed the calculations; All authors analysed and discussed the data; C.K. wrote the paper.

Funding: The publication was written at VIRTUAL VEHICLE Research Center in Graz and partially funded by the COMET K2—Competence Centers for Excellent Technologies Programme of the Federal Ministry for Transport, Innovation and Technology (bmvit), the Federal Ministry for Digital, Business and Enterprise (bmdw), the Austrian Research Promotion Agency (FFG), the Province of Styria and the Styrian Business Promotion Agency (SFG). Furthermore, we acknowledge the partial financial support of the Austrian Science Fund (FWF): P27806-N30.

Conflicts of Interest: The authors declare no conflict of interest.

References

1. Holmberg, K.; Erdemir, A.; The impact of tribology on energy use and CO_2 emission globally and in combustion engine and electric cars. *Tribol. Int.* **2019**, *135*, 389–396.
2. Holmberg, K.; Andersson, P.; Erdemir, A.; Global energy consumption due to friction in passenger cars. *Tribol. Int.* **2012**, *47*, 221–234.
3. Schwaderlapp, M.; Koch F.; Dohmen J.; Friction Reduction—The Engine's Mechanical Contribution to Saving Fuel. In Proceedings of the FISITA World Automotive Congress, Seoul, Korea, 12–15 June 2000.
4. Grebe, U.D. *Weiterentwicklung des Otto-Motors*; Lecture notes; Technical University Vienna: Vienna, Austria, 2015; Chapter 2.
5. Wong, V.W.; Tung, S.C. Overview of automotive engine friction and reduction trends—Effects of surface, material, and lubricant-additive technologies. *Friction* **2016**, *4*, 1–28.
6. Melby, J. Internal Combustion Engine Friction Testing and Virtual Modeling. Masters Thesis, Norwegian University of Science and Technology, Trondheim, Norway, 2016.
7. Mufit, R.A.; Priest, M. Effect of Engine Operating Conditions and Lubricant Rheology on the Distribution of Losses in an Internal Combustion Engine. *ASME. J. Tribol.* **2009**, *131*, 37–43.
8. Mufti, R.A. Total and Component Friction in a Motored and Firing Engine. Ph.D. Thesis, University of Leeds, Leeds, UK, 2004.
9. Dowson, D.; Taylor, C.M.; Yang, L. Friction Modelling for Internal Combustion Engines. In *The Third Body Concept Interpretation of Tribological Phenomena*; Dowson, D., Taylor, C.M., Childs, T.H.C., Dalmaz, G., Berthier, Y., Flamand, L., Georges, J.-M., Lubrecht, A.A., Eds.; Elsevier Science B.V.: Amsterdam, The Netherlands, 1996; pp. 301–318.
10. Fischer, G.D. Expertenmodell zur Berechnung der Reibungsverluste von Ottomotoren. Ph.D. Thesis, Technische Universität Darmstadt, Darmstadt, Germany, 2000.
11. Sylvester, J.R. Characterization and Modeling of Rubbing Friction in a Motored Four-Cylinder Internal Combustion Enginge. Master's Thesis, McMaster University, Hamilton, ON, Canada, 2012.
12. Sopouch, M. Reibungsanalyse an Komponenten von Dieselmotoren durch Vergleiche von Messung und Berechnung. Master's Thesis, Montanuniversität Leoben, Leoben, Austria, 1995.
13. Gießauf, G. Bewertung unterschiedlicher reibungsrelevanter Maßnahmen beim PKW-Dieselmotor. Master's Thesis, Graz University of Technology, Graz, Austria, 2013.
14. Schaffer, K.M. Maßnahmen zur Verbesserung des Arbeitsprozesses und des Reibverhaltens von Pkw Dieselmotoren. Ph.D. Thesis, Graz University of Technology, Graz, Austria, 2011.
15. Shayler, P.J.; Leong, D.K.W.; Murphy, M. Contributions to Engine Friction During Cold, Low Speed Running and the Dependence on Oil Viscosity. *SAE Int. J. Engines* **2005**, *114*, 1191–1201.
16. Taylor, R.I. Engine Friction Lubricant Sensitivities: A Comparison of Modern Diesel and Gasoline Engines. *Tribotest J.* **2000**, *7*, 37–43.
17. Wichtl, R. Wettbewerbsvergleich zweier Ottomotoren mit Aufladung und Direkeinspritzung. Master's Thesis, Graz University of Technology, Graz, Austria, 2012.
18. Penninger, M. Vergleich von PKW-Dieselmotoren mit einer Reibungsanalyse. Master's Thesis, Graz University of Technology, Graz, Austria, 2011.
19. Michaelis, K.; Geiger, J.; Moser, K.; Stahl, K.; Beulshausen, J.; Pischinger, S. *Low Friction Powertrain, General Report of the Research Cluster Low Friction Powertrain*; Final report, FVV Heft 1000; FVV: Frankfurt am Main, Germany, 2013.

20. Golloch, R. *Downsizing bei Verbrennungsmotoren—Ein wirkungsvolles Konzept zur Kraftstoffverbrauchssenkung*; Golloch, R., Ed.; Springer: Berlin/Heidelberg, Germany, 2005.
21. Knauder, C.; Allmaier, H.; Sander, D.E.; Sams, T. Investigations of the friction losses of different engine concepts. Part 1: A combined approach for applying sub-assembly-resolved friction loss analysis on a modern passenger car diesel engine. *Lubricants* **2019**, *7*, 39.
22. Sander, D.E.; Knauder, C.; Allmaier, H.; Damjanovic-Le Baleur, S.; Mallet, P. Friction Reduction Tested for a Downsized Diesel Engine with Low-Viscosity Lubricants Including a Novel Polyalkylene Glycol. *Lubricants* **2017**, *5*, 9.
23. Sreenath, A.V.; Raman, N. Running-in wear of a compression ignition engine: Factors influencing the conformance between cylinder liner and piston rings. *Wear* **1976**, *38*, 271–289.
24. Dowson, D. *The Running-in Process in Tribology*; Dowson, D., Taylor, C., Godet, M., Berthe, D., Eds.; Butterworth-Heinemann: Oxford, UK, 1982.
25. Knauder, C.; Allmaier, H.; Salhofer, S.; Sams, T. The impact of running-in on the friction of an automotive gasoline engine and in particular on its piston assembly and valve train. *Proc. Inst. Mech. Eng. J.* **2017**, *232*, 749–756.
26. Zhmud, B. In-manufacture Running-in of Engine Components by Using the Triboconditioning® Process. In Proceedings of the 7th International Conference on Fracture Fatigue and Wear, FFW 2018, Ghent, Belgium, 9–10 July 2018; pp. 671–681.
27. Carden, P.; Pisani, C.; Lainè, E.; Field, I.; Devine, M.; Schoeni, A.; Beyer, P. Calculation of crank train friction in a heavy duty truck engine and comparison to measured data. *Proc. Inst. Mech. Eng. J.* **2013**, *227*, 168–184.
28. Adams, D.R. Tribological considerations in internal combustion engines. In *Tribology and Dynamics of Engine and Powertrain*; Rhanejat, H., Ed.; Woodhead Publishing Limited: Sawston, UK, 2010; pp. 251–283.
29. Sandoval, D. An Improved Friction Model For Spark Ignition Engines. Bachelor of Science Thesis, Massachusetts Institute of Technology, Cambridge, MA, USA, 2013.
30. Schwarzmeier, M. Der Einfluss des Arbeitsprozeßverlaufs auf den Reibmitteldruck von Dieselmotoren. Ph.D. Thesis, Technische Universität München, München, Germany, 1992.

4.3 Friction reduction potentials and risk assessment at the sub-assembly level

In the foreseeable future, diversity in passenger car vehicles' propulsion systems will grow. Driven by the electrification of the power train, the pure ICE driven vehicle will decrease. Nevertheless, the usage of the ICE in hybrid propulsion systems will increase at the same time. Therefore, the ICE will stay the predominant propulsion technology in the transportation sector with 75% purely driven and about 90% in electrified hybrid propulsion systems. [14], [95] For this reason, the reduction of fuel consumption and pollutant emissions will continue to be necessary and the minimisation of friction losses will be an essential element in achieving this objective. Today a widespread use of continuously lower viscosity lubricants in engines to achieve lower fuel consumption is present.

The friction losses in the hydrodynamic lubrication regime are dominated by the inner resistance of the lubricant during shearing processes between sliding surfaces (lubricant viscosity). The friction loss in that lubrication regime is directly proportional to lubricant viscosity, assuming pure or at least strongly dominating hydrodynamic lubrication. A reduction in lubricant viscosity subsequently reduces the friction losses. At the same time, the lubrication film height is decreasing. Friction reduction is possible up to the point where the lubricating gap height has been reduced until contact between the previously separated surfaces starts. In a first phase of the mixed lubrication regime, this happens at the roughness peaks of the technical surfaces. When the lubrication gap is further decreasing by lowering the lubricant viscosity, increasing the load or decreasing the sliding velocity solid to solid contact between the surfaces is increased and the mixed lubrication regime is becoming more and more pronounced. Increased friction and the onset of wear are the result of these unfavourable lubrication conditions, affecting the performance and service life of engine components.

By determining the quantity of present mechanical friction losses, no insight can be gained about potential harmful boundary friction and increased risk of failure for the lubricated contacts in the sub-assembly system. Increased wear, component degradation, surface damage or bearing seizure are potential risks that arise from reduced oil film heights.

The approach used to investigate the lubrication conditions for the three engines and their sub-systems is as follows: by varying the media temperature of the engine under test, the lubrication conditions in all contacts are simultaneously affected. A viscosity reduction is achieved by increasing the temperature, thus simulating the use of a low-viscosity engine oil. Consequently, the friction losses of the three engines are determined, analysed and compared for different media temperatures: 70 °C and 90 °C. If the determined friction losses for the increased media temperature do not change or even increase, this indicates the presence of significant amounts of mixed lubrication.

This work therefore investigates the friction increase (risk) and friction decrease (reduction potential) using the previously presented combined experimental and numerical approach. The novelty of this work is that the lubrication analysis is performed not only for the three full base engines, but also to their subsystems.

The details of the chosen approach as well as the results of the friction reduction potentials and risk assessment at the sub-assembly level are described in [45] and can be found in section 4.3.2. Prior to this, the research findings of the publication are summarized.

4.3.1 Summary of research findings

- The evaluation is not carried out by strip tests to determine the friction losses of the individual components, but by applying the combined methodology developed to the overall system.
- The investigations on the individual piston assembly, main and big end bearings, and combined valve train/timing drive systems of the engines are performed on passenger car engines of the same size with the same or twice the specific power. This enables the friction potential and risk assessment analysis in relation to conventional and down-sized concepts.
- At the base engine level, for example of gasoline engine 2, the arising risks are rather small between 0 % and -2 % at low engine speeds and high loads. However, when analyzing the friction reduction at the sub-assembly level, arising risks are identified at the piston group and valve train system.
- A reduction of the lubricant viscosity is very well suited to reduce friction losses at the main and big end bearings at all three engines. Large reduction potentials between 16 % and 30 % indicate an operation mainly in the hydrodynamic lubrication regime.
- The potential analysis of piston group friction provides different results.
- For the piston group system of the diesel engine and gasoline engine 1, friction reduction potentials up to 16 % are found, but in different operating conditions. For gasoline engine 1, reduction potentials are found at low speed and low load operation, while reduction potentials for the diesel engine are found at medium speed and low load operation. Both engines reveal beginning mixed lubrication to a minor extent with a friction increase of up to 7 % for low engine speeds and high load operation.
- For low load operation, friction reduction potentials up to 23 % are obtained at the piston group system of gasoline engine 2. The most significant results are obtained at low engine speed and high load operation. Arising risks are present at engine speeds below n = 2000 rpm and peak cylinder pressures above pcyl = 50 bar. At these operation points, disadvantages of up to 29 % are identified.
- A temperature increase at the valve train system (including timing drive and crankshaft seals) results in an increase of the friction losses. Dependent on the valve train design, the friction increase is more or less significant. For the flat tapped based valve actuation system of gasoline engine 1, friction losses increase between 9 % and 18 %. A strong dependency on the engine speed of the roller type follower systems of valve train system of the diesel engine and gasoline engine 2 was found. While the friction losses for the diesel valve train system are increasing by 9 % and 11 %, minor reduction potentials up to 3 % at gasoline engine 2 are found at engine speeds between n=2000 rpm and n=4000 rpm. At lower engine speeds, friction losses increase up to 9 % and considerably at higher engine speeds up to 22 %.
- Potential harmful increase of friction loss of a single sub-system cannot be identified when the entire base engine is evaluated. For instance, friction reduction in the bearings may cancel the increase of friction in the valve train or the piston assembly system, leading to possible misinterpretations.

4.3.2 Paper III [45]

lubricants

MDPI

Article

Investigations of the Friction Losses of Different Engine Concepts: Part 3: Friction Reduction Potentials and Risk Assessment at the Sub-Assembly Level

Christoph Knauder [1,*], Hannes Allmaier [1], David E. Sander [1], and Theodor Sams [2,3]

1 Virtual Vehicle Research GmbH, Inffeldgasse 21A, 8010 Graz, Austria; hannes.allmaier@v2c2.at (H.A.); david.sander@v2c2.at (D.E.S.)
2 AVL List GmbH, Hans-List-Platz 1, 8020 Graz, Austria; theodor.sams@avl.com (T.S.)
3 Institute of Internal Combustion Engines and Thermodynamics - Graz University of Technology, Inffeldgasse 19, 8010 Graz, Austria
* Correspondence: christoph.knauder@v2c2.at

Received: 10 February 2020; Accepted: 25 March 2020; Published: 31 March 2020

Abstract: One of the biggest requirements of today's engine development process for passenger cars is the need to reduce fuel consumption. A very effective and economic approach is the use of low-viscosity lubricants. In this work, sub-assembly resolved friction reduction potentials and risks are presented for three different engine concepts. By using a developed combined approach, the friction losses of the base engines are separated to the sub-assemblies piston group, crankshaft journal bearings, and valve train over the full operation range of the engines. Unique analyzing of boundary conditions makes it possible for the first time to compare friction reduction potentials and possible risks, not only between diesel and gasoline engines for passenger car applications, but also with particular focus on the power density of the three engines. Firstly, the engines have been specifically chosen regarding their specific power output. Secondly, one identical SAE 5W30 lubricant suitable for all engines is used to neglect influences from different lubricant properties. Thirdly, identical test programs have been conducted at the same thermal boundary conditions at engine media supply temperatures of 70 °C and 90 °C. For the crankshaft journal bearings, high reduction potentials are identified, while risks arising occur at the valve train and the piston group systems.

Keywords: engine friction; friction reduction; friction reduction potential analysis; mixed lubrication; hydrodynamic lubrication; ICE; friction loss distribution; sub-assembly friction; valve train; journal bearings; main bearings; big end bearings; piston group.

1. Introduction

A reliable lubrication system is of key importance for internal combustion engines. For emission legislation, the focus relies on the mechanical friction losses of the engine, as these directly contribute to fuel consumption. Consequently, OEMs continually work to reduce these to a minimum. [1] However, there are different regimes of friction that are usually represented by the Stribeck curve: purely hydrodynamic lubrication, boundary friction, and the mixed lubrication regime, where both of these forms of friction coexist. These different schemes are shown for a statically loaded journal bearing in Figure 1.

Lubricated contacts which are present in internal combustion engines might be assumed to operate in purely hydrodynamic lubrication. With this form of lubrication, a sufficiently thick oil film separates the two gliding surfaces from each other and the friction in this oil film generates the observed losses. Purely hydrodynamic lubrication is advantageous in principle as there is no actual contact between the surfaces and consequently no wear can occur. The reality is more complex as the

Lubricants **2020**, *8*, 39

transient nature of operation for internal combustion engines prevents pure hydrodynamic lubrication (for example, during starting).

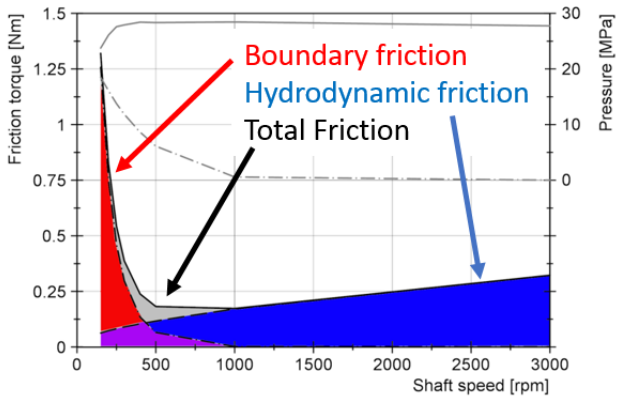

Figure 1. Stribeck curve for a statically loaded journal bearing (from [2]). As can be seen, decreasing shaft speed mixed lubrication starts early at about 1000 rpm and steadily increases. The total friction reaches its minimum at about 500 rpm, where significant mixed lubrication is present, and accounts for about one-third of the total friction.

Furthermore, the Stribeck curve shows that the minimum of the friction losses is located in the mixed lubrication regime where some surface contact is present. Consequently, the continued efforts to reduce the friction losses in internal combustion engines have led to the regular appearance of mixed lubrication. Excessive wear is typically countered with either oil additive chemistry or surface coatings, and is often combined with a very smooth surface topography.

In the previous two parts of this series, a novel method to investigate friction in internal combustion engines was presented (see part 1 [3]), and applied to three engines from different engine architectures (see part 2 [4]). The friction losses were investigated by combining experimental testing with accurate simulation techniques.

However, by merely determining the quantity of present mechanical friction losses [5], no insight can be gained about the dominant form of friction or how close the engine is to the minimum friction point. Furthermore, potential harmful boundary friction and increased risk of failure for lubricated contacts cannot be located without investigating the engine's sub-systems. Potential risks that arise from reduced oil viscosity, and consequently by enhanced metal to metal contact are, for example, increased wear, component degradation, surface damage, or bearing seizures. Therefore, the third part of this series aims to extend the basis provided by the previous works, by analyzing the lubrication regime of these three investigated engines.

In contrast to published works that investigate the lubrication regime only in a global context [6,7], or for specific parts of an engine [8,9], like, for example, the main and big end bearings [10], the piston assembly [11–15], valve train [16–18] or even of rotary crank shaft seals [19], the present work analyzes all individual sub-assemblies (main and big end bearings, piston assembly, and combined valve-train/timing drive) of the same specific engines for the entire range of operating conditions, including engine load.

The approach used to investigate the lubrication conditions for the three engines and their sub-systems is as follows: by varying the media temperature of the engine under test, the lubrication conditions in all contacts are simultaneously affected. A viscosity reduction is achieved by increasing the temperature, thus simulating the use of a low-viscosity engine oil. Consequently, the friction losses of the three engines are determined for different media temperatures: 70 °C and 90 °C. Conventional motor oils show a strong dependency of dynamic viscosity on temperature [20]; therefore,

Lubricants **2020**, *8*, 39

a temperature increase of 20 °C corresponds roughly to reducing the oil viscosity in half. The following Figure 2 shows the behavior of the lubricant viscosity for the SAE (Society of Automotive Engineers) 5W30 lubricant used in this work when increasing the lubricant temperature. When increasing the temperature from 70 °C to 90 °C, the dynamic viscosity decreases from 20.18 mPas to 11.83 mPas, respectively, which represents a viscosity reduction of 41%. For comparison, the use of engine oils with a difference of two SAE classes (for example, SAE 30 and SAE 16) is given here.

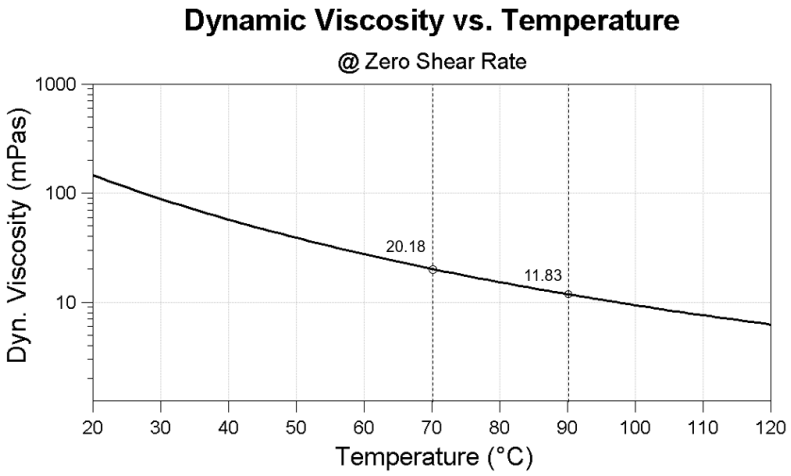

Figure 2. Dynamic viscosity decrease when increasing the lubricant temperature for the 5W30 lubricant used in this study.

The friction loss due to hydrodynamic shear stress in a lubricating film is directly proportional to lubricant viscosity [2]. Therefore, assuming pure—or at least strongly dominating—hydrodynamic lubrication, reducing viscosity also reduces the friction losses correspondingly. This is the same argument that led to the widespread use of continuously lower viscosity lubricants in engines to achieve lower fuel consumption. However, if the determined friction losses for the increased media temperature do not change or even increase, this indicates the presence of significant amounts of mixed lubrication (see also Figure 1). This work therefore investigates the friction increase (risk) and friction decrease (reduction potential) using the previously presented combined experimental and numerical approach.

The novelty of this work is that the lubrication analysis is performed not only for the three full base engines, but also to their subsystems. However, the evaluation is not carried out by strip tests to determine the friction losses of the individual components, but by applying the combined methodology developed to the overall system. In addition, the investigations on the individual piston assembly, main and big end bearings, and combined valve train/timing drive systems of the engines are performed on passenger car engines of the same size with the same or twice the specific power. This enables the friction potential and risk assessment analysis in relation to conventional and down-sized concepts.

2. Test Program and Test Procedure

The applied analysis used a specifically coordinated procedure [3], combining predictive journal bearing simulations and accurate measurements. The investigations are carried out on three different engines for passenger car applications, two gasoline engines, and one diesel engine. The engines have been specifically chosen according to their power density. This allows the analysis of the friction losses not only between diesel and gasoline engine architectures, but also with a focus on the specific power output. Table 1 lists the main technical data of the engines investigated in this work.

Table 1. Technical data of the engines under test.

Parameter	Diesel Engine	Gasoline Engine 1	Gasoline Engine 2
Volume displacement	1995 cm^3	1781 cm^3	1991 cm^3
Compression ratio	16.5:1	9.5:1	8.6:1
Bore	84 mm	81 mm	83 mm
Stroke	90 mm	86.4 mm	92 mm
Nominal torque	380 Nm	235 Nm	422 Nm
Nominal Power	135 kW	130 kW	265 kW
Specific power	68 kW/L	73 kW/L	133 kW/L
Maximum Speed	4600 rpm	6600 rpm	6700 rpm
Cylinder distance	91 mm	88 mm	90 mm
Conrod length	138 mm	144 mm	138.7 mm
Main bearing diameter	55 mm	54 mm	55 mm
Main bearing width	25 mm	22 mm	19 mm
Main bearing clearance (cold)	20 µm	20 µm	20 µm
Big-End bearing diameter	50 mm	47.8 mm	48 mm
Big-End bearing width	24 mm	25 mm	19.4 mm
Valve-train	DOHC	DOHC	DOHC
Timing drive	chain	belt	chain
Valve-train type	roller-type cam follower	flat-base tappet	roller-type cam follower
Valves	4 per cylinder	5 per cylinder	4 per cylinder
Connecting rod ratio	0.326	0.3	0.332

The diesel engine and gasoline engine 1 represent conventional engine concepts with almost the same specific power output. Gasoline engine 2 is designed as a high-power downsized engine concept, and has the doubled power density in comparison to the conventional concepts. The following Figure 3 shows the overview of the used procedure to conduct the potential analysis on the sub-assembly level of the base engines.

The determination of the total friction losses is done experimentally using the IMEP (indicated mean effective pressure)-method. For the sake of completeness, the main equations when using the IMEP-method are presented here (for example, see textbook [21]),

$$FMEP = IMEP - BMEP \tag{1}$$

where the FMEP is calculated by a subtraction of the IMEP and BMEP (brake mean effective pressure) according to Equation (1).

For the calculation of the BMEP (Equation (2)), the measured brake torque at the crankshaft (T) is related to the corresponding mean effective pressure (BMEP)

$$BMEP = \frac{W}{V_D} = \frac{4\pi T}{V_D} \tag{2}$$

where W refers to the work per cycle and V_D to the volume displacement of the investigated four-stroke engine.

Equation (3) describes the calculation of the IMEP by integrating the measured cylinder pressure ($pcyl$) over a working cycle divided by the volume displacement of the engine:

$$IMEP = \frac{\oint pdV}{V_D} \tag{3}$$

For all three engines investigated in this work, the same analysis procedure (see Figure 3) is used after disassembling the full engine to the base engine level. By combination and subtraction of the individual friction losses received at the respective engine media supply temperatures (70 °C and 90 °C), the resulting friction loss reduction and increase are calculated.

Lubricants **2020**, *8*, 39

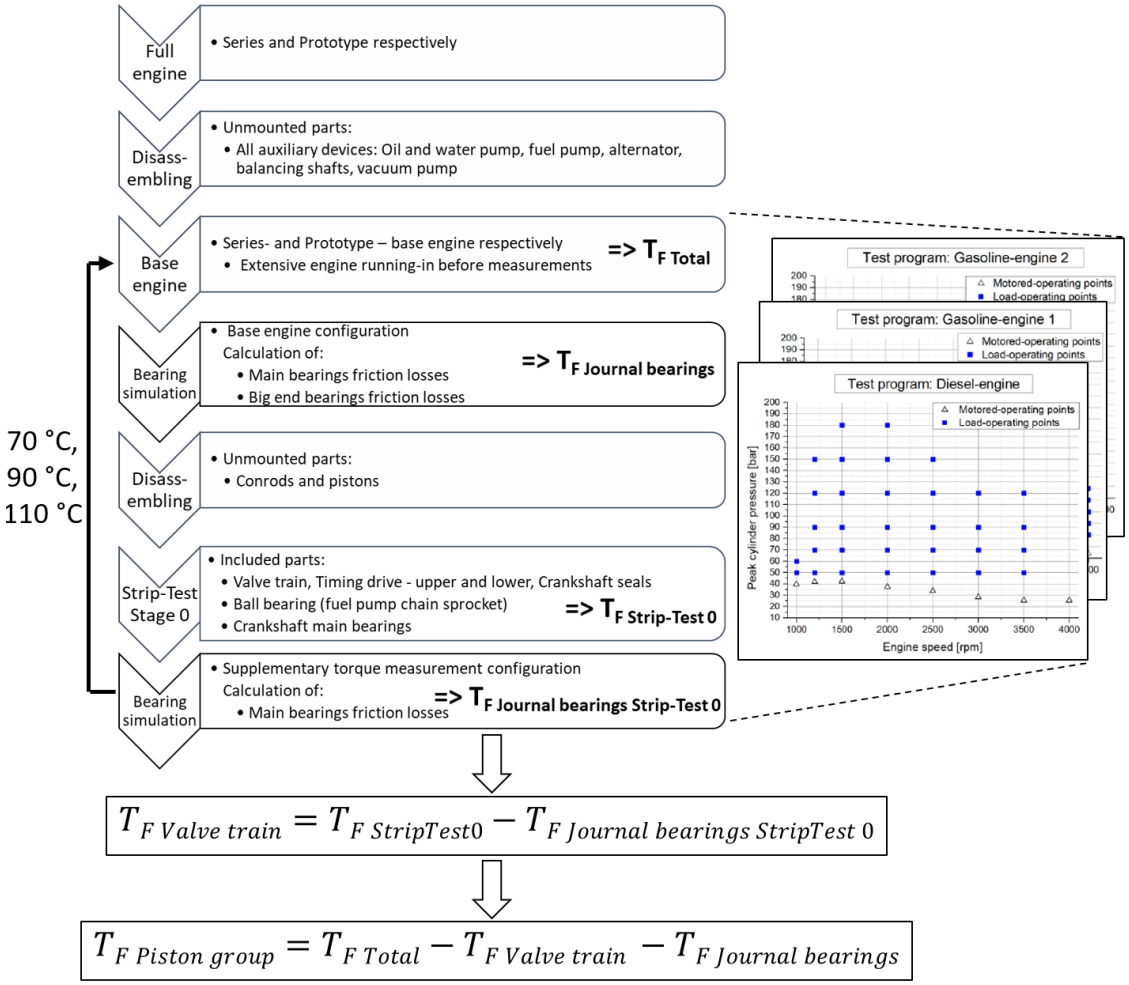

Figure 3. Analysis procedure to investigate the friction reduction potential and risk at the sub-assembly level of the base engines.

The risk assessment in this work is conducted by analyzing the increase in friction when temperature is increased. An increased temperature lowers the viscosity, and it is expected that friction in the mixed and boundary lubrication regime increases due to more severe metal to metal contact. More severe metal to metal contact is potentially harmful to components in the lubricated contacts, and, therefore, it is considered to be a risk when friction increases.

3. Sub-Assembly Resolved Friction Reduction Potentials and Risks

In the following section, the sub-assembly resolved friction reduction potentials and risks are presented for the diesel engine, gasoline engine 1, and gasoline engine 2, when increasing the lubricant and water supply temperature from 70 °C to 90 °C. For each of the three engines, the results are plotted in one figure including all four sub-assembly systems investigated.

Diesel engine: The results of the potential analysis for the diesel engine when increasing the engine media supply temperature from 70 °C to 90 °C are presented in Figure 4. It is interesting to note that the crankshaft journal bearings (main and big end bearings) revealed a significant decrease of the friction losses when increasing the lubricant supply temperature between 16% and 30%, which indicates an operation mainly in the hydrodynamic lubrication regime. For the piston group, the same trend is found for a wide range of engine operation. Especially at low load operation and engine speeds between n = 1500 rpm and n = 2500 rpm, the FMEP decreases by 16%. For engine speeds lower than n = 2000 rpm and high engine loads, the FMEP values partially increase up to 7% indicating

mixed lubrication. On the other hand, the valve train friction losses share (including crankshaft seals and timing drive) increase with increasing engine media supply temperature in the range of 9% to 11%. It was found in part 1 of this publication series [3] that the disadvantages at the combined valve train/timing drive system arise largely from the timing drive part.

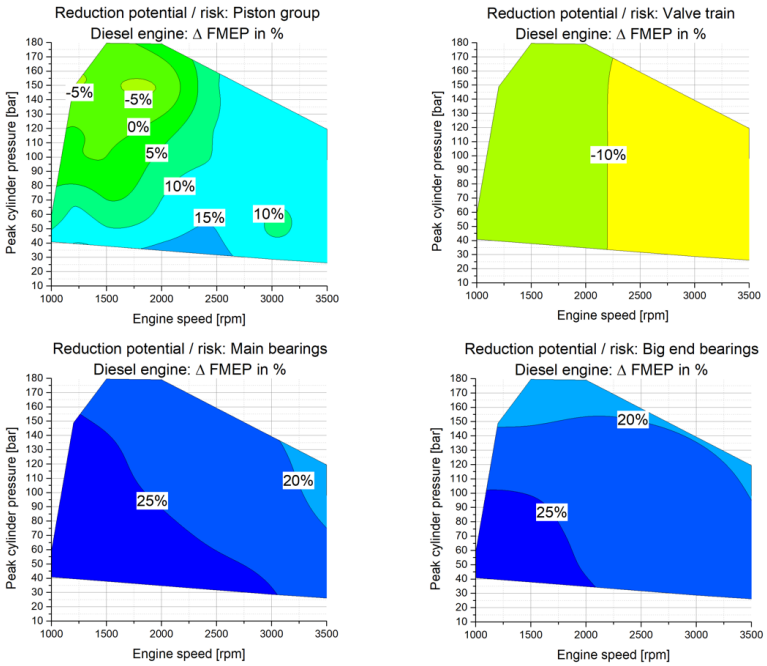

Figure 4. Diesel engine: Sub-assembly resolved friction reduction potential/risk when increasing the engine media supply temperature from 70 °C to 90 °C (positive values represent friction benefits); **top left**: piston group, **top right**: valve train, **bottom left**: main bearings, **bottom right**: big end bearings.

Gasoline engine 1: The results of the friction reduction potential analysis for the gasoline engine 1 when increasing the engine media supply temperature from 70 °C to 90 °C are presented in Figure 5.

For the crankshaft main bearings and big end bearings, it was found that a temperature increase of the engine media (cooling water and lubricant) results in significant friction reduction in the range of 18% to 32%. The results for the crankshaft journal bearings indicate an operation in the hydrodynamic lubrication regime. For the piston group assembly, advantages of up to 19% are investigated at very low loads and engine speeds below n = 1500 rpm. Beyond low speeds and low loads, the friction loss potential analysis at the piston group shows both disadvantages up to −5% indicating mixed lubrication regimes, as well as reduction potentials up to 10%. It is further interesting to note that, for the valve train system which is designed as flat-tappet based valve actuation system, the friction losses are strongly affected by the lubricant supply temperature. Similar results for the flat-tappet based based systems are found in [22]. The friction losses increase between 9% at high engine speeds and 18% at low engine speeds. Especially at low engine speeds, the friction losses increase to a greater extent, where subsequently reduced rotational speeds are present at the interaction between flat tappet and cam.

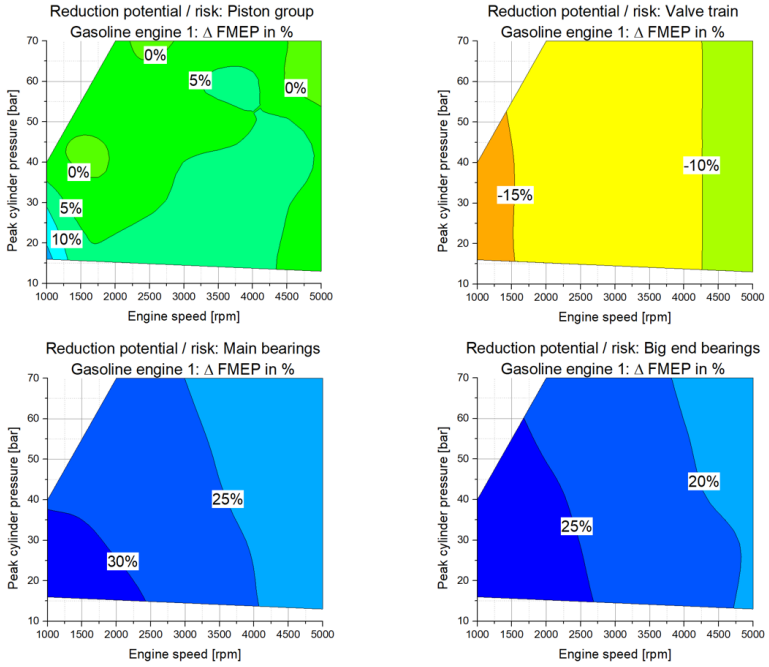

Figure 5. Gasoline engine 1: Sub-assembly resolved friction reduction potential/risk analysis when increasing the engine media supply temperature from 70 °C to 90 °C (positive values represent friction benefits); **top left**: piston group, **top right**: valve train, **bottom left**: main bearings, **bottom right**: big end bearings.

Gasoline engine 2: For gasoline engine 2, the friction potential investigation has been carried out for identical thermal boundary conditions compared to the other engines. The engine media supply temperature has been varied from 70 °C to 90 °C and the following Figure 6 shows the results of the friction potential analysis.

For the crankshaft journal bearings, a friction reduction in the range of 16% to 29% results from the conducted potential analysis. This indicates an operation of the journal bearings in the hydrodynamic lubrication regime. For the piston group, varying results are obtained, while, at engine speeds above n = 2500 rpm, friction reduction potentials of up to 23% are investigated, the behavior at low engine speeds is different. Especially at engine speeds below n = 2000 rpm and high load conditions, significant disadvantages of up to −29% arise indicating significant mixed lubrication regimes in the piston group sub-assembly. The results for the piston group clearly show the high requirements for high power downsized engine architectures. Particularly at low loads and low engine speeds, the limit between operation in hydrodynamic and mixed lubrication regime is reached, and limits possible friction reduction when the viscosity of the lubricant is reduced. For the valve train friction losses (incl. timing drive and crankshaft seals friction losses), it is interesting to note that, for engine speeds below n = 2000 rpm, the friction losses increase up to 9% when increasing the engine media supply temperature. Additionally, for high engine speeds above n = 4000 rpm, the friction losses significantly increase up to 22%. For engine speeds in the range between n = 2000 rpm and n = 4000 rpm, the friction reduction potential is to a minor extent. The reduction potential/risk is small ranging between an advantage of 3% and a disadvantage of −1%.

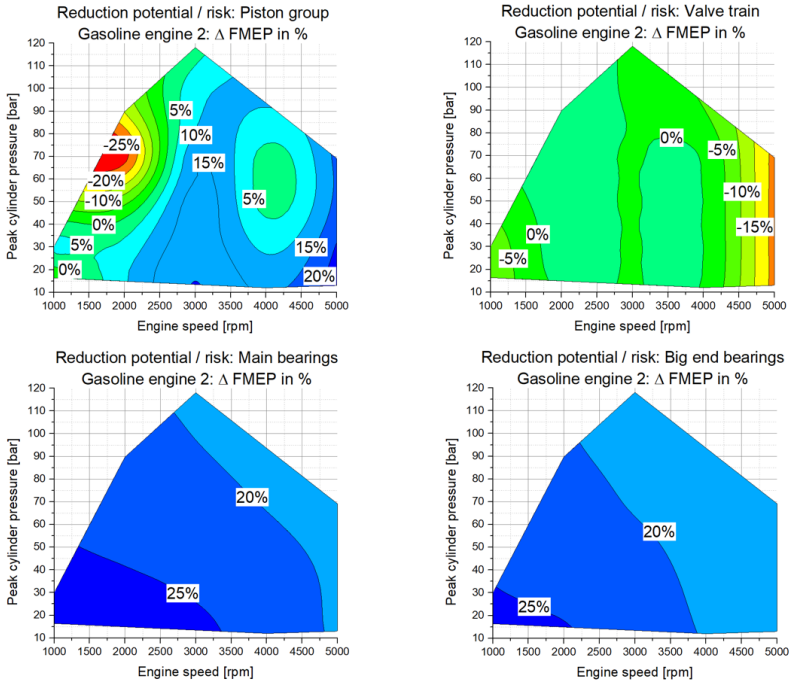

Figure 6. Gasoline engine 2: Sub-assembly resolved friction reduction potential/risk analysis when increasing the engine media supply temperature from 70 °C to 90 °C (positive values represent friction benefits); **top left**: piston group, **top right**: valve train, **bottom left**: main bearings, **bottom right**: big end bearings.

4. Base Engine Friction Losses and Resulting Global Potentials and Risks

The total friction losses ($T_{F\,Total}$) of the three engine concepts have been investigated according to the analysis procedure presented in Figure 3. Since the base engine friction results are obtained at engine media supply temperatures of 70 °C and 90 °C, the friction reduction potential analysis can be performed not only at the sub-assembly level of the engines, but also at the global base engine level. This is done by subtraction of the FMEP results at the individual temperature level, and enables comparison of the global potential and risks at the base engine level. Subsequently, possible advantages using the presented combined approach are explained in detail. The resulting FMEP-maps at the base engine level of the investigated engine architectures are presented in Figure 7 (see also [4]).

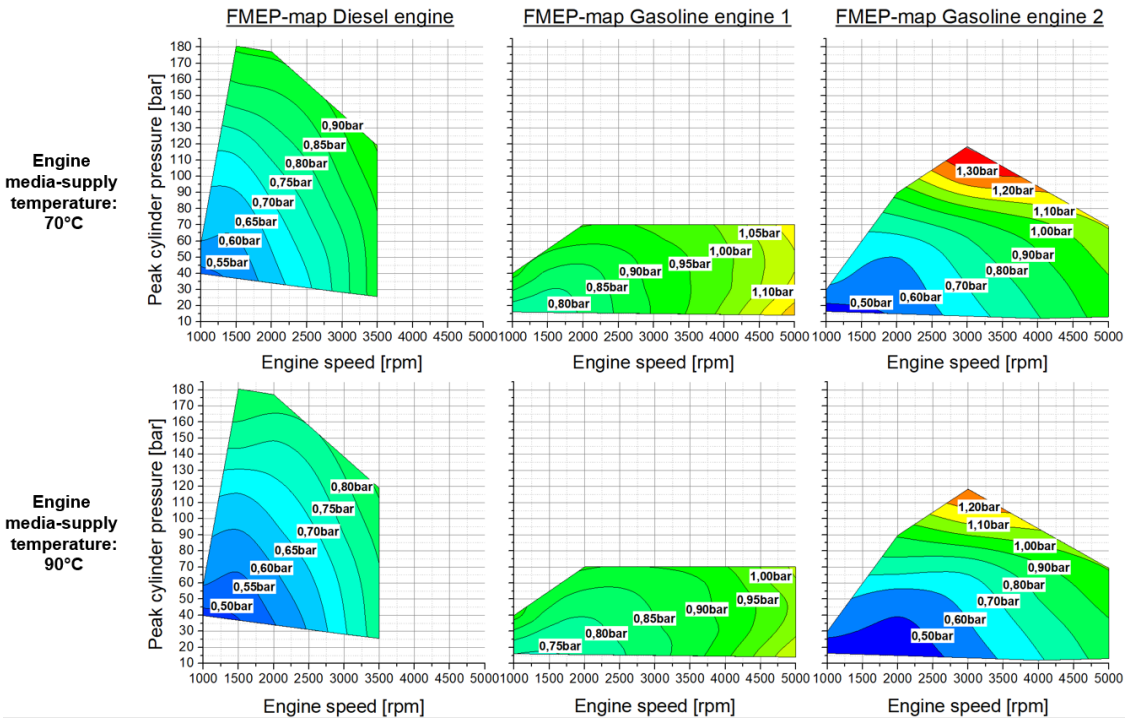

Figure 7. Resulting FMEP-maps for different engine media supply temperatures: (**left**) diesel engine; (**middle**) gasoline engine 1; (**right**) gasoline engine 2.

By increasing the lubricant supply temperature, a significant decrease of the lubricant viscosity is obtained (see Figure 2), and friction reduction potentials, as well as possible risks due to beginning mixed lubrication regimes are studied. The following Figure 8 shows the calculated friction reduction/risk potential when increasing the engine media supply temperature of the base engines from 70 °C to 90 °C.

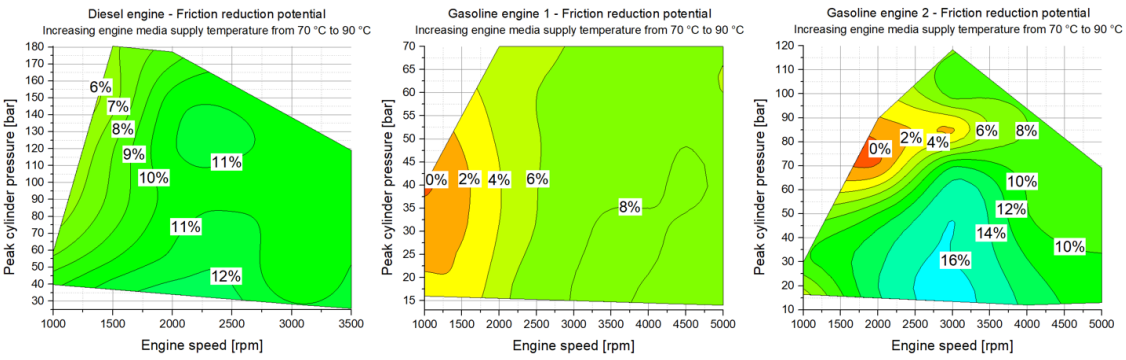

Figure 8. Base engine friction reduction potentials/risks when increasing the oil supply temperature (negative values represent disadvantages): **left** Diesel engine; **middle** Gasoline engine 1; **right** Gasoline engine 2.

Diesel engine:

The increase in engine media supply temperature shows friction reduction potentials over the entire engine speed and load range, and advantages up to 13% are investigated. The most significant advantages result at engine speeds higher than n = 1500 rpm. At lower engine speeds between n = 1000 rpm and 1500 rpm, the friction reduction potential is in the range of 6% (at high load operation) to 11% (at low load operation).

Gasoline engine 1:

When the engine media supply temperature is increased from 70 °C to 90 °C for gasoline engine 1, areas of friction reduction potential near 0% and below signal arising risks (see Figure 8 middle). At low engine speeds and high loads, disadvantages (risks) of up to −2% arise, indicating mixed lubrication regimes. Furthermore, the overall friction reduction potential ranges between −2% and 9%. This shows that the overall friction reduction potential for this engine is smaller in comparison to the other engines. It is interesting to note that friction reduction potentials above 6% are investigated for engine speeds higher than n = 2000 rpm and low load conditions.

Gasoline engine 2:

Increasing the engine media supply temperature from 70 °C to 90 °C at gasoline engine 2 results in areas of friction reduction potential near 0% and below (see Figure 8 right). It is interesting to note that, for engine operation at low loads, significant reduction potential results. For engine speeds above n = 1500 rpm and peak cylinder pressures below pcyl = 50 bar, reduction potentials between 10% and 17% are investigated. When the engine load is increased especially at engine speeds below n = 3000 rpm, the reduction potential decreases and enters levels between −1% and 6%. The results indicate mixed lubrication at engine speeds below n = 2000 rpm and peak cylinder pressures above pcyl = 70 bar.

5. Discussion

The results of the friction potential analysis and risk assessment at the base engine level represents a good example of the advantages when using the combined approach for friction analysis presented in the publicatiosn series [3,4]. At the base engine level, for example of gasoline engine 2, the arising risks are rather small between 0% and −2% at low engine speeds and high loads. However, when analyzing the friction reduction at the sub-assembly level (see Figure 6), arising risks are identified at the piston group system and valve train system. Therefore, the presented analysis procedure enables to place specific focus on measures for developing future engine generations at the relevant sub-assembly systems.

The main and big end bearings at all three engines show large reduction potentials between 16% and 30% and indicate an operation mainly in the hydrodynamic lubrication regime. For the piston group system of the diesel engine and gasoline engine 1, friction reduction potentials up to 16% are found. It is interesting to note that the reduction potential at the piston group system are identified at different areas of engine operation, while, for gasoline engine 1, reduction potentials are found at low speed and low load operation, reduction potentials for the diesel engine are found at medium speed and low load operation. Both engines reveal beginning mixed lubrication to a minor extent when increasing the engine media supply temperature from 70 °C to 90 °C for low engine speeds and high load operation. Here, the friction levels increase up to 7%.

The most significant results are obtained for the piston group of gasoline engine 2, which is designed as a high-power downsizing concept. For low load operation friction, reduction potentials up to 23% are obtained, and the results at low engine speed and high load operation are significantly different. It is found that arising risks are present at engine speeds below n = 2000 rpm and peak cylinder pressures above pcyl = 50 bar. At these operation points, disadvantages of up to 29% are identified.

The analysis of the valve train system for the diesel and gasoline engine 1 reveal that friction losses increase between 9% and 11% for the diesel engine, and between 9% and 18% for gasoline engine 1 when the engine media supply temperature is increased from 70 °C and 90 °C. For the valve train system of gasoline engine 2, a slight friction reduction potential of up to 3% is investigated at engine speeds between n = 2000 rpm and n = 4000 rpm. However, at engine speeds below n = 2000 rpm and above n = 4000 rpm, the friction losses increase when the supply temperature is increased

from 70 °C to 90 °C, while, at the low engine speeds, the increase is up to 9%, and the increase at high engine speeds is significant with 22%.

6. Conclusions

The sub-assembly resolved friction reduction potentials and risks when reducing the lubricant viscosity are investigated for three different engine concepts for passenger car applications. By using a developed combined approach, the friction losses of one diesel engine, a gasoline engine with the same specific power, and a gasoline engine with doubled power density are analyzed. The base engine friction losses are separated into the sub-assemblies piston group, crankshaft journal bearings, and valve train over the full operation range of the engines.

One suitable 5W30 lubricant is chosen for all three engines to exclude influences from different lubricants. By supplying the engine media (lubricant and cooling water) by external supply units, identical thermal boundary conditions are realized for the investigations. The viscosity reduction is achieved by increasing the supply temperature from 70 °C to 90 °C.

The results of the conducted friction reduction potential analysis show significant differences at the sub-assembly systems. The main bearings and big-end bearings show a high potential to reduce friction by increasing the lubricant temperature. A contrary behavior shows the valve train where a temperature increase results in an increase in friction losses. Dependent on the valve train design, the friction increase is more or less significant. The piston assembly shows varying friction reduction potential over the investigated speed and load range. Generally, the friction losses are reduced at high speed and at low loads. At high load and low speed conditions, the friction benefit vanishes or turns into a friction increase in particular for the investigated gasoline engine 2.

Furthermore, it is shown that a potential harmful increase of friction loss of a single sub-system cannot be identified when the entire base engine is evaluated. For instance, friction reduction in the bearings may cancel the increase of friction in the valve train or the piston assembly. Therefore, a friction analysis of the engine's sub-systems is essential.

Author Contributions: Conceptualization, C.K., H.A., and D.E.S.; Data curation, C.K., H.A., and D.E.S.; Funding acquisition, H.A.; Investigation, C.K., H.A., and D.E.S.; Methodology, C.K., H.A., and D.E.S.; Supervision, H.A. and T.S.; Validation, C.K., H.A., D.E.S., and T.S.; Writing—original draft, C.K. All authors have read and agreed to the published version of the manuscript.

Acknowledgments: The authors gratefully acknowledge funding of the Austrian Science Fund (FWF) for the project P27806-N30. The publication was written at Virtual Vehicle Research GmbH in Graz and partially funded by the COMET K2—Competence Centers for Excellent Technologies Programme of the Federal Ministry for Climate Action (bmk), the Federal Ministry for Digital and Economic Affairs (bmdw), the Austrian Research Promotion Agency (FFG), and the Province of Styria and the Styrian Business Promotion Agency (SFG).

Conflicts of Interest: The authors declare no conflict of interest.

References

1. Sander, D.E.; Knauder, C.; Allmaier, H. Potentiale und Risiken von (Ultra-)Leichtlaufölen zur Senkung der Motorreibung. In *Reibung in Antrieb und Fahrzeug*; Springer Vieweg: Wiesbaden, Germany, 2018; pp. 179–190.
2. Sander, D.E.; Allmaier, H.; Priebsch, H.H., Witt, M., Skiadas, A. Simulation of journal bearing friction in severe mixed lubrication—Validation and effect of surface smoothing due to running-in. *Tribol Int* **2016**, *96*, 173–183.
3. Knauder, C.; Allmaier, H.; Sander, D.E.; Sams, T. Investigations of the friction losses of different engine concepts. Part 1: A combined approach for applying sub-assembly resolved friction loss analysis on a modern passenger car diesel engine. *Lubricants* **2019**, *7*, 39.
4. Knauder, C.; Allmaier, H.; Sander, D.E.; Sams, T. Investigations of the friction losses of different engine concepts. Part 2: Sub-assembly resolved friction loss comparison of three engines. *Lubricants* **2019**, *7*, 109.
5. Kovach, J.T.; Tsakiris, E.A.; Wong, L.T. Engine friction reduction for improved fuel economy. *SAE Tech. Paper* **1982**. doi:10.4271/820085.

6. Wong, V.W.; Tung, S.C. Overview of automotive engine friction and reduction trends—Effects of surface, material, and lubricant-additive technologies. *Friction* **2016**, *4*, 1–28.
7. Coy, R.C. Practical applications of lubrication models in engines. *Tribol. Int.* **1998**, *31*, 563–571.
8. Priest, M.; Taylor, C.M. Automobile engine tribology—Approaching the surface. *Wear* **2000**, *241*, 193–203.
9. Offner, G. Friction power loss simulation of internal combustion engines considering mixed lubricated radial slider, axial slider and piston to liner contacts. *Trib. Trans.* **2013**, *56*, 503–515.
10. Knauder, C.; Allmaier, H.; Sander, D.E.; Salhofer, S.; Reich, F.; Sams, T. Analysis of the journal bearing friction losses in a heavy-duty diesel engine. *Lubricants* **2015**, *3*, 142–154.
11. Kim, K.; Shah, P.; Takiguchi, M.; Aoki, S. Part 3: A study of friction and lubrication behavior for gasoline piston skirt profile concepts. *SAE Tech. Paper* **2009**. doi:10.4271/2009-01-0193.
12. Westerfield, Z.; Totaro, P.; Kim, D.; Tian, T. An experimental study of piston skirt roughness and profiles on piston friction using the floating liner engine. *SAE Tech. Paper* **2016**. doi:10.4271/2016-01-1043.
13. Ma, M.T.; Sherrington, I.; Smith, E.H. Analysis of lubrication and friction for a complete piston-ring pack with an improved oil availability model: Part 1: Circumferentially uniform film. *Proc. Inst. Mech. Eng. J.* **1997**, *211*, 1–15.
14. Ma, M.T.; Smith, E.H.; Sherrington, I. Analysis of lubrication and friction for a complete piston-ring pack with an improved oil availability model: Part 2: Circumferentially variable film. *Proc. Inst. Mech. Eng. J.* **1997**, *211*, 17–27.
15. Taylor, R.I.; Brown, M.A.; Thompson, D.M.; Bell, J.C. The influence of lubricant rheology on friction in the piston ring-pack. *SAE Trans.* **1994**, *103*, 1390–1399.
16. Taylor, C.M. Valve train-cam and follower: Background and lubrication analysis. *Tribol. Ser.* **1993**, *26*, 159–181.
17. Mufti, R.A.; Priest, M. Experimental and theoretical study of instantaneous engine valve train friction. *J. Trib.* **2003**, *125*, 628–637.
18. Staron, J.T.; Willermet, P.A. An analysis of valve train friction in terms of lubrication principles. *SAE Trans.* **1983**, *92*, 625–639.
19. Knauder, C.; Allmaier, H.; Sander, D.E.; Sams, T. Measurement of the crankshaft seals friction losses in a modern passenger car diesel engine. *Proc. Inst. Mech. Eng. J.* **2019**. doi:10.1177/1350650119870353.
20. Allmaier, H.; Priestner, C.; Sander, D.E.; Reich, F.M. Friction in automotive engines. In *Tribology in Engineering*; Pihtili, H., Ed.; Intech: Rijeka, Croatia, 2013; pp. 149–184.
21. Heywood, J.B. Engine friction and lubrication. In *Internal Combustion Engine Fundamentals*; Holman, J.P., Ed.; McGraw-Hill, Inc.: New York, NY, USA, 1988; pp. 712–747.
22. Taylor, R.I.; Morgan, N.; Mainwaring, R.; Davenport, T. How much mixed/boundary friction is there in an engine—In addition, where is it? *Proc. Inst. Mech. Eng. J.* **2019**. doi:10.1177/1350650119875316.

4.4 The impact of running-in on the friction of an automotive gasoline engine and in particular on its piston assembly and valve train

The roughness conditions during the running-in of a new engine lead to direct contact between the two surfaces involved, e.g. camshaft and valve actuation or bearing journal and bearing shell, especially in the case of highly stressed contacts. This occurs inevitably under certain operating conditions also with hydrodynamic bearings, which are in conventional operation completely separated by a lubricating film [83].

The running-in process at the beginning of the service life of an engine is a criterion that must be considered as a significant source of error if it is not observed. Subsequently, the performance of friction measurements requires precise boundary conditions and processes in order to achieve meaningful results for the realization of comparability between tests. It is an essential point when carrying out friction measurements to ensure a uniform, run-in initial state of the engines to be tested.

With the main focus in this thesis on performing friction measurements and comparison of the results obtained, the newly developed method is used as an application example to determine the duration until stable boundary conditions are reached by measuring the friction torque. The capability of the developed method to break down the friction losses to the sub-assembly level of the base engine is used to investigate the running-in phase with specific focus at gasoline engine 1. In this term, special focus was placed on the valve train and piston group assemblies. To ensure uniform initial conditions, the components of the valve train and piston group were replaced by new parts.

As it is generally known from the literature, after the running-in phase has been completed, a stable plateau of the frictional torque on the base engine is reached, representing steady state operating conditions. The control of the running-in condition during the tests in this work is checked by repeated measurements after the test program has been run through and comparison with the value after the running-in phase.

An additional aim of the investigations was to determine the duration of time until the end of the running-in process. Derived from this investigation, a running-in program is to be defined which will be used in the engine tests in this thesis.

The details of the application example investigating the running-in behaviour of gasoline engine 1 are described in [46] and can be found in section 4.4.2. Prior to this, the research findings of the publication are summarized in the subsection hereafter.

4.4.1 Summary of research findings

- A series of tests have been conducted at gasoline engine 1 to gain insight into the influence and duration of the engine running-in phase.
- As the temperature of the lubricant has a profound influence on the viscosity in the contact, the investigations are carried out at different engine media supply temperatures ranging from 70 °C to 110 °C.
- The main components of the valve train and piston group assembly have been replaced by new parts with specific focus on the running-in of these components.
- The running-in time of 60 hours is sufficiently long to achieve a stable friction torque plateau and the running-in processes are finished.

- The running-in process causes significant change in the base engine FMEP, e.g. 0.06 bar at 3000 rpm operation point and full load. This result is equivalent to about 6 % of the initial FMEP of the engine at the initial testing phase of 1.03 bar.
- The greatest part of friction change occurs very quickly; between the first and second test of the repeated four stage test programme already 0.04 bar change occurred which is about 70 % of the total change. This corresponds to an operating time of about 15 hours. Between the second and third test, 20 % of the entire change in FMEP due to running-in is occurring and 10 % between the third and fourth test.
- The derived results regarding necessary engine operation revealed that engine operation at low and high speeds and low and high loads are necessary to obtain steady state operation over the full engine map. In addition, the operation of the engine at low and high engine media supply temperatures during the running-in phase is recommended. While the lubrication film is smallest at highest supply temperatures, specific oil additives may be activated at certain temperature levels to protect the surfaces in contact.
- The influence of running-in is about as large as the temperature difference between 70 °C and 90 °C and its impact on engine friction. The running-in process caused a 0.04-0.06 bar reduction in the friction losses of the full engine for full load operation. The 20 °C temperature change causes an FMEP reduction of about 0.08 bar.
- The influence of running-in directly correlates with the amount of mixed lubrication, which is strongest for low engine speed.
- The influence of running-in reduces with increasing engine speeds.
- For the direct acting valve train of gasoline engine 1 always significant mixed lubrication is present, even at high engine speeds. The systems are affected the strongest by the running-in process with 0.06 bar, which represents about 18 % of the total valve train FMEP at the same operating point. The influence of running-in is strongest at low engine speeds, where the sliding speeds are smallest and mixed lubrication is strongest.
- At the piston assembly, a stronger effect of running-in on the FMEP is resulting with increasing peak cylinder pressure, but the influence is of minor extent compared to the valve train system with about 0.03 bar.
- For valve train systems working according to the direct acting principle, the impact of running-in can be significantly larger than for the piston assembly. An FMEP change by about 0.02 - 0.04 bar for the piston assembly compared to 0.03 - 0.06 bar for the direct acting valve train with 20 valves in total has been investigated in this work. The high number of five valves per cylinder in combination with the fact that no coatings are employed at the system justify the observed results. While in the piston assembly both the piston ring faces as well as the piston skirt are coated and are therefore more resistant to wear.

4.4.2 Paper IV [46]

Original Article

Institution of MECHANICAL ENGINEERS
Journal of ENGINEERING TRIBOLOGY

Proc IMechE Part J:
J Engineering Tribology
0(0) 1–8

DOI: 10.1177/1350650117727231
journals.sagepub.com/home/pij
SAGE

The impact of running-in on the friction of an automotive gasoline engine and in particular on its piston assembly and valve train

Christoph Knauder[1], Hannes Allmaier[1], Stefan Salhofer[1] and Theodor Sams[2,3]

Abstract

Generally, mating surfaces that are in tribological contact undergo a running-in process at the beginning of their operational lifetime. During this running-in phase, the tribological operating condition changes significantly leading ideally to long-term operation with a minimum of continuous wear. While this process and its duration are rather well understood for single machine elements like journal bearings, it is the aim of this work to investigate the running-in behaviour of more complex systems like an internal combustion engine and its sub-assemblies. To gain insight into the influence and duration of this running-in phase, a series of tests have been performed under realistic engine operating conditions. To be able to separate the running-in processes for the individual subsystems' piston assembly, valve train and journal bearings of the crank train, a large series of tests have been conducted for a conventional gasoline passenger car engine. The results show a strong influence of the running-in process on total engine friction, which can be attributed mostly to the direct acting valve train and to a considerably lesser extent to the piston assembly.

Keywords

Running-in, friction, measurement, simulation, friction break down, automotive engine

Date received: 1 February 2017; accepted: 4 July 2017

Introduction

In the automotive and transportation sector, the efficiency of the powertrain and in particular of the employed internal combustion engine (ICE) is of great interest and in the focus of research and development engineers for considerable time.[1] Not only increasingly strict emission legislation, but also the customer demand due to increasing fuel costs motivates the continuous work to improve the efficiency by lowering the friction power losses. The general term friction refers commonly to the largest part of the lifetime of the tribological system, where the initial running-in phase has been finished and the parts operate with minimal wear. From a tribological viewpoint, the running-in phase is central to obtain a long-term state with a minimum of continuous wear[2] and a better understanding of its influence on the tribological properties and on its duration would be beneficial. In addition, current trends in emission legislation put further focus on the friction losses over the entire lifetime by employing continuous monitoring systems.

While this process and its duration is rather well investigated for single machine elements like journal bearings,[3–5] the running-in behaviour of more complex systems like an ICE and its sub-assemblies is considerably more challenging. Although the major subsystems of the engine, namely the valve train, the piston assembly and the journal bearings of the crank train, operate with the same lubricant and have been developed to have similar operating lifetime, the tribological conditions for these subsystems are distinctly different. It is commonly understood that the valve train operates in significant mixed lubrication,[6–8] the piston assembly in dominantly hydrodynamic lubrication with severe mixed lubrication

[1]Virtual Vehicle Research Center, Graz, Austria
[2]AVL List GmbH, Graz, Austria
[3]Institute of Internal Combustion Engines and Thermodynamics, Graz University of Technology, Graz, Austria

Corresponding author:
Christoph Knauder, Virtual Vehicle Research Center, Inffeldgasse 21A, Graz 8010, Austria.
Email: christoph.knauder@v2c2.at

only occurring for short periods[9–11] and the journal bearings in dominantly hydrodynamic lubrication conditions.[12,13] These different lubrication conditions certainly influence the running-in behaviour. The quantitative influence of running-in on engine friction as well as its duration is the scope of this work.

To gain insight into the influence and duration of this running-in phase, a series of tests have been conducted. As it is known that the running-in depends on the operating conditions (e.g. Allmaier[3] and Sander et al.[5]), a broad range of operating conditions were covered to ensure that the running-in does not depend significantly on the chosen operating condition.

The friction power losses of the complete engine were obtained over a large range of operating conditions including low and full load operation as well as the full rotational speed range of the engine. As the temperature of the lubricant has a profound influence on the viscosity in the contact and, consequently, on the tribological conditions, the engine was operated with different lubricant temperatures ranging from 70 to 110 °C. In addition, the friction power losses of the valve train (and timing drive) were also obtained experimentally. As the journal bearings of the crank train (main and big end bearings) were already run-in, their friction losses did not change during the tests. Therefore, by subtracting the valve train contribution from the full engine friction losses all remaining influence of the running-in process can be attributed to the piston assembly.

Table 1. Technical data of the in-line four cylinder turbocharged engine under test.

Volume displacement	1781 cm^3
Compression ratio	9.5:1
Bore	81 mm
Stroke	86.4 mm
Nominal torque	235 N m
Nominal power	132 kW
Cylinder diameter	88 mm
Con-rod length	144 mm
Main bearing diameter	54 mm
Main bearing width	22 mm
Big-end bearing diameter	47.8 mm
Big-end bearing width	25 mm
Valve train	DOHC
Timing drive	(dry) belt
Valve train type	Direct acting on Bucket tappet
Valves	Five per cylinder

DOHC: double overhead camshaft.

Table 2. Lubricant data.

SAE class	5W30
Dynamic viscosity at 40°C	59.88 mPa s
Dynamic viscosity at 100°C	9.98 mPa s
Density at 15°C	853 kg/m^3

SAE: society of automotive engineers.

Testing

The engine under test

The passenger car engine put to test is an in-line four cylinder, turbo charged, spark ignition engine with a nominal volume displacement of 1.8 l and a nominal power of 132 kW; more technical details of the engine are listed in Table 1. To be able to test the running-in behaviour of the base engine, all auxiliary devices like oil and water pump, alternator, etc. have been removed from the engine. To realize external temperature and pressure control of the media, several parts of the engine, e.g. the oil module and the oil pan, have been modified. The coolant and engine oil are supplied from an external supply unit which also controls supply temperatures and pressures, which are measured directly at the coolant circuit and oil gallery of the engine, respectively. The oil and coolant supply temperature was controlled externally with an accuracy of about ±0.5 °C. The oil and coolant pressure were controlled externally with an accuracy of about ±0.05 bar. The cylinder pressure is measured in all four cylinders using piezoelectric pressure sensors.

The tested engine employs a direct acting valve train with two overhead camshafts and five valves per cylinder, conventional aluminium pistons with coated piston skirts and coated piston rings in a cast iron crank case. Even brand new engines have already been operated by the manufacturer during the end-of-line testing, so an alternative approach has been used. A used engine was employed and all parts of the piston assembly and all relevant parts of the valve train were replaced with new parts. However, the already run-in journal bearings of the crank train (main and big-end bearings) were kept and not replaced.

As the running-in behaviour of the journal bearings of the crank train was investigated in previous works,[3,4] the focus of this work is on the piston assembly and valve train. Therefore, the already run-in journal bearings have been used and it was checked at the beginning and end of the tests that their contribution to the total engine friction did not change.

To lubricate the engine under test a standard 5W30 grade automotive lubricant was used and its basic rheological data are given in Table 2.

The dynamometer

For the measurements a pressurized motoring test rig has been used. In contrast to fired engine operation,

a pressurized air dynamometer supplies air under pressure to the engine intake. In combination with the intrinsic compression of the engine, realistic peak cylinder pressures of up to 200 bar can be realized in the combustion chamber.[10,14] This method has the major advantage of much higher measurement accuracy compared to fired engine tests. The main reason for the improved accuracy is the strongly reduced (by a factor of about 4) indicated mean effective pressure (IMEP) in comparison to fired operation. Therefore, torque transducers with a much smaller measurement range and, consequently, much higher absolute accuracy can be used. In addition, in fired engine tests, the variations between individual cycles can be very large, in particular for gasoline engines, where it is common to see more than 20% variation in peak cylinder pressure. The main drawback of pressurized motoring is the different thermal situation in the piston assembly. However, a direct comparison of friction measurements for the same engine in fired operation and pressurized motoring showed very similar results.[10]

The pressurized motoring technique uses the well-known IMEP method to determine the friction mean effective pressure (FMEP) by subtracting the brake mean effective pressure (BMEP)

$$\mathrm{FMEP} = \mathrm{IMEP} - \mathrm{BMEP} \tag{1}$$

with the minor difference being that the signs of the IMEP and BMEP are negative in comparison to fired engine operation. When using the IMEP method to investigate the friction losses of an engine it is essential to determine two quantities, the indicated power and the brake power of the engine with highest possible accuracy. The reason for this is that IMEP and BMEP are two large and very similarly sized quantities which are subtracted from each other to determine a rather small difference (FMEP). Therefore, any significant error in the determination of the BMEP and IMEP can easily lead to a measurement error of the same magnitude as the to-be-determined FMEP.

Practically, the IMEP is measured using piezoelectric sensors in the combustion chamber. However, the BMEP cannot be measured directly as pressure but is commonly measured as brake torque. Following equation relates the mean effective pressure p_{me} to the corresponding torque T

$$p_{me} = \frac{W}{V_D} = \frac{4\pi T}{V_D} \tag{2}$$

where W refers to the work per cycle and V_D to the volume displacement of the investigated four-stroke engine.

At the friction dynamometer test rig a high accuracy torque measurement system (HBM T12) with built-in engine speed sensor is used for the brake torque and engine speed measurement. For the IMEP determination it is essential to determine the position of the top dead centre (TDC) of the piston to great precision. To this task, a capacitive TDC sensor (AVL OT428) was used to ensure a high accuracy TDC determination. Ideally, the TDC determination should be done for every operating condition as the engine load and even the oil temperature influence the exact position of the TDC. A working compromise is to perform TDC determination for an important operating condition, which was defined as 2000 rpm. Figure 1 shows the capacitive TDC sensor installed in the opening for the spark plug of cylinder #1[a] during the TDC determination.

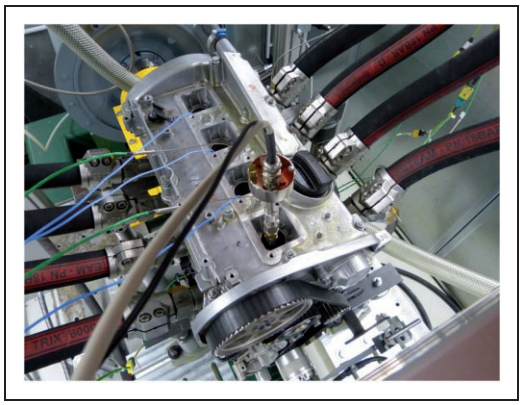

Figure 1. Mounted capacitive TDC sensor during TDC determination in cylinder #1[a].
TDC: top dead centre.

Test procedure

As shortly discussed in 'Introduction' section, to ensure the proper running-in of all engine components a wide range of engine operation conditions ranging from low to high engine speeds at low and high engine loads were performed for three different coolant/oil temperatures. For the tests the oil and coolant supply temperatures were kept identical; therefore, the term *media temperature* will be used for brevity in the following.

The engine operating conditions (speeds and loads) for the tests are listed in Figure 2. These engine operating conditions were performed for 70/90/110 °C media temperature (in increasing order as listed). The increasing media temperatures are intended to promote a more gradual running-in process as mixed lubrication generally increases with increasing media temperature.

Full engine tests

The largest part of the experimental investigations comprises tests with the complete base engine. One set of measurements consists of all engine operating

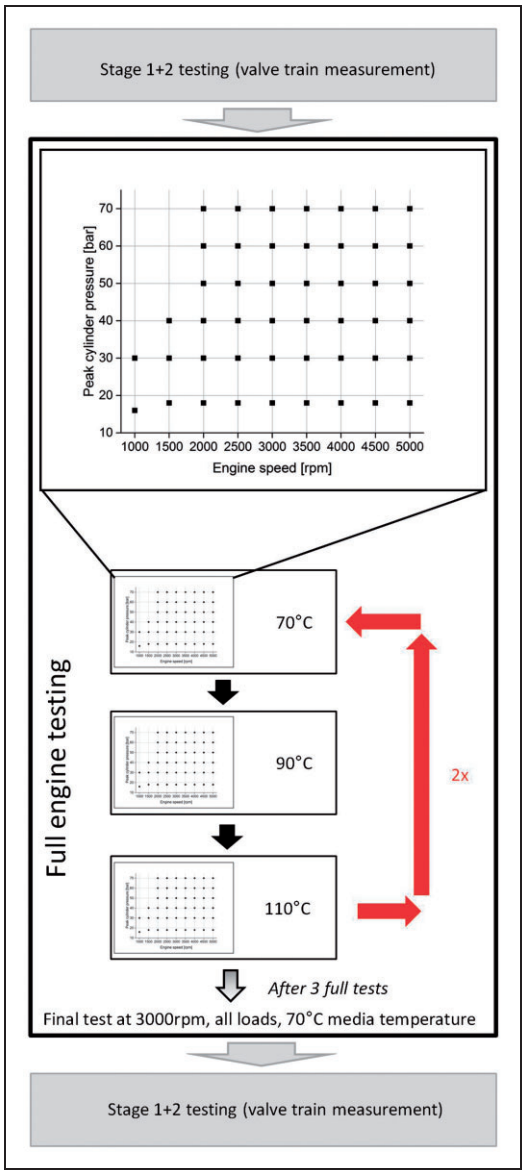

Figure 2. Flowchart of the tested engine operating conditions. The tests covered the full range of operating conditions of the engine (in terms of speed and load), were performed for three different media temperatures (70, 90 and 110°C) and conducted three times in total. At the end, a final test at 3000 rpm was performed for all loads ranging from motoring to full load and 70°C media temperature. At the beginning and at the end measurements for the stage 1 + 2 configuration were conducted to obtain the friction torque of the valve train (see 'Testing' section).

points (speeds and loads) shown as inset in Figure 2. Such a test set was conducted for three different media temperatures 70, 90, 110 °C (in this order) and then repeated starting again from 70 °C media temperature. In total, three such tests were performed (denoted as test 1/2/3). After these three tests,

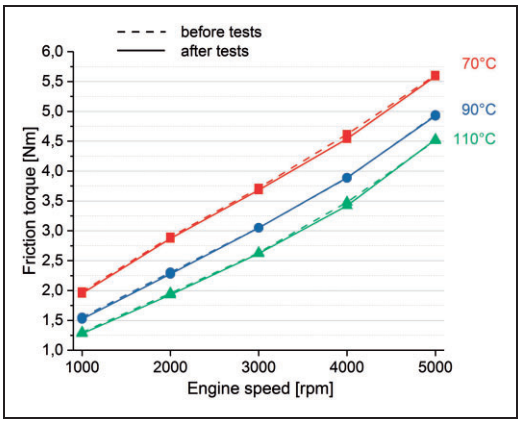

Figure 3. Comparison of the measured friction torque for the stage 2 engine configuration (motoring only the main bearings of the crank train and rotary shaft seals, see text) before and after the full engine test programme.

additional measurements only for 3000 rpm engine speed were performed for all engine loads and for 70 °C media temperature (denoted as test 4). Therefore, the tests 1/2/3/4 correspond to similarly spaced, increasing operating times of the engine. The total engine operating time was about 60 h.

Additional tests

Before and after the full engine measurements additional measurements were conducted to obtain the friction contributions from the valve train with timing drive and the crankshaft main bearings with rotary shaft seals.

In *Stage 1* all four piston assemblies (pistons with con-rods) have been removed from the engine. As a replacement for the removed masses and to seal the oil supply holes in the crank shaft pin, master weights were mounted onto the crank shaft for this test. To summarize, in the stage 1 configuration the crankshaft supported by the main bearings, the rotary shaft seals, the timing belt and valve train is motored. As the largest part of the measured friction torque in this engine configuration is attributed to the valve train, this stage is called valve-train friction torque for simplicity in the following.

Stage 2 comprises the modifications from stage 1 and in addition the timing belt is removed from the engine under test. This allows the measurement of the crank train main bearings and rotary shaft seals. By subtracting the results from stage 1 with the results from stage 2, the friction contribution of the valve train is obtained. In addition, this stage 2 test serves as a check at the beginning and end of the tests that the friction power losses of the main bearings do not change during the testing. Figure 3 shows the measurements of this stage 2 configuration at the beginning and at the end of the measurements and confirms that

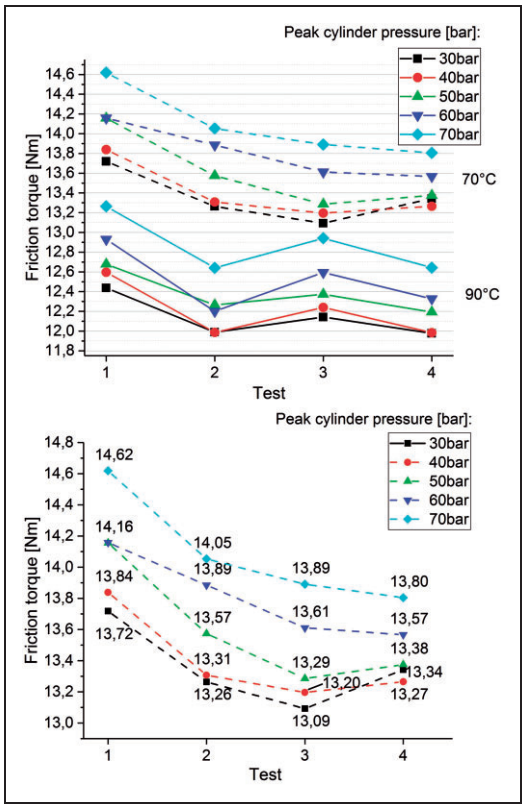

Figure 4. Change of full engine friction torque with the number of tests shown for a rotational speed of 3000 rpm: the top plot shows the results for 70 and 90°C media temperatures, the bottom plot shows the 70°C results in more detail.

indeed the main bearings (and rotary shaft seals) do not change detectably.

Results and discussion

This section discusses the results of the investigated running-in processes of the tested engine. Figure 4 shows the measured friction torques for the full engine after four different operating durations (as discussed in 'Test procedure' section). The results indicate that the chosen total running time of 60 h is sufficiently long so that the running-in process is almost completely finished and a stable friction torque is achieved for most operating points. Already the second test indicates that most of the running-in process is finished and only small changes in the friction torque occur in the later tests. The running-in process causes a significant change in full engine friction torque as is found from the results. For example, the full load (70 bar peak cylinder pressure) operating point at 70 °C media temperature, a total change due to running-in of 0.82 N m is observed, which is equivalent to about 6% of the initial friction torque of 14.62 N m. Also the change in friction torque is strongly regressive with the most part of the change occurring very quickly. Between the first and the second test already 0.57 N m change occurred, which is 70% of the total change. Between the second and third test only a change of 0.16 N m is observed, which corresponds to about 20%. The remaining 10% change are seen between the third and fourth test with an absolute change in friction torque of 0.09 N m. For the other operating conditions similar behaviour is observed.

As can be seen from Figure 4, the measured decreasing trends appear not to be entirely perfect. To put this into perspective, the smallest observed differences in the friction torques are of the magnitude of 0.04–0.1 N m, which corresponds to less than about 0.7% of the maximum measured motoring (BMEP) torque of about 60 N m and corresponds to even only 0.04% when related to the maximum nominal torque of the engine (235 N m, see Table 1). It was found that the cleanest results with the smallest fluctuations were obtained for 70 °C media temperature, so these will be investigated in particular in the following.

Several interesting points can be observed from Figure 4: notably the influence of running-in is about as large as the temperature difference between 70 and 90 °C media temperature and its impact on engine friction. In numbers, the running-in process caused a 0.6–0.8 N m reduction in the full engine friction torque for 70 bar peak cylinder pressure (for both 70 and 90 °C media temperature), whereas the 20 °C difference in media temperature caused a change of about 1.2 N m in friction torque. Also the influence of the engine load (peak cylinder pressure) is of the same magnitude with about 0.6–0.8 N m change in friction torque between 30 and 70 bar peak cylinder pressure.

While the results for the full engine tests provide a global perspective, it is interesting to investigate the influence of running-in and its effect on the subassemblies valve train and piston assembly (the journal bearings of the crank train do not change during the tests as discussed previously in 'Additional tests' section and shown in Figure 3).

Running-in results for the valve train

In Figure 5 the friction torques of the valve train before and after the tests are shown for different media temperatures and Figure 6 shows the corresponding change in friction torque for 70 °C media temperature.

As it is to be expected from lubrication theory, the influence of running-in directly correlates with the amount of mixed lubrication which is strongest for low engine speeds. This is supported by the shown plots (Figures 5 and 6) as the influence of running-in reduces with increasing engine speed. From the results it becomes apparent that for the investigated direct acting valve train always significant mixed lubrication

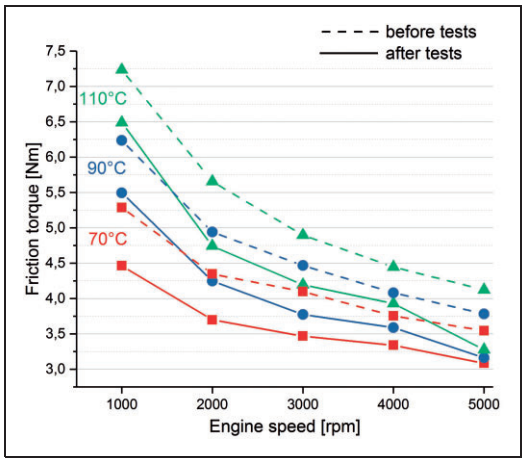

Figure 5. Comparison of the friction torque of the valve train before and after the running-in tests.

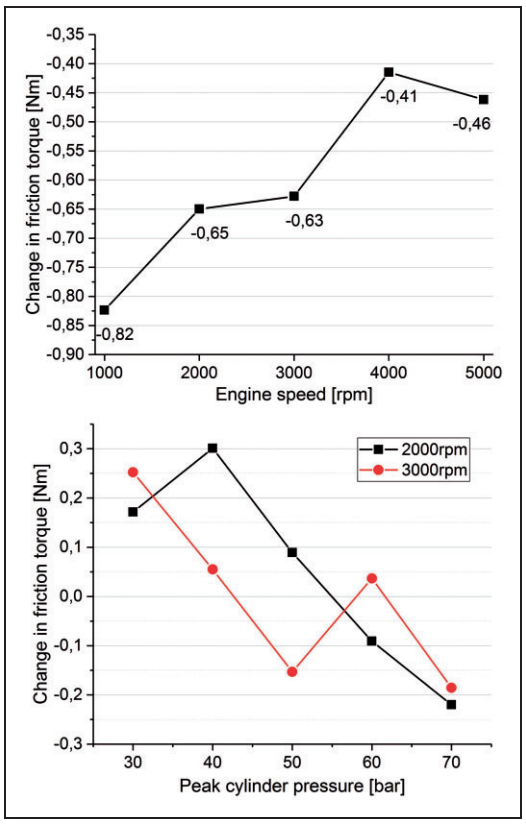

Figure 6. Difference of the friction torque of the valve train before and after the running-in tests for 70°C media temperature; the bottom plot shows the change in friction torque for the piston assembly for 3000 rpm engine speed before and after three full testing maps. For comparison, also the results for 2000 rpm are shown before and after two testing maps (all for 70°C media temperature).

is present; even at the highest engine speed a change due to running-in can be observed for all three media temperatures.

Running-in results for the piston assembly

Figure 6 shows the change in friction torque for the piston assembly by subtracting the friction torque of the valve train from the full engine friction torque before and after the entire testing procedure. The results are shown for an engine speed of 2000 and 3000 rpm, which are the engine speeds where most mixed lubrication is expected.

While the results for both engine speeds show very similar trends, it is necessary to point out that these two engine speeds correspond to different engine running times. Only the engine speed of 3000 rpm was tested at the end of the three test sets (see 'Full engine tests' section), therefore the results for the 2000 rpm engine speed were taken from the last of the three tests and correspond to a shorter engine running time. Consequently, the 2000 rpm engine results in this figure shall only serve to confirm the 3000 rpm results.

Apparently the modifications to the engine and/or to the test rig caused a measurement offset as the change in friction torque obtained for the piston assembly is positive for low peak cylinder pressures. This increase would mean that the running-in process causes an increase in friction of the piston assembly for low peak cylinder pressures, which – even if it might be physically possible – appears unlikely. Also the obtained results are on the border of the measurement accuracy of the test rig, therefore, the focus is only on the observed trend in the following.

Neglecting this change in absolute torque offset, a trend can be identified for the piston assembly. With increasing peak cylinder pressure a stronger effect of running-in on the friction torque can be seen for the piston assembly. This is consistent with the understanding of the occurrence of mixed lubrication in the piston assembly where increasing peak cylinder pressure leads to increased mixed lubrication. Therefore, running-in optimizes the mating of the surfaces in contact and this improvement is expected to gain influence with increasing peak cylinder pressure.

Further, it is interesting to note that the impact of running-in is considerably smaller for the piston assembly than for the valve train: the friction torque of the piston assembly changes by about 0.3–0.5 N m, whereas the friction torque of the valve train changes by about 0.4–0.8 N m in comparison. A possible explanation for these results might be that the valve train does not employ coatings neither on the cams nor on the bucket tappets. In contrast, both the piston rings and piston skirts are coated which commonly reduces wear. In addition, the valve train employs the direct acting principle, where the cam directly

acts on the tappet without any (roller) finger follower. This working principle leads to a highly loaded sliding contact[6–8,15–18] which in combination with the unusually high number of five valves per cylinder is the likely explanation for the observed magnitude of the valve-train friction power losses.

Conclusions

The influence of running-in on the friction torque of a four-cylinder gasoline engine was investigated with a series of tests for different engine speeds, loads and media temperatures using a conventional 5W30 lubricant. With the exception of the journal bearings of the crank train, the engine can be considered to be like new at the beginning of the tests. By removing the pistons and con-rods before and after the measurement campaign, the change in friction torque of the valve train with timing drive can be assessed. As the friction torque of the full engine and the valve train is measured and the journal bearings of the crank train did not change during the tests, the influence of running-in for the piston assembly can be derived in addition.

The results for the full engine indicate that the running-in process is almost finished after the investigated operating time of about 60 h. After this total 60 h operating time, the friction torque decreased by about 6% from its initial value. The largest change in friction torque (about 70% of the entire change) occurs already between the first and second test, which corresponds to an operating time of about 15 h. The change in friction torque due to running-in observed between the second and third test is about 20% and between the third and fourth test is about 10% of the entire change in friction torque due to running-in.

From the results it is further found that the direct acting valve train with five valves per cylinder is strongest affected by the running-in process. The friction torque of the valve train changes by a maximum of about 0.8 N m which represents about 18% of the total valve-train friction torque (referring to the same operating point). As expected, the influence of running-in is strongest for low engine speeds where the sliding speeds are smallest and mixed lubrication is strongest.

In contrast, the influence of running-in on the piston assembly is minor. While the piston assembly contributes considerably more friction torque than the valve train[b] a maximum change in friction torque due to running-in of merely about 0.4 N m is observed. However, an increasing influence of running-in with increasing peak cylinder pressure could be identified from the results.

A possible explanation for this unexpected result is unusually high number of five valves per cylinder and, in particular, the lack of coatings in the valve train (neither on cam or tappet).[18,19] While in the piston assembly both the piston ring faces as well as the piston skirt are coated and are, therefore, more resistant to wear.

Finally, it is interesting to compare the results to the running-in behaviour of the crank train journal bearings. In a previous work,[3] the running-in behaviour of journal bearings with similar size and operating conditions was investigated by employing a combination of simulation and experiment. It was found that the running-in process of journal bearings is finished very quickly; the most significant part of running-in was observed in the first 20 min of testing on the journal bearing test rig. Also in terms of influence on friction, the magnitude of the friction torque changed by about 10% in the first 20 min of operation and was already insignificant for longer operating times. Summarizing, it is concluded that for the investigated engine the running-in process affects most strongly the valve train where the observed change in friction torque is largest with about 18%. By considering the results from the previous work, it appears that the journal bearings of the crank train are also significantly affected by the running-in process with a roughly 10% change in friction torque. Finally, the piston assembly shows the smallest change for the investigated engine.

Future work could address the running-in process of a diesel engine as the considerably higher peak cylinder pressures of up to 200 bar might involve a stronger running-in behaviour for the piston assembly.

Declaration of Conflicting Interests

The author(s) declared no potential conflicts of interest with respect to the research, authorship, and/or publication of this article.

Funding

The author(s) disclosed receipt of the following financial support for the research, authorship, and/or publication of this article: The authors would like to acknowledge the financial support of the 'COMET – Competence Centres for Excellent Technologies Programme' of the Austrian Federal Ministry for Transport, Innovation and Technology (bmvit), the Austrian Federal Ministry of Science, Research and Economy (bmwfw), the Austrian Research Promotion Agency (FFG), the Province of Styria and the Styrian Business Promotion Agency (SFG). Furthermore, we acknowledge the partial financial support of the Austrian Science Fund (FWF): P27806-N30.

Notes

a. The used numbering of the cylinders starts from the side opposite of the clutch where most engines have the timing drive.
b. While the absolute contribution of the piston assembly to the measured friction torque cannot be accessed using this approach, it is estimated to be at about 6 N m for 3000 rpm engine speed, full load and 70 °C media temperature.

References

1. Dowson D, Taylor C, Godet M, et al. *The running-in process in tribology*. UK: Butterworth-Heinemann, 1982.
2. Blau PJ. On the nature of running-in. *Tribol Int* 2006; 38: 1007–1012.
3. Allmaier H, Sander D, Priebsch H, et al. Non-Newtonian and running-in wear effects in journal bearings operating under mixed lubrication. *Proc IMechE, Part J: J Engineering Tribology*, Epub ahead of print 16 July 2015. DOI: 10.1177/1350650115594191.
4. Sander DE, Allmaier H, Priebsch H, et al. Edge loading and running-in wear in dynamically loaded journal bearings. *Tribol Int* 2015; 92: 395–403.
5. Sander DE, Allmaier H, Witt M, et al. Journal bearing friction and wear in start/stop applications. *MTZ Worldwide* 2017; 78: 46–50.
6. Dyson A. Elastohydrodynamic lubrication and wear of cams bearing against cylindrical tappets. *SAE technical paper*. USA: SAE International, 1977.
7. Schamel A, Grischke M and Bethke R. Amorphous carbon coatings for low friction and wear in bucket tappet valvetrains. *SAE technical paper*. USA: SAE International, 1997.
8. Priest M and Taylor C. Automobile engine tribology – approaching the surface. *Wear* 2000; 241: 193–203.
9. Tian T. Dynamic behaviours of piston rings and their practical impact. Part 2: oil transport, friction and wear of ring/liner interface and the effects of piston and ring dynamics. *Proc IMechE, Part J: J Engineering Tribology* 2002; 216: 229–248.
10. Allmaier H, Knauder C, Salhofer S, et al. An experimental study of the load and heat influence from combustion on engine friction. *Int J Engine Res* 2016; 17: 347–353.
11. Priest M, Dowson D and Taylor C. Predictive wear modelling of lubricated piston rings in a diesel engine. *Wear* 1999; 231: 89–101.
12. Allmaier H, Priestner C, Sander D, et al. Friction in automotive engines. In: Pihtili H (ed) *Tribology in engineering*. Croatia: Intech, 2013, http://www.intechopen.com/books/tribology-in-engineering/friction-in-automotive-engines (accessed 7 February 2017).
13. Sander D, Allmaier H and Priebsch H. Friction and wear in automotive journal bearings operating in today's severe conditions. In: Darji PPH (ed) *Advances in Tribology*. Croatia: Intech, 2016, http://www.intechopen.com/books/advances-in-tribology/friction-and-wear-in-automotive-journal-bearings-operating-in-today-s-severe-conditions (accessed 7 February 2017).
14. Sander D, Allmaier H and Reich F. Determination of friction losses in combustion engines – combination of measurement and validated EHD journal bearing simulation. USA. *VDI-Berichte 2202* 2013; 10: 165–175.
15. Colgan T and Bell JC. A predictive model for wear in automotive valve train systems. In: *SAE technical paper*. SAE International, 1989.
16. Katoh A and Yasuda Y. An analysis of friction reduction techniques for the direct-acting valve train system of a new-generation lightweight 3-liter V6 Nissan engine. In: *SAE technical paper*. USA: SAE International, 1994.
17. Masuda M, Ujino M, Shimoda K, et al. Development of titanium nitride coated shim for a direct acting OHC engine. In: *SAE technical paper*. USA: SAE International, 1997.
18. Lawes S, Hainsworth S and Fitzpatrick M. Impact wear testing of diamond-like carbon films for engine valve-tappet surfaces. *Wear* 2010; 268: 1303–1308.
19. Gangopadhyay A, Soltis E and Johnson MD. Valvetrain friction and wear: Influence of surface engineering and lubricants. *Proc IMechE, Part J: J Engineering Tribology* 2004; 218: 147–156.

Bibliography

[1] Adams, D. Tribological considerations in internal combustion engines. In *Tribology and dynamics of engine and powertrain*. Woodhead Publishing Limited, 2010, pp. 251–283.

[2] Affenzeller, J., and Gläser, H. *Lagerung und Schmierung von Verbrennungsmotoren*. Springer Wien, 1996.

[3] Allmaier, H., Priestner, C., Reich, F. M., Priebsch, H. H., Forstner, C., and Novotny-Farkas, F. Predicting friction reliably and accurately in journal bearings–The importance of extensive oil-models. *Tribology International 48* (2012), 93–101.

[4] Allmaier, H., Priestner, C., Reich, F. M., Priebsch, H. H., and Novotny-Farkas, F. Predicting friction reliably and accurately in journal bearings—Extending the EHD simulation model to TEHD. *Tribology International 58* (2013), 20–28.

[5] Allmaier, H., Priestner, C., Six, C., Priebsch, H. H., Forstner, C., and Novotny-Farkas, F. Predicting friction reliably and accurately in journal bearings—A systematic validation of simulation results with experimental measurements. *Tribology International 44*, 10 (2011), 1151–1160.

[6] Allmaier, H., Sander, D. E., Damjanovic, S., and Mallet, P. Analysing engine friction in view of the new WLTC driving cycle. *MTZ Worldw 78* (2017), 16–21.

[7] Allmaier, H., Sander, D. E., Priebsch, H. H., Witt, M., Füllenbach, T., and Skiadas, A. Non-Newtonian and running-in wear effects in journal bearings operating under mixed lubrication. *Proceedings of the Institution of Mechanical Engineers, Part J: Journal of Engineering Tribology 230*, 2 (2016), 135–142.

[8] Alshwawra, A., Pohlmann-Tasche, F., Stelljes, F., and Dinkelacker, F. Enhancing the geometrical performance using initially conical cylinder liner in internal combustion engines—A numerical study. *Appl. Sci. 10* (2020).

[9] Archard, J. Contact and rubbing of flat surfaces. *Journal of Applied Physics 24*, 8 (1953), 981–988.

[10] Beulshausen, J., Geiger, J., Pischinger, S., and Höhn, B.-R. Increase in powertrain efficiency through friction reduction. *ATZ worldwide 115* (2013), 58–65.

[11] Blaxill, H., Reader, S., Mackay, S., Lerch, B., and Rueckauf, J. Development of a friction optimized engine. In *SAE World Congress & Exhibition* (2009), SAE International.

[12] Bonneau, D., Fatu, A., and Souchet, D. *Hydrodynamic Bearings*. ISTE, London and John Wiley & Sons, New York, 2014.

[13] Bowyer, S., Tomazic, D., and Rogers, G. Fuel economy optimization. In *Encyclopedia of Automotive Engineering*. Woodhead Publishing Limited, 2014.

[14] Brett, S., Spulber, A., Modi, S., and Fiorelli, T. Technology roadmaps: Intelligent mobility technology, materials and manufacturing processes, and light duty vehicle propulsion. *Technology Roadmaps* (2017).

[15] Caruana, C., Farrugia, M., and Sammut, G. The determination of motored engine friction by use of pressurized 'shunt' pipe between exhaust and intake manifolds. *SAE Technical Paper*, 2018-01-0121 (2018).

[16] Caruana, C., Farrugia, M., Sammut, G., and Pipitone, E. Further experimental investigation of motored engine friction using shunt pipe method. *SAE Int. J. Adv. & Curr. Prac. in Mobility 1* (2018), 1444–1453.

[17] Caruana, C., Farrugia, M., Sammut, G., and Pipitone, E. Experimental investigation on the use of argon to improve FMEP determination through motoring method. *SAE Technical Paper*, 2019-24-0141 (2019).

[18] Chen, H. *Modeling the Lubrication of the Piston Ring Pack in Internal Combustion Engines Using the Deterministic Method*. PhD thesis, Massachusetts Institute of Technology, 2011.

[19] Chun, S. M. Simulation of engine life time related with abnormal oil consumption. *Tribology International 44*, 4 (2011), 426–436.

[20] Cui, H., Hall, D., and Lutsey, N. Update on the global transition to electric vehicles through 2019. *International Council On Clean Transportation: Briefing July 2020* (2020).

[21] D'Agostino, V., and Senatore, A. Fundamentals of lubrication and friction of piston ring contact. In *Tribology and dynamics of engine and powertrain*. Woodhead Publishing Limited, 2010, pp. 343–386.

[22] Department of Education and Science. Lubrication (tribology) education and research (Jost report). *Her Majesty's Stationery Office (HMSO)* (1966).

[23] Dolatabadi, N., Forder, M., Morris, N., Rahmani, R., Rahnejat, H., and Howell-Smith, S. Influence of advanced cylinder coatings on vehicular fuel economy and emissions in piston compression ring conjunction. *Applied Energy 259* (2020).

[24] Dowson, D., Taylor, C., and Yang, L. Friction modelling for internal combustion engines. In *The Third Body Concept Interpretation of Tribological Phenomena*. Elsevier Science B.V., 1996, pp. 301–318.

[25] Dursunkaya, Z., Keribar, R., and Ganapathy, V. A model of piston secondary motion and elastohydrodynamic skirt lubrication. *Journal of Tribology 116*, 4 (1994), 777–785.

[26] ExxonMobil. OEM engine oil lubricant specifications. *White paper* (2018).

[27] Fischer, G. D. *Expertenmodell zur Berechnung der Reibungsverluste von Ottomotoren*. PhD thesis, Technische Universität Darmstadt, 2000.

[28] Fraidl, G., Kapus, P., Mitterecker, H., and Weissbäck, M. Internal combustion engine 4.0. *MTZ Worldw 79* (2018), 28–35.

[29] Gangopadhyay, A., McWatt, D. G., Zdrodowski, R. J., Simko, S. J., Matera, S., Sheffer, K., and Furby, R. S. Valvetrain friction reduction through thin film coatings and polishing. *Tribology Transactions 55:1* (2012), 99–108.

[30] Gießauf, G. *Bewertung unterschiedlicher reibungsrelevanter Maßnahmen beim PKW-Dieselmotor*. Master's thesis, Graz University of Technology, 2013.

[31] Golloch, R. *Downsizing bei Verbrennungsmotoren: Ein wirkungsvolles Konzept zur Kraftstoffverbrauchssenkung*. Springer Vieweg, 2005.

[32] Greenwood, J., and Tripp, J. The contact of two nominally flat rough surfaces. *Proceedings of the Institution of Mechanical Engineers 185*, 1 (1970), 625–633.

[33] Greenwood, J., and Williamson, J. Contact of nominally flat surfaces. *Proceedings of the Royal Society of London. Series A, Mathematical and Physical Sciences 295* (1966), 300–319.

[34] Heywood, J. B. Engine friction and lubrication. In *Internal combustion engine fundamentals*. McGraw-Hill, Inc., New York, 1988, pp. 712–747.

[35] Holmberg, K., Andersson, P., and Erdemir, A. Global energy consumption due to friction in passenger cars. *Tribology International 47* (2012), 221–234.

[36] Holmberg, K., and Erdemir, A. Influence of tribology on global energy consumption, costs and emissions. *Friction 5* (2017), 263–284.

[37] Hopfner, W., Lösch, S., Satschen, S., and Winklhofer, E. Friction test procedures in engine development. *Proceedings of the 5th Györer Tribologie- und Effizienztagung* (2018), 53–66.

[38] Hu, Y., Cheng, H. S., Arai, T., Kobayashi, Y., and Aoyama, S. Numerical simulation of piston ring in mixed lubrication—A nonaxisymmetrical analysis. *Journal of Tribology 116*, 3 (1994), 470–478.

[39] Infineum, I. Infineum additives seminar. `https://www.infineuminsight.com/en-gb/resources/infineum-additives-seminar/`, 7 2020.

[40] Jikuya, H., Mori, S., Yamamori, K., and Hirano, S. Development of firing fuel economy engine dyno test procedure for JASO ultra low viscosity engine oil standard (JASO GLV-1). In *2019 JSAE/SAE Powertrains, Fuels and Lubricants* (2019), SAE International.

[41] Kirner, C., Halbhuber, J., Uhlig, B., Oliva, A., Graf, S., and Wachtmeister, G. Experimental and simulative research advances in the piston assembly of an internal combustion engine. *Tribology International 99* (2016), 159–168.

[42] Knauder, C., Allmaier, H., Salhofer, S., and Sams, T. The impact of running-in on the friction of an automotive gasoline engine and in particular on its piston assembly and valve train. *Proceedings of the Institution of Mechanical Engineers, Part J: Journal of Engineering Tribology 232*, 6 (2017), 749–756.

[43] Knauder, C., Allmaier, H., Sander, D. E., and Sams, T. Investigations of the friction losses of different engine concepts. Part 1: A combined approach for applying subassembly-resolved friction loss analysis on a modern passenger-car diesel engine. *Lubricants 7*, 5 (2019), 35.

[44] Knauder, C., Allmaier, H., Sander, D. E., and Sams, T. Investigations of the friction losses of different engine concepts. Part 2: Sub-assembly resolved friction loss comparison of three engines. *Lubricants 7*, 12 (2019), 19.

[45] Knauder, C., Allmaier, H., Sander, D. E., and Sams, T. Investigations of the friction losses of different engine concepts. Part 3: Friction reduction potentials and risk assessment at the sub-assembly level. *Lubricants 8*, 4 (2020), 12.

[46] Knauder, C., Allmaier, H., Sander, D. E., and Sams, T. Measurement of the crankshaft seals friction losses in a modern passenger car diesel engine. *Proceedings of the Institution of Mechanical Engineers, Part J: Journal of Engineering Tribology 234*, 7 (2020), 1106–1113.

[47] Koch, F., Geiger, U., and Hermsen, F.-G. Piffo - piston friction force measurements during engine operation. *SAE technical paper*, 960306 (1996).

[48] Köhler, E., and Flierl, R. *Verbrennungsmotoren: Motormechanik, Berechnung und Auslegung des Hubkolbenmotors*. Springer Vieweg, 2016.

[49] Lemazurier, L., Shidore, N., Kim, N., Moawad, A., Rousseau, A., Bonkoski, P., and Delhom, J. Impact of advanced engine and powertrain technologies on engine operation and fuel consumption for future vehicles. *SAE Technical Paper*, 2015-01-0978 (2015).

[50] Lösch, S., Priestner, C., Thonhauser, B., Zieher, F., and Hick, H. Advances in determination of piston group friction losses at high speeds and loads using the AVL FRISC single-cylinder engine. In *Proceedings Reibungsminimierung im Antriebsstrang*. Springer Vieweg, Wiesbaden, 2015, pp. 184–202.

[51] Lutsey, N. Modernizing vehicle regulations for electrification. *International Council On Clean Transportation: Briefing October 2018* (2018).

[52] MAHLE, G. *Kolben und motorische Erprobung*. Springer Vieweg, 2011.

[53] MAHLE, G. *Ventiltrieb: Systeme und Komponenten*. Springer Vieweg, 2013.

[54] MAHLE, G. *Zylinderkomponenten: Eigenschaften, Anwendungen, Werkstoffe*. Springer Vieweg, 2015.

[55] Mauke, D., Dolt, R., Stadler, J., Huttinger, K., and Bargende, M. Methods of measuring friction under motored conditions with external charging. *Kistler Group* (2016).

[56] Maurizi, M., and Hrdina, D. New MAHLE steel piston and pin coating system for reduced TCO of CV engines. *SAE Int. J. Commer. Veh. 9*, 2 (2016), 6.

[57] McKinsey. Roads towards a low-carbon future: Reducing CO_2 emissions from passenger vehicles in the global road transportation system. *Report* (2009).

[58] Merker, G. P., and Teichmann, R. *Grundlagen Verbrennungsmotoren: Funktionsweise, Simulation, Messtechnik*. Springer-Vieweg, 2014.

[59] Merkle, A., Kunkel, S., and Wachtmeister, G. Analysis of the mixed friction in the piston assembly of a SI engine. *SAE Int. J. Engines 5*, 3 (2012), 1487–1497.

[60] Mock, P. Real-driving emissions test procedure for exhaust gas pollutant emissions of cars and light commercial vehicles in Europe. *International Council On Clean Transportation Policy Update* (2017).

[61] Mock, P. European vehicle market statistics 2019/20. *International Council On Clean Transportation: European Vehicle Market Statistics Pocketbook 2019/20* (2019).

[62] Mock, P., and Diaz, S. European vehicle market statistics 2020/21. *International Council On Clean Transportation: European Vehicle Market Statistics Pocketbook 2020/21* (2020).

[63] Morgenstern, R., Kiessling, W., and Reichstein, S. Reduced friction losses and wear by DLC coating of piston pins. *Proceedings of the ASME 2008 Internal Combustion Engine Division Spring Technical Conference* (2008), 289–297.

[64] Morris, N., Moammadpour, M., Rahmani, R., Johns-Rahnejat, P., Rahnejat, H., and Dowson, D. Effect of cylinder deactivation on tribological performance of piston compression ring and connecting rod bearing. *Tribology International 120* (2018), 243–254.

[65] Mufti, R. A., and Priest, M. Experimental evaluation of piston-assembly friction under motored and fired conditions in a gasoline engine. *Journal of Tribology 127*, 4 (2005), 826–836.

[66] Mufti, R. A., and Priest, M. Technique of simultaneous synchronized evaluation of the tribological components of an engine under realistic conditions. *Proceedings of the Institution of Mechanical Engineers, Part D: Journal of Automobile Engineering 223*, 10 (2009), 1311–1325.

[67] Noorman, M. T., Assanis, D. N., Patterson, D. J., Tung, S. C., and Tseregounis, S. I. Overview of techniques for measuring friction using bench tests and fired engines. *SAE Transactions 109*, Section 4: Journal of fuels and lubricants (2000), 890–900.

[68] Okuda, S., Saito, H., Nakano, S., Koike, Y., Sagawa, T., Kawamura, S., and Yoshida, K. Development of JASO GLV-1 0W-8 low viscosity engine oil for improving fuel efficiency considering oil consumption and engine wear performance. In *WCX SAE World Congress Experience* (2020), SAE International.

[69] Okuyama, Y., Shimokoji, D., Sakurai, T., and Maruyama, M. Study of low-viscosity engine oil on fuel economy and engine reliability. In *SAE 2011 World Congress & Exhibition* (2011), SAE International.

[70] Patir, N., and Cheng, H. An average flow model for determining effects of three-dimensional roughness on partial hydrodynamic lubrication. *ASME, Transactions, Journal of Lubrication Technology 100* (1978), 12–17.

[71] Patir, N., and Cheng, H. Application of average flow model to lubrication between rough sliding surfaces. *ASME, Transactions, Journal of Lubrication Technology 101* (1979), 220–230.

[72] Peklenik, J. Paper 24: New developments in surface characterization and measurements by means of random process analysis. *Proceedings of the Institution of Mechanical Engineers, Conference Proceedings 182*, 11 (1967), 108–126.

[73] Pischinger, F., Adomeit, P., Dorenkamp, R., Schindler, K.-P., Baar, R., Greiner, J., Gumpoltsberger, G., Sasse, C., Steinel, K., Lanzer, H., Pecnik, H., Kurz, G., Stüttem, M., Beck, M., Pingen, B., Drescher, I., and Heinl, E. Antriebe. In *Vieweg Handbuch Kraftfahrzeugtechnik*. Springer-Vieweg, 2011, pp. 158–378.

[74] Plank, R., Hosenfeldt, T., Karbacher, R., Musayev, Y., Schulz, E., and Weber, J. Tribological optimization in the powertrain. In *Encyclopedia of Automotive Engineering*. John Wiley & Sons, 2015, pp. 1485–1497.

[75] Priebsch, H. H., and Krasser, J. Simulation of the oil film behaviour in elastic engine bearings considering pressure and temperature dependent oil viscosity. *Tribology Series 32* (1997), 651–659.

[76] Priestner, C., Allmaier, H., Priebsch, H. H., and Forstner, C. Refined simulation of friction power loss in crank shaft slider bearings considering wear in the mixed lubrication regime. *Tribology International 46*, 1 (2012), 200–207.

[77] Rahnejat, H., Balakrishnan, S., King, P., and Howell-Smith, S. In-cylinder friction reduction using a surface finish optimization technique. *Proceedings of the Institution of Mechanical Engineers, Part D: Journal of Automobile Engineering 220*, 9 (2006), 1309–1318.

[78] Sadeghi, F. Elastohydrodynamic lubrication. In *Tribology and dynamics of engine and powertrain*. Woodhead Publishing Limited, 2010, pp. 171–221.

[79] Sander, D., Knauder, C., Allmaier, H., Damjanovi-Le Baleur, S., and Mallet, P. Friction reduction tested for a downsized diesel engine with low-viscosity lubricants including a novel polyalkylene glycol. *Lubricants 5*, 2 (2017), 9.

[80] Sander, D. E. *A Validated Elasto-Hydrodynamic Simulation for Journal Bearings Operating Under Severe Conditions*. PhD thesis, Technische Universität Graz, 2016.

[81] Sander, D. E., Allmaier, H., and Priebsch, H. H. Friction and wear in automotive journal bearings operating in today's severe conditions. In *Advances in Tribology*, P. H. Darji, Ed. IntechOpen, Rijeka, 2016, ch. 7.

[82] Sander, D. E., Allmaier, H., Priebsch, H. H., Reich, F. M., Witt, M., Füllenbach, T., Skiadas, A., Brouwer, L., and Schwarze, H. Impact of high pressure and shear thinning on journal bearing friction. *Tribology International 81* (2015), 29–37.

[83] Sander, D. E., Allmaier, H., Priebsch, H. H., Reich, F. M., Witt, M., Skiadas, A., and Knaus, O. Edge loading and running-in wear in dynamically loaded journal bearings. *Tribology International 92* (2015), 395–403.

[84] Sander, D. E., Allmaier, H., Priebsch, H. H., Witt, M., and Skiadas, A. Simulation of journal bearing friction in severe mixed lubrication–validation and effect of surface smoothing due to running-in. *Tribology International 96* (2016), 173–183.

[85] Sander, D. E., Allmaier, H., and reich, F. M. Ermittlung der Reibungsverluste in Serienmotoren. *VDI-Berichte Nr.2202* (2013), 165–175.

[86] Sandoval, D. *An Improved Friction Model For Spark Ignition Engines*. Bachelor's thesis, Massachusetts Institute of Technology, 2003.

[87] Schommers, J., Lagemann, V., Böhm, J., and Binder, S. Direkte Messung der Kolbengruppenreibung. *MTZ Motortech Z 76* (2015), 16–23.

[88] Schreiner, K. *Basiswissen Verbrennungsmotor*. Springer Vieweg, 2011.

[89] Schwaderlapp, M., Dohmen, J., Janssen, P., and Schürmann, G. Friction reduction – The contribution of engine mechanics to fuel consumption reduction of powertrains. *In Proceedings of the 22nd Aachen Colloquium Automobile and Engine Technology, Aachen, Germany, 7–9 October 2013* (2013), 1273–1292.

[90] Schwarzmeier, M. *Der Einfluss des Arbeitsprozeßverlaufs auf den Reibmitteldruck von Dieselmotoren*. PhD thesis, Technische Universität München, 1992.

[91] Stachowiak, G., and Batchelor, A. W. *Engineering Tribology*. Butterworth-Heinemann, Oxford, 2014.

[92] Tian, T. Dynamic behaviours of piston rings and their practical impact. Part 1: Ring flutter and ring collapse and their effects on gas flow and oil transport. *Proceedings of the Institution of Mechanical Engineers, Part J: Journal of Engineering Tribology 216* (2002), 209–228.

[93] Tian, T. Dynamic behaviours of piston rings and their practical impact. Part 2: Oil transport, friction and wear of ring/liner interface and the effects of piston and ring dynamics. *Proceedings of the Institution of Mechanical Engineers, Part J: Journal of Engineering Tribology 216* (2002), 229–248.

[94] Tietge, U., Mock, P., and Dornoff, J. CO_2 emissions from new passenger cars in the European Union: Car manufacturers' performance in 2018. *International Council On Clean Transportation Briefing* (2019).

[95] Toyota, N. Toyota aims for sales of more than 5.5 million electrified vehicles including 1 million zero-emission vehicles per year by 2030. `https://global.toyota/en/newsroom/corporate/20353243.html`, 7 2020.

[96] Ullmann, K. Die mechanischen Verluste des schnelllaufenden Dieselmotors und ihre Ermittlung im Schleppversuch. *Deutsche Kraftfahrtforschung 34* (1939).

[97] Ullmann, K. Die Reibungs- und Pumpverluste des schnellaufenden Otto- und Dieselmotors. *ATZ - Automobiltechnische Zeitschrift 42* (1939), 397–406.

[98] van Basshuysen, R., and Schäfer, F. *Handbuch Verbrennungsmotor: Grundlagen, Komponenten, Systeme, Perspektiven*. Springer Vieweg, 2015.

[99] Werner, M., Graf, S., Merkle, A., and Wachtmeister, G. Direkte Messung der Kolbengruppenreibung. *MTZ Motortech Z 75* (2014), 72–79.

[100] Wichtl, R., Eichlseder, H., Mallinger, W., and Peterek, R. Friction investigations on the diesel engine in combustion mode - A new measuring method. *MTZ Worldw 78* (2017), 26–31.

[101] Wichtl, R., Schneider, M., Grabner, P., and Eichlseder, H. Experimental and simulative friction analysis of a fired passenger car diesel engine with focus on the cranktrain. *SAE Int. J. Engines 9*, 4 (2016), 2227–2241.

[102] Wong, V. W., and Tung, S. C. Overview of automotive engine friction and reduction trends–effects of surface, material, and lubricant-additive technologies. *Friction 4*, 1 (2016), 1–28.

[103] Woydt, M., Gradt, T., Hosenfeldt, T., Luther, R., Rienäcker, A., Wetzel, F.-J., and Wincierz, C. Tribology in Germany: Interdisciplinary technology for the reduction of CO_2-emissions and the conservation of resources. *Expert Study of the German Society for Tribology (Gesellschaft für Tribologie e.V. – GfT)* (2019).

[104] Yang, Z., and Bandivadekar, A. Light-duty vehicle greenhouse gas and fuel economy standards. *International Council On Clean Transportation: Global Update 2017* (2017).

[105] Yoshida, S., Yamamori, K., Hirano, S., Sagawa, T., Okuda, S., Miyoshi, T., and Yukimura, S. The development of JASO GLV-1 next generation low viscosity automotive gasoline engine oils specification. In *WCX SAE World Congress Experience* (2020), SAE International.

[106] Zhao, F., Kangda, C., Hao, H., and Liu, Z. Challenges, potential and opportunities for internal combustion engines in China. *Sustainability 12*, 4955 (2020), 15.

List of Figures

List of Tables